LIMIT DESIGN OF REINFORCED CONCRETE SLABS - OPENINGS AND SLAB-COLUMN CONNECTIONS

A thesis presented for

the degree of Doctor of Philosophy

in Civil Engineering

in the University of Canterbury,

Christchurch, New Zealand.

by

S. ISLAM

1973

ABSTRACT

This thesis is concerned with two aspects of the limit design methods of reinforced concrete slabs.

The first part deals with a theoretical investigation of uniformly loaded two-way rectangular slabs with four positions of rectangular openings, namely the slab centre, the slab corner, the centre of a short side and the centre of a long side. Yield-line theory was used to derive equations and design charts suitable for the limit design of such slabs reinforced orthotropically with edges either all fixed or all simply supported.

The second part involves theoretical and experimental investigations on the transfer of shear and unbalanced moments at interior flat plate-column connections. Tests were conducted on half scale reinforced concrete models under monotonic and cyclic loading to determine the deterioration of load carrying capacity and ductility which would occur under earthquake loadings. Ultimate strength procedures were developed to predict the load carrying capacity of slab-column connections with and without shear reinforcement. Good agreement was obtained between the experimental and theoretical strength of such connections. Of the various types of shear reinforcement tested (cranked bars, structural steel shearheads and vertical closed stirrups) the use of closed stirrups passing round the top and bottom slab bars in the vicinity of the column faces proved to be most effective.

ACKNOWLEDGEMENTS

I gratefully acknowledge the assistance received during the course of this project and extend my thanks to:

Professor H.J. Hopkins, Head of Civil Engineering Department, under whose overall guidance this study was made;

Professor R. Park, supervisor for this study, for his continued encouragement and valuable guidance throughout the project, and for his helpful advice during the preparation of this thesis;

Messrs. H.T. Watson and P.C. Dawson, Technical Officers, and the Technical Staff of the Civil Engineering Department for their assistance in the experimental programme. I wish to particularly thank Mr. A.G. Foot, Senior Technician, for his conscientious preparation of the test equipment and test specimens and Mr. N.W. Prebble, Senior Technician, for preparing the formwork;

Mrs. A. Watt for typing the manuscript;

Mr. W. McClelland for draughting assistance;

Mr. H. Patterson for photographic work;

The University Grants Committee, for financial assistance in the form of a Commonwealth Scholarship;

Certified Concrete (Christchurch) Ltd, for their assistance in casting the specimens and the concrete blocks.

Finally I wish to thank my wife for her encouragement and help.

CONTENTS

		Page
1.	INTRODUCTION AND SCOPE OF RESEARCH	
1.1	INTRODUCTION	1
1.2	SCOPE OF RESEARCH	2
1.3	FORMAT	3
2.	PART I : UNIFORMLY LOADED TWO WAY REINFORCED CONCRETE SLABS WITH OPENINGS	
	SUMMARY	5
2.1	INTRODUCTION	5
2.2	YIELD-LINE THEORY APPROACH	6
2.3	ULTIMATE LOAD EQUATIONS FOR SLABS WITH OPENINGS ...	9
2.4	MINIMIZATION OF ULTIMATE LOAD	25
2.5	DESIGN CHARTS	25
2.6	ACCURACY OF DERIVED CHARTS	26
2.7	EFFECT OF OPENINGS ON ULTIMATE LOAD	39
2.8	CONCLUSIONS	44
3.	PART II : TRANSFER OF UNBALANCED MOMENT AND SHEAR FROM REINFORCED CONCRETE FLAT PLATES TO INTERIOR COLUMNS	
	SUMMARY	45
3.1	INTRODUCTION	45
3.2	REVIEW OF PREVIOUS WORK	49
	Summary	49
3.2.1	Introduction	49
3.2.2	Investigations Without Shear Reinforcement	50
	(i) Di Stasio and Van Buren	51
	(ii) Moe	54

		Page
	(iii) ACI-ASCE Committee 326	56
	(iv) Commentary on ACI Building Code (ACI 318-63)	57
	(v) Hanson and Hanson	58
	(vi) Revised Building Code Requirements for Reinforced Concrete (ACI 318-71)	61
	(vii) Hawkins and Corley	62
3.2.3	Discussion of Methods of Analaysis Without Shear Reinforcement	66
3.2.4	Investigations With Shear Reinforcement	71
	(i) Full Scale Test by Hollings	71
	(ii) PCA Tests	74
3.2.5	Effectiveness of Shear Reinforcement in Resisting Punching Shear	76
	(i) Recommendation by ACI Building Code (ACI 318-71)..	76
	(ii) New Evaluation of Punching Shear Tests by Herzog..	77
	(iii) Discussion of Effectiveness of Shear Reinforcement	79
3.2.6	Tests at British Research Station	80
3.2.7	Seismic Resistance of Flat Plates	83
3.2.8	Conclusions	84
3.3	EXPERIMENTAL STUDY OF INTERIOR FLAT PLATE-COLUMN CONNECTIONS	85
	Summary	85
3.3.1	Introduction	85
3.3.2	Design of Test Specimens	86
	(i) Selection of Test Specimen	86
	(ii) Discussion of Method of Loading	88
	(iii) The Prototype Structure	89
	(iv) Details of Test Specimens	89
3.3.3	Test Equipment and Procedure	97
3.3.4	Test Results	103
	(i) Description of Loading Cycle	104

		Page
	(ii) Strength and Ductility of Connections	104
	(iii)Behaviour of Specimen 1	106
	(iv) Behaviour of Specimen 2	111
	(v) Behaviour of Specimen 3C	116
	(vi) Behaviour of Specimen 4S	122
	(vii)Behaviour of Specimen 5S	127
	(viii)Behaviour of Specimen 6CS	134
	(ix) Behaviour of Specimen 7CS	141
	(x) Behaviour of Specimen 8CS	147
3.3.5	Discussion of Test Results	152
	(i) Strength	152
	(ii) Ductility	153
	(iii) Stresses in Slab Bars and Shear Reinforcement ...	154
	(iv) Effect of Bending Moment Reversals	157
	(v) Effectiveness of Various Shear Reinforcement Arrangements	157
	(vi) Junction Failure Mechanisms	158
	(vii) Effective Width and Stiffness of Slab-Column Specimens	160
3.3.6	Conclusions	163
3.4	THEORY FOR SHEAR-FLEXURE FAILURE OF SLAB-COLUMN CONNECTIONS WITHOUT SHEAR REINFORCEMENT	165
	Summary	
3.4.1	Introduction	165
3.4.2	Assumptions	167
3.4.3	Moment Transfer by Flexure	169
3.4.4	Effect of Membrane Action	170
3.4.5	Moment Transfer by Vertical Shear Stresses	172
3.4.6	Moment Transfer by Torsion	173
3.4.7	Strength Equations	174

		Page
3.4.8	Comparison with Test Results	175
3.4.9	Discussion of the Theory Presented	187
3.4.10	Conclusions	188
3.5	THEORY FOR SHEAR-FLEXURE FAILURE OF SLAB-COLUMN CONNECTIONS WITH SHEAR REINFORCEMENT	189
	Summary	189
3.5.1	Introduction	189
3.5.2	Inclined Cranked Bars	189
3.5.3	Vertical Closed Stirrups	193
3.5.4	Structural Steel Shearhead	194
3.5.5	Comparison with Test Results	197
3.5.6	Discussion of the Theory Presented	200
3.5.7	Conclusions	201
3.6	THEORY FOR FLEXURAL FAILURE OF SLAB-COLUMN CONNECTIONS	202
	Summary	202
3.6.1	Introduction	202
3.6.2	Development of Equations	203
3.6.3	Comparison with Test Results	208
3.6.4	Conclusions	211
3.7	CONCLUSIONS AND SUGGESTED FUTURE RESEARCH	212
3.7.1	General	212
3.7.2	Summary of Conclusions	212
3.7.3	Suggested Future Research	213
APPENDIX A :	BIBLIOGRAPHY	A1
APPENDIX B :	MATERIALS, EQUIPMENT AND TESTING PROCEDURE ...	B1
B.1	MATERIALS	B1

		Page
B.1.1	Concrete	B1
B.1.2	Steel	B3
B.2	FABRICATION	B7
B.2.1	Formwork	B7
B.2.2	Placing Reinforcement	B8
B.2.3	Placing Concrete	B8
B.3	TEST EQUIPMENT AND PROCEDURE	B12
B.3.1	Test Frame	B12
B.3.2	Load Application and Measurement	B12
B.3.3	Deflections	B14
B.3.4	Steel Strains	B14
B.3.5	Crack Detection	B20
B.3.6	Sequence of Operations	B20

LIST OF FIGURES

Figure		Page
2.1	Slabs with Openings	7
2.2	Yield-line Patterns for Central Openings	10
2.3	Yield-line Patterns for Corner Opening	14
2.4	Yield-line Patterns for Opening at a Short Side	19
2.5	Yield-line Patterns for Opening at a Long Side	22
2.6	Central Opening $r' = 0$	27
2.7	Central Opening $r' = 1$	28
2.8	Central Opening $r' = 2$	29
2.9	Corner Opening $r' = 0$	30
2.10	Corner Opening $r' = 1$	31
2.11	Corner Opening $r' = 2$	32
2.12	Opening at Centre of Short Edge $r' = 0$	33
2.13	Opening at Centre of Short Edge $r' = 1$	34
2.14	Opening at Centre of Short Edge $r' = 2$	35
2.15	Opening at Centre of Long Edge $r' = 0$	36
2.16	Opening at Centre of Long Edge $r' = 1$	37
2.17	Opening at Centre of Long Edge $r' = 2$	38
2.18	Effect of Opening Size and Position on Ultimate Load of a Slab	43
3.1	Interior Slab-Column Connection	46
3.2	Assumed Critical Sections and Shear Stress Distributions	52
3.3	Hanson and Hanson's Test Specimen and Loading Methods	59
3.4	Hawkins and Corley's Analysis	63
3.5	Details of Hollings' Test Structure	73
3.6	PCA Test Specimens	75
3.7	BRS Model Slabs	81

		Page
3.8	Selection of Slab-Column Test Specimen	87
3.9	Slab-Column Test Specimen	91
3.10	Details of Reinforcement	92
3.11	Details of Joint without Shear Reinforcement	93
3.12	Inclined Cranked Bars for Specimen 4S	94
3.13	Shearhead for Specimen 5S	95
3.14	Closed Stirrups for Specimen 6CS	98
3.15	Closed Stirrups for Specimens 7CS and 8CS	99
3.16	Slab-Column Specimen in the Test Rig	100
3.17	Upward Load-Displacement Curve for Specimen 1	107
3.18	Downward Load-Displacement Curve for Specimen 1	107
3.19	Stresses in Slab Bars of Specimen 1	109
3.20	Crack Pattern of Specimen 1 at 2 in. deflection	110
3.21	Failure Surface of Specimen 1	110
3.22	Deflected Shape of Specimen 1	114
3.23	Upward Load-Displacement Curve for Specimen 2	112
3.24	Downward Load-Displacement Curve for Specimen 2	112
3.25	Stresses in Slab Bars of Specimen 2	113
3.26	Crack Pattern of Specimen 2 at failure	114
3.27	Failure Surface of Specimen 2	115
3.28	View of Specimen 2 after Removal of Broken Concrete ..	115
3.29	Loading Cycles for Specimen 3C	117
3.30	Load-Displacement Curve for Edge A of Specimen 3C	118
3.31	Load-Displacement Curve for Edge B of Specimen 3C	118
3.32	Stresses in Slab Bars of Specimen 3C	119
3.33	Crack Pattern of Specimen 3C after Cycle 1	120
3.34	Crack Pattern of Specimen 3C after Cycle 5	120
3.35	Crack Pattern of Specimen 3C after Cycle 9	121

		Page
3.36	Failure Surface of Specimen 3C	121
3.37	Upward Load-Displacement Curve for Specimen 4S	123
3.38	Downward Load-Displacement Curve for Specimen 4S	123
3.39	Stresses in Slab Bars of Specimen 4S	124
3.40	Stresses in Cranked Bars of Specimen 4S	125
3.41	Crack Pattern of Specimen 4S	126
3.42	Failure Surface of Specimen 4S	126
3.43	Load-Displacement Curve for Edge A of Specimen 5S	128
3.44	Load-Displacement Curve for Edge B of Specimen 5S	129
3.45	Stresses in Slab Bars of Specimen 5S	130
3.46	Stresses in Shearhead of Specimen 5S	131
3.47	Crack Pattern of Specimen 5S	132
3.48	Specimen 5S at 4 in. Edge Displacement	132
3.49	Loading Cycles for Specimens 6CS, 7CS and 8CS	135
3.50	Load-Displacement Curves for Edge A of Specimen 6CS ..	136
3.51	Load-Displacement Curves for Edge B of Specimen 6CS ..	136
3.52	Stresses in Slab Bars of Specimen 6CS	137
3.53	Stresses in Stirrups of Specimen 6CS	138
3.54	Crack Pattern of Specimen 6CS at Cycle 5	139
3.55	Crack Pattern of Specimen 6CS at Cycle 5	139
3.56	Specimen 6CS at Edge Displacement of 7.2 in.	140
3.57	Specimen 6CS at the End of Testing	140
3.58	Load-Displacement Curves for Edge A of Specimen 7CS ..	142
3.59	Load-Displacement Curves for Edge B of Specimen 7CS ..	142
3.60	Stresses in Slab Bars of Specimen 7CS	144
3.61	Stresses in Stirrups of Specimen 7CS	145
3.62	View of Specimen 7CS after Test	146
3.63	Deflected Shape of Specimen 7CS after Test	146
3.64	Load-Displacement Curves for Edge A of Specimen 8CS ..	148

		Page
3.65	Load-Displacement Curves for Edge B of Specimen 8CS ...	148
3.66	Stresses in Slab Bars of Specimen 8CS	149
3.67	Stresses in Stirrups of Specimen 8CS	150
3.68	Crack Pattern of Specimen 8CS after Test	151
3.69	View of Specimen 8CS after Removal of Broken Concrete..	151
3.70	Computation of Edge Displacement	161
3.71	Moments and Forces at Slab-Column Connection	166
3.72	Membrane Action	171
3.73	Interaction Diagrams for Hanson and Hanson's Specimens A1, A2 and A12	178
3.74	Interaction Diagrams for Hanson and Hanson's Specimens B7 and B16	179
3.75	Interaction Diagrams for Hanson and Hanson's Specimens C8 and C17	180
3.76	Interaction Diagrams for Moe's Specimens M2, M2A, M3 and M4A	181
3.77	Interaction Diagrams for Moe's Specimens M6, M7 and M9	182
3.78	Interaction Diagrams for Moe's Specimens M8 and M10 ...	183
3.79	Interaction Diagrams for Author's Specimens 1, 2 and 3C	184
3.80	Inclined Cranked Bars	190
3.81	Shearhead Reinforcement	196
3.82	Yield-line Pattern A1	204
3.83	Yield-line Pattern A2	206
3.84	Yield-line Pattern B1 for Moe's Specimens	210
B.1	Stress-Strain Curves for Steel	B5
B.2	Load-deflection Curve for Shearhead	B6
B.3	Formwork and Reinforcement	B9
B.4	Inclined Cranked Bars in Specimen 4S	B9
B.5	Shearhead in Specimen 5S	B10
B.6	Closed Stirrups in Specimen 6CS	B11

		Page
B.7	Closed Stirrups in Specimens 7CS and 8CS	B11
B.8	Test Frame	B15
B.9	Method of Applying Line Load at Edge	B16
B.10	Method of Applying Edge Load Through 4 Points ..	B16
B.11	Application of Column Load	B15
B.12	Application of Upward Edge Load	B17
B.13	Application of Downward Edge Load	B17
B.14	Load-Strain Plot for High Tensile Bar	B18
B.15	Dial Gauge Locations	B19

LIST OF TABLES

Table		Page
2.1	$wL_x^2/12m_y$ from Eq. (2.13)	40
2.2	$wL_x^2/12m_y$ from Eq. (2.5)	41
3.1	Actual Values of K from Test Results	68
3.2	Moment and Ductility Characteristics of Test Specimens	105
3.3	Comparison of Maximum Steel Stresses as a Proportion of the Yield Stress Reached in Slab Bars Across the Slab	155
3.4	Comparison of Calculated and Measured Edge Displacement	162
3.5	Strength for Slab-Column Specimens without Shear Reinforcement	176
3.6	Strengths for Slab-Column Specimens with Shear Reinforcement	198
B.1	Concrete Properties at Time of Testing	B2
B.2	Steel Properties	B4

INDEX OF NOTATION

(Greek letters are listed at end)

A, $\bar{A}$, A_c = area of concrete in assumed critical section

A_s = area of one leg of closed stirrups

A_{s1} = area of one reinforcing bar parallel to the torsion face of the column

A_v = area of shear reinforcement

a = distance from centroidal axis to the most remote part of the critical section

b = perimeter of column

c = side dimension of a square column

c_1 = side dimension of column parallel to the direction of bending

c_2 = side dimension of column transverse to the direction of bending

d = effective depth of slab

d_1 = effective depth for face AD or BC of the critical section

d_1' = distance from extreme compression fibre to centroid of compression steel for face AD

d_2 = effective depth for face AB or CD of the critical section

d' = distance between the bottom face and the centroid of bottom reinforcement

d'' = distance between the top face and the centroid of top reinforcement

f_c' = cylinder compressive strength of concrete

f_{sp} = splitting tensile strength of concrete

f_y = yield stress of reinforcement

h = depth of structural steel shapes in shearhead

J, $\bar{J}$, J_c = polar moment of inertia of the surface described by the critical section passing through the slab thickness about its centroid

K = moment reduction factor that specifies the part of unbalanced moment producing shear stress on the critical section

kL_x , kL_y = dimension of the opening in the x and y directions

L_c = length of shearhead arm measured from the column face

L_x , L_y = spans of the slab in the x and y directions ($L_y > L_x$)

M = total unbalanced moment

M_{AB} , M_{BC} = bending moment acting on face AB, BC, etc. of the critical section

M_{ABO}, M_{BCO} = ultimate resisting moment for face AB, BC, etc. of the critical section

M_{flex} = ultimate flexural capacity of the slab

M_o = ultimate unbalanced moment capacity without shear transfer

M_u = total ultimate unbalanced moment capacity

M_w = service load unbalanced moment capacity without shear transfer

M_v = part of moment resisted by shear stresses acting on faces AB and CD of the critical section

M_{test} = maximum measured unbalanced moment

m_{AB} , m_{CD} = working stress design moment acting on faces AB and CD of the critical section

m_r = sum of flexural moments acting on faces AB and CD of critical section, calculated by working stress design method

m_p = plastic moment capacity of a shearhead arm

m_t = plastic torque of a shearhead arm

m_u = positive ultimate flexural capacity of face AB per unit length

m'_u = negative ultimate flexural capacity of face CD per unit length

m_x , m_y = sagging or positive yield moments, per unit width, in the x and y directions

m'_x , m'_y = hogging or negative yield moments, per unit width, in the x and y directions

r = m_x/m_y

r' = $m'_x/m_x = m'_y/m_y$

s = spacing of stirrups

s_1 = spacing of reinforcing bars parallel to the torsion face of the column

T = total torsional moment acting on the side faces AD and BC of the critical section

T_{AD} , T_{BC} = ultimate resisting torsional moment acting on faces AD, BC of the critical section in combination with shear

T_o = ultimate resisting torsional moment in pure torsion

T_s = torsional moment resisted by stirrups

T_u = ultimate resisting torsional moment in combination with shear

t = total thickness of slab

U_e = external virtual work

U_i = internal virtual work

V = total shear around the critical section

V' = difference between the measured ultimate load and the calculated shear resistance of slab without the assistance of actual shear reinforcement

V_{flex} = shear force at which flexural failure takes place

V_o = ultimate shear capacity without moment transfer

V_s = shear force carried by shear reinforcement

V_u = total ultimate shear transferred

V_w = service load shear capacity without moment transfer

V_{AB} , V_{BC} = shear force acting on face AB, BC, etc. of the critical section

V_{ABO}, V_{BCO} = ultimate resisting shear for face AB, BC, etc. of the critical section

v_1 , v_2 = unit vertical shear stress

v_{max} = maximum shear stress

v_u = nominal ultimate shear stress

v_{AB} , v_{BC} = shear stress induced by V_u on faces AB, BC, etc. of the critical section

w = ultimate uniformly distributed load, per unit area

x_o = dimension of critical section parallel to the direction of bending

y_o = dimension of critical section transverse to the direction of bending

α = L_x/L_y or inclination of cranked bars with the horizontal axis

β_1 , β_2 , β_3 = ratios of yield line dimensions to respective spans

η = efficiency of shear reinforcement

ρ = bottom reinforcement ratio

ρ' = top reinforcement ratio

τ_{AD} , τ_{BC} = nominal ultimate torsional shear stress on the face AD or BC of the critical section

Ω = coefficient = $0.66 + 0.33\frac{(c_1 + d_2)}{(d_1 - d_1')}$

$= 0.66 + \frac{0.33x_o}{t-d'-d''}$ but not greater than 1.5 .

1. INTRODUCTION AND SCOPE OF RESEARCH

1.1 INTRODUCTION

In the design of reinforced concrete slabs most codes of practice allow approximate methods based on the elastic plate theory and give moment coefficients for regular panels. The use of the actual elastic theory distribution of moments is too complicated for practical design. Further, once concrete is cracked and strains in the concrete and steel get into the inelastic region, the assumptions of the elastic theory remain no longer valid. A more rational method to be used in conjunction with ultimate strength proportioning of reinforced concrete slabs is one which is based on their actual behaviour at failure and takes inelastic strains into consideration when determining the distribution of bending moments and forces in the entire floor system. Such a design approach is called limit design which recognises that due to plasticity the distribution of moments in the slab may be different at failure or collapse from the elastic distribution. By using this method simple accurate solutions can be obtained, even when designing slabs of unusual shape and boundary conditions.

Although in recent years the limit design method has become widely recognised as an accepted design procedure for reinforced concrete slabs, several aspects of the theory require further investigation and clarification. Two such aspects are slabs with openings and flat plate-column connections transferring shear and unbalanced moment.

To meet the functional requirements of architects and planners for service ducts in buildings, openings of considerable size are often placed at various positions in the floor slabs. The analysis of such slabs always presents a problem to structural designers. An investigation is needed to study the effect of openings on the ultimate strength of slabs.

The use of beamless flat plate construction has become a popular structural system because of its aesthetic features and economical considerations resulting from reduced floor heights and simplified formwork. The design of a flat plate structure is generally controlled by the behaviour of the slab-column connection which is the most critical part of such a structure and is vulnerable to premature shear failure in the slab around the column. When a flat plate floor is subjected to unbalanced gravity loads, wind or earthquake loadings, there may be a transfer of substantial unbalanced moment in addition to shear between the slab and the column. For such connections only a limited theoretical and experimental work has been done. Very little information is available on test data or design procedures for connections containing some form of shear reinforcement. Further in countries requiring design for earthquake loading design engineers have generally been cautious regarding the seismic resistance of flat plate structures. The main reason for caution is the shortage of experimental evidence on the behaviour and performance of slab-column connections under earthquake conditions. A study is necessary to obtain further insight into these aspects of the slab-column connection behaviour.

1.2 SCOPE OF RESEARCH

The first part of this investigation concerned the limit design of uniformly loaded two-way slabs with openings. Rectangular slabs with a range of rectangular openings were considered. The openings occupied four positions, namely, central opening, corner opening, opening at the centre of a short side and opening at the centre of a long side. The edges of the slab were assumed to be either all fixed or all simply supported. The slab reinforcement was considered to be orthotropic.

The second part of the investigation concerned the transfer of shear and unbalanced moment at interior flat plate-column connections.

Experimental work was carried out on one-half scale reinforced concrete models of slab-column specimens with square columns. Methods to increase the shear strength of slab-column connections by using various types of shear reinforcement in the form of cranked bars, shearheads and closed vertical stirrups were investigated. Two types of loading methods were used. In order to make an appraisal of the existing design procedures and to substantiate the theory developed here the slab-column connections were loaded to failure with dead load plus live load and with monotonically increasing moment. The deterioration of load carrying capacity and ductility which would occur under seismic loading conditions were examined by subjecting the connections to cycles of bending moment reversals with the same vertical loading. Theoretical procedures were developed for predicting the unbalanced moment capacity of interior slab-column connections with and without shear reinforcement.

1.3 FORMAT

The chapters of this thesis have been limited to three and arranged as follows:

Part I of the thesis appears under Chapter 2 which covers all the work including derivation of ultimate load equations and design charts executed in connection with the limit design of uniformly loaded two-way slabs with openings.

Chapter 3 contains Part II of the thesis and is divided into several sections. In Section 3.2 a review of previous investigations on the transfer of shear and moment is presented and the need for an improved theory is pointed out.

The experimental work and test results are contained in Section 3.3. The variables in the test sequence included the use of various types of shear reinforcement and loading methods which are of monotonic and cyclic types.

Sections 3.4 and 3.5 present theories developed for shear-flexure failures of slab-column connections with and without shear reinforcement and Section 3.6 considers the flexural failure of such connections. These theories are compared with test results reported in this thesis as well as with those reported by other investigators.

The conclusions that have been reached are summarised in Section 3.7 and suggestions are made for future research. Generally the conclusions for each section of the work appear at the end of appropriate sections, and consequently the formal conclusions in this section are comparatively brief.

2. PART I : UNIFORMLY LOADED TWO-WAY REINFORCED CONCRETE SLABS WITH OPENINGS

SUMMARY

Yield-line theory is used to derive equations and charts suitable for the limit design of uniformly loaded rectangular reinforced concrete slabs with rectangular openings. Four positions of openings are considered: the slab centre, the slab corner, the centre of a short side and the centre of a long side. The ratios of the corresponding lengths of the sides of the opening and the slab are kept the same and sizes of opening of up to 0.6 of the length of the slab sides are considered. The edges of the slab are assumed to be either all fixed or all simply supported. Design charts are plotted for various values of the ratio of negative to positive yield moments and for the ratio of the yield moments in the two directions.

2.1 INTRODUCTION

Two-way reinforced concrete slabs often contain openings of considerable size for ducts, pipes, and other services. Elastic theory analysis indicates high peaks of bending moment in the corners of such openings but in reinforced concrete slabs such peaks of bending moment are reduced by moment redistribution and a limit design incorporating an isotropic or orthotropic reinforcement arrangement may be used. The ultimate strength of such slabs may be conveniently determined using the yield-line theory due to Johansen[1]. The draft British Code[2] recommends

yield-line theory as one of the possible methods of slab design. Lash and Banerjee[3] and Zaslavsky[4] have produced ultimate load equations for uniformly loaded slabs with central openings, and Johansen[5] has produced some equations for openings in various positions. Here design equations and charts are produced for uniformly loaded two-way rectangular slabs with edges either all fixed or all simply supported and with a range of rectangular openings.

In Fig. 2.1 four possible positions of the opening are shown: (a) central opening, (b) corner opening, (c) opening at the centre of a short side and (d) opening at the centre of a long side. Various sizes of opening are considered and in order to simplify the plotting of design charts the ratios of the lengths of the sides of the opening and the lengths of the sides of the slab are kept the same. The design charts are plotted for orthotropic reinforcement with various values for the ratio of negative to positive yield moments and for the ratio of the yield moments in the two directions.

2.2 YIELD-LINE THEORY APPROACH

When a reinforced concrete slab reaches ultimate load it is converted into a mechanism by a system of lines of intense cracking across which the tension steel has yielded. Once the system of yield lines at collapse has been postulated the ultimate load of the slab may be determined by using either the virtual work equation or the equations of equilibrium for the segments between the yield lines. Here the virtual work method will be used since the ultimate load is not particularly sensitive to small changes in the dimensions defining the positions of the yield lines and

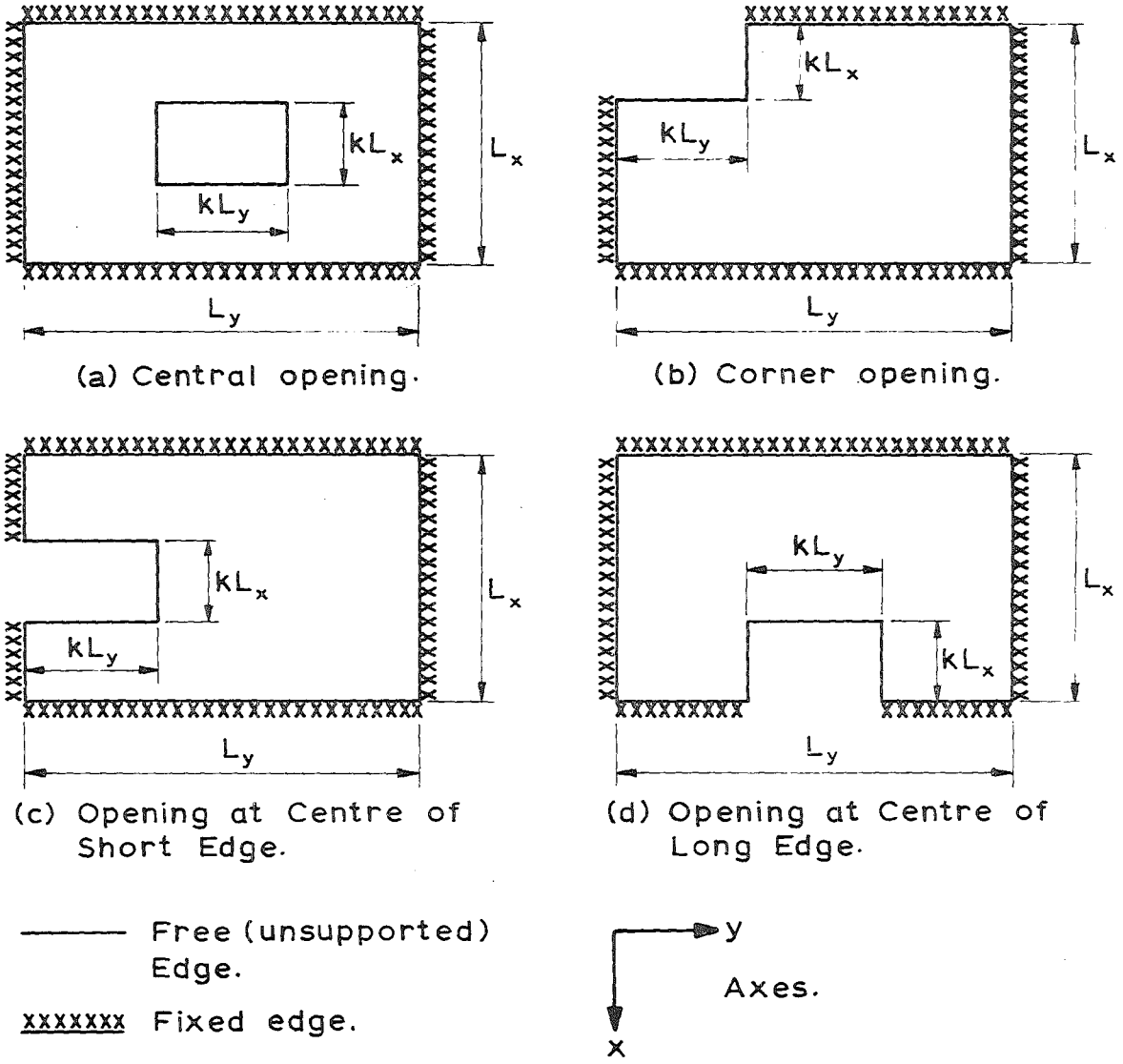

FIG. 2.1 SLABS WITH OPENINGS

the method suits well the numerical procedure of solution that will be used.

The ultimate load is found by giving the slab in the collapse condition a small virtual displacement in the direction of the loading and equating the external work done by the load in moving through the virtual displacements to the internal work done by the bending moments at the yield lines as the segments rotate about the support axes. The virtual work equation may be written as

$$\iint w.\delta(x,y)dx.dy = \sum (m_x\theta_x y_1 + m_y\theta_y x_1) \qquad \ldots\ (2.1)$$

where

w = ultimate load per unit area

$\delta(x,y)$ = virtual displacement in the direction of the loading at the element of area of dimensions dx by dy

m_x , m_y = yield moments per unit width in the x and y directions

θ_x , θ_y = components of the virtual rotation of the slab segments in the x and y directions

x_1 , y_1 = the projected lengths of the yield lines in x and y directions.

When Eq. (2.1) is written for a particular slab it will generally include terms β_1 , β_2 , β_3 etc. which define the positions of the node points of the yield lines. The values of β_1 , β_2 , β_3 etc. to be used in the equation are those which give the minimum load to cause failure.

Since yield-line theory is an upper bound method care must

be taken to examine all the possible yield-line patterns to ensure that the most critical collapse mode is considered because otherwise the load carrying capacity of the slab will be overestimated. There are several possible yield-line patterns associated with the four types of openings to be investigated.

The effect of corner levers will be ignored. In each corner region the yield line will be considered to run straight into the corner. Corner levers theoretically cause a small reduction in the ultimate load but it is felt that their effect can justifiably be neglected since tests have generally shown yield-line theory to be conservative because of the neglect of the effect of membrane action.

2.3 ULTIMATE LOAD EQUATIONS FOR SLABS WITH OPENINGS

Uniformly loaded two-way rectangular slabs with the exterior edges either fixed or simply supported and with the four types of rectangular openings shown in Fig. 2.1(a),(b),(c) and (d) will be investigated. The slab will be considered to be reinforced orthotropically by steel in the top and the bottom running parallel to the edges except that in the case of simply supported edges it will be assumed that no top steel is present. The following equations are derived for slabs with fixed edges but the case of simply supported edges may be obtained by putting $r' = o$. The uniform load is only considered to be acting over the region of the slab where there is no opening, i.e. the slab is not carrying load over the area of the opening.

2.3.1 Central Opening

The three yield-line patterns considered for a slab with a central opening are shown in Fig. 2.2. Only one unknown

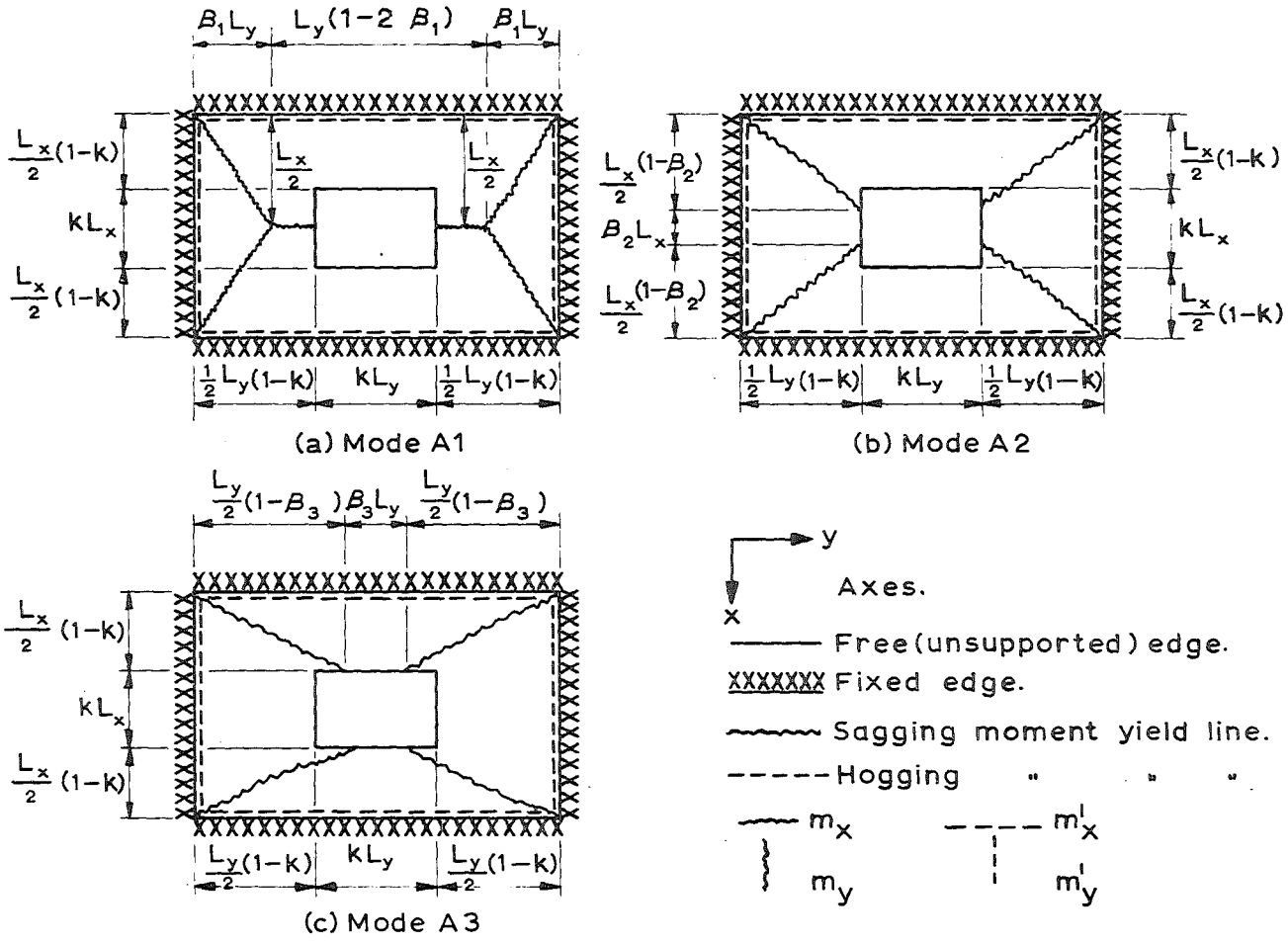

FIG. 2.2 YIELD-LINE PATTERNS FOR CENTRAL OPENING

dimension is necessary to define the positions of the yield lines fully. The ultimate load equations for these yield-line patterns are derived as follows:

Mode A1 (Fig. 2.2a)

Let m_x , m_y be the sagging yield moments per unit width and m'_x , m'_y the hogging yield moments per unit width in the x and y directions. The ratio of yield moments is defined by $r = \frac{m_x}{m_y}$ and $r' = \frac{m'_x}{m_x} = \frac{m'_y}{m_y}$.

Let L_x , L_y be the spans of the slab in the x and y directions $(L_y > L_x)$ and kL_x , kL_y the dimensions of the opening in the x and y directions. $\alpha = \frac{L_x}{L_y}$ defines the ratio of the spans of the slab in the x and y directions and β_1 , β_2 β_3 define the ratio of yield line dimensions to respective spans. Let w be the ultimate uniformly distributed load per unit area.

The internal work done by the yield lines is given by

$$U_i = 2\left[\frac{m'_x L_y^2}{L_x} + \frac{m_x L_y (1-k)^2}{L_x} + \frac{m'_y L_x}{\beta_1 L_y} + \frac{m_y L_x}{\beta_1 L_y}\right]$$

$$= \frac{2m_y}{\alpha\beta_1}\left[2\beta_1 r (r' + 1 - k) + \alpha^2 (r' + 1)\right]$$

The external work done by the loading is obtained as

$$U_e = \frac{4}{3} w\beta_1 L_y \frac{L_x}{2} + \frac{wL_x}{2} L_y (1 - k - 2\beta_1) + \frac{wL_x}{2} kL_y (1-k)^2$$

$$= \frac{wL_x^2}{6\alpha}\left[3 (1 - 2k^2 + k^3) - 2\beta_1\right]$$

Equating $U_i = U_e$, one obtains

$$w = \frac{12m_y}{L_x^2}\left[\frac{2\beta_1\, r(r' + 1 - k) + \alpha^2 (r' + 1)}{3\beta_1 (1 - 2k^2 + k^3) - 2\beta_1^2}\right] \quad \ldots\ldots (2.2)$$

Mode A2 (Fig. 2.2b)

The internal work done by the yield line is given by

$$U_i = 2\left[\frac{m'_x L_y^{\,2}}{L_x (1-\beta_2)} + \frac{m_x L_y (1-k)^2}{L_x (1-\beta_2)} + \frac{m'_y L_x^{\,2}}{L_y (1-k)} + \frac{m_y L_x (1-\beta_2)^2}{L_y (1-k)}\right]$$

$$= \frac{4m_y}{\alpha}\left[\frac{r(1 - k)(r' + 1 - k) + \alpha^2 (1 - \beta_2)(r' + 1 - \beta_2)}{(1 - \beta_2)(1 - k)}\right]$$

The external work done by the loading is given by

$$U_e = \frac{4}{3}\left[w \frac{L_y}{2}(1-k)\frac{L_x}{2}(1-\beta_2) + w\beta_2 L_x \frac{L_y}{2}(1-k)\right.$$

$$\left. + wkL_y \frac{L_x}{2}(1-k)\frac{(1-k)}{(1-\beta_2)}\right]$$

$$= \frac{wL_x^2}{6\alpha}\,\frac{[2(1-k)(1-\beta_2)^2 + 3\beta_2(1-k)(1-\beta_2) + 3k(1-k)^2]}{(1 - \beta_2)}$$

Equating $U_i = U_e$

$$w = \frac{24\, m_y}{L_x^2}\left[\frac{r(1-k)(r' + 1 - k) + \alpha^2 (1-\beta_2)(r' + 1 - \beta_2)}{2(1-k)^2 (1-\beta_2)^2 + 3\beta_2(1-k)^2(1-\beta_2) + 3k(1-k)^3}\right] \ldots (2.3)$$

Mode A3 (Fig. 2.2c)

$$U_i = 2\left[\frac{m'_y L_x^{\,2}}{L_y (1-\beta_3)} + \frac{m_y L_x (1-k)^2}{L_y (1-\beta_3)} + \frac{m'_x L_y^{\,2}}{L_x (1-k)} + \frac{m_x L_y (1-\beta_3)^2}{L_x (1-k)}\right]$$

$$= \frac{4m_y}{\alpha}\left[\frac{\alpha^2(1-k)(r'+1-k)+r(1-\beta_3)(r'+1-\beta_3)}{(1-\beta_3)(1-k)}\right]$$

$$U_e = \frac{4}{3}\,w\,\frac{L_y}{2}(1-\beta_3)\,\frac{L_x}{2}(1-k) + \frac{w}{2}\,L_x(1-k)\beta_3 L_y$$

$$+ \frac{w}{2}\,L_y(1-\beta_3)\,kL_x\,\frac{(1-\beta_3)}{(1-k)}$$

$$= \frac{wL_x^2}{6\alpha}\left[\frac{2(1-\beta_3)(1-k)^2+3\beta_3(1-k)^2+3k(1-\beta_3)^2}{(1-k)}\right]$$

Equating $U_i = U_e$,

$$w = \frac{24m_y}{L_x^2}\left[\frac{\alpha^2(1-k)(r'+1-k)+r(1-\beta_3)(r'+1-\beta_3)}{2(1-\beta_3)^2(1-k)^2+3\beta_3(1-k)^2(1-\beta_3)+3k(1-\beta_3)^3}\right]$$

.....(2.4)

The special case when the yield lines enter the opening at the corners may be obtained from either Eq. (2.3) or (2.4) by putting either $\beta_2 = k$ or $\beta_3 = k$.

2.3.2 Corner Opening

The four yield-line patterns considered for a slab with a corner opening are shown in Fig. 2.3. In all cases three unknown dimensions are required to define the positions of the yield lines fully. Mode B1 is likely to be the governing pattern for small openings and the other modes for larger openings. The derivation of the ultimate load equations for these yield-line patterns is given below.

Mode B1 (Fig. 2.3a)

$$U_i = \left(m_y + m'_y\right)\frac{L_x(1-k)k}{\beta_1(1-\beta_3)L_y} + \left(m_x + m'_x\right)\frac{L_y}{\beta_3 L_x}$$

$$+ \left(m_y + m'_y\right)\frac{L_x}{\beta_2 L_y} + \frac{m_x L_y(1-\beta_1)}{L_x(1-\beta_3)} + \frac{m'_x L_y(1-k)}{L_x(1-\beta_3)}$$

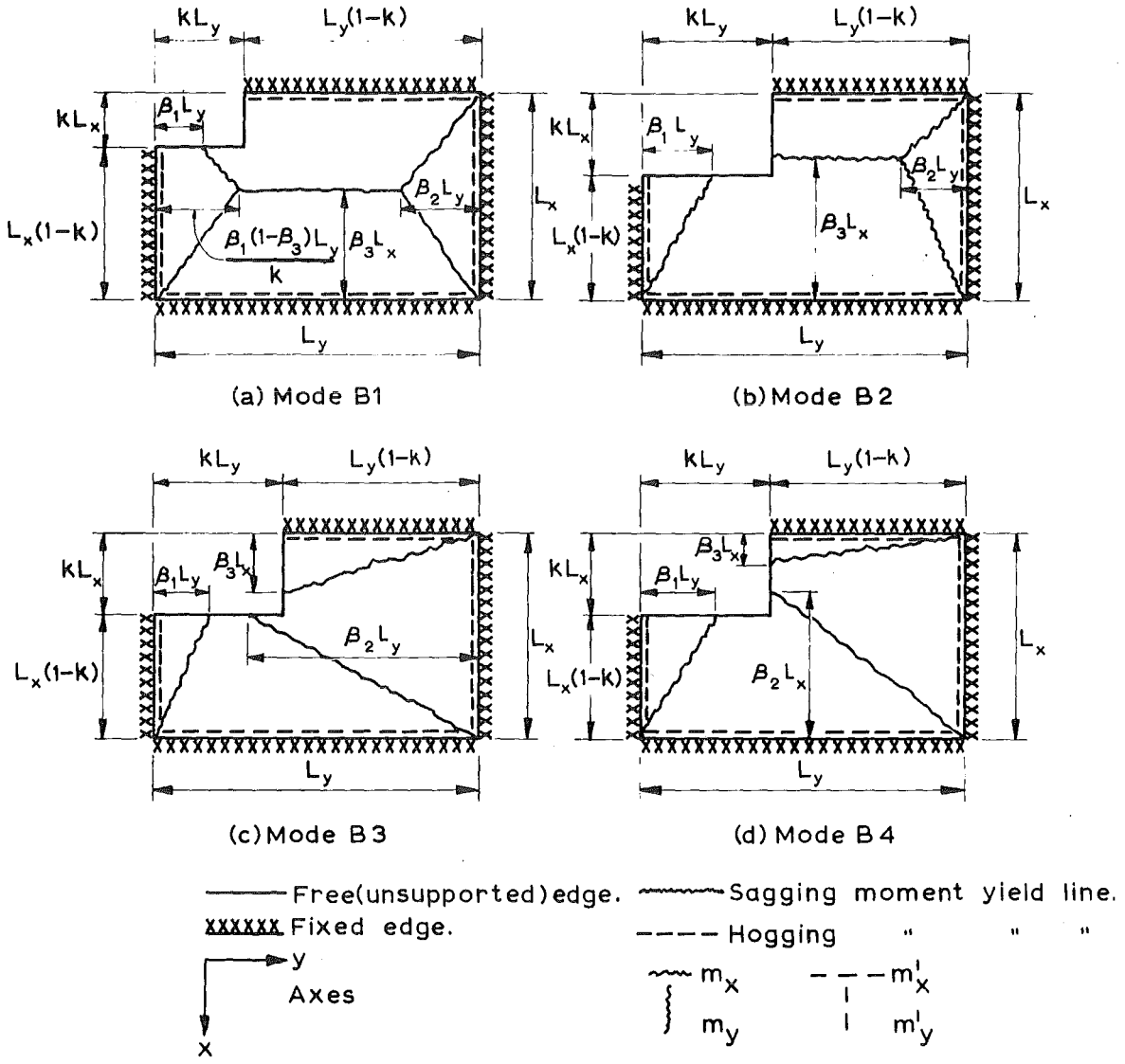

FIG. 2.3 YIELD-LINE PATTERNS FOR CORNER OPENING

$$= m_y \left[\frac{(1+r')(1-k)\alpha k}{\beta_1 (1-\beta_3)} + \frac{r(1+r')}{\alpha\beta_3} + \frac{\alpha(1+r')}{\beta_2} + \frac{r(1-\beta_1 + r' - r'k)}{\alpha(1-\beta_3)} \right]$$

$$U_e = \frac{w}{3} \beta_2 L_y L_x + \frac{w}{2} L_x L_y \left[1-\beta_2-\frac{\beta_1(1-\beta_3)}{k} \right] + \frac{w}{3} L_x L_y \frac{\beta_1(1-\beta_3)}{k}$$

$$- \frac{w}{3} \beta_1 L_y kL_x \frac{k}{1-\beta_3} - \frac{w}{2} kL_x L_y (k-\beta_1) \frac{k}{1-\beta_3}$$

$$= \frac{wL_x^2}{6\alpha} \left[3 - \beta_2 - \frac{\beta_1 (1-\beta_3)}{k} - \frac{k^2 (3k - \beta_1)}{1 - \beta_3} \right]$$

From $U_i = U_e$,

$$w = \frac{6m_y}{L_x^2} \frac{k \left[\alpha^2 k(1+r')(1-k)\beta_2\beta_3 + r(1+r')(1-\beta_3)\beta_1\beta_2 + \alpha^2(1+r')(1-\beta_3)\beta_1\beta_3 + r(1-\beta_1+r'-r'k)\beta_1\beta_2\beta_3 \right]}{\beta_1 \beta_2 \beta_3 \left[(3-\beta_2)(1-\beta_3)k - \beta_1 (1-\beta_3)^2 - k^3 (3k-\beta_1) \right]} \quad \ldots\ldots(2.5)$$

Mode B2 (Fig. 2.3b)

$$U_i = \left(m_y + m_y' \right) \frac{L_x}{\beta_2 L_y} + \frac{m_x' L_y}{\beta_3 L_x} + \frac{m_x \beta_1 L_y}{\beta_3 L_x} + \frac{m_x L_y (1-k)}{\beta_3 L_x}$$

$$+ \left(m_y + m_y' \right) \frac{L_x (1-k)(1-k)}{\beta_1 \beta_3 L_y} + \left(m_x + m_x' \right) \frac{L_y (1-k)}{L_x (1-\beta_3)}$$

$$= m_y\left[\frac{\alpha(1+r')}{\beta_2} + \frac{(1+r')(1-k)^2\alpha}{\beta_1\beta_3} + \frac{r(1+r'+\beta_1-k)}{\alpha\beta_3} + \frac{r(1+r')(1-k)}{\alpha(1-\beta_3)}\right]$$

$$U_e = \frac{2}{3} w\beta_2 L_y \frac{L_x}{2} + \frac{w}{2} L_y (1-k-\beta_2) L_x + \frac{w}{2} L_y (k-\beta_1) L_x (1-k)\frac{(1-k)}{\beta_3}$$

$$+ \frac{w}{3} \beta_1 L_y L_x (1-k) \frac{(1-k)}{\beta_3}$$

$$= \frac{wL_x^2}{6\alpha\beta_3}\left[\beta_3 (3-3k-\beta_2) + (1-k)^2 (3k-\beta_1)\right]$$

From $U_i = U_e$,

$$w = \frac{6m_y}{L_x^2} \frac{\left[\alpha^2(1+r')\beta_3\beta_1(1-\beta_3) + \alpha^2(1+r')(1-k)^2\beta_2(1-\beta_3) + r(1+r'+\beta_1-k)\beta_1\beta_2(1-\beta_3) + r(1+r')(1-k)\beta_1\beta_2\beta_3\right]}{\beta_1\beta_2(1-\beta_3)\left[\beta_3(3-3k-\beta_2) + (1-k)^2(3k-\beta_1)\right]}$$

.....(2.6)

Mode B3 (Fig. 2.3c)

$$U_i = \left(m_y + m_y'\right)\frac{L_x(1-k)}{\beta_1 L_y} + \frac{m_x' L_y}{L_x(1-k)} + \frac{m_x \beta_1 L_y}{L_x (1-k)} + \frac{m_x \beta_2 L_y}{L_x (1-k)}$$

$$+ \frac{m_y' L_x}{\beta_2 L_y} + \frac{m_y L_x(1-\mu)}{\beta_2 L_y} + \frac{m_y \beta_3 L_x}{\beta_2 L_y} + \left(m_x + m_x'\right)\frac{L_y(1-k)}{\beta_3 L_x}\frac{(1-k)}{\beta_2}$$

$$= m_y\left[\frac{\alpha(1-k)(1+r')}{\beta_1} + \frac{\alpha(r'+1-k+\beta_3)}{\beta_2} + \frac{r(r'+\beta_1+\beta_2)}{\alpha(1-k)} + \frac{r(1+r')(1-k)^2}{\alpha\beta_2\beta_3}\right]$$

$$U_e = \frac{w}{3}\beta_1 L_y L_x (1-k) + \frac{w}{2} L_x (1-k) L_y(1-\beta_1-\beta_2) + \frac{w}{3}\beta_2 L_y L_x (1-k)$$

$$+ \frac{w}{2} L_y(1-k)\, L_x(k-\beta_3)\, \frac{(1-k)}{\beta_2} + \frac{w}{3} L_y(1-k)\, \beta_3\, L_x \frac{(1-k)}{\beta_2}$$

$$= \frac{wL_x^2\,(1-k)}{6\alpha\beta_2} \left[(3-\beta_1-\beta_2)\beta_2 + 3(k-\beta_3)(1-k) + 2\beta_3(1-k) \right]$$

From $U_i = U_e$

$$w = \frac{6m_y}{L_x^2} \; \frac{\left[\alpha^2(1+r')\beta_2\beta_3(1-k)^2 + \alpha^2(r'+1-k+\beta_3)\beta_1\beta_3(1-k) + r(r'+\beta_1+\beta_2)\beta_1\beta_2\beta_3 + r(1+r')(1-k)^3\,\beta_1\right]}{\beta_1\,\beta_3\,(1-k)^2\left[(3-\beta_1-\beta_2)\beta_2 + 3(k-\beta_3)(1-k) + 2\beta_3(1-k)\right]}$$

.....(2.7)

Mode B4 (Fig. 2.3d)

$$U_i = \left(m_y + m_y'\right) \frac{L_x(1-k)}{\beta_1\, L_y} \frac{(1-k)}{\beta_2} + \frac{m_x' L_y}{\beta_2 L_x} + \frac{m_x \beta_1 L_y}{\beta_2 L_x} + \frac{m_x L_y(1-k)}{\beta_2 L_x}$$

$$+ \frac{m_y' L_x}{L_y(1-k)} + \frac{m_y \beta_2 L_x}{L_y(1-k)} + \frac{m_y \beta_3 L_x}{L_y(1-k)} + \left(m_x + m_x'\right) \frac{L_y(1-k)}{\beta_3 L_x}$$

$$= m_y \left[\frac{(1+r')\alpha(1-k)^2}{\beta_1\,\beta_2} + \frac{\alpha(r'+\beta_2+\beta_3)}{(1-k)} + \frac{r(r'+1+\beta_1-k)}{\alpha\beta_2} + \frac{r(1-k)(1+r')}{\alpha\beta_3} \right]$$

$$U_e = \frac{w}{3} L_x(1-k)\, \beta_1 L_y \frac{(1-k)}{\beta_2} + \frac{w}{2} L_y\,(k-\beta_1)\, L_x(1-k)\frac{(1-k)}{\beta_2} + \frac{w}{3} \beta_2 L_x L_y(1-k)$$

$$+ \frac{w}{2} L_x(1-\beta_2-\beta_3)\, L_y(1-k) + \frac{w}{3} L_y(1-k)\, \beta_3 L_x$$

$$= \frac{wL_x^2(1-k)}{6\alpha\beta_2} \left[2\beta_1(1-k) + 3(k-\beta_1)(1-k) + \beta_2(3-\beta_2-\beta_3) \right]$$

From $U_i = U_e$,

$$w = \frac{6m_y}{L_x^2} \frac{\left[\alpha^2(1+r')(1-k)^3\beta_3+\alpha^2(r'+\beta_2+\beta_3)\beta_1\beta_2\beta_3+r(r'+1+\beta_1-k)\beta_1\beta_3(1-k) + r(1+r')\beta_1\beta_2(1-k)^2\right]}{\beta_1\beta_3(1-k)^2\left[(3-\beta_2-\beta_3)\beta_2 + 3(k-\beta_1)(1-k) + 2\beta_1(1-k)\right]} \quad \ldots\ldots\ldots (2.8)$$

The special cases where one or more yield lines enter the opening at the corner may be obtained from the above equations.

2.3.3 Opening at a Short Side

The three yield-line patterns considered for a slab with an opening at the centre of a short side are shown in Fig. 2.4. Only two unknown dimensions are required to define the positions of the yield lines fully in each case. Mode C1 will govern if the opening is of small size; modes C2 and C3 will govern for larger size openings. The ultimate load equations derived for these yield-line patterns using the virtual work Eq. (2.1) are as follows:

Mode C1 (Fig. 2.4a)

$$U_i = \frac{m_y L_x}{\beta_1 L_y} + \frac{m'_y L_x(1-k)}{\beta_1 L_y} + \left(m_x + m'_x\right)L_y \frac{2}{L_x} + \left(m_y + m'_y\right)\frac{L_x}{\beta_2 L_y}$$

$$+ \left(m_x + m'_x\right) L_y \frac{2}{L_x}$$

$$= \frac{m_y}{\alpha\beta_1\beta_2}\left[\alpha^2(1+r'-r'k)\beta_2 + 4r\beta_1\beta_2(1+r') + \alpha^2\beta_1(1+r')\right]$$

$$U_e = \frac{w}{3}\beta_1 L_y L_x + \frac{w}{3}\beta_2 L_y L_x + \frac{w}{2} L_x L_y(1-\beta_1-\beta_2) - \frac{w}{2} kL_y \, kL_x \frac{k}{\beta_1}$$

$$= \frac{wL_x^2}{6\alpha\beta_1}\left[\beta_1(3-\beta_1-\beta_2) - 3k^3\right]$$

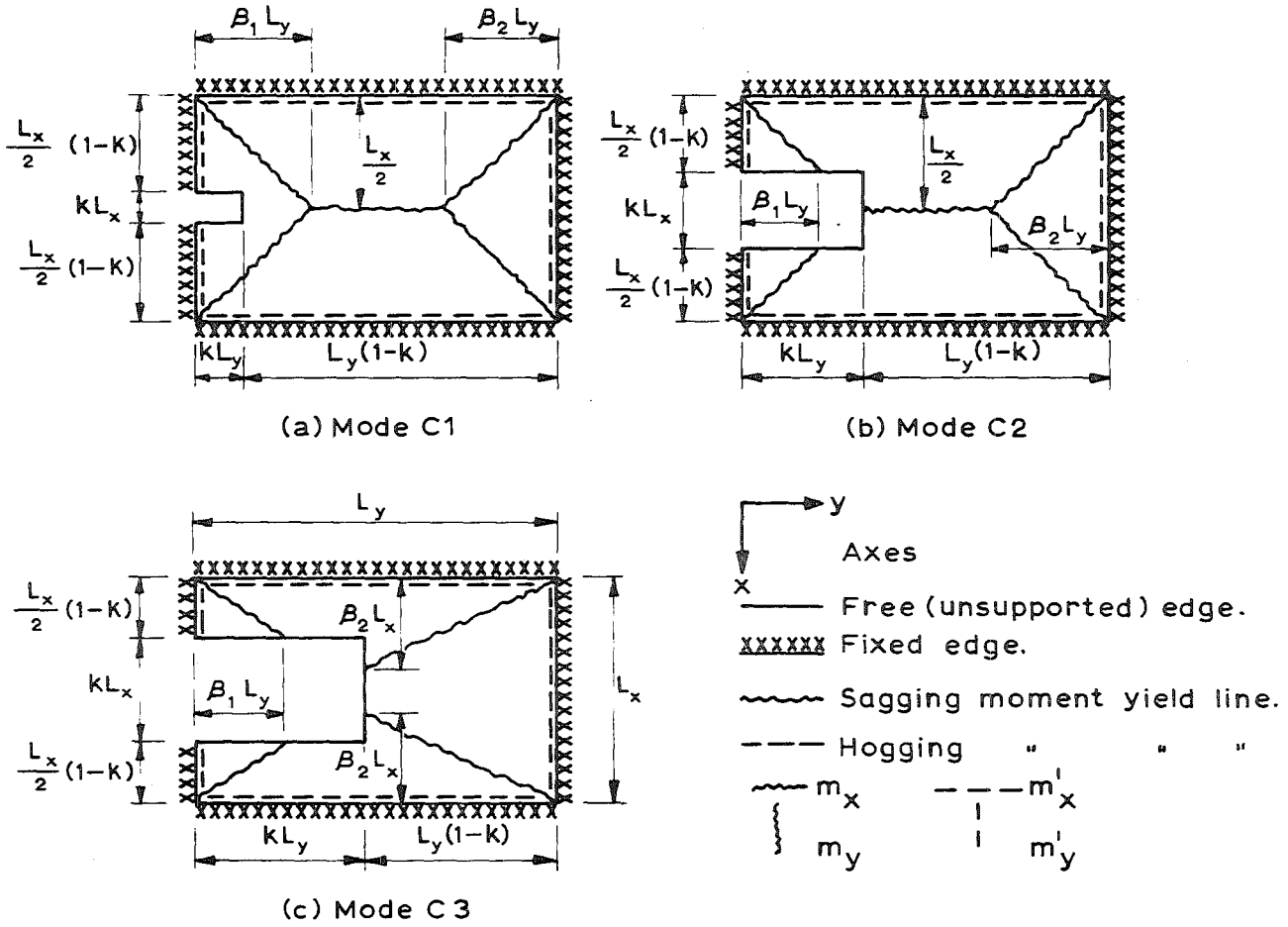

FIG. 2.4 YIELD-LINE PATTERNS FOR OPENING AT A SHORT SIDE

From $U_i = U_e$,

$$w = \frac{6m_y}{L_x^2} \quad \frac{\left[\alpha^2\beta_2\,(1+r'-r'k) + 4r\beta_1\beta_2\,(1+r') + \alpha^2\beta_1\,(1+r')\right]}{\left[\beta_1\,\beta_2\,(3-\beta_1-\beta_2) - 3\beta_2\,k^3\right]} \qquad \text{.....(2.9)}$$

Mode C2 (Fig. 2.4b)

$$U_i = 2\left(m_y + m'_y\right)\frac{L_x}{2}(1-k)\,\frac{(1-k)}{\beta_1 L_y} + 2m_x\,\beta_1\,L_y\,\frac{2}{L_x} + 2m_x\,L_y\,(1-k)\,\frac{2}{L_x}$$

$$+ 2m'_x\,L_y\,\frac{2}{L_x} + \left(m_y + m'_y\right)\frac{L_x}{\beta_2 L_y}$$

$$= m_y\left[\alpha^2(1+r')(1-k)^2\,\beta_2 + 4r\beta_1\beta_2(1+\beta_1+r'-k) + \alpha^2(1+r')\beta_1\right]$$

$$U_e = \frac{w}{3}\,\beta_2\,L_y\,L_x + \frac{w}{2}\,L_x\,L_y\,(1-k-\beta_2) + 2\,\frac{w}{2}\,L_y\,(k-\beta_1)\,\frac{L_x}{2}(1-k)^2$$

$$+ 2\,\frac{w}{3}\,\beta_1\,L_y\,\frac{L_x}{2}(1-k)^2$$

$$= \frac{wL_x^2}{6\alpha}\left[2\beta_2 + 3\,(1-k-\beta_2) + (1-k)^2\,(3k-\beta_1)\right]$$

From $U_i = U_e$

$$w = \frac{6m_y}{L_x^2} \quad \frac{\left[\alpha^2(1+r')(1-k)^2\beta_2 + 4r\beta_1\beta_2(1+\beta_1+r'-k) + \alpha^2(1+r')\beta_1\right]}{\beta_1\,\beta_2\left[3(1-k) + (1-k)^2\,(3k-\beta_1) - \beta_2\right]}$$

..... (2.10)

Mode C3 (Fig. 2.4c)

$$U_i = \left(m_y + m'_y\right)\frac{L_x\,(1-k)}{\beta_1\,L_y}\,\frac{(1-k)}{2\beta_2} + 2\left[\frac{m_x\,\beta_1\,L_y}{\beta_2\,L_x} + \frac{m_x\,L_y(1-k)}{\beta_2\,L_x} + \frac{m'_x\,L_y}{\beta_2\,L_x}\right]$$

$$+ \frac{2m_y \beta_2 L_x}{L_y (1-k)} + \frac{m'_y L_x}{L_y (1-k)}$$

$$= m_y \left[\frac{\alpha(1+r')(1-k)^2}{2\beta_1 \beta_2} + \frac{2r\,(1+\beta_1-k+r')}{\alpha\beta_2} + \frac{\alpha(2\beta_2 + r')}{(1-k)} \right]$$

$$U_e = 2 \frac{w}{3} \beta_1 L_y \frac{L_x(1-k)}{2} \frac{(1-k)}{2\beta_2} + 2 \frac{w}{2} \frac{L_x(1-k)}{2} L_y(k-\beta_1) \frac{(1-k)}{2\beta_2}$$

$$+ 2 \frac{w}{3} \beta_2 L_x L_y (1-k) + \frac{w}{2} L_x (1-2\beta_2) L_y (1-k)$$

$$= \frac{wL_x^2 (1-k)}{12\alpha\beta_2} \left[(1-k)(3k-\beta_1) + 2\beta_2 (3-2\beta_2) \right]$$

From $U_i = U_e$,

$$w = \frac{6m_y}{L_x^2} \frac{\left[\alpha^2(1+r')(1-k)^3 + 4r(1+\beta_1-k+r')\beta_1(1-k) + 2\alpha^2(2\beta_2+r')\beta_1\beta_2\right]}{\beta_1 (1-k)^2 \left[(1-k)(3k-\beta_1) + 2\beta_2 (3-2\beta_2)\right]}$$

.....(2.11)

2.3.4 Opening at a Long Side

The three yield-line patterns considered for a slab with an opening at the centre of a long side are shown in Fig. 2.5. Only two unknown dimensions are required to define the positions of the yield lines fully in each case. The ultimate load equations derived for these yield-line patterns using the virtual work Eq. (2.1) are as follows:

Mode D1 (Fig. 2.5a)

$$U_i = \left(m_y + m'_y\right) \frac{L_x}{\beta_1 L_y} + \frac{m_x L_y}{\beta_2 L_x} + \frac{m'_x L_y (1-k)}{\beta_2 L_x} + \left(m_y + m'_y\right) \frac{L_x}{\beta_1 L_y}$$

$$+ \left(m_x + m'_x\right) \frac{L_y}{L_x (1-\beta_2)}$$

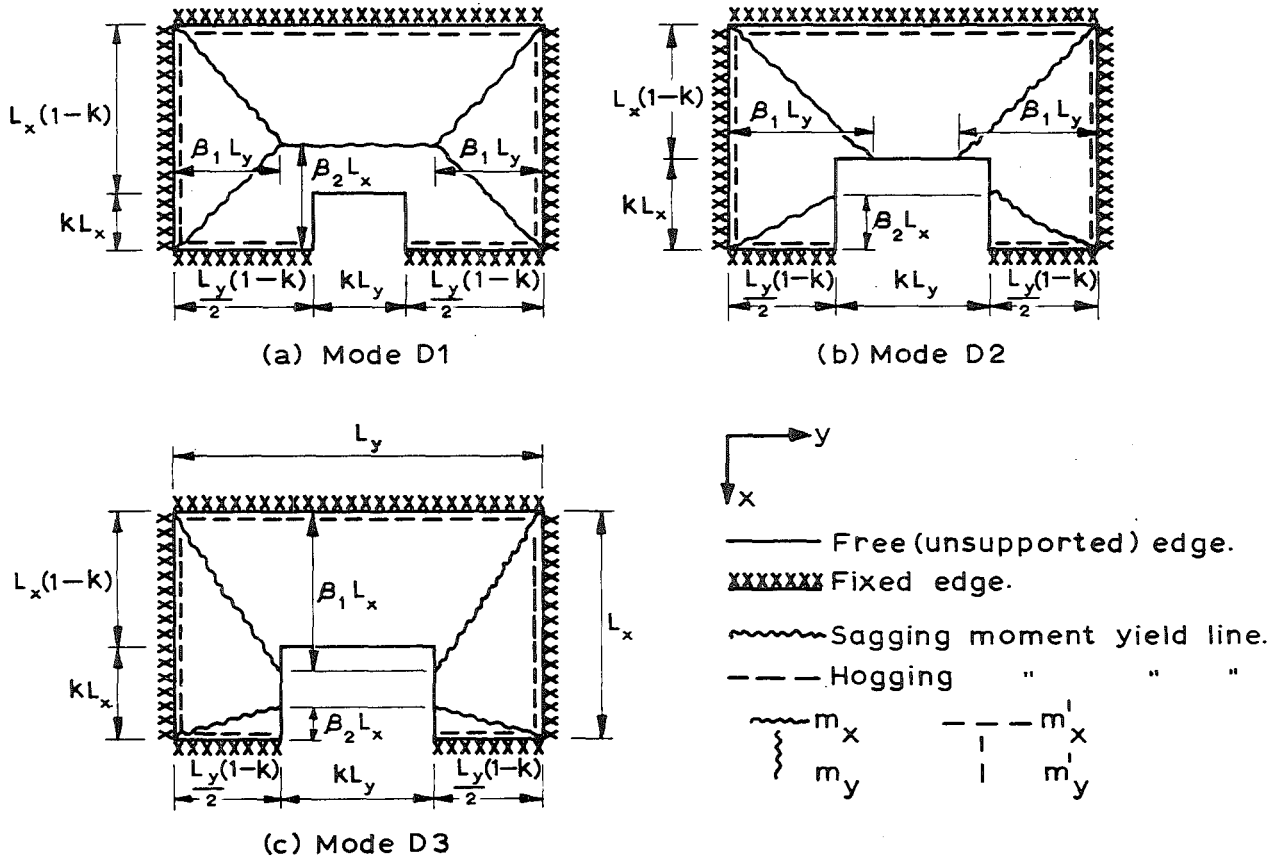

FIG. 2.5 YIELD-LINE PATTERNS FOR OPENING AT A LONG SIDE

$$= m_y \left[\frac{2\alpha(1+r')}{\beta_1} + \frac{r(r'-r'k+1)}{\alpha\beta_2} + \frac{r(1+r')}{\alpha(1-\beta_2)} \right]$$

$$U_e = 2\frac{w}{3}\beta_1 L_y L_x + \frac{w}{2} L_y (1-2\beta_1) L_x - \frac{w}{2} kL_x kL_y \frac{k}{\beta_2}$$

$$= \frac{wL_x^2}{6\alpha\beta_2}\left[(3-2\beta_1)\beta_2 - 3k^3\right]$$

From $U_i = U_e$,

$$w = \frac{6m_y}{L_x^2} \frac{\left[2\alpha^2(1+r')\beta_2(1-\beta_2) + r(r'-r'k+1)\beta_1(1-\beta_2) + r(1+r')\beta_1\beta_2\right]}{\beta_1(1-\beta_2)\left[(3-2\beta_1)\beta_2 - 3k^3\right]}$$

..... (2.12)

Mode D2 (Fig. 2.5b)

$$U_i = 2\left(m_x + m_x'\right)\frac{L_y(1-k)}{2\beta_2 L_x}\frac{(1-k)}{2\beta_1} + 2\left[\frac{m_y \beta_2 L_x}{\beta_1 L_y} + \frac{m_y L_x(1-k)}{\beta_1 L_y} + \frac{m_y' L_x}{\beta_1 L_y}\right]$$

$$+ \frac{2m_x \beta_1 L_y}{L_x(1-k)} + \frac{m_x' L_y}{L_x(1-k)}$$

$$= m_y\left[\frac{r(1+r')(1-k)^2}{2\beta_1\beta_2\alpha} + \frac{2\alpha(1+\beta_2+r'-k)}{\beta_1} + \frac{r(2\beta_1+r')}{\alpha(1-k)}\right]$$

$$U_e = \left[2\frac{w}{3}\frac{L_y}{2}(1-k)\beta_2 L_x + 2\frac{w}{2}L_x(k-\beta_2)\frac{L_y}{2}(1-k)\right]\frac{(1-k)}{2\beta_1}$$

$$+ 2\frac{w}{3}\beta_1 L_y L_x(1-k) + \frac{w}{2}L_y(1-2\beta_1)L_x(1-k)$$

$$= \frac{wL_x^2(1-k)}{12\alpha\beta_1}\left[(1-k)(3k-\beta_2) + 2\beta_1(3-2\beta_1)\right]$$

From $U_i = U_e$,

$$w = \frac{6m_y}{L_x^2} \frac{\left[r(1+r')(1-k)^3 + 4\alpha^2(1+\beta_2+r'-k)\beta_2(1-k) + 2r(2\beta_1+r')\beta_1\beta_2\right]}{\beta_2(1-k)^2\left[(1-k)(3k-\beta_2) + 2\beta_1(3-2\beta_1)\right]}$$

.....(2.13)

Mode D3 (Fig. 2.5c)

$$U_i = 2\left(m_x + m'_x\right)\frac{L_y}{2}(1-k)\frac{1}{\beta_2 L_x} + 2\left[\frac{m_y\beta_2 L_x}{L_y(1-k)} + \frac{m_y\beta_1 L_x}{L_y(1-k)} + \frac{m'_y L_x}{L_y(1-k)}\right]$$

$$+ \frac{m'_x L_y}{\beta_1 L_x} + \frac{m_x L_y (1-k)}{\beta_1 L_x}$$

$$= m_y\left[\frac{r(1+r')(1-k)}{\alpha\beta_2} + \frac{4\alpha(\beta_2+\beta_1+r')}{(1-k)} + \frac{r(r'+1-k)}{\alpha\beta_1}\right]$$

$$U_e = 2\frac{w}{3}\beta_2 L_x\frac{L_y}{2}(1-k) + 2\frac{w}{2}\frac{L_y}{2}(1-k)L_x(1-\beta_1-\beta_2)$$

$$+ 2\frac{w}{3}\beta_1 L_x\frac{L_y}{2}(1-k) + \frac{w}{2}L_x(1-k)kL_y\frac{(1-k)}{\beta_1}$$

$$= \frac{wL_x^2(1-k)}{6\alpha\beta_1}\left[(3-\beta_1-\beta_2)\beta_1 + 3k(1-k)\right]$$

From $U_i = U_e$,

$$w = \frac{6m_y}{L_x^2} \frac{\left[r(1+r')\beta_1(1-k)^2 + 4\beta_1\alpha^2(\beta_1+\beta_2+r')\beta_2 + r(r'+1-k)\beta_2(1-k)\right]}{\beta_2(1-k)^2\left[(3-\beta_1-\beta_2)\beta_1 + 3k(1-k)\right]}$$

.....(2.14)

2.4 MINIMIZATION OF ULTIMATE LOAD

The ultimate load equations (2.2) to (2.14) contain the unknown terms β_1 , β_2 and β_3 which define the positions of the yield lines. The values of β_1 , β_2 and β_3 which make the ultimate load in each case a minimum are sought. The required values of these unknown terms may be found by solving simultaneously the equations $\frac{\partial w}{\partial \beta_1} = 0$, $\frac{\partial w}{\partial \beta_2} = 0$ and $\frac{\partial w}{\partial \beta_3} = 0$ for each expression for w , but the resulting simultaneous equations are non-linear and the algebraic work involved is lengthy. Also, for some yield-line patterns, for example modes A2 and C2, the minimum ultimate load given by the equations may not occur when the magnitude of the unknown dimension lies within the allowable range of variation. Because of these difficulties a numerical procedure has been adopted. Computer programmes were written to calculate the values of $\frac{wL_x^2}{12m_y}$ from Equs. (2.2) to (2.14) for various values of the dimensions β_1 , β_2 and β_3 within their allowable ranges thus allowing the minimum value of $\frac{wL_x^2}{12m_y}$ for the yield-line patterns considered to be determined. In this analysis the values of β_1 , β_2 and β_3 were varied at increments of either 0.01 or 0.02.

2.4 DESIGN CHARTS

Using the above method for determining the ultimate load, design charts have been prepared for slabs for each of the four types of opening considered. The charts are shown in Figs. 2.6 to 2.17 and plot $\frac{wL_x^2}{12m_y}$ versus k , the ratio of opening size to slab span for various ratios of $\alpha = \frac{L_x}{L_y}$, $r = \frac{m_x}{m_y}$ and $r' = \frac{m'_x}{m_x} = \frac{m'_y}{m_y}$. The range of α values plotted varies between 1 and $\frac{1}{3}$. The r values plotted vary between 1 and 5 thus ensuring that the greater yield

moment is in the direction of the short span. This is in accordance with the elastic theory distribution of bending moments. The values of r' plotted are 0 (applying to the case of simply supported edges) and 1 and 2 (applying to the case of fixed edges). In order to ensure that the crack widths and deflections of the slab at working load are not excessive it is important that the ratios of the resisting moments at the various sections do not show large differences from the elastic theory distribution of moments.

In the preparation of the design charts only the minimum values of $\frac{wL_x^2}{12m_y}$ from all the possible yield-line patterns have been plotted. For example, in the case of a slab with the opening at a short side (Fig. 2.4), for particular values of $r = 2.0$, $r' = 1.0$, $\alpha = \frac{2}{3}$ and $k = 0.3$, the minimum value of $\frac{wL_x^2}{12m_y}$ given by Mode C1 (Eq.2.9) is 4.977 ($\beta_1 = 0.43$, $\beta_2 = 0.30$), by Mode C2 (Eq. 2.10) is 4.743 ($\beta_1 = 0.18$, $\beta_2 = 0.30$), and by Mode C3 (Eq. 2.11) is 5.376 ($\beta_1 = 0.18$, $\beta_2 = 0.50$). Hence Mode C2 is the governing yield-line pattern and the value of $\frac{wL_x^2}{12m_y} = 4.743$ has been plotted in the design chart shown in Fig. 2.13. Thus the design charts can be used directly without knowing the governing modes. The discontinuities in the slope which occur at various points in the curves of the charts arise when the governing yield-line pattern changes from one mode to another. Some of the curves show a distinct cusp where the governing pattern changes.

2.6 ACCURACY OF DERIVED CHARTS

The magnitude of the ultimate load calculated by the virtual work method is relatively insensitive to small changes of the yield line positions from the correct yield-line pattern. The equations derived for slabs with a central opening contain one unknown dimension which

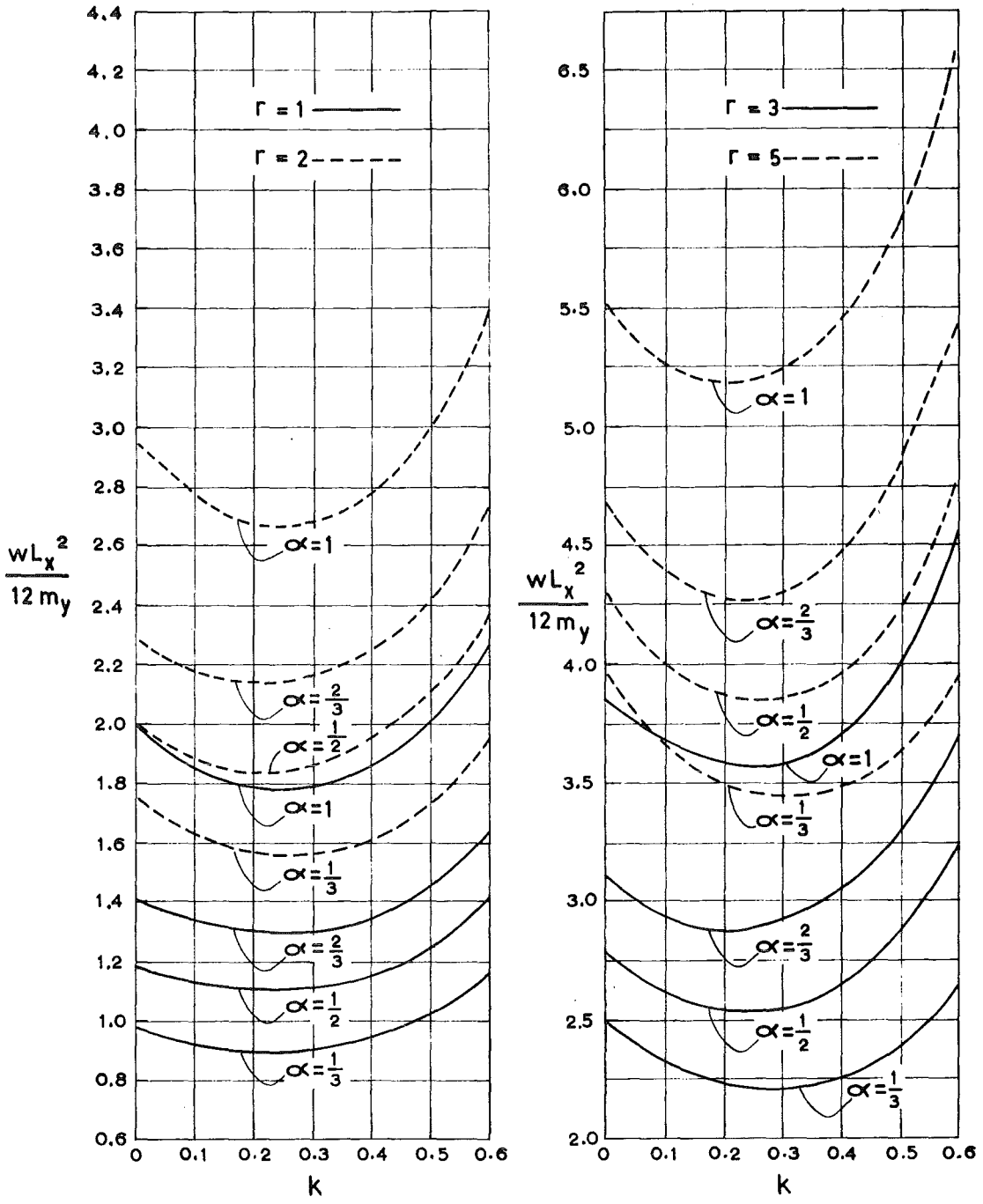

FIG. 2.6 CENTRAL OPENING r' = 0

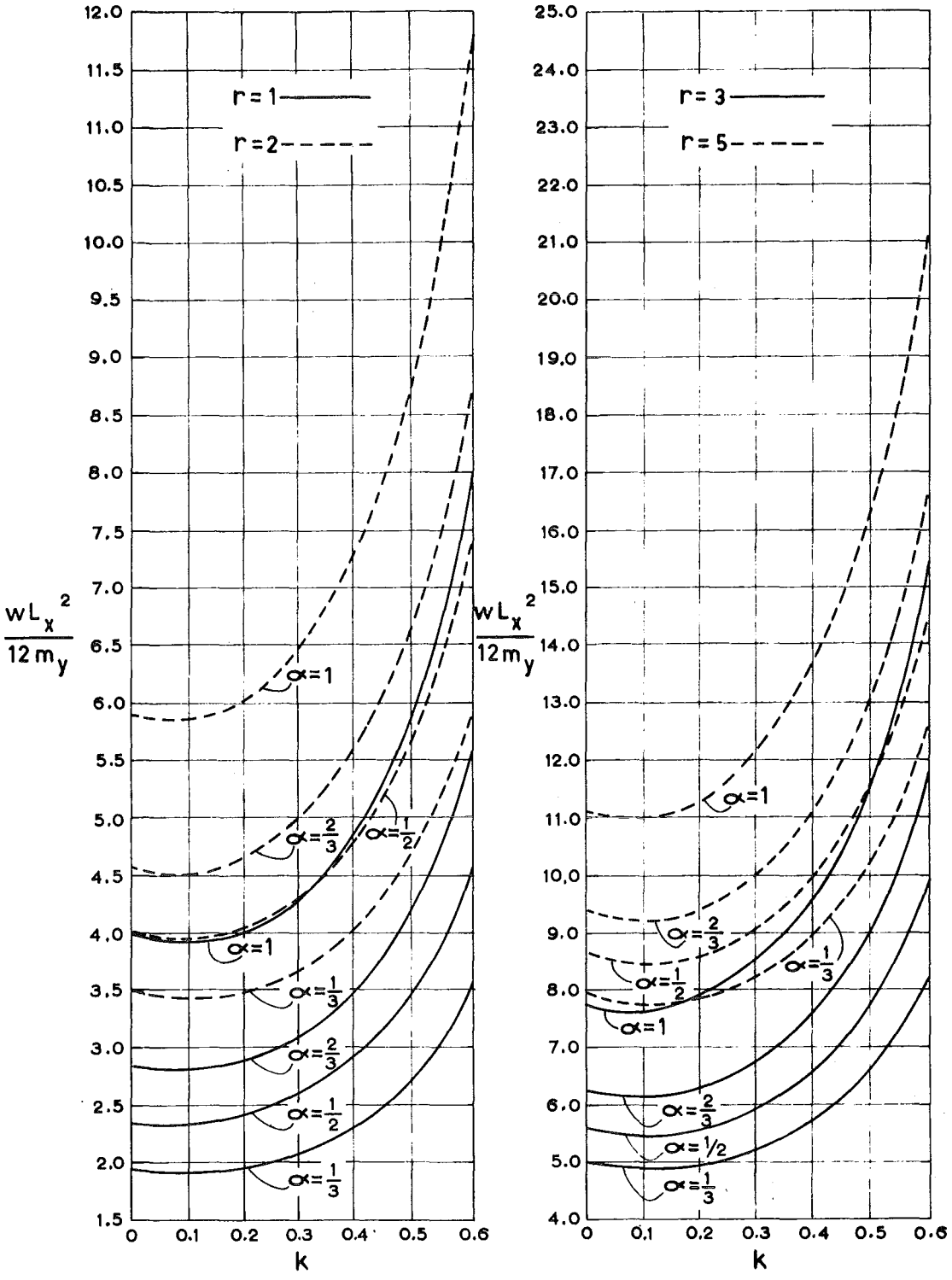

FIG. 2.7 CENTRAL OPENING r' = 1

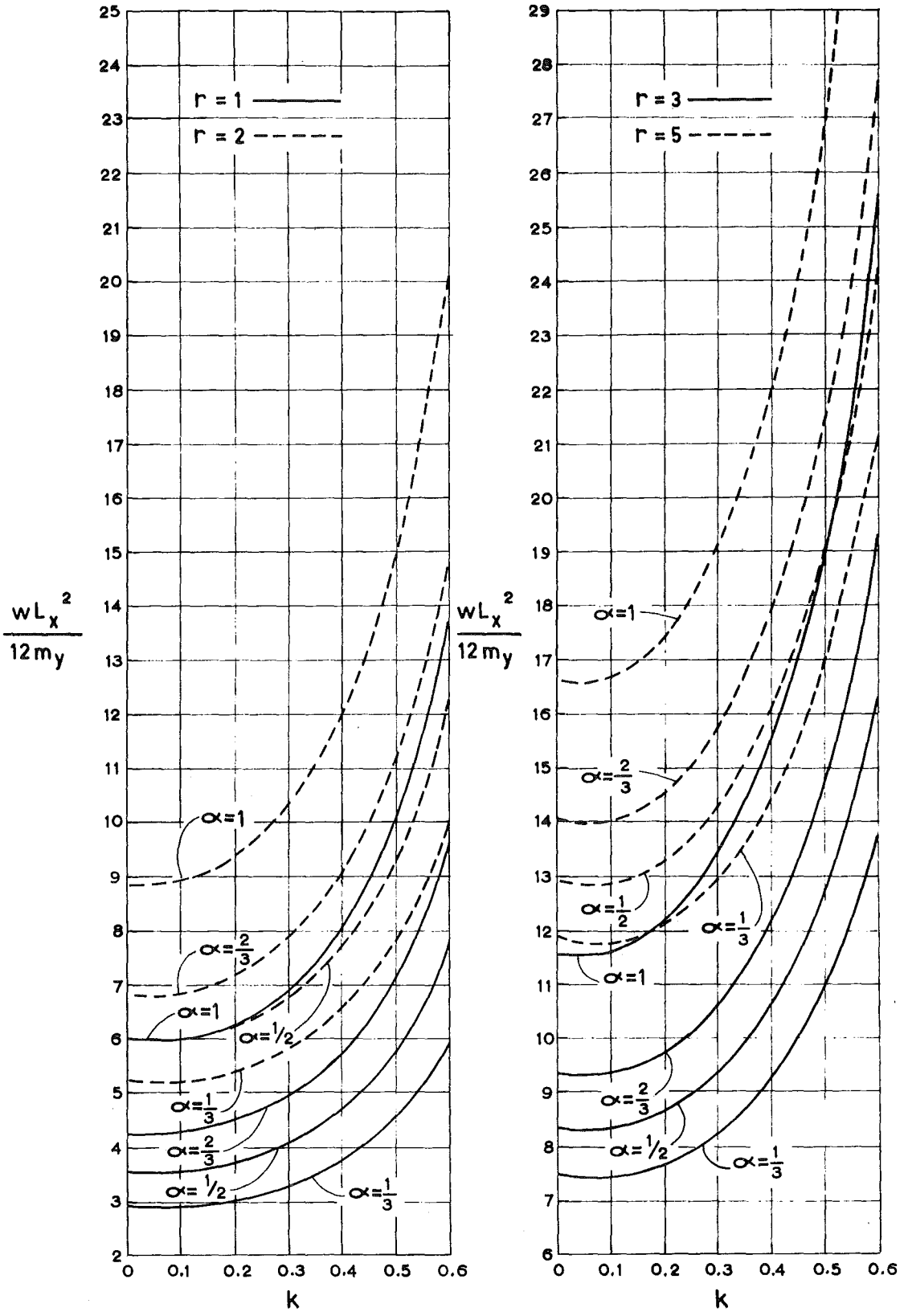

FIG. 2.8 CENTRAL OPENING r'=2

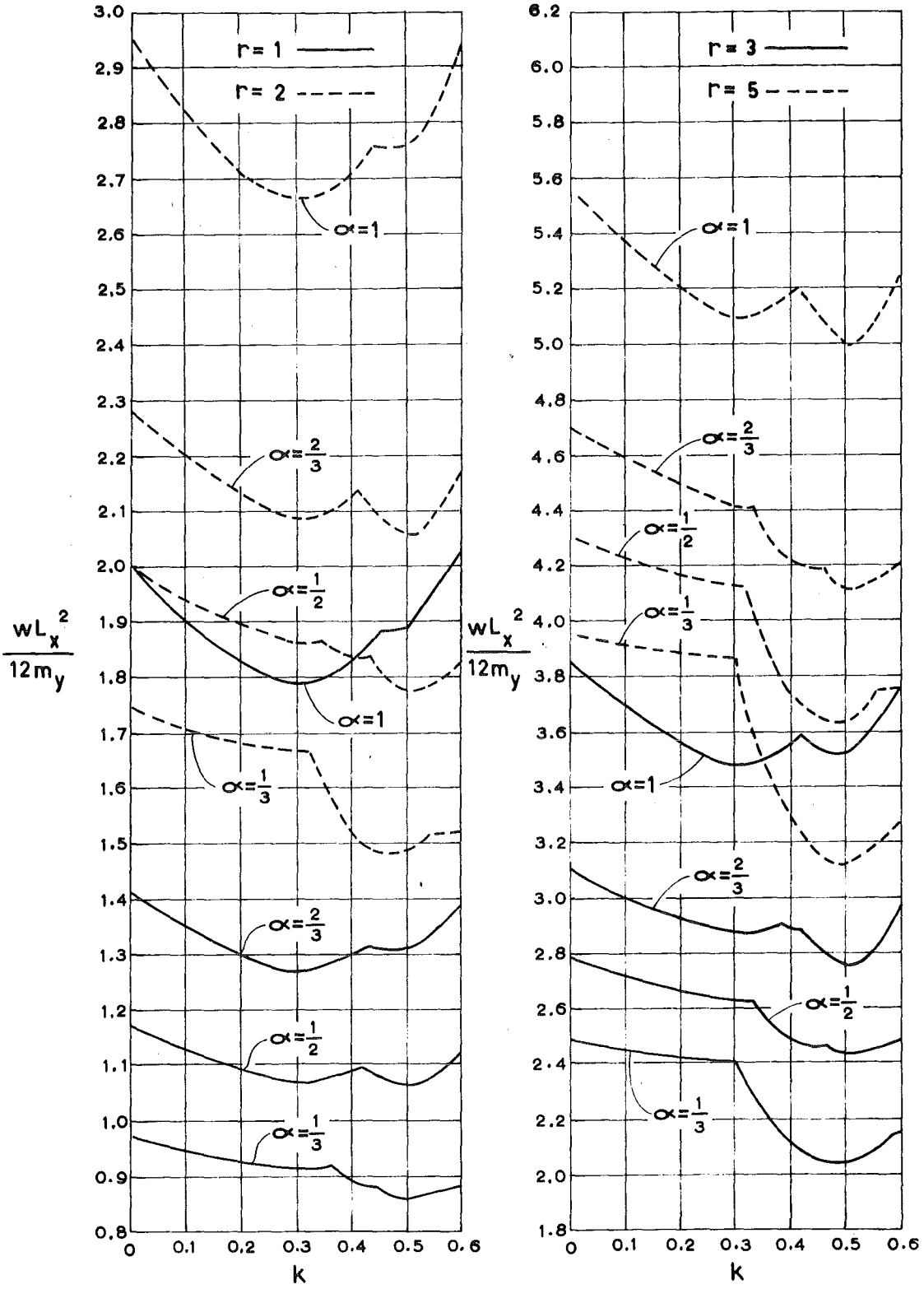

FIG. 2.9 CORNER OPENING r' = 0

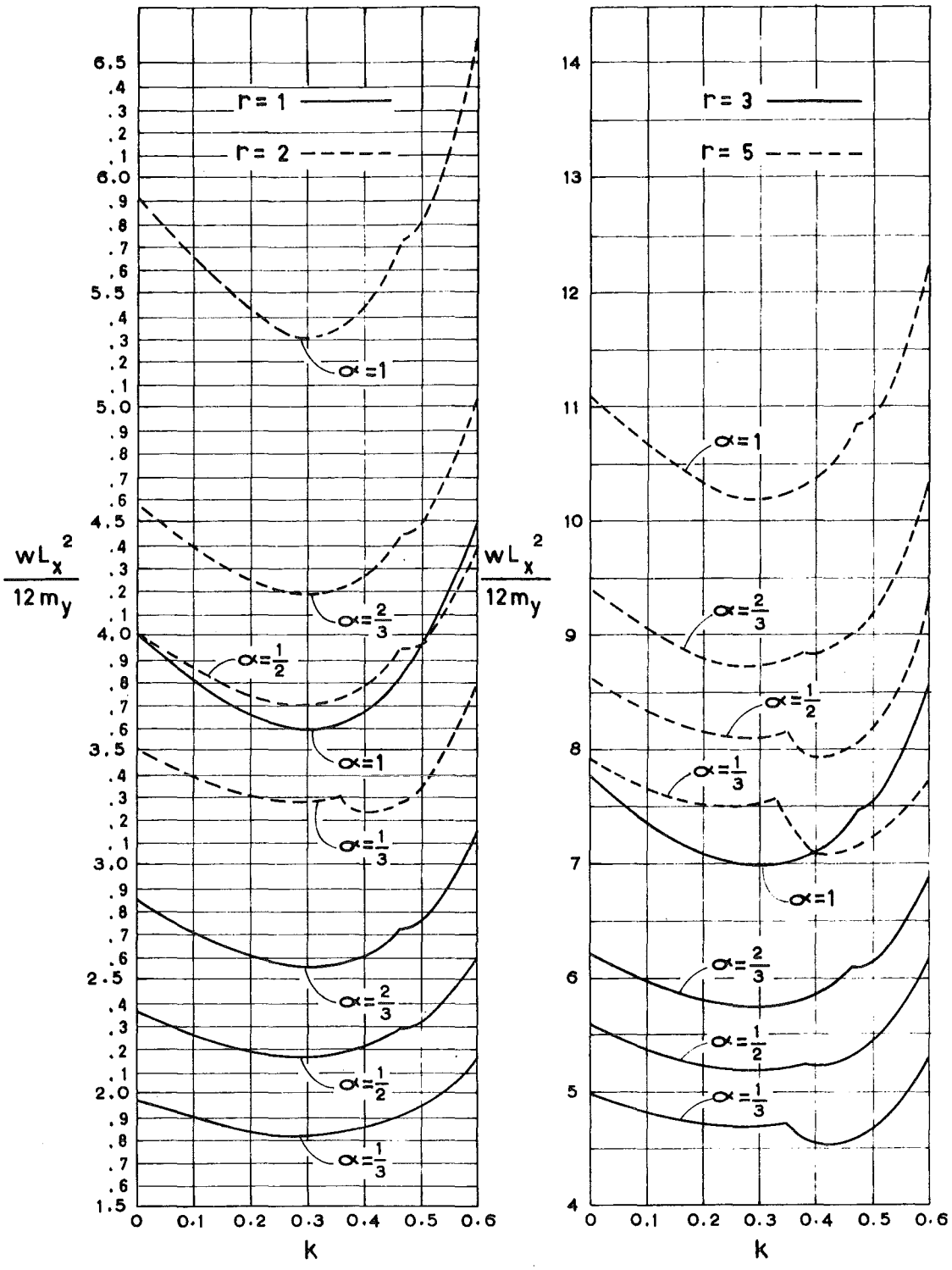

FIG. 2.10 CORNER OPENING r'=1

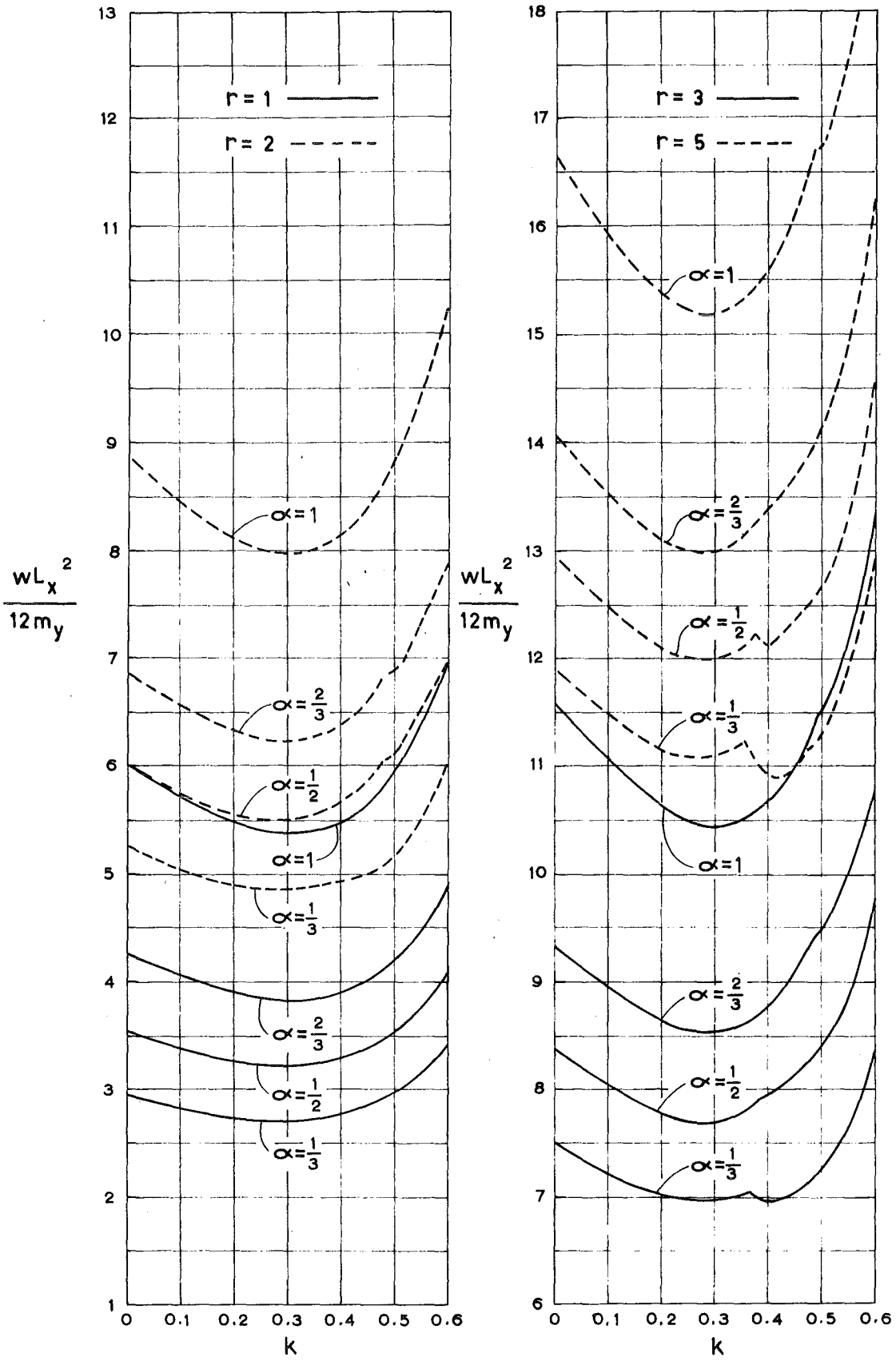

FIG. 2.11 CORNER OPENING r' = 2

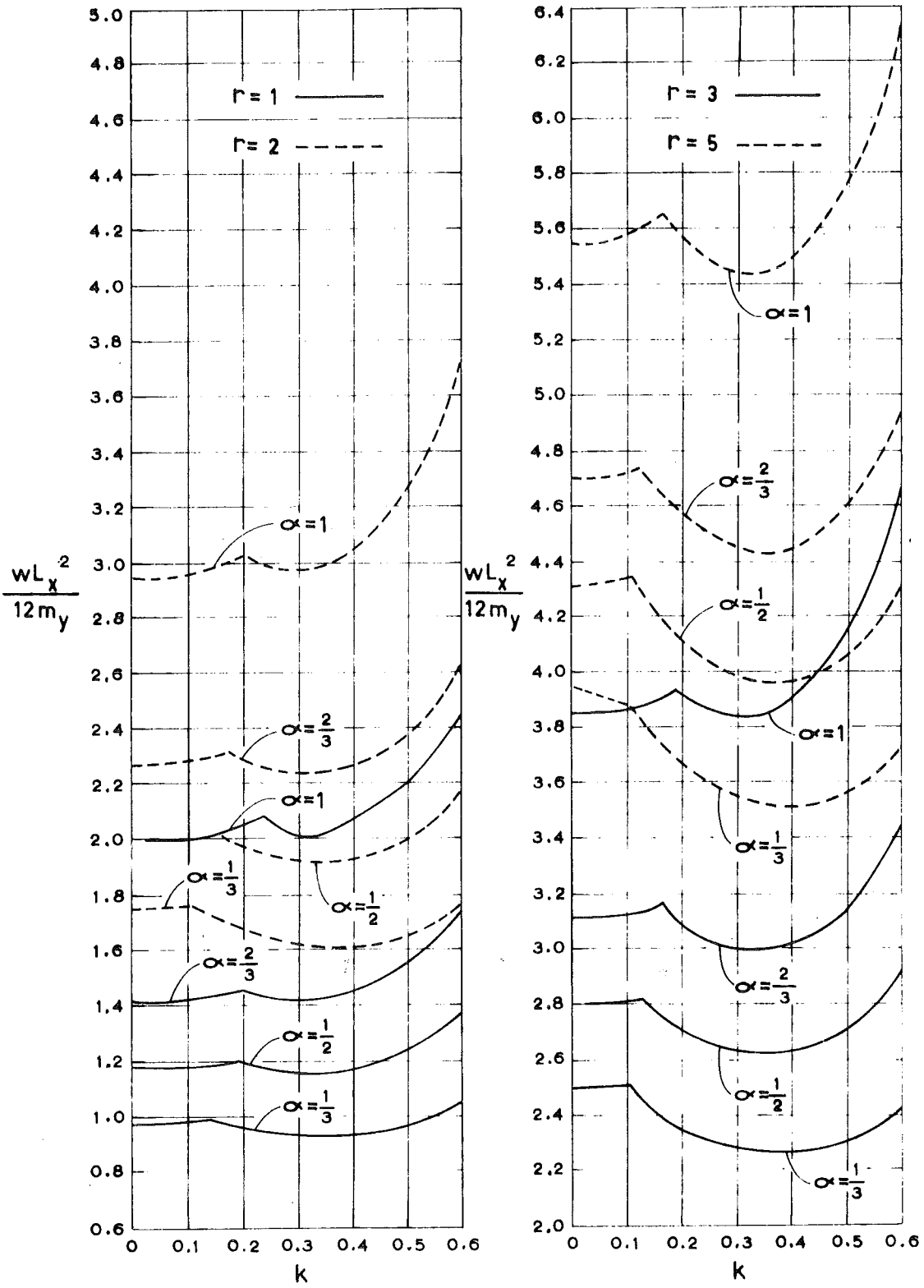

FIG. 2.12 OPENING AT CENTRE OF SHORT EDGE r' = 0

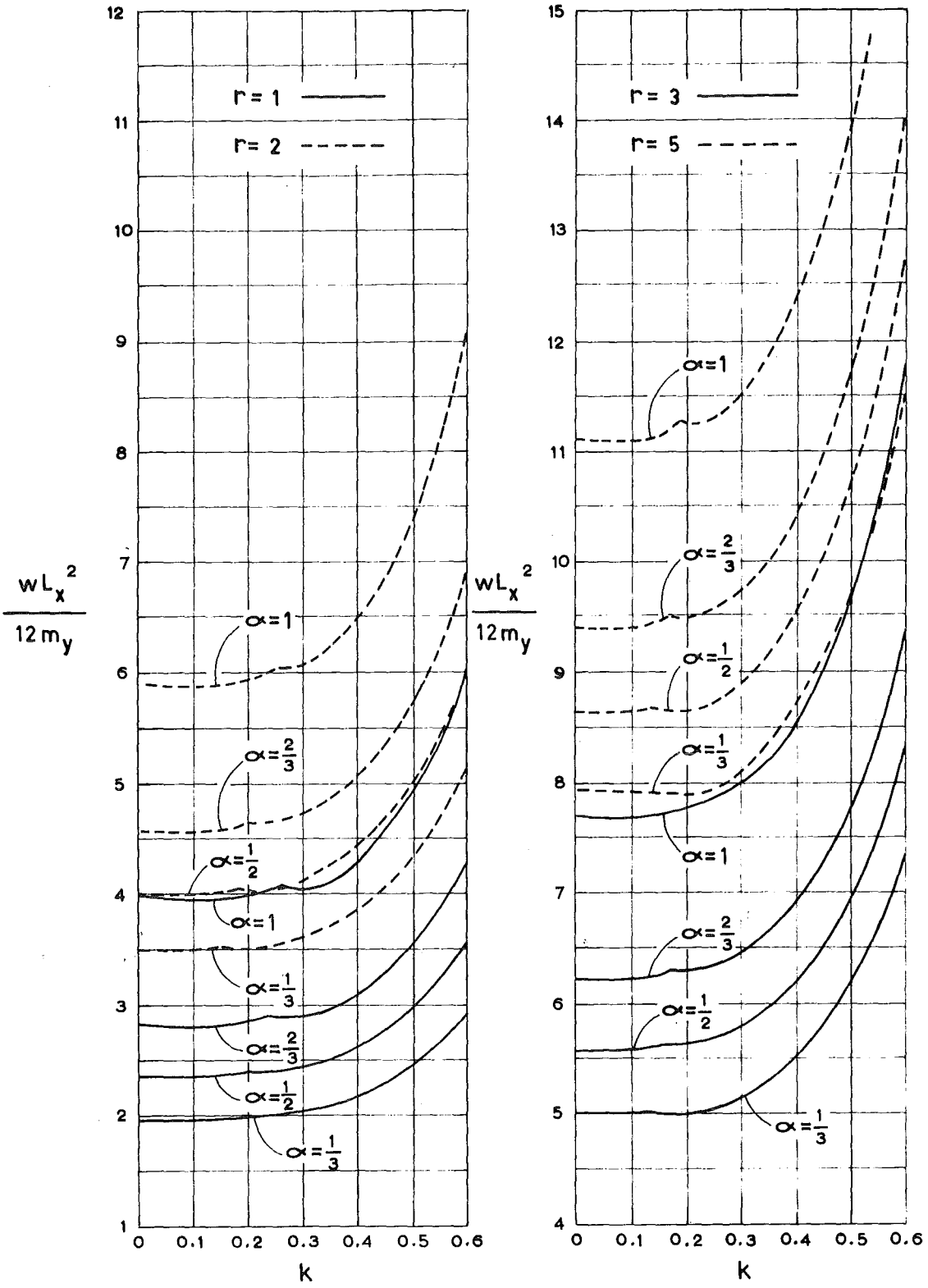

FIG. 2.13 OPENING AT CENTRE OF SHORT EDGE r'=1

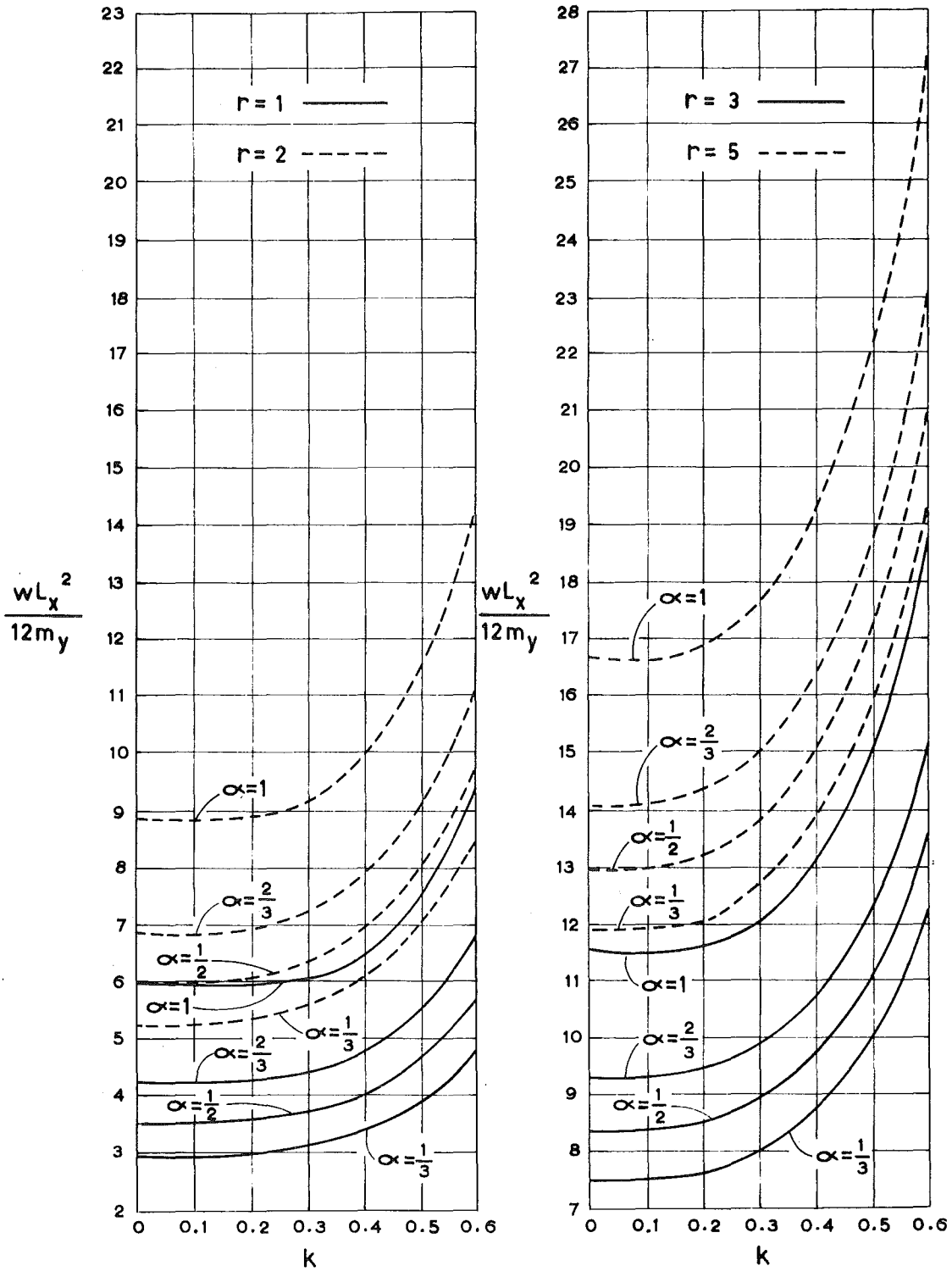

FIG. 2.14 OPENING AT CENTRE OF SHORT EDGE r'=2

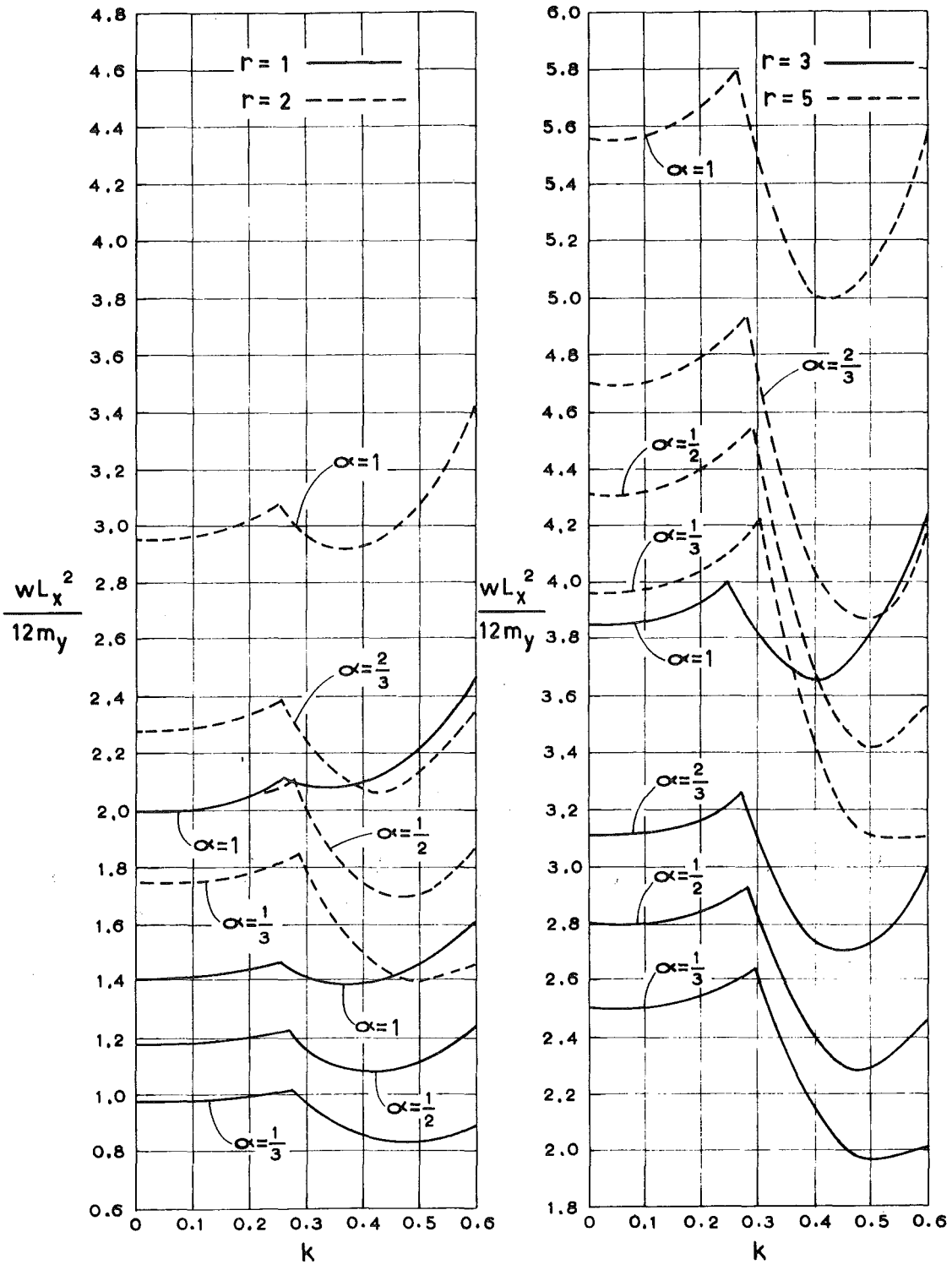

FIG. 2.15 OPENING AT CENTRE OF LONG EDGE r'=0

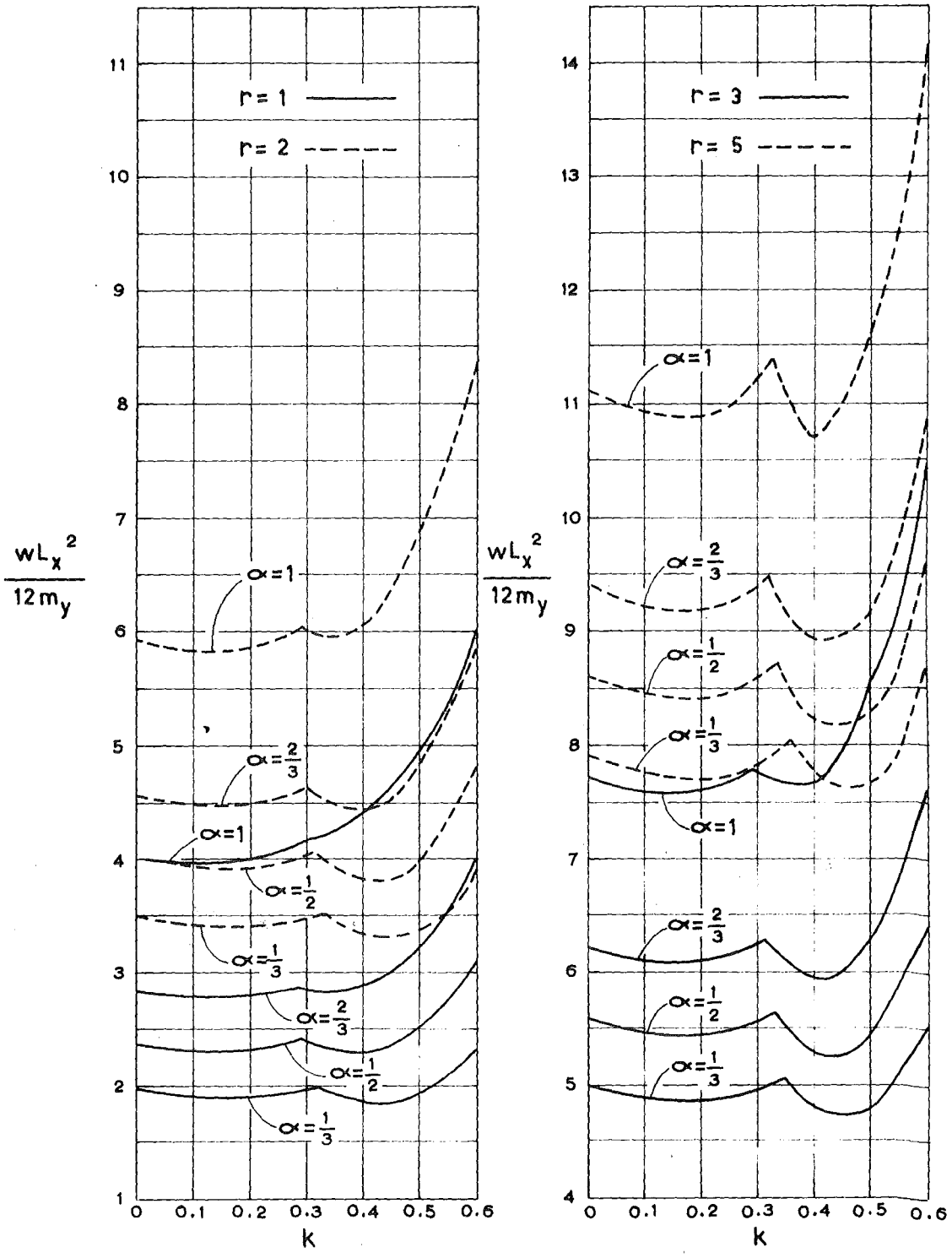

FIG. 2.16 OPENING AT CENTRE OF LONG EDGE r'=1

defines the pattern fully. Those for slabs with an opening at the short or long side contain two unknown dimensions and those for slabs with a corner opening contain three unknown dimensions. When determining the ultimate loads the unknown β values were varied at increments of 0.01 for patterns with a single unknown and at 0.02 for patterns with two or more unknowns. To illustrate the magnitude of error involved in determining the minimum ultimate load from these increments, the effect of small variations in the unknown dimensions on the minimum ultimate load is shown for two cases in Tables 2.1 and 2.2. The variations in the ultimate load in the tables near the minimum ultimate load are small and it is evident that the chosen increments result in negligible error. For example, in Table 2.2 the minimum ultimate load calculated using an increment of 0.02 is only approximately 0.2 percent different from the minimum using an increment of 0.01.

2.7 EFFECT OF OPENINGS ON ULTIMATE LOAD

Openings in two-way slabs tend to attract the yield lines to them since they represent regions of zero flexural strength in the slab. On the other hand the slab is not required to carry load over the area of the opening and hence the total load to be carried is smaller than for a slab without openings. Hence the ultimate load per unit area of a slab with an opening may be either smaller or greater than that of a slab without an opening. The effect of opening size on the ultimate load per unit area is illustrated in Figs. 2.6 to 2.17. The reduction in load carrying capacity per unit area is greatest for slabs with simply supported edges because for this case openings cause a greater reduction in the total lengths of yield lines than in fixed-edge slabs.

For slabs with central openings the largest reduction in the ultimate load per unit area is about 13 percent occurring when

TABLE 2.1

$wL_x^2/12m_y$ from Equation (2.13) when r = 1.0 , r' = 1.0 , α = 0.5 and k = 0.5 .

β_1	β_2	$wL_x^2/12m_y$
0.30	0.45	2.5349
0.30	0.46	2.5342
0.30	0.47	2.5339
0.31	0.45	2.5342
0.31	0.46	2.5334*
0.31	0.47	2.5332**
0.32	0.45	2.5353
0.32	0.46	2.5345
0.32	0.47	2.5343

* Result plotted

** Minimum for 0.01 increment

TABLE 2.2

$wL_x^2/12m_y$ from Equation (2.5) when r = 5.0 , r' = 1.0 , $\alpha = \frac{1}{3}$ and k = 0.3 .

β_1	β_2	β_3	$wL_x^2/12m_y$
0.19	0.11	0.53	7.6279
0.19	0.11	0.54	7.6197
0.19	0.11	0.55	7.6178
0.19	0.12	0.53	7.6247
0.19	0.12	0.54	7.6165
0.19	0.12	0.55	7.6145**
0.19	0.13	0.53	7.6268
0.19	0.13	0.54	7.6185
0.19	0.13	0.55	7.6165
0.20	0.11	0.53	7.6437
0.20	0.11	0.54	7.6337
0.20	0.11	0.55	7.6299
0.20	0.12	0.53	7.6406
0.20	0.12	0.54	7.6305*
0.20	0.12	0.55	7.6267
0.20	0.13	0.53	7.6427
0.20	0.13	0.54	7.6326
0.20	0.13	0.55	7.6288
0.21	0.11	0.53	7.6603
0.21	0.11	0.54	7.6484
0.21	0.11	0.55	7.6428
0.21	0.12	0.53	7.6571
0.21	0.12	0.54	7.6452
0.21	0.12	0.55	7.6396
0.21	0.13	0.53	7.6594
0.21	0.13	0.54	7.6474
0.21	0.13	0.55	7.6417

* Result plotted

** Minimum for 0.01 increment

$k = 0.2$ to 0.3 for simply supported edges; when $k > 0.4$ to 0.6 the ultimate load per unit area becomes greater than that for the case without an opening. For fixed-edge slabs with a central opening when $r' = 1$ or 2, the reduction in ultimate load is much smaller. At large k values the ultimate load of the slab increases very significantly.

Corner openings in simply supported slabs cause a reduction in the ultimate load per unit area of up to 21 percent when $k = 0.3$ to 0.5. A reduction in the ultimate load of up to 10 percent occurs even when $r' = 2$. Slabs with corner openings do not show such a significant increase in load carrying capacity as the opening size increases.

Openings placed at the short side of a simply supported slab cause a maximum reduction in the ultimate load per unit area of about 11 percent when $k = 0.3$ to 0.4. Fixed-edge slabs do not show any reduction in strength and the ultimate load increases significantly with large k values.

When the opening is at the long side of a simply supported slab the maximum reduction in ultimate load per unit area is about 22 percent when $k = 0.5$. The reduction in strength becomes less significant when the edges of the slab are fixed.

Fig. 2.18 shows the effect of opening size on the ultimate load of a slab for each of the four types of openings for particular values of $r = 2$, $r' = 1$ and $\alpha = 0.5$. In this case the only significant reduction in ultimate load occurs in the case of a corner opening.

Although only rectangular openings have been considered here it is evident that the design charts will also give a very good indication of the effect of openings of other shapes.

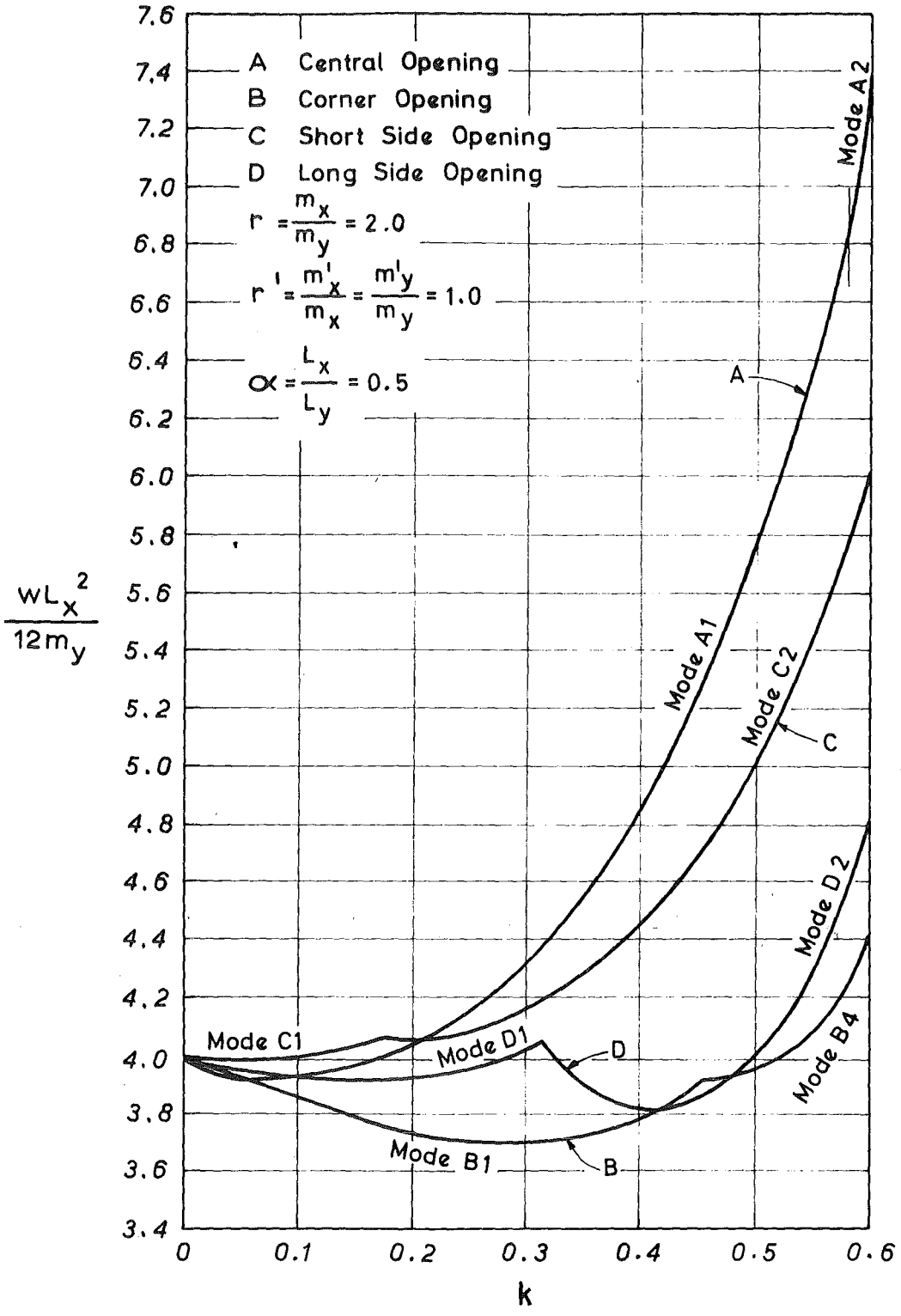

FIG. 2.18 EFFECT OF OPENING SIZE AND POSITION ON ULTIMATE LOAD OF A SLAB

2.8 CONCLUSIONS

Design charts may be drawn up for uniformly loaded two-way slabs with openings in various positions. A reduction in the ultimate load per unit area of up to 22 percent can occur in the case of slabs with an opening either at a corner or at the centre of a long side. The reduction in ultimate load is greater for simply supported slabs than for fixed-edge slabs.

The openings tend to attract yield lines to them since they represent regions of zero strength in the slab. To improve the serviceability of the slab the total amount of reinforcement may be distributed more densely near the opening than near the supports.

3. PART II: TRANSFER OF UNBALANCED MOMENT AND SHEAR FROM REINFORCED CONCRETE FLAT PLATES TO COLUMNS

SUMMARY

A review of previous work on the transfer of unbalanced moment and shear from reinforced concrete flat plates to columns indicates the need for more test results and improved theory for designing slab-column connections which transfer moment. Tests on half scale reinforced concrete models simulating interior slab-column connections under monotonic and cyclic loadings are described. The tests studied the effectiveness of various shear reinforcement arrangements and their performance under seismic conditions. Ultimate strength procedures are developed to determine the shear and moment capacity of such connections with and without shear reinforcement. Predicted strengths are shown to compare favourably with test results and the use of closed stirrups proved to be most effective in increasing the ductility of the connection.

3.1 INTRODUCTION

The slab-column connection is a critical part of a reinforced concrete flat plate structure because the design is often governed by the shear strength of the slab around the column. In many cases column capitals and drop panels are necessary to increase the strength of the connections. The critical nature of the shear in the slab around the column is further aggravated when lateral forces due to wind or earthquake loadings cause substantial unbalanced moments to be transferred between the slab and the column. In order to examine the manner by which this transfer of moment can take place a portion of the slab surrounding an interior column as shown in Fig. 3.1 may be considered. The forces and moments acting on some critical section ABCD within the slab and contributing to the transfer of the applied shear V and moment M between the slab and the

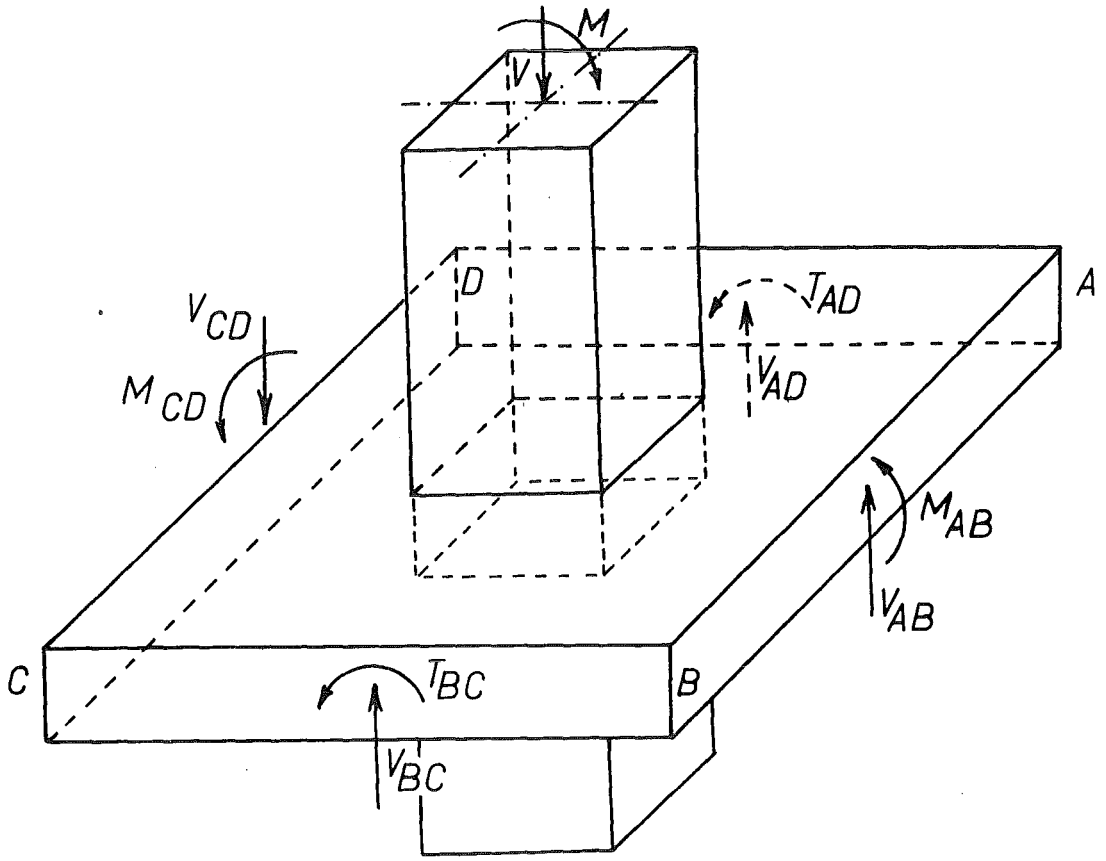

FIG. 3.1 - INTERIOR SLAB-COLUMN CONNECTION

column are indicated in the figure.

Part of the unbalanced moment M is resisted by flexural moments M_{AB} and M_{CD} acting on faces AB and CD of the critical section and part of the moment is resisted by the torsional moments T_{BC} and T_{AD} acting on faces BC and AD. The remainder of the moment is resisted by the vertical shear forces acting on the faces. Thus moment is transferred between the slab and the column by three actions, namely (i) flexure, (ii) torsion and (iii) shear. It is also evident that the shear stresses induced by the transfer of moment will make shear more critical for this case than for gravity loads alone. One of the objectives of this study is to develop an ultimate strength procedure for determining the unbalanced moment capacity of the slab-column junction by considering the individual contributions of flexure, torsion and shear in resisting the applied loads.

Since the shear strength of the slab around the column often indicates the load carrying capacity of flat plate floors some form of shear reinforcement could be used to increase the shear strength of the connection. At present no suitable design methods are available for proportioning shear reinforcement for slab-column connections which are subjected to both shear and unbalanced moment loadings. In slabs shear reinforcement may consist of bars or structural shearheads. The effectiveness of bars, which may be in the form of stirrups or inclined cranked bars, as shear reinforcement in thin slabs is still a matter of concern for structural designers and needs to be examined further. The role of shear reinforcement is to transfer shear force across a diagonal tension crack and to fulfil this purpose the shear reinforcement must be securely anchored at both ends. The anchorage of stirrups or cranked bars can be developed by transferring the force in the shear bar either to the concrete by bond and bearing or to other reinforcement, such as by rigidly attaching stirrups to longitudinal reinforcement, or by tightly wrapping stirrups around the longitudinal reinforcement. In slabs, anchorage of shear reinforcement is a problem

which becomes more critical with the decrease in the slab thickness.

The effectiveness of various types of shear reinforcement can only be determined from tests which will help to develop a guide to their design provisions. To find methods of increasing the shear strength of slab-column connections by using various reinforcement arrangements is another objective of this investigation.

The most important benefit that could be derived from effectively shear reinforced connections is the enhancement of ductility. In countries which require design for earthquake loading ductility is an important consideration. The present standards for seismic design assume that in the case of a severe earthquake the structure has sufficient ductility to absorb energy by post-elastic deformation without collapse. Very little is known about the seismic resistance of flat plate-column connections and this aspect requires particular attention.

During an earthquake the slab-column connections of a multistorey flat plate structure will be subjected to repeated reversals of bending moment. Such reversals may lead to a shear failure in the slab around the column. Information is needed on the extent of the deformation which may occur under earthquake conditions and on the deterioration of load carrying capacity of slab-column connections due to bending moment reversals so that the designer can take appropriate steps to ensure the integrity of the structure.

3.2 REVIEW OF PREVIOUS WORK

SUMMARY

A review of previous investigations on transfer of shear and moment from reinforced concrete flat plates to columns is presented. Existing design methods and test results for slab-column connections without shear reinforcement and limited work done on connections with shear reinforcement are discussed.

3.2.1 INTRODUCTION

Many tests [6,7,8,9,10] have been performed to investigate the strength of symmetrically loaded flat plate-column connections which transfer shear without moment from the slab to the column. These tests have led to several semi-empirical design procedures [6,7,8,9,10,11]. For such a symmetrically loaded slab-column junction the current design practice is to consider a critical section at a distance $d/2$ from the face of the column and to compute a nominal shear stress by assuming that the shear force is uniformly distributed over a vertical area defined by the periphery of the critical section and the effective depth of the slab. This nominal shear stress is then limited to $4\sqrt{f'_c}$ psi for slabs without shear reinforcement [12,13].

In contrast, for an eccentrically loaded flat plate-column junction, which transfers both shear and moment, the amount of investigation carried out is only limited and can be classified into two main categories. The first category deals with slab-column junctions without any shear reinforcement while the second category deals with junctions containing some form of shear reinforcement. For the first category some methods of analysis [8,12,14,15] as well as some test data [8,16,17] are available. For the

second category no method of design or analysis of strength is available and only a few test results[18,19] are available.

3.2.2 INVESTIGATIONS WITHOUT SHEAR REINFORCEMENT

As late as 1960 when Di Stasio and Van Buren[14] first published a paper for determining stresses at a flat plate floor-column junction transferring moment and shear, structural designers had no access to any method of analysis for designing slab to column junctions which transferred moment. In 1961 Moe[8] reported the first test results and proposed an ultimate strength equation connecting the shear V and the moment M transferred to the column. The ACI-ASCE Committee 326[12] considered these two investigations and in addition studied 15 more test results, of which 10 were taken from preliminary work by Hanson and Hanson[16] and 5 from Frederick and Pollauf's work reported by Kreps and Reese[17]. Committee 326[12] recommended a design procedure in 1962. Another method appeared in Commentary on Building Code Requirements for Reinforced Concrete (ACI 318-63)[15] in 1965.

All the four methods referred to so far are somewhat related to each other as will be shown later. Because of extremely complex stress distribution on the critical section, these four methods assume a linear distribution of shear stresses along the critical sections. The concept of an equivalent polar moment of inertia of the critical peripheral section is used in all the methods to determine the shear stresses induced by the moment.

Apart from these four methods, one more new approach to design has been reported recently by Hawkins and Corley[20]. A design recommendation has been included in the new ACI Building Code (ACI 318-71)[13] for the first time. A brief review of all these methods is given below.

(i) Di Stasio and Van Buren[14]

Di Stasio and Van Buren proposed a working stress design method for determining stresses at the junction between a flat-plate floor and a column under combined shear and unbalanced moment. The critical section shown by dotted lines in Fig. 3.2(a) is taken at a distance $(t - 1\frac{1}{2})$ in. from the column periphery. The combined vertical shear stress is assumed to be distributed as shown in Fig. 3.2(e) for an interior column-slab junction.

The unit vertical shear stresses are given by the following equations:

$$v_1 = \frac{8t}{7d}\left[\frac{V}{A} - \frac{(M - m_{AB} - m_{CD})\,a}{J}\right] \quad \ldots (3.1)$$

$$v_2 = \frac{8t}{7d}\left[\frac{V}{A} + \frac{(M - m_{AB} - m_{CD})\,a}{J}\right] \quad \ldots (3.2)$$

where

$$A = 2t\,(x_o + y_o)$$

$$J = \frac{tx_o^3}{6} + \frac{x_o t^3}{6} + \frac{ty_o x_o^2}{2}$$

$$a = \frac{x_o}{2}$$

In the above equations

t = total thickness of slab

d = effective depth of slab

V = total shear around the critical section

A = area of concrete in assumed critical section

M = total unbalanced moment

m_{AB} = working stress design moment acting on face AB of the critical section

m_{CD} = working stress design moment acting on face CD of the critical section

a = distance from centroidal axis to the most

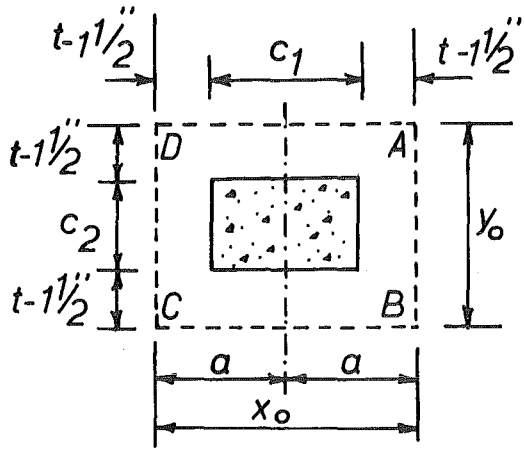

(a) Di Stasio & Van Buren

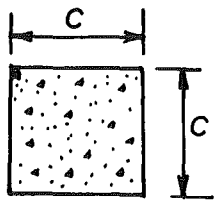

(b) Moe

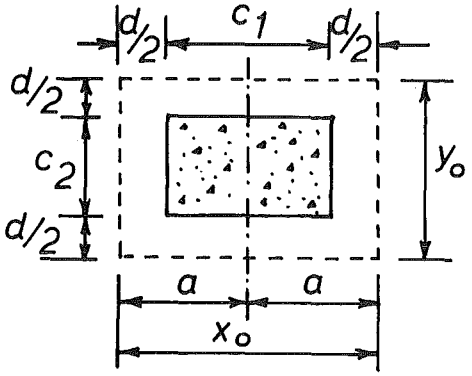

(c) ACI Committee 326

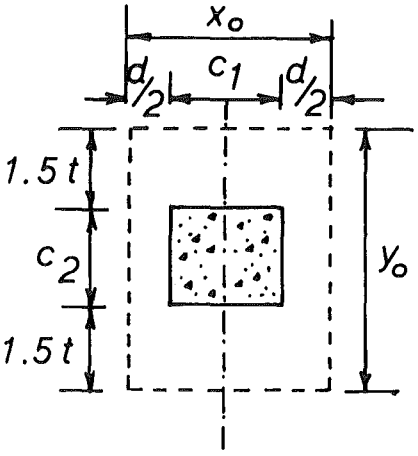

(d) Commentary on ACI 318-63

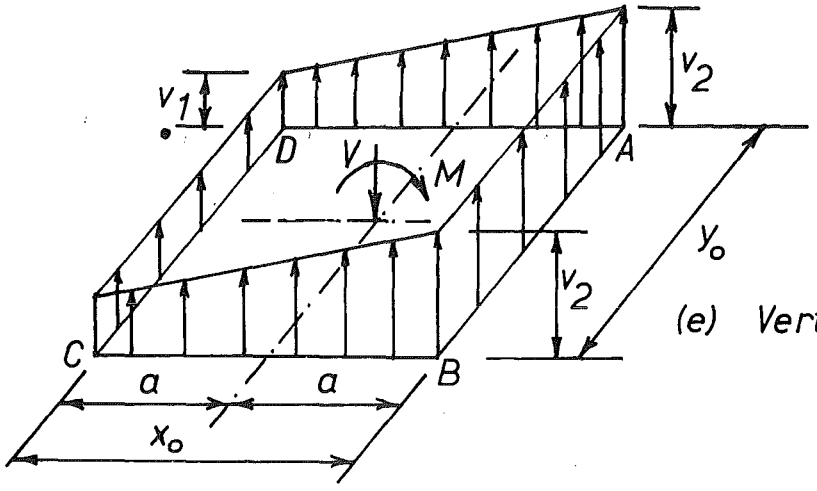

(e) Vertical Shear Stress

FIG. 3.2 ASSUMED CRITICAL SECTIONS AND SHEAR STRESS DISTRIBUTION

remote part of critical section

J = polar moment of inertia of the surface described by the critical section passing through the slab thickness about its centroid

x_o = dimension of critical section parallel to the direction of bending

y_o = dimension of critical section transverse to the direction of bending

Thus the total unbalanced moment M acting at the centre of the joint is resisted by flexural moments m_{AB} and m_{CD} acting on the faces AB and CD of the critical section respectively and a torsional moment T acting on either side faces AD and BC . The equation of moment about the centre of the joint is

$$M = m_{AB} + m_{CD} + T$$

from which the total torsional moment on the two side faces is obtained as

$$T = M - m_{AB} - m_{CD} \qquad \ldots (3.3)$$

Limiting values of m_{AB} and m_{CD} are taken as resisting moments of the slab section on sides AB and CD of the critical section and they are calculated on the basis of working stress design principles.

In Eqs. (3.1) and (3.2) $\frac{V}{A}$ represents the average vertical shear stress due to V and $\frac{T.a}{J}$ is the additional vertical shear stress due to the torsional moment T . The factor $\frac{t}{d}$ is required to transform A and J in terms of the effective depth and $j = \frac{7}{8}$ is used to conform to the design practice[21] current in 1960 of calculating shear stress by $\frac{V}{bjd}$. To allow for additional resistance developed through the dowel action of the reinforcing bars they recommended an increase in both A and J by multiplying the individual terms by the factor $[1 + (n - 1)\, \rho_t]$, in which ρ_t is the percentage of total reinforcement crossing the perimeter of the critical section and n is the modular ratio.

They considered it necessary to investigate two sections, one along the perimeter of the column for maximum punching shear which was limited to $0.0625f'_c$ and the other along the periphery parallel to column faces at a distance $(t - 1\frac{1}{2})$ in. from the column face for diagonal tension. The maximum vertical shear stress on this section was limited to $0.03f'_c$ as specified in the diagonal tension recommendations of the ACI Building Code (ACI 318-56)[21].

Similar analyses were presented for moment transfer at exterior columns with or without spandrel beams.

(ii) Moe[8]

Moe developed an ultimate strength analysis for moment transfer at an interior column by performing 12 tests on 6 ft. square, 6 in. thick slabs which were simply supported along all four edges. All but two of his slabs had reinforcement only near the bottom face. Load was applied through a centrally located square column stub at different eccentricities.

He proposed the following ultimate strength equation connecting the ultimate shear V_u and the ultimate moment M_u transferred to the column.

$$V_u = \frac{V_o}{1 + \frac{3KM_u}{V_u c}} \qquad \ldots (3.4)$$

where

V_u = total ultimate shear transferred

V_o = shearing capacity of the slab for zero eccentricity

K = moment reduction factor determined experimentally

M_u = total ultimate moment transferred

c = side length of loaded area of square shape or side length of a square column

Moe considered critical section to be directly adjacent to the periphery of the column. The slab was assumed to fail in shear when the ultimate unit shear stress reached a value equal to

$$v_u = \frac{V_u}{bd} = \frac{15\,(1 - 0.075\,\frac{c}{d})\sqrt{f'_c}}{1 + \frac{5.25bd\sqrt{f'_c}}{V_{flex}}} \qquad \ldots (3.5)$$

where

v_u = nominal ultimate shear stress

b = perimeter of the column

d = effective depth of the slab

c = side length of a square column

V_{flex} = shear force at which flexural failure takes place

For design purposes V_u is taken equal to V_{flex} and Eq. (3.5) becomes

$$v_u = (9.75 - 1.125\,\frac{c}{d})\,\sqrt{f'_c} \qquad \ldots (3.6)$$

Eq. (3.4) proposed by Moe can also be expressed in a different way. Substitution of $b = 4c$ and $V_o = v_u\,bd = v_u \times 4cd$ in Eq. (3.4) results in the following equation

$$v_u = \frac{V_u}{4cd} + \frac{KM_u}{\frac{2}{3}c^3 d}\left(\frac{c}{2}\right)$$

$$= \frac{V_u}{\bar{A}} + \frac{KM_u}{\bar{J}}\left(\frac{c}{2}\right) \qquad \ldots (3.7)$$

where

$\bar{A}$ = $4cd$ = area of the critical section

$\bar{J}$ = $\frac{dc^3}{6} + \frac{c\,d\,c^2}{2} = \frac{2}{3}c^3 d$ = polar moment of inertia of the critical section about its centroid.

Moe determined the value of K from his test data. He found that the ultimate strengths of all his slabs could be predicted satisfactorily

with a standard deviation of 0.103 if the value of K was taken as $\frac{1}{3}$, thus indicating that approximately 33 percent of the total moment could be assumed to be transferred by shear stresses.

(iii) ACI-ASCE Committee 326[12]

ACI-ASCE Committee 326 reviewed the investigations on moment transfer between concrete slabs and columns carried out by Di Stasio and Van Buren[14] as well as by Moe[8]. They found that Moe's Eq. (3.6) for ultimate shear stress of concrete slabs could not be applied to either very large or very small values of $\frac{c}{d}$. Consequently Committee 326 selected a limiting shear stress formula

$$v_u = 4 \left(\frac{d}{c} + 1\right) \sqrt{f'_c} \qquad \ldots (3.8)$$

which could be applicable to full practical range of $\frac{c}{d}$ ratios. The critical section continued to be the periphery of the column. The Committee also pointed out that the variable $\frac{c}{d}$ in Eq. (3.8) could also be taken into account by choosing a critical section located at a distance d/2 from the column periphery and limiting the shear stress to $4\sqrt{f'_c}$.

To be consistent with the design procedure the Committee adopted the following formula

$$v_u = \frac{V_u}{A_c} + \frac{KM_u a}{J_c} < 4\sqrt{f'_c} \qquad \ldots (3.9)$$

where, for an interior column,

$$A_c = 2d\ (x_o + y_o)$$

$$J_c = \frac{dx_o^3}{6} + \frac{x_o d^3}{6} + \frac{dy_o\, x_o^2}{2}$$

$$a = \frac{x_o}{2}$$

All other terms are as defined previously.

The assumed critical section taken at a distance d/2 from the face of the column is shown in Fig. 3.2(c) and the assumed shear stress

distribution on the critical section is shown in Fig. 3.2(e). In calculating A_c and J_c, the effective depth d was used instead of the total thickness t. No increase in shear resistance due to dowel action was allowed.

In order to specify a safe design value for the moment reduction factor K, the Committee studied 25 test results, of which 10 were taken from preliminary works of Hanson and Hanson[16], 10 from Moe's[8] work and 5 from Frederick and Pollauf's[17] work.

Using Di Stasio and Van Buren's Eqs. (3.1) and (3.2), where the term $(M - m_{AB} - m_{CD})$ was replaced by KM, they determined the best value of K and the average value of $\frac{v_{Test}}{\sqrt{f'_c}}$ for these 25 tests at distances 0, t/2 and d outside the column with full dowel action considered and without any dowel action considered. The best correlation with the test data was obtained when the shear stresses were calculated at a distance d outside the column with full dowel action considered. The value of K = 0.487 gave the best coefficient of variation of 0.121 and the average value of the maximum shear stress at ultimate strength was $4\sqrt{f'_c}$ psi. With the Committee's recommended Eq. (3.9) a constant K = 0.2 gave a coefficient of variation of 0.259 and an average value of calculated ultimate shear stress $v_u = 4.47\sqrt{f'_c}$. So $v_u = 4\sqrt{f'_c}$ was considered as a safe design value.

Based on this evaluation the Committee recommended limiting the shear stress to $4\sqrt{f'_c}$ on a design critical section located at a distance d/2 from the column face and assuming K = 0.2.

(iv) Commentary on ACI Building Code (ACI 318-63)[15]

This method presented in the "Commentary"[15] was similar to the Di Stasio and Van Buren's[14] working stress design method. For an interior column the maximum shear stress v_2 is calculated by

$$v_2 = \frac{V}{A_c} + \frac{(M - m_{AB} - m_{CD})\, a}{J_c} \qquad \ldots (3.10)$$

The dimensions of the critical section x_o and y_o as shown in Fig. 3.2(d) are assumed to be equal to $c_1 + d$ and $c_2 + 3t$ respectively. All other terms are as defined previously. This calculated shear stress is limited to the permissible value of $2\sqrt{f'_c}$ as specified in the 1963 ACI Building Code[22].

(v) Hanson and Hanson[16]

In their study[16] on the strength of flat slabs near columns, Hanson and Hanson reported the results of 17 tests involving combined shear and unbalanced moment loadings. Sixteen specimens measuring 84 in. by 48 in. had 6 in. square or 12 in. by 6 in. interior columns at the centre while one specimen D15 measuring 48 in. by 45 in. contained a 6 in. square column located adjacent to and centred along the longer edge. All the slabs were 3 in. thick and were reinforced with $\frac{3}{8}$ in. diameter deformed bars spaced at 3 in. centres in each direction both at the top and bottom. A typical test specimen and the methods of loading are shown in Fig. 3.3. Eight of the specimens with square columns had pairs of 6 in. by 1 in. holes which were located adjacent to the column and were either parallel to the longer side or the shorter side of the slab indicated by the letters L or C respectively on specimen numbers.

They made a comparative study of the four design methods presented by Di Stasio and Van Buren[14], Moe[8], ACI-ASCE Committee 326[12] and the Commentary on ACI Building Code (318-63)[15] by evaluating their test results[16] and Moe's test data[8].

The interaction equation derived for the two working stress design methods[14, 15] was given by

$$\frac{V_u}{V_w} = 2 - \frac{M_u - 2m_r}{M_w - m_r} \qquad \ldots (3.11)$$

where

V_w = service load shear capacity without moment transfer

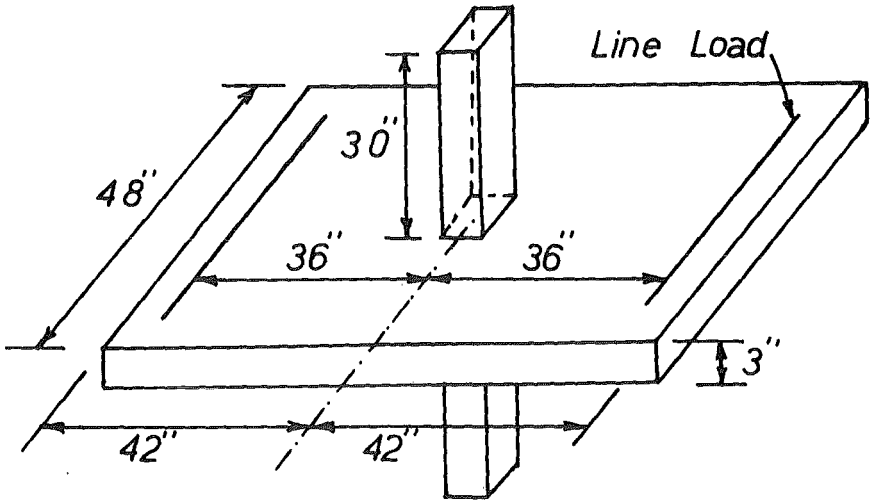

(a) Test Specimen

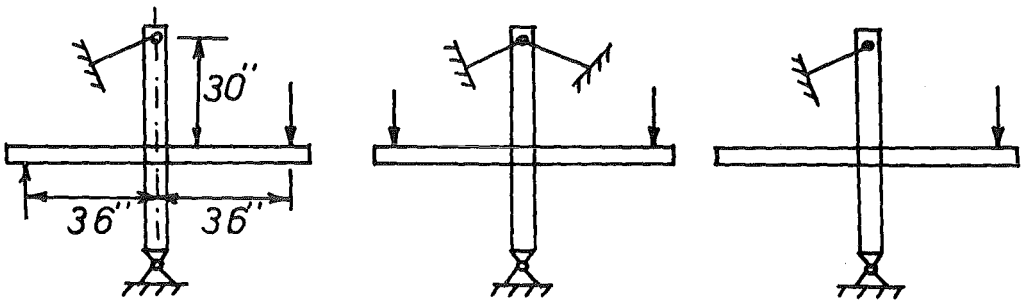

(b) Loading Methods

FIG. 3.3 HANSON AND HANSON'S TEST SPECIMEN AND LOADING METHODS

V_u = ultimate shear

M_w = service load unbalanced moment capacity without shear transfer

M_u = ultimate unbalanced moment

m_r = sum of flexural moments acting on faces AB and CD of critical section, calculated by working stress design method

In this derivation of Eq. (3.11) it was assumed that the service load shear, V and moment, M for the test specimens were one half of the ultimate shear, V_u and ultimate moment, M_u. The nominal service load shear stress was assumed to be $2\sqrt{f'_c}$.

Values of $\frac{V_u}{V_w}$ and $\frac{M_u - 2m_r}{M_w - m_r}$ for the test specimens[8,16] were computed by Di Stasio and Van Buren's method[14] which was modified to conform to the requirements of the 1963 ACI Building Code[22]. These values when plotted as an interaction diagram were all found to be outside the interaction line representing Eq. (3.11), indicating that a nominal service load shear stress of $2\sqrt{f'_c}$ was conservative for a factor of safety of 2 when using Di Stasio and Van Buren's method.

The method given in the Commentary[15] on the 1963 ACI Building Code was found to be satisfactory for the tests reported by Hanson and Hanson but it led to a factor of safety less than 2 for all but three of Moe's tests.

The interaction equation derived for the two ultimate strength methods[8,12] given by Moe and ACI Committee 326[12] was

$$\frac{V_u}{V_o} = 1 - \frac{M_u}{M_o} \qquad \ldots (3.12)$$

where

V_u = ultimate shear

V_o = ultimate shear capacity without moment transfer

M_u = ultimate unbalanced moment capacity

M_o = ultimate unbalanced moment capacity without shear transfer

Values of $\frac{V_u}{V_o}$ and $\frac{M_u}{M_o}$, assuming $K = \frac{1}{3}$ were calculated by Moe's method and plotted as an interaction diagram. It was found that Moe's method conservatively predicted the ultimate strength of all the tests on interior column-slab junctions.

The method of Committee 326 with $K = 0.2$ was found to overestimate the strength of many of the test specimens.

Hanson and Hanson concluded from their examination of test data by studying the interaction diagrams that the ultimate strength design method recommended by ACI-ASCE Committee 326[12] would give a good prediction of the strength of the slab-column junction when the moment reduction factor K was changed from 0.2 to 0.4 .

(vi) Revised Building Code Requirements for Reinforced Concrete (ACI 318-71)[13]

For the first time a design provision has been included in the revised ACI Building Code (ACI 318-71)[13] . Section 11.13.2 of the revised Code states that "when unbalanced gravity load, wind, earthquake or other lateral forces cause transfer of bending moment between slab and column, a fraction of the moment given by

$$1 - \frac{1}{1 + \frac{2}{3}\sqrt{\frac{c_1 + d}{c_2 + d}}}$$

shall be considered transferred by eccentricity of the shear about the centroid of the critical section defined in Section 11.10.2. Shear stresses shall be taken as varying linearly about the centroid of the critical section and the shear stress v_u shall not exceed $4\sqrt{f'_c}$ ". In Section 11.10.2 it is stated that "the critical section shall be perpendicular to the plane of the slab and located so that its periphery is a minimum and approaches no closer than $d/2$ to the periphery of the concentrated load or reaction area".

The fraction mentioned in the Code may be simply expressed as

$$K = \frac{1}{1 + 1.5\sqrt{\frac{c_2 + d}{c_1 + d}}} \qquad \ldots (3.13)$$

where

c_1 = column size in the direction in which moments are being determined

c_2 = column size transverse to the direction of moment

The method of design given in the "Commentary[23] on Building Code Requirements for Reinforced Concrete (ACI 318-71)" is similar to the one recommended by ACI-ASCE Committee 326[12] as modified later by Hanson and Hanson[16]. In the Commentary[23] it was pointed out that most of the data were obtained from tests of square columns. For square columns Eq. (3.13) gives $K = 0.4$ as suggested by Hanson and Hanson. For rectangular columns it has been assumed that the percent of moment transferred by flexure increases as the width of the face of the critical section resisting flexure increases.

(vii) Hawkins and Corley[20]

Hawkins and Corley developed an ultimate strength procedure for interior and exterior column-slab connections based on a beam analogy. The slab framing into each column face was idealized as beams running in two directions at right angles. The ultimate capacity of the connection was obtained by summing the ultimate bending moment, torsional moment and shear forces of the beams for the given loading condition.

Figs. 3.4(a) and 3.4(b) show the view and section of a slab adjacent to an interior column. Two possible modes of failure were considered. The first, termed as "moment-torsion", involves failure on all four column faces. The ultimate torsional strength is reached on side faces BC and AD and the ultimate flexural strength on faces AB and CD. The second

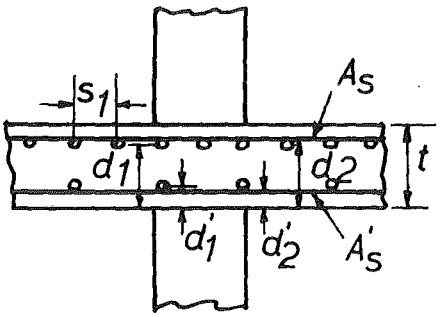

(a) Section - X X Direction

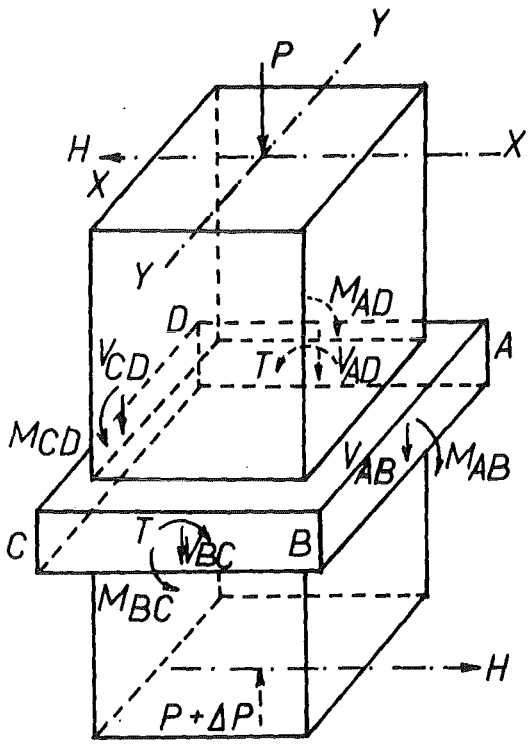

(b) Moments and Forces

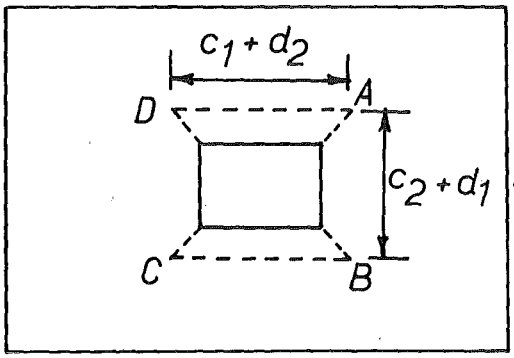

(c) Critical Section for Moment - Torsion

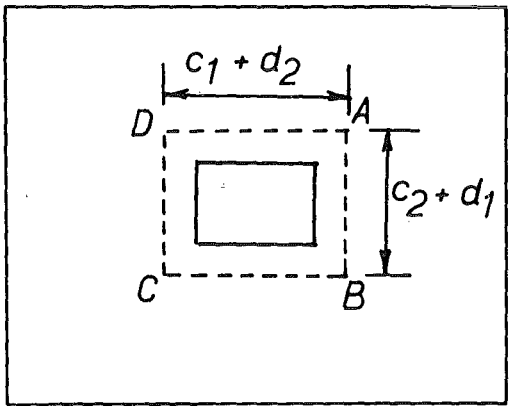

(d) Critical Section for Shear - Torsion

FIG. 3.4 HAWKINS AND CORLEY'S ANALYSIS

mode, referred to as "shear-torsion", requires failure on three faces only. This mode dominates when the shear transferred is significant. For moderate values of shear the ultimate torsional strength is reached on the side faces and the ultimate shear strength on the face AB. For high shears the ultimate shear strength is also reached on the face CD.

The critical section assumed for a moment-torsion failure is shown in Fig. 3.4(c). The total moment capacity for a moment-torsion failure is given by

$$M_t = M_{ABO} + M_{CDO} + 2 T_O \qquad \ldots (3.14)$$

where

M_t = total moment capacity for a moment-torsion failure

M_{ABO}, M_{CDO} = ultimate resisting moments for faces AB , CD of the critical section

T_O = ultimate resisting torsional moment for face BC or AD in pure torsion

M_{ABO} and M_{CDO} are calculated from the ultimate strength design formula for a rectangular reinforced concrete section. The limiting value of the torsional moment is calculated by using Hsu's[24,25,26,27] expressions for torsional strength mainly because Hsu tested beams with breadth to depth ratios comparable to $\frac{c + d}{t}$ ratios likely in slabs. THe ultimate torque in pure torsion is given by

$$T_o = \frac{0.36 t^2}{\sqrt{t}} \left(c_1 + d_2\right) f_{sp} + \frac{\Omega \, (c_1 + d_2) \, (d_1 - d_1') \, A_{s1} f_y}{s_1} \qquad \ldots (3.15)$$

where

t = thickness of slab

c_1 = width of column face parallel to direction of applied moment

d_1 = effective depth for face AD

d_1' = distance from extreme compression fibre to centroid of compression steel for face AD

f_{sp} = splitting tensile strength of concrete

Ω = coefficient = $0.66 + 0.33 \frac{(c_1 + d_2)}{(d_1 - d_1')}$ but not more than 1.5

A_{s1} = area of one reinforcing bar parallel to the torsion face of the column

f_y = yield stress of reinforcing bars

s_1 = spacing of reinforcing bars parallel to the torsion face of the column

For torsion in combination with shear and moment the ultimate torque assumed is

$$T_u = T_o \sqrt{1 - \frac{V_{AD}}{V_{ADO}}} \qquad \ldots (3.16)$$

$$\text{if } \frac{M_{AD}}{M_{ADO}} < 0.5$$

or

$$T_u = T_o \left(1.7 - 1.4 \frac{M_{AD}}{M_{ADO}}\right) \sqrt{1 - \left(\frac{V_{AD}}{V_{ADO}}\right)^2} \qquad \ldots (3.17)$$

$$\text{if } \frac{M_{AD}}{M_{ADO}} > 0.5$$

where

V_{AD} = shear force acting on face AD

V_{ADO} = ultimate resisting shear for face AD

M_{AD} = moment acting on face AD

M_{ADO} = ultimate resisting moment for face AD

For a shear-torsion failure a diagonal tension crack is assumed to extend across the full width of the face AB in Fig. 3.4(d). The load on the area tributary to this face is equal to or greater than the ultimate shear strength for this face, which is given by

$$V_{ABO} = 0.6 f_{sp} (c_2 + d_1) d_2 > 4 \sqrt{f_c'} (c_2 + d_1) d_2 \qquad \ldots (3.18)$$

where

V_{ABO} = ultimate resisting shear for face AB

f_{sp} = splitting tensile strength of concrete

c_2 = width of column face transverse to direction of moment

d_1 = effective depth for face AD

d_2 = effective depth for face AB

For a shear-torsion failure the critical section follows the broken line in Fig. 3.4(d). The torsional strength T_u is obtained from Eq. (3.16) or (3.17) as appropriate with V_{AD} taken as the load on the area tributary to the face of AD plus $\frac{V_{AB} - V_{ABO}}{2}$. The shear-torsion moment can be calculated as

$$M_s = M_{ABO} + M_{CDO} + 2\,T_u \qquad \ldots (3.19)$$

where M_s = total moment capacity for a shear-torsion failure.

Hawkins and Corley found that their method resulted in accurate predictions of the measured strengths for the slabs without openings tested by Hanson and Hanson[16]. They had to make a number of assumptions to analyse Moe's[8] test data by their method because loads acting on the areas tributary to each column face could not be measured in Moe's tests. In terms of practical applications their method appears to be quite involved. In idealizing the behaviour of the slab-column connection as beam elements their procedure permits a better understanding of the factors controlling the strength of the connection.

3.2.3 DISCUSSION OF METHODS OF ANALYSIS WITHOUT SHEAR REINFORCEMENT

Apart from the recently proposed method of Hawkins and Corley[20], the early methods[8,12,14,15] reviewed are similar in basic approach. These related methods assume a linear variation of vertical shear stresses from the centroidal axis and this assumption leads to Eqs. (3.1), (3.2), (3.7), (3.9) and (3.10). The methods differ mainly in location of the critical sections and in selection of the factor K which is the portion of the total unbalanced moment M producing shear stresses on the

critical section.

The two working stress methods of Di Stasio and Van Buren[14] and the Commentary[15] on the 1963 ACI Building Code give $K = (M - m_{AB} - m_{CD})/M$. Considering the service load moment M to be one half the ultimate moment M_u, K can be expressed as

$$K = \frac{M_u - 2(m_{AB} + m_{CD})}{M_u} \qquad \ldots (3.20)$$

For square columns Moe[8] suggests $K = \frac{1}{3}$ and the ACI Building Code (ACI 318-71)[13] suggests $K = 0.4$. In Moe's method K is that part of the total moment which produces only vertical shear stresses. In case of the ACI method K is that part of the total moment which produces both vertical and horizontal shear stresses and it is, therefore, expected to be greater than Moe's value.

Values of K calculated from test results are given in Table 3.1 for the methods recommended by ACI[12,23], Moe[8] and Di Stasio and Van Buren[14]. The ratios of measured to theoretical strengths for the tests by Moe[8] and Hanson and Hanson[16] can be obtained by dividing the recommended value of K by the actual values of K obtained from test results and these are also given in Table 3.1.

A study of Table 3.1 reveals the same conclusions as reached by Hanson and Hanson[16] by means of their interaction diagrams. All K values computed by Moe's method are less than $\frac{1}{3}$, indicating safe results. If the value of K is taken as 0.2 by the ACI method[12,23], many specimens will produce unsafe results but a value of $K = 0.4$ will mean that all K values computed by the ACI method from the test results will be less than 0.4, thus pointing to safe results. The ACI method is also seen to produce scattered results for the slabs tested by Moe. This is because all but two of Moe's slabs had reinforcement on one face only. The capacity of the resisting moments of the slab sections should be a factor in deciding the proportion of moment to be transferred by shear.

TABLE 3.1

ACTUAL VALUES OF K FROM TEST RESULTS

INVESTIGATOR	SPECIMEN NO.	ACI METHOD		MOE'S METHOD		DI STASIO & VAN BUREN	
		K_{ACI} Eq.(3.9)	$\frac{0.4}{K_{ACI}}$	K_{MOE} Eq.(3.7)	$\frac{0.33}{K_{MOE}}$	K_{DV} Eq.(3.20)	$\frac{K_{DV}}{K_{ACI}}$
HANSON & HANSON[16]	A1	0.298	1.34	0.241	1.38	0.735	2.47
	A2	0.283	1.41	0.227	1.47	0.754	2.66
	A12	0.266	1.50	0.223	1.49	0.855	3.21
	B7	0.397	1.01	0.314	1.06	0.870	2.19
	B16	0.382	1.05	0.302	1.10	0.895	2.34
	C8	0.341	1.17	0.268	1.24	0.685	2.01
	C17	0.369	1.08	0.266	1.25	0.795	2.15
MOE[8]	M2A	0.241	1.66	0.243	1.37	0.601	2.49
	M4A	0.357	1.12	0.298	1.12	0.718	2.01
	M2	0.168	2.38	0.182	1.83	0.745	4.43
	M3	0.269	1.49	0.236	1.41	0.727	2.70
	M6	0.238	1.68	0.223	1.50	0.725	3.05
	M7	-	-	0.183	1.82	0.158	-
	M8	0.302	1.32	0.232	1.44	0.678	2.25
	M9	0.103	3.88	0.184	1.81	0.533	5.17
	M10	0.242	1.65	0.200	1.67	0.627	2.59

From Table 3.1 it is also seen that the ratios of K values obtained by Di Stasio and Van Buren's method[14] to those obtained by the ACI method[12,23] are greater than 2, thus indicating a factor of safety greater than 2. The actual values of K computed by the method given in the Commentary[15] on the 1963 ACI Code will be less than those given by the method of Di Stasio and Van Buren because in the former case m_{AB} and m_{CD} in Eq. (3.20) will be increased by the factor $\frac{c_2 + 3_t}{c_2 + d}$. Hanson and Hanson[16] showed that this method gave a factor less than 2 for many specimens tested by Moe.

Regarding the empirical value of K for rectangular sections given by Eq. (3.13) it may be pointed out that specimens C8 and C17 tested by Hanson and Hanson[16] produce rather lower K values than the recommended value. For these two specimens with $c_1 + d = 8.44$ in. and $c_2 + d = 14.44$ in. the value of K given by Eq. (3.13) is 0.34 whereas actual values of K obtained from tests are 0.34 and 0.37 for C8 and C17 respectively. Hence Eq. (3.13) when used with the current ACI proposal[13,23] may not give safe results for $\frac{c_2 + d}{c_1 + d} > 1.7$.

The polar moment of inertia, J, for square and rectangular sections has been expressed as

$$J = \frac{dx_o^3}{6} + \frac{x_o d^3}{6} + \frac{dy_o x_o^2}{2}$$

$$\text{and } \frac{J}{a} = \frac{J}{x_o/2} = \frac{dx_o^2}{3} + \frac{d^3}{3} + y_o dx_o \qquad \ldots (3.21)$$

In balancing the applied moment the first term $\frac{dx_o^2}{3}$ in Eq. (3.21) gives the contribution of linearly varying vertical shearing stresses along faces BC and AD of the critical section, the 2nd term $\frac{d^3}{3}$ gives the contribution of horizontal shear stresses acting on faces BC and AD and the last term $y_o dx_o$ gives the contribution of vertical shear stresses acting on transverse faces AB and CD. The term $\frac{d^3}{3}$ is very small compared with the other terms and this means

that the contribution of horizontal shear stress in balancing the applied moment may not be duly considered. In Moe's method the term $\frac{d^3}{3}$ has been dropped in calculating J but this has been compensated to some extent by selecting a lower value of K. Since the overall depths of slabs tested were equal to or less than half the side dimension, c_1 of the columns, the contribution of torsional moments were small and as a result there was not any large discrepancy between the test results and the theoretical results due to this factor.

On the whole Di Stasio and Van Buren's[14] working stress method has been found to produce safe results with a factor of safety greater than 2. Since this method is based on working stress design principles, use of straight-line variation of stresses and the concept of polar moment of inertia may be regarded as a useful design tool with some justification.

However, the same cannot be said about the ultimate strength design procedures recommended by Moe[8] and the ACI[12,13,23]. These methods predict ultimate strengths with a varying degree of safety but they are in a true sense regarded as empirical design methods. The concept of straight-line variations of stresses and use of polar moment of inertia are not in keeping with the ultimate strength design philosophy.

In contrast the method proposed by Hawkins and Corley[20] is in a real sense an ultimate strength design procedure. They have idealised the slab to column connection as intersecting beams for which separate expressions for moment, shear and torque have been developed. In Eq. (3.15) the contribution of slab reinforcement in providing torsional resistance seems to have been overestimated because this does not comply with the limitation of maximum nominal ultimate torsional shear stress in concrete which, due to pure torsion, is given as $12\sqrt{f'_c}$ in the ACI Building Code (318-71)[13].

In none of the slabs analysed by them closed hoops were provided. For effective development of torsional resistance in reinforced concrete

beams it is essential to provide both closed hoops and adequate longitudinal reinforcement as can be demonstrated by a space truss analogy. In the absence of closed hoops, the second term of Eq. (3.15), which gives the contribution of slab reinforcement towards the ultimate resisting torsional moment, cannot be considered as fully effective in providing the same torsional resistance as would be given by the closed stirrups because the vertical shear stresses may not be balanced within the slab.

Excellent correlations that exist between their theory and the test results could be attributed to overestimation of steel component in calculating the torsional moment. It is also believed that the torsional moment capacity of the slab-section which is assumed to frame into the column will increase due to warping restraint and the flexural capacity of the slab section is expected to increase due to inplane compressive forces imposed on the slab by the restraint of the column.

3.2.4 INVESTIGATIONS WITH SHEAR REINFORCEMENT

The shearing strength of the flat plate-column junction can be increased by using shear reinforcement formed from bars or shearheads fabricated from steel I or channel shapes. Although shearhead reinforcement has been in use in flat plate construction for a long time no detailed test data or design procedure was available until Corley and Hawkins[28] conducted tests and proposed a design procedure for concentrically loaded slab-column junctions. For a slab-column junction containing shear reinforcement or a shearhead, which transfers both shear and moment there would appear to be no design procedures available. Of the few known tests on such a junction one has been carried out by Hollings[18] and four or five tests have been performed at the Portland Cement Association Laboratory[19,29]. A review of these tests is given below.

(i) Full Scale Test by Hollings[18]

A full scale test simulating the large deformations possible in a

very severe earthquake was carried out by Hollings[18] on a reinforced concrete flat plate to column connection containing a steel shearhead. The object of the test was to prove that the particular flat plate to column connection used in the construction of a 16 storeyed structure could survive repeated floor to floor horizontal deflections of 2 in. without loss of the vertical load carrying capacity of the connection. The details of the test specimen and the method of testing are shown in Fig. 3.5.

The steel shearhead made of 2 pairs of I-sections, each of size 3 in. x 2 in. x 4.5 lbs, was selected without calculation to fulfil the following criteria:

(a) The nominal shear stresses on the concrete section outside the shearhead must be very low for the worst condition of moment and shear.

(b) The shearhead must be easy to build and light in weight.

(c) It must fit between the layers of reinforcing bars.

In his method of testing full vertical load conditions with a small load factor were simulated by placing a stack of concrete blocks on the test slab which together with the concrete blocks weighed 144 psf. Equal and opposite loads were applied in 0.5 ton increments by hydraulic jacks at the centre of each slab edge to simulate earthquake loading conditions.

A total of 4 tests were performed on the same test specimen. Test 1 was discontinued at 8 tons on each jack because of doubtful stability of the loading strut. At this loading the test slab had reached 85% of its ultimate moment capacity and an average deflection of 2.3 in. was reached at the jacks. A pattern of light cracking with a maximum crack width of 0.03 in. and limited to a few square feet around the column could be observed at this stage. In test 2 the load cells were removed and loading was continued in the same direction to the limit of stability of the jacking apparatus. This was reached at an average slab edge deflection

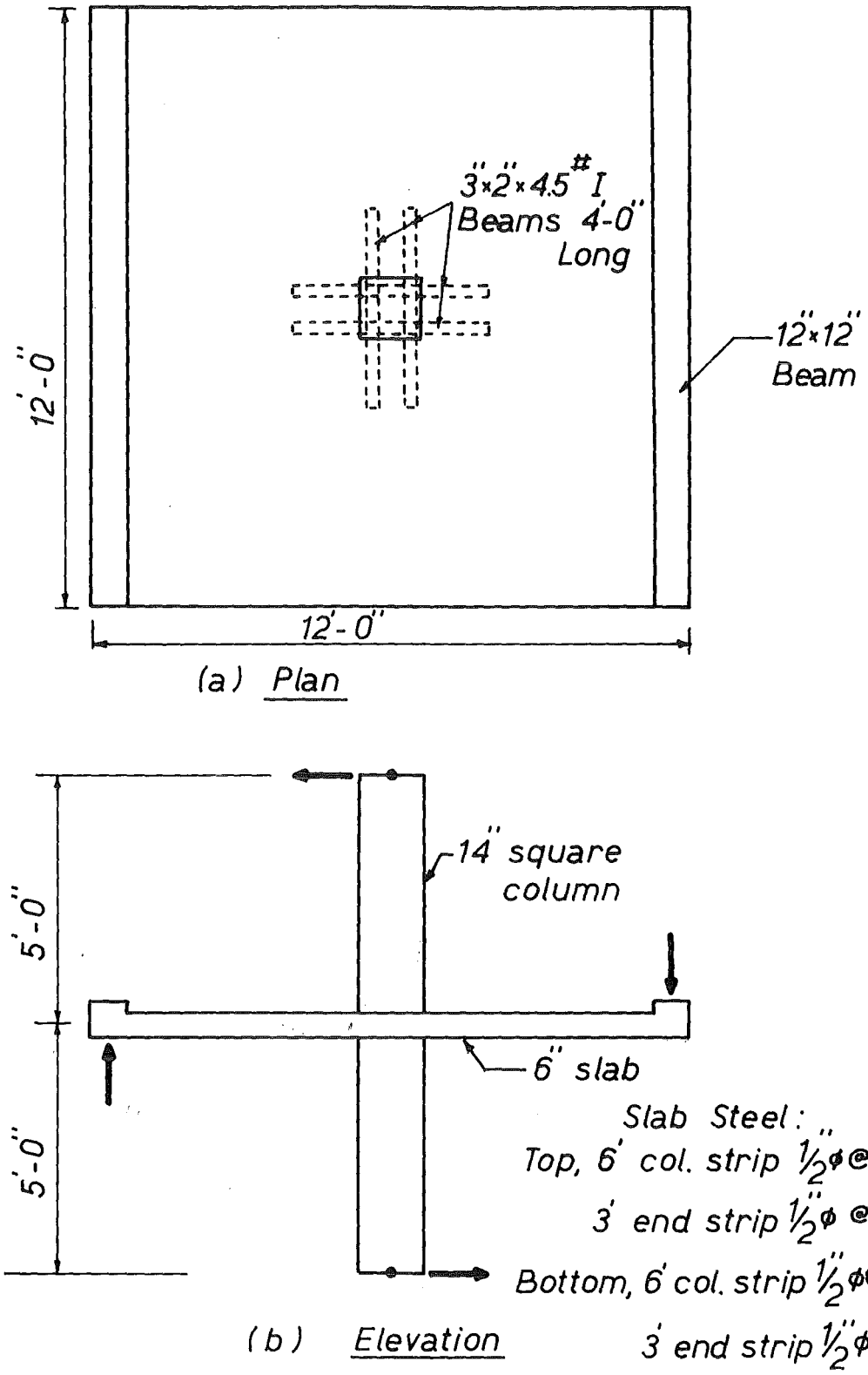

FIG. 3.5 DETAILS OF HOLLINGS' TEST STRUCTURE

of 4.25 in. and the crack pattern was only slightly extended from that of test 1. On unloading the slab edge recovered 2.25 in. In test 3 the jacking points were reversed and the permanent deflection left in the slab after test 2 was jacked back to zero. Then a further edge deflection of 2.5 in. was applied. Similar cracks patterns to those of test 1 appeared on the reverse faces of the slab. In test 4 both edges of the slab were jacked downwards to the limit of jack travel, which was 4 in. This produced wide cracking across the full width of the slab on or near the column centre line.

The test successfully showed that the particular flat plate to column connection can survive repeated floor to floor deflections of the order of 3 to 4 in. without loss of the vertical shear capacity of the connection.

(ii) P.C.A. Tests[19,29]

Experimental work has been in progress at the Portland Cement Association Laboratories, U.S.A., on the seismic resistance of the flat plate to column connection. Results of their tests have not yet been published except that of the 5th test which appeared in the ACI Journal[19] as a discussion of proposed revisions of the 1963 ACI Building Code. Some details of their specimens and loading arrangements as shown in Fig. 3.6 have been obtained from a private communication[29] from the P.C.A.

The test specimens measured 19 ft. x 13 ft. 1 in. with a $7\frac{1}{2}$ in. thick slab. The size of the column was 18 in. square and 10 ft. 9 in. in height. Their test procedure was to attach dead weights to the slab to bring the total shear up to the equivalent of dead load plus partitions plus 15 psf live load, then to apply equal and opposite deflections at the stiffening beams placed along the shorter edges to simulate the unbalanced moment. Seismic loading cycles were simulated by reversing the edge beam deflections in sign several times.

The main variable in their tests was the use of different shear reinforcements at the slab-column junction. Their first specimen

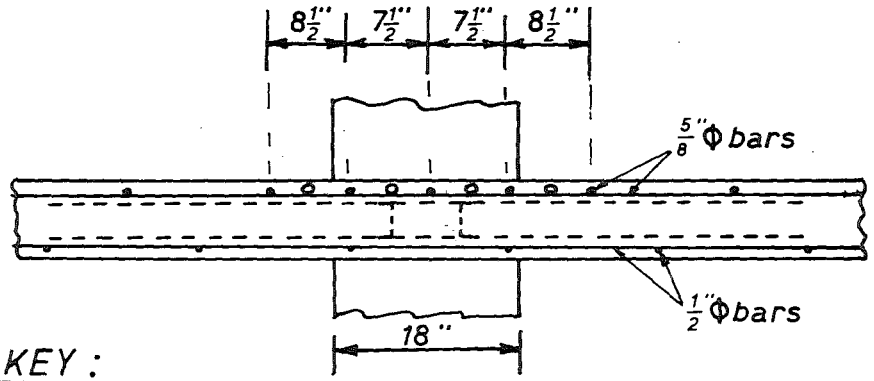

KEY :

- ○ 7/8" Φ Bars in Specimens 2 and 4
- Shearhead 3 [7.1 in Specimens 3 and 4

Reinforcement Details — Section A-A

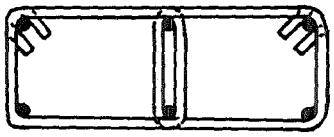

3/8" Φ Slab Stirrups for Specimen 5
Spacings 36 @ 3" centres from column face and remainder @ 6" centres

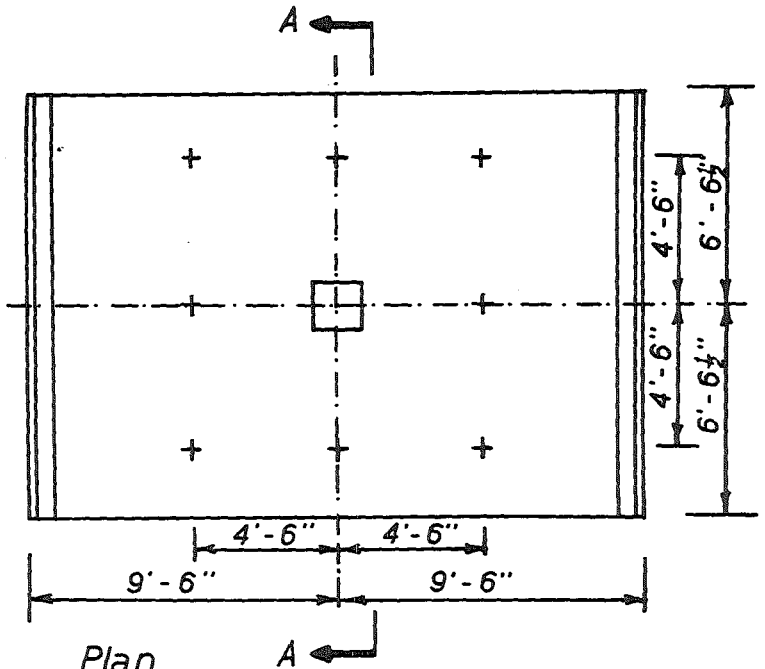

Plan

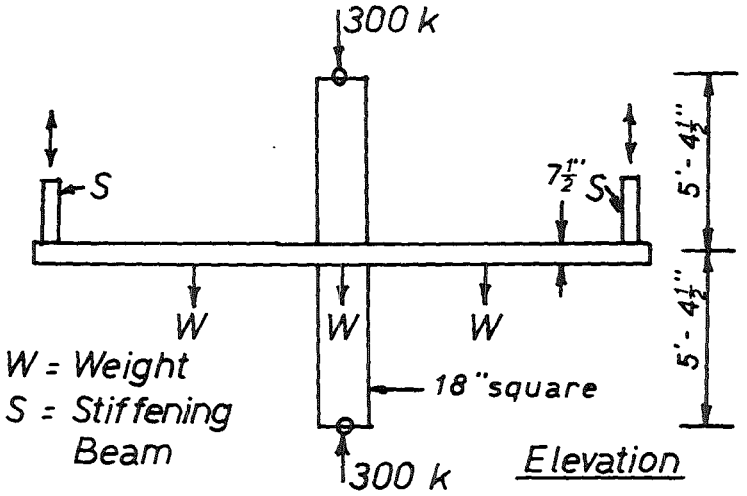

Elevation

FIG. 3.6 P. C. A. TEST SPECIMENS

contained only the basic reinforcement pattern without any shear reinforcement. Four $\frac{7}{8}$ in. diameter bars were added each way in the 2nd specimen. A shearhead made of two pairs of channels was added to the basic pattern for the 3rd test and both $\frac{7}{8}$ in. diameter bars and the shearhead were added for the 4th specimen. All these four specimens failed in shear before reaching general slab yielding. The maximum edge deflection attained was about 2 in. in 9 ft.

In the fifth specimen, the "integral beam" shear reinforcement shown in Fig. 3.6 was used. Closed hoops made of $\frac{3}{8}$ in. diameter bars at a maximum spacing of d/2 were used. Under application of unbalanced moment the test specimen was intact after sustaining slab end deflections of 8 in. in 9 ft. The integral beams maintained a high load carrying capacity in spite of extreme cracking and deformations.

Their test showed that closed stirrups can be adequately anchored in a slab less than 10 in. thick and that adequately anchored bars can be considered as fully effective shear reinforcement for slabs. Their proposal for a change in the shear reinforcement provisions in slabs has been adopted in Section 11.11.1 of the revised ACI Building Code (ACI 318-71)[13].

3.2.5 EFFECTIVENESS OF SHEAR REINFORCEMENT IN RESISTING PUNCHING SHEAR

(i) Recommendation by ACI Building Code (318-71)[13]

Until the publication of the latest ACI Building Code (ACI 318-71)[13] shear reinforcement formed from bars was considered entirely ineffective in slabs with a total thickness less than 10 in. This restriction on the use of shear reinforcement in slabs resulted from inadequately anchored shear reinforcement in the test specimens[6,8,31] considered in the report by ACI-ASCE Committee 326[12]. As a result of the test carried out at the Portland Cement Association Laboratory[19] on a $7\frac{1}{2}$ in. thick flat plate-

column specimen with shear reinforcement in the form of closed stirrups ACI Committee 318 revised the shear reinforcement provisions for slabs in the new ACI Building Code (ACI 318-71)[13] and Section 11.11.1 of the revised Code now reads:-

"Shear reinforcement consisting of bars or wires anchored in accordance with Section 12.13 may be provided in slabs. For design of such shear reinforcement, shear stresses shall be investigated at the critical section defined in Section 11.10.2 and at successive sections more distant from the support; and the shear stress v_c carried by the concrete at any section shall not exceed $2\sqrt{f'_c}$. Where v_u exceeds v_c, the shear reinforcement shall be provided according to Section 11.6".

(ii) New Evaluation of Punching Shear Tests by Herzog[30]

Herzog[30] made a new evaluation of the earlier punching shear tests[6,7,8] etc and derived three empirical equations in order to determine the effectiveness of shear reinforcement in the form of inclined bars, stirrups or shearheads.

For slabs without shear reinforcement Herzog[30] considered the nominal ultimate shear stress divided by the tensile strength of the concrete and the relative yield force of the flexural reinforcement as the two principal variables on which the punching shear strength of the slabs depended. The nominal ultimate stress in punching shear on a critical section taken at a distance d from the column face was given as

$$\frac{v_u}{\sqrt{f'_c}} = 2.64 + 0.00477\, \rho f_y < 6.3 \qquad \ldots (3.22)$$

where

v_u = nominal ultimate shear stress

f'_c = cylinder compressive strength of concrete

ρ = ratio of area of tension reinforcement to effective area of concrete

f_y = yield stress of reinforcement

For slabs with shear reinforcement in the form of inclined bars or

stirrups the efficiency of the shear reinforcement was calculated by the formula

$$\eta = \frac{A_v f_y \sin \alpha}{V'} \qquad \ldots (3.23)$$

where

η = efficiency of shear reinforcement

$A_v f_y \sin \alpha$ = vertical component of the yield strength of the actual shear reinforcement inclined at an angle α with the horizontal

V' = difference between the measured ultimate load and the punching resistance of the slab calculated from Eq. (3.22), ignoring the assistance of the actual shear reinforcement

From the 57 evaluated punching tests[6,8,10,31,32,33,34] on slabs with shear reinforcement Herzog found that the efficiency given by Eq. (3.23) could be taken as 39% with an unsatisfactory accuracy, the coefficient of variation amounting to 49.5%. Nevertheless, the punching load can be predicted sufficiently accurately with a coefficient of variation of 18.1%. It was found possible to increase the resistance to punching by 62% by providing shear reinforcement in the form of inclined bars or stirrups.

For slabs with shearheads, the calculated punching resistance, ignoring the assistance of the actual shearheads, was obtained from Eq. (3.22), and subtracted from the measured ultimate load. The resulting difference, multiplied by the unsupported length of the shearhead arm measured from the column face and divided by the sum of the plastic moments of all shearhead arms, was taken as the efficiency of the shearhead.

Herzog showed that the results of 16 punching tests by Corley and Hawkins[28] could be represented by the following formula

$$\eta = \frac{V' L_c}{\Sigma m_p} = 0.05 + 0.6 \left(\frac{L_c}{h} - 2.2 \right) \qquad \ldots (3.24)$$

where

V' = difference between the measured ultimate load and the punching resistance of the slab calculated from Eq. (3.22), ignoring the assistance of the actual shearheads

L_c = length of shearhead arm measured from the column face

Σm_p = sum of the plastic moments of all sheahead arms

h = depth of steel shapes in shearhead

The coefficient of variation for the efficiency of the shearhead was 25.9% for these 16 test results. The punching load could be predicted with a coefficient of variation of 5.9%. In the foregoing tests it was found possible to increase the punching resistance by 68% by providing shearheads.

(iii) Discussion of Effectiveness of Shear Reinforcement

The main purpose of shear reinforcement in slabs is to increase the resistance to punching sufficiently in order to secure full utilisation of the flexural capacity of the slabs. It is also necessary to know the effectiveness of various systems of shear reinforcement in relatively thin slabs. The P.C.A. Test[19] has successfully demonstrated that closed stirrups may be regarded as fully effective shear reinforcement. The ACI Building Code (318-71)[13] recommends shear reinforcement in the form of bars as 100% effective in slabs of any thickness, provided the shear reinforcement is adequately anchored. The effectiveness of this type of shear reinforcement is yet to be proved in slabs thinner than $7\frac{1}{2}$ in. which was the thickness of the P.C.A. test specimen.

Herzog's[30] finding that shear reinforcement in the form of bent bars or stirrups is only 39% effective in slabs may be attributed to the results of punching shear tests of many slabs[6,8,31] with inadequately anchored shear reinforcement. This will also explain the large coefficient of variation

of 49.5% of his evaluation of the efficiency figure of 39%.

In evaluating the efficiency of the shearhead Herzog[30] has put forward an alternative design procedure for shearhead reinforcement in slabs. However, his findings are based on concentrically loaded slabs.

Although the difference in effectiveness of shear reinforcement when provided as inclined bars or as stirrups could not be observed from the tests considered by Herzog, it has been found possible to increase the resistance of slabs to punching by 62% by providing bent bars or stirrups and by 68% by providing shearheads.

3.2.6 TESTS AT BRITISH RESEARCH STATION

Russell[35] has reported some preliminary tests carried out at the British Research Station on flat plates supported on several columns, which had to resist both vertical loads and horizontal wind loads. The object was to determine the potential limitations of flat slab construction and to assess the design requirements.

A total of six tests were conducted; one full size specimen and five $\frac{1}{3}$ scale models. The full size specimen or the prototype measured 21 ft. by 21 ft. with a 6 in. thick slab and was supported on four 12 in. square columns on a square grid of 15 ft. centres. The total height of each column was 10 ft., 5 ft. above and 4 ft. 6 in. below the surfaces of the 6 in. thick slab.

These tests could be divided into two groups. Group No. 1 consisted of the full size specimen and two exact models (Nos. 1 and 3) of the prototype. Model No. 1 had very weak columns and Model No. 3 had very strong columns. Group No. 2 comprised three models (Nos. 2, 4 and 5). No. 2 consisted of a single square panel with the columns at the corners. The column centres and dimensions were the same as models 1 and 3. The slab thickness was increased to 2 in. for this group compared with 1.8 in. for group no. 1. Models 4 and 5 both consisted of a square panel similar

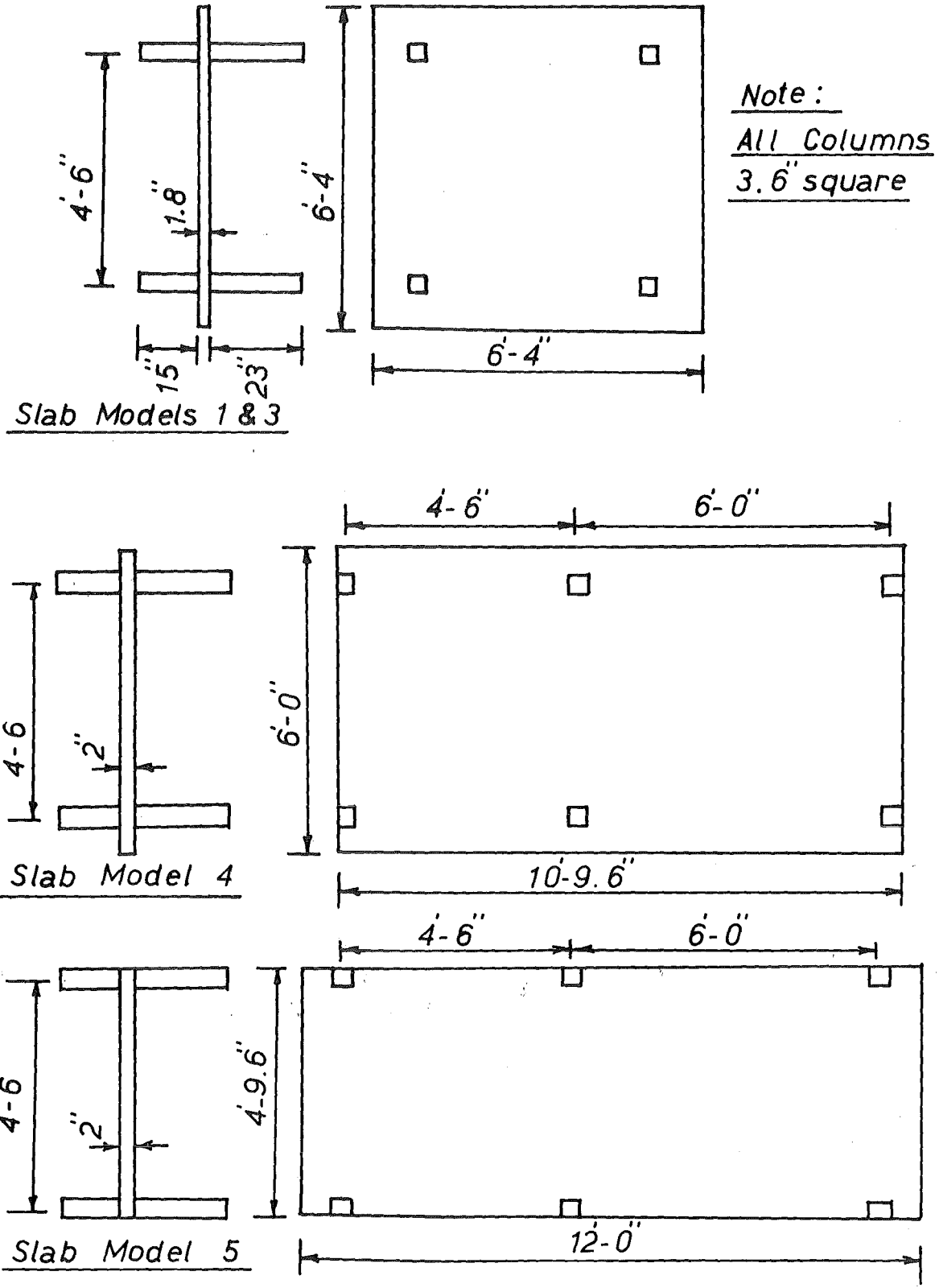

FIG. 3.7 - B. R. S. MODEL SLABS

to slab 2 with an adjoining rectangular panel. The column centres and dimensions of models 4 and 5 were the same but the locations of the slab edge with respect to columns differed. The details of the specimens are given in Fig. 3.7.

All specimens were subjected to three sets of loads - a uniformly distributed load on the slab, a vertical axial load on the column and a horizontal load on the column.

The prototype was designed for ultimate loads of 87 psf dead load, 200 psf imposed load and 3035 lb/column wind load on the basis of a collapse mechanism consisting of two parallel yield lines across the slab - a negative yield line directly above the leeward supports and a positive yield line on the windward side of the centre line. Failure did not take place at these loads. The cracks tended to be parallel to the faces of the columns or to radiate out from them in a manner resembling fan mechanism but none of the cracks extended the full width of the slab. Further increase in the loads caused local failure around the columns and the collapse mechanism consisted of a punching failure on two sides of the column.

In order to determine the punching shear strength of the prototype two punching shear slabs measuring 7 ft. square and 6 in. thick with a 12 in. square column in the centre of the slab were tested. The arrangement of the reinforcement was identical to the negative reinforcement in the column strip of the prototype. In punching slab no. 1 the load was applied axially to the column and the ultimate load of punching was in close agreement to that predicted by the empirical ultimate load equations[6,8,9,10,11] for punching shear strength of concentrically loaded slabs. In punching slab no. 2 an axial force and a bending moment in the N-S direction were applied through the upper column and an axial force and bending moments in both N-S direction and E-W direction were provided at the lower columns. The collapse mechanism and ultimate loads of the punching slab no. 2 and the

prototype were very similar.

In all but one of the tests the models failed by punching around the columns, usually on one or two sides but never on four sides. Model 1 failed in flexure because the columns were undersized for the ultimate bending moment.

Their tests show that it is possible for flat slab construction to resist combined vertical and horizontal loads but the omission of lateral bracing may lead to a very flexible structure and deflections could be excessive. No design recommendation was put forward for slab-column junctions transmitting both moment and shear.

From their tests it is also evident that the failure patterns and the ultimate loads of isolated slab-column tests are similar to those of multi-panel flat plate structures.

3.2.7 SEISMIC RESISTANCE OF FLAT PLATES

Tsuboi and Kawaguchi[36] carried out experimental studies to study the behaviour of flat slabs under column top moments. Their 100 cm. square 3 cm. thick slabs contained centrally located 20 cm. square column stubs. Monotonously increasing and reciprocally repeated moment loadings were applied through the column stub while two opposite slab edges were supported and the other two edges left free. Three of the nine specimens were made of plain mortar but the other six slabs had varied distribution of reinforcement, the total amount of which was constant in all six specimens. They found that the distribution of longitudinal reinforcement affected the punching shear resistance around the column and repeated load reduced the punching shear resistance. The concept of effective width was found to be useful for the practical design of flat slabs and from test results they obtained the effective width to be equal to 0.58 to 0.61 of the side dimension of the square slabs in the elastic state.

None of their specimens contained any form of shear reinforcement.

They did not propose any theoretical procedure for calculating the ultimate strength of slab-column connections.

3.2.8 CONCLUSIONS

For flat plate-column junctions without shear reinforcement transferring moment and shear, Di Stasio and Van Buren's[14] working stress design method gives a factor of safety greater than 2 when compared with the tests reported by Moe[8], and Hanson and Hanson[16].

The methods recommended by Moe[8], ACI Committee 326[12] and ACI Committee 318[13,23] predict the ultimate strengths of the test specimens[8,16] with a varying degree of safety and this variation is primarily due to adoption of a constant value of K by each of these methods. Factors such as moment to shear ratio, relative stiffness of the column and the slab and the flexural capacity of the slab are likely to influence the proportion of moment transferred by shear stresses. These methods are good design tools but cannot be regarded as true ultimate strength design procedures.

Hawkins and Corley's[20] ultimate strength method gives more accurate results than the previous methods. However, their method needs some modifications and in its present form it is too involved to be used as a design method.

Very little is known from the existing literature about the method of design for flat plate to column connections with shear reinforcement transferring moment and shear. More investigations are needed to assess their design requirements and to determine the effectiveness of various forms of shear reinforcement in preventing punching shear failures.

Seismic resistance of flat plate to column junctions with or without shear reinforcement needs to be examined in respect of ductility available at the junctions and loss in load carrying capacity due to reversal of applied bending moments.

3.3 EXPERIMENTAL STUDY OF INTERIOR FLAT PLATE-COLUMN CONNECTIONS

SUMMARY

A series of eight tests were conducted on half scale models of reinforced concrete interior flat plate-column specimens under combined vertical and lateral loadings. Three specimens were without any shear reinforcement at the slab-column junctions while the remaining five contained various shear reinforcement arrangements. The results presented include the experimental failure loads, modes of failure, load deflection graphs, stresses in slab bars and shear reinforcement and the ductility available at junctions with or without shear reinforcement, particularly under seismic loading conditions.

3.3.1 INTRODUCTION

In recent years, with the increase in the popularity of flat plate concrete structures as a structural system, there is a growing need for experimental study of the ability of flat plate-column junctions to transfer moment and shear, particularly under earthquake loading conditions. The objects of this experimental study are threefold.

Firstly, more test results are sought to substantiate the existing theories and the theory presented in Section 3.4 on the strength of slab-column junctions transferring moment and shear.

Secondly, tests are required to be carried out to find methods of increasing the shear strength of junctions by using various reinforcement arrangements in the form of bars or structural steel sections. These tests will enable one to determine the effectiveness of various types of shear reinforcement and to develop a guide to their design provisions.

Thirdly, there is a lack of information on the seismic resistance of

slab-column junctions with or without shear reinforcement. The deterioration of the load carrying capacity due to reversal of bending moments and the ductility that is available at such junctions require a close examination. Tests need to be conducted to study these aspects of slab-column junctions under seismic loading conditions.

In order to fulfil these objectives a series of eight tests were conducted on half scale models of reinforced concrete interior flat plate-column specimens under combined vertical and lateral loadings. Three of the specimens designated as 1 , 2 and 3C did not contain any shear reinforcement while the remaining five specimens designated as 4S , 5S , 6CS , 7CS and 8CS had various arrangements of shear reinforcement at the slab-column junctions in the form of inclined cranked bars, shearheads fabricated from structural steel shapes and vertical closed stirrups. Reversals of loading simulating earthquake effects were applied to the specimens identified by the letter C following their numbers. The letter S indicates the specimens with shear reinforcement.

A detailed description of the material properties, test equipment and testing procedure used in these tests is given in Appendix B.

3.3.2 DESIGN OF TEST SPECIMENS

(i) Selection of Test Specimen

The test specimens are intended to represent half scale models of an interior column and the surrounding slab, which form part of a multistorey flat plate structure, shown shaded in Fig. 3.8(a). The deformed shape of the structure under vertical and horizontal loadings is shown in Fig.3.8(b). An isolated view of the internal slab-column junction under consideration is shown in Fig. 3.8(c). An imposed horizontal displacement, Δ , induces horizontal and vertical reactions H and X respectively. In Fig. 3.8(d) the entire slab-column junction has been rotated until the two column

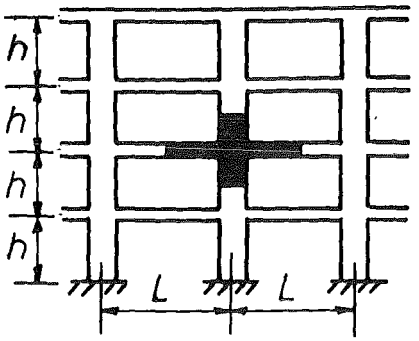

(a) Flat Plate Structure

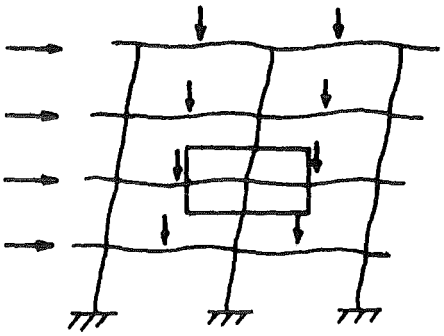

(b) Deformed Shape of Structure

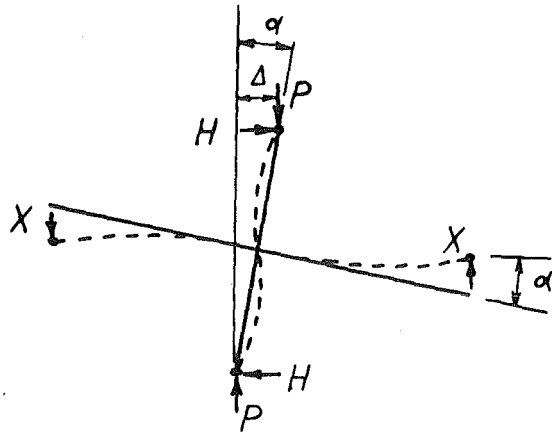

(c) Isolated Slab-Column Specimen

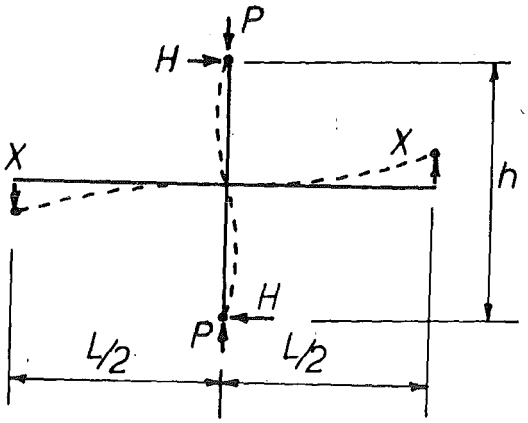

(d) Test Slab-Column Specimen Rotated Through Angle α

FIG. 3.8 — SELECTION OF SLAB-COLUMN TEST SPECIMEN

inflection points are on the same vertical line, giving a more convenient orientation for testing purposes. The column axial load P represents the loading due to the weight of the building above the particular junction as well as due to the overturning moment on the structure. The vertical load, X , applied at the ends of the slab and the reactive lateral loads, H , induced at the ends of the column represent the forces applied by the lateral loading.

The test specimens have been selected on the basis of Fig. 3.8(d) which is assumed to simulate the behaviour of the real structure.

(ii) Discussion of Method of Loading

The longitudinal plan dimensions of the slab surrounding the interior column are chosen to coincide with the points of contraflexure, which are assumed to be located at 0.5 L from the column centre line, where L denotes the span between columns. In the actual test of the specimens the upward and downward vertical forces X of Fig. 3.8(d) were applied at the two opposite ends of the slab. These loads were applied along the edge by equal and opposite edge displacements. Elastic analysis[37,41] shows that internal actions resulting from the applied moment at the slab-column junction are confined to a localised portion of the slab in the vicinity of the column and are not greatly influenced by the outer boundary conditions of the floor plate. Thus the test results are unlikely to be influenced by the exact manner of application of the loads at the midspan region of the slab. The equal and opposite edge displacements consisted of either line loads applied along the whole width of the slab edges or point loads applied to the edges through several loading points. In testing specimen 1 line loads were used (vide Appendix B) but owing to difficulties in spreading the load uniformly across the entire slab width this method was abandoned in all subsequent tests. Instead the slab edges were loaded by four equal point loads in the remaining tests (vide Appendix B).

(iii) The Prototype Structure

The prototype structure on which the test specimens were modelled was chosen as representative of a flat plate structure with design loads and dimensions as used for multistorey apartment buildings. The prototype consisted of 18 in. square columns at 20 ft. centres on a square grid with interstorey heights of 10 ft. The slab was designed as an interior flat plate floor with a service live load of 60 lb/ft^2 and a dead load of 87.5 lb/ft^2, giving a total service load of 147.5 lb/ft^2. The material strengths used in the design of the slab by the ultimate strength design method were a concrete cylinder strength of 4,000 lb/in^2 and a steel yield stress of 40,000 lb/in^2.

The slab thickness of the prototype was found to be 7 in. and the following spacings of $\frac{3}{4}$ in. diameter bars were required in each direction:

	Column Strip	Middle Strip
Top	7 in.	14 in.
Bottom	14 in.	14 in.

In the prototype it was necessary to use $\frac{3}{4}$ in. diameter bars so that the reduction in scale to the test specimens, in which $\frac{3}{8}$ in. diameter deformed bars were used, could be made directly. Otherwise it would not have been possible to use deformed bars in the test specimens as deformed bars are not available in smaller diameters than $\frac{3}{8}$ in. in New Zealand.

(iv) Details of Test Specimens

As the test specimens were half scale models of the prototype structure the overall depth of the model slab became $3\frac{1}{2}$ in. and the size of the column was reduced to 9 in. x 9 in. with the height as 5 ft. The reinforcement required for the column strip in the prototype was used as the general reinforcement pattern in all the test specimens. This resulted in $\frac{3}{8}$ in. diameter deformed bars spaced at $3\frac{1}{2}$ in. centres in the top and at 7 in. centres in the bottom in each direction.

The column was reinforced with eight $\frac{3}{4}$ in. diameter deformed bars which were necessary to make the ultimate flexural capacity of the column greater than that of the slab. This ensured that any failure would occur in the slab and not in the column. Ties made of $\frac{1}{4}$ in. diameter plain bars spaced at 8 in. centres were used in the column outside the slab region.

Since the test specimens were subjected to an unbalanced moment in one direction only, the side of the slab transverse to the direction of bending was condensed to 3/4th of its length for the sake of ease in handling the specimens in the laboratory as well as reducing the size of the test rig. The overall size of the slab-column specimens became 10 ft. x 7 ft. 6 in. in plan with the height of the column as 5 ft. The details of the specimen dimensions and the basic reinforcement pattern used in all the eight tests are shown in Figs. 3.9 and 3.10.

The details of reinforcement at the slab-column joint regions of the specimens were as follows:

Specimen Nos. 1 , 2 and 3C

Fig. 3.11 shows the details of reinforcement at the slab-column junctions. These three specimens did not contain any shear reinforcement at the slab-column junctions.

Specimen No. 4S

This specimen was provided with shear reinforcement in the form of 4 Nos. $\frac{3}{8}$ in. diameter inclined cranked bars placed in each direction. The details are shown in Fig. 3.12. The design was based on shear stresses computed by the method of ACI 318-71 for a combined vertical load of 8040 lb. and the ultimate flexural capacity of 527,000 lb.in. The vertical load represented the prototype dead load and a live load of 20 lb/ft^2. The ultimate flexural capacity was then arrived at by considering the yield-line pattern A1 shown in Fig. 3.82. The cranked bars were provided with sufficient anchorage lengths according to the ACI 318-71 Building Code.

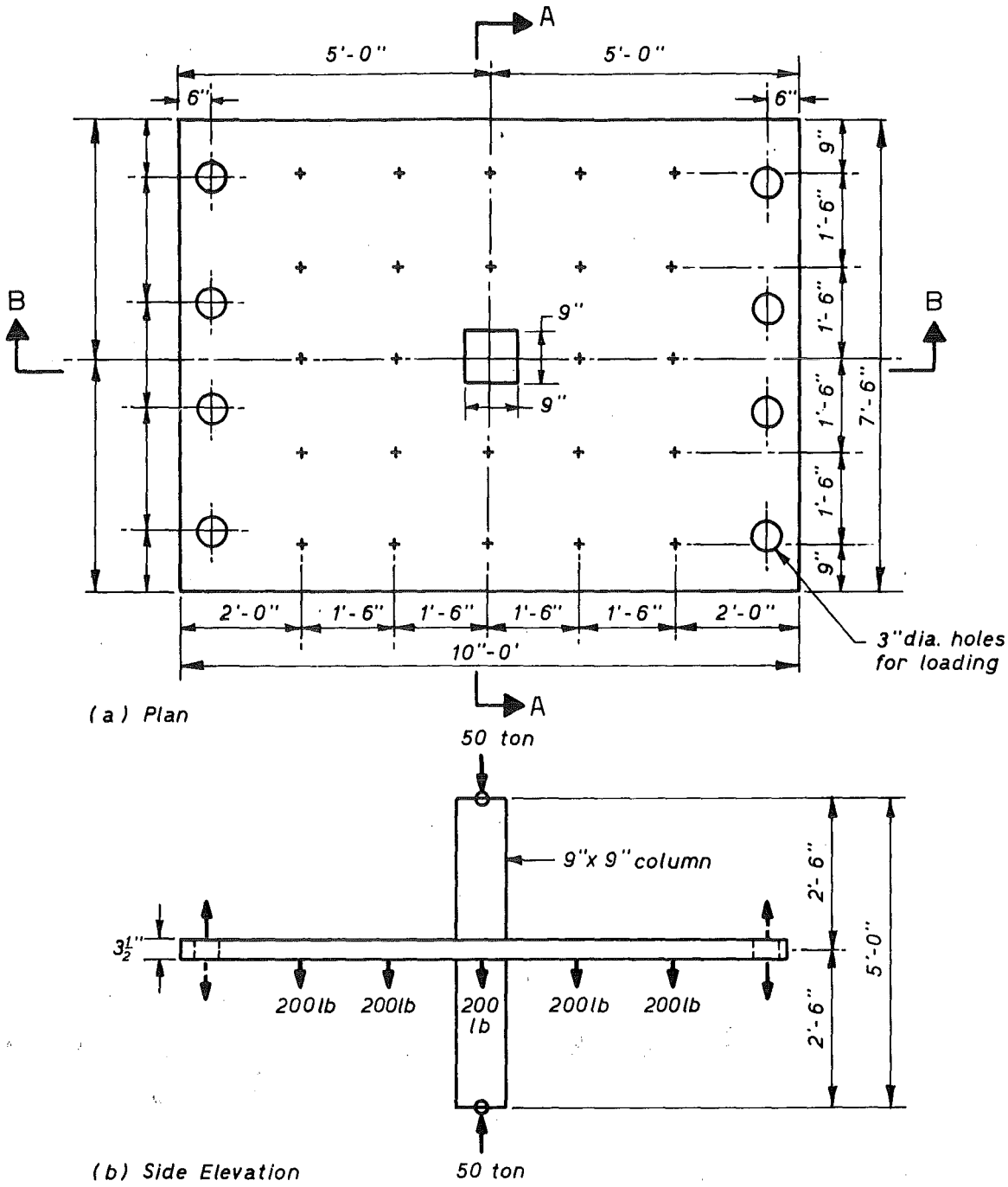

FIG 3.9 SLAB-COLUMN TEST SPECIMEN

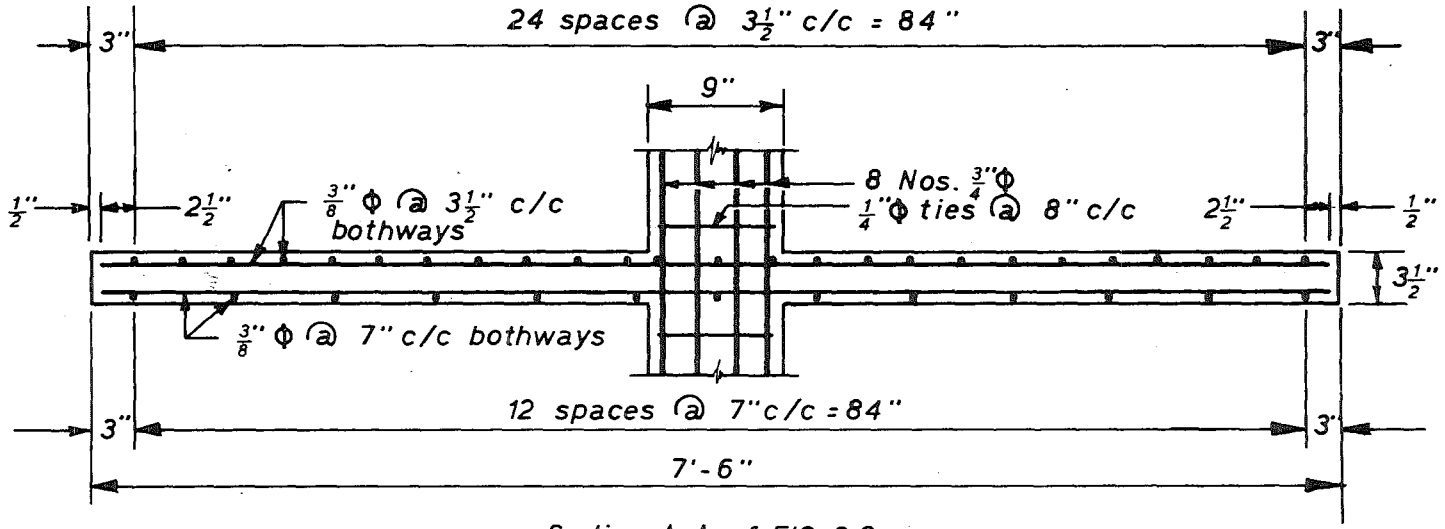

Section A-A of FIG. 3.9

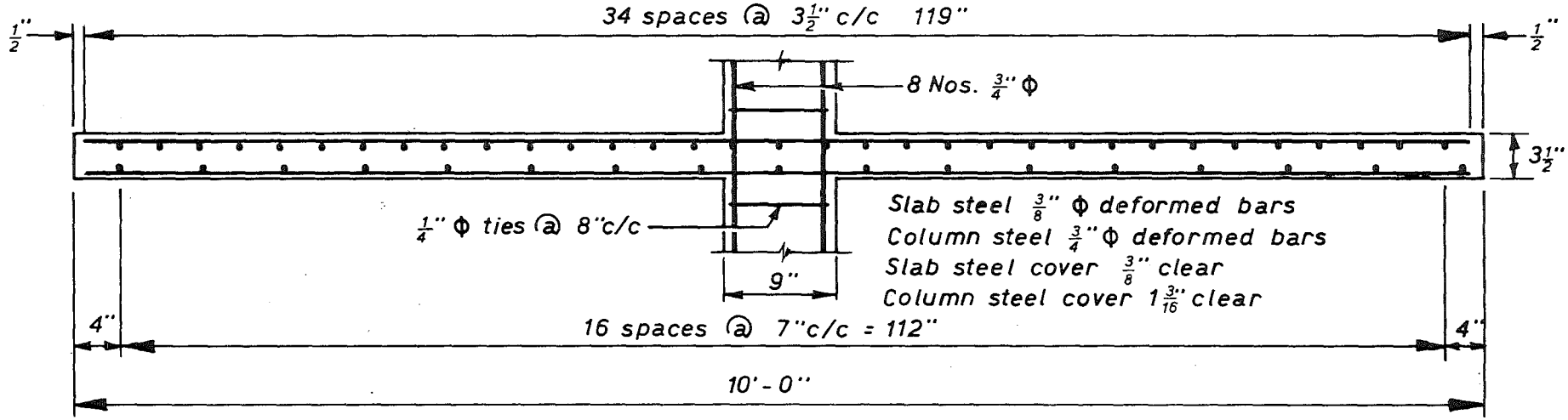

Section B-B of FIG. 3.9

FIG. 3.10 DETAILS OF REINFORCEMENT

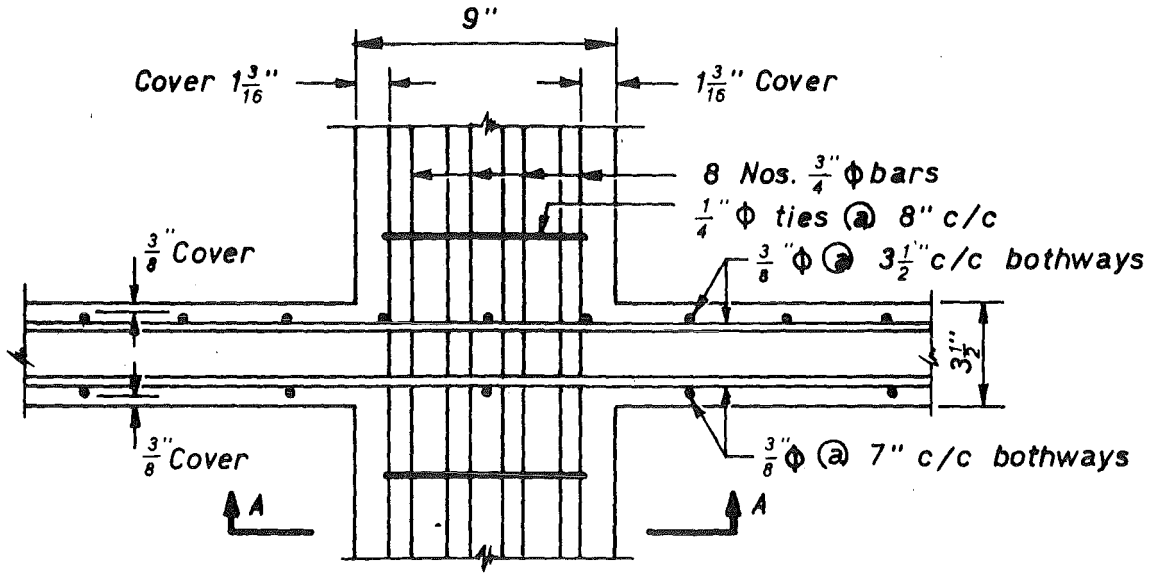

(a) Slab-Column Junction

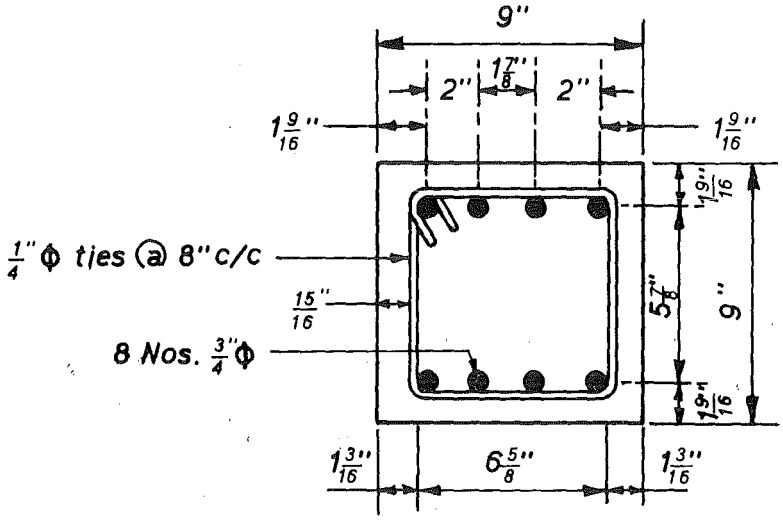

(b) Section A-A Column Cross Section

FIG. 3.11 DETAIL OF JOINT WITHOUT SHEAR REINFORCEMENT

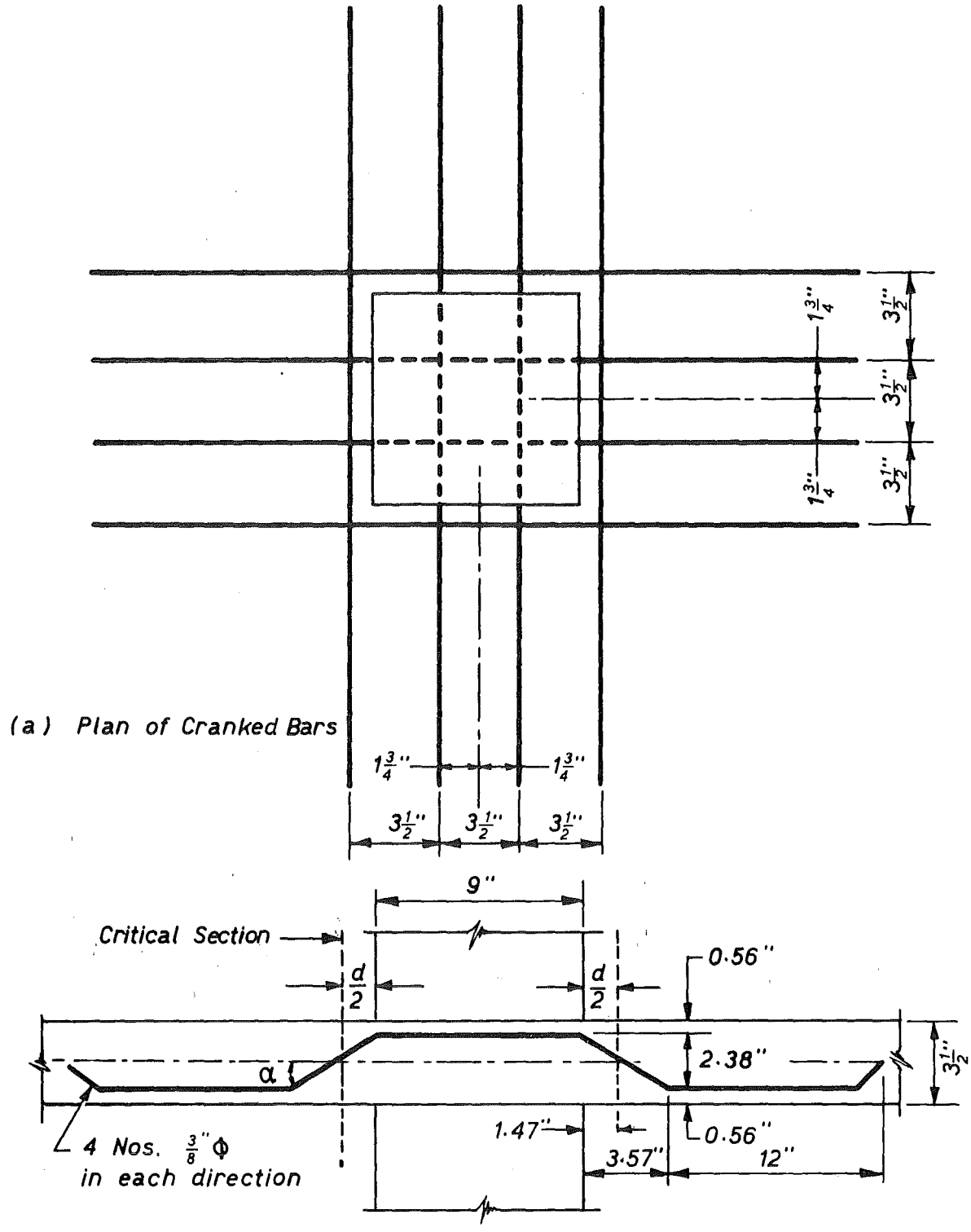

FIG 3.12 INCLINED CRANKED BARS FOR SPECIMEN 4S

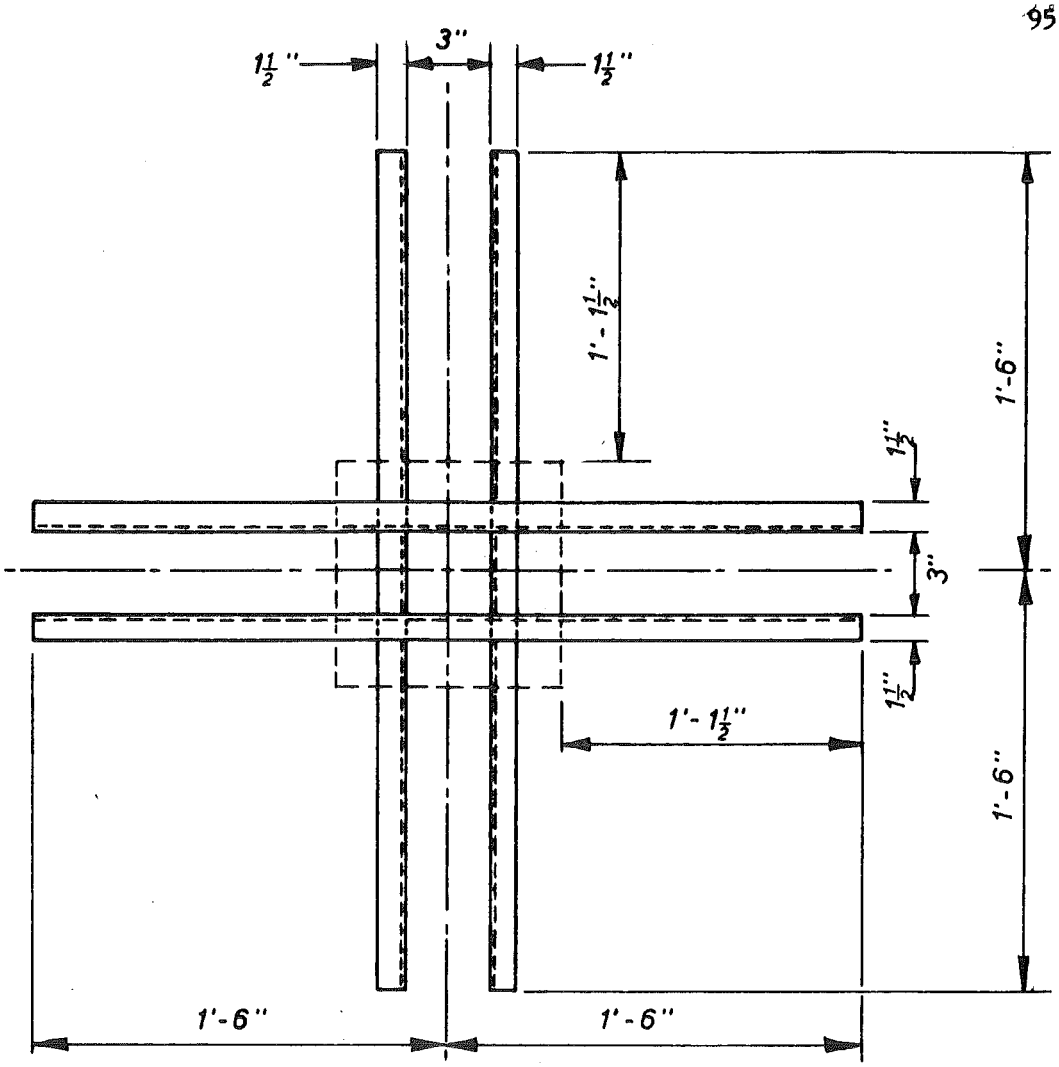

(a) Plan at Column - Slab Junction

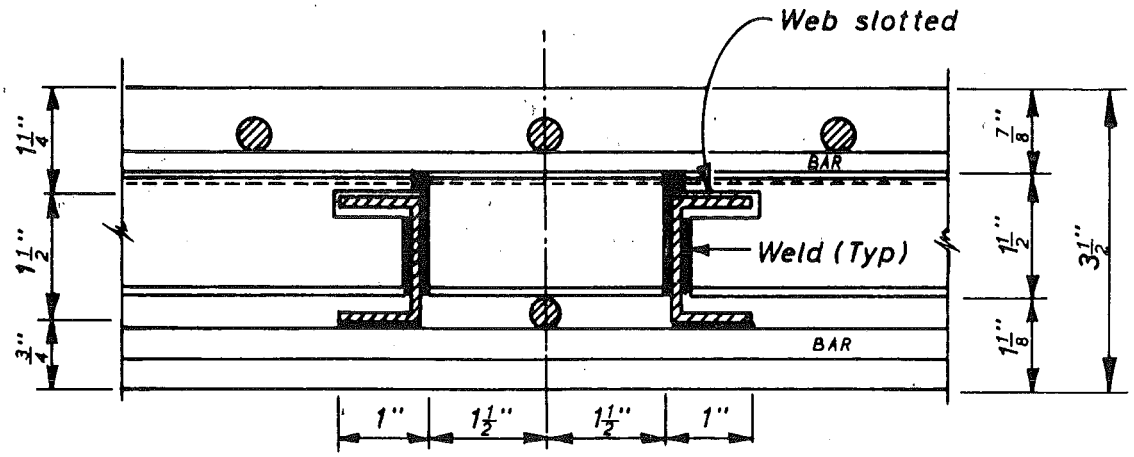

(b) Section Through Slab Showing Intersection of 1½"x 1"x 0.128"thick Channel Sections

FIG. 3.13 SHEARHEAD FOR SPECIMEN 5S

Specimen No. 5S

Fig. 3.13 shows the details of the shearhead reinforcement used in this specimen. The shearhead consisted of pairs of $1\frac{1}{2}$ in. (depth) x 1 in. (wide) x 0.128 in. (thick) channel sections placed 3 in. apart back to back in both directions. One pair was continuous and the other pair had to be fabricated and welded to get the final shape shown in Fig. B.5. The channel section mentioned above was the largest possible size that could be placed within the slab and column reinforcement. As standard channel section of this size was not available, these sections had to be cut from rectangular hollow sections and finished off by machining to get the required dimensions.

Since there was no established procedure available for designing shearheads for flat plate-column junctions under combined shear and bending moment it was necessary to make an estimate of the size required. The junction needed to be capable of transferring a vertical shear of 8040 lb. and an ultimate moment of 527,000 lb.in. First, the strength of the unreinforced junction was computed by Eq. (3.9) as recommended by the ACI 318-71 and was found to be 277,000 lb. in. This meant that an additional moment of 250,000 lb. in. was required to be transferred by the shearhead alone. The moment which could be transferred by each $1\frac{1}{2}$ in. x 1 in. x 0.128 in. channel section was estimated as 68,400 lb. in. due to its own flexural capacity plus the moment couple due to upward and downward web shear acting at transverse faces of the critical section. The total number of channel sections required in each direction was found to be 4 . The limited space available within the reinforcement at the slab-column junction and the difficulty in fabricating and welding 4 channel sections in each direction ruled out the possibility of using this design. It was, therefore, decided to use 2 channels in each direction at the slab-column junction. The total length of the shearhead was arrived at by using Eq. (3.42).

Specimen 6CS

For this specimen vertical closed type of stirrups consisting of 4 legged 3/16 in. diameter plain bars were used as shown in Fig. 3.14. The stirrups enclosed 3 bars at top and 3 bars at bottom where it was necessary to provide two additional bars. The maximum shear stress was calculated on the critical section by using Eq. (3.9) of the method of ACI 318-71 due to a combined shear of 8040 lb. and unbalanced moment of 527,000 lb. in. The area of shear reinforcement was computed for nominal stresses in excess of $4\sqrt{f'_c}$ psi. It was found that 4 legs of 3/16 in. diameter bars placed at a spacing of $1\frac{1}{2}$ in. centres met the necessary requirements. One additional stirrup was placed within the column section on each face of the column. Stirrups were provided up to a distance of half the span of the slab measured from the column face.

Specimen No. 7CS

In this case the area and the extent of shear reinforcement was kept the same as those used for specimen No. 6CS. Here 2 legged $\frac{1}{4}$ in. diameter plain bars were used in place of 4 legged 3/16 in. diameter bars. The details are shown in Fig. 3.15.

Specimen No. 8CS

As shown in Fig. 3.15 this specimen contained 2 legs of 3/16 in. diameter plain bars at a spacing of $1\frac{1}{2}$ in. centres in each direction. The area of shear reinforcement required was halved in this case in order to compare its performance with specimen No. 6CS and 7CS.

3.3.3 TEST EQUIPMENT AND PROCEDURE

The test rig with a slab-column specimen in position is shown in Fig. 3.16. The top and bottom ends of the column were grouted into steel caps. The steel caps had semicircular grooves to accommodate steel pins and the specimen was supported by placing the column vertically between

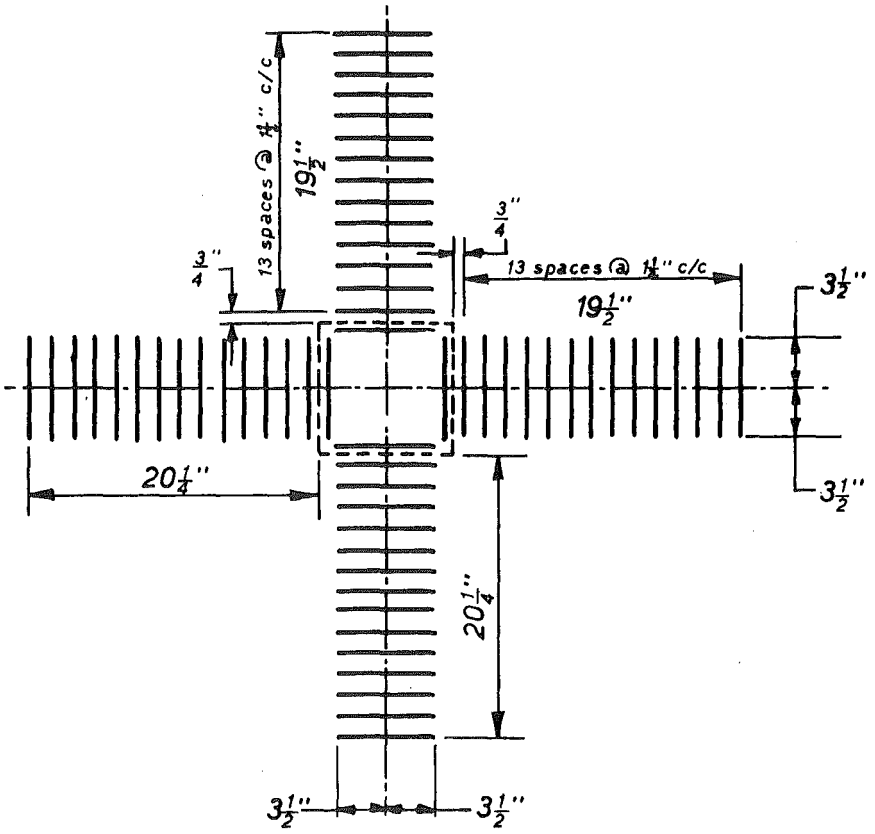

(a) Plan of Closed Vertical Stirrups

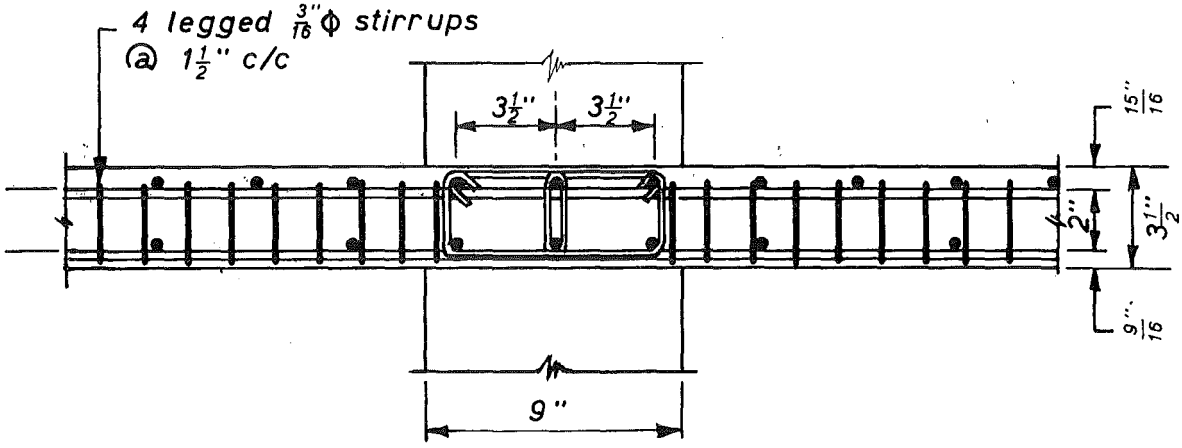

(b) Typical Section through Slab showing Stirrups for Specimen 6C

FIG 3.14 CLOSED STIRRUPS FOR SPECIMEN 6CS

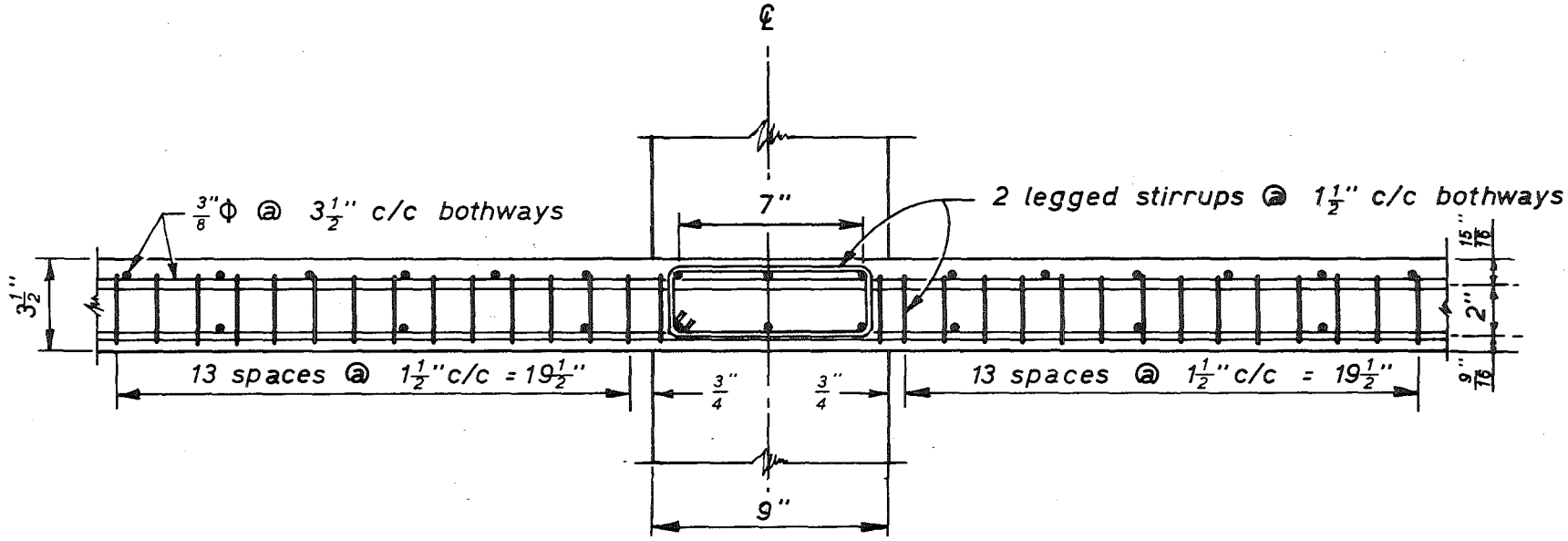

Section Through Slab Showing Stirrups

Diameter of stirrups for Specimen 7CS = $\frac{3}{16}$ in.
" " " " " 8CS = $\frac{1}{4}$ in

FIG 3.15 CLOSED STIRRUPS FOR SPECIMENS 7CS AND 8CS

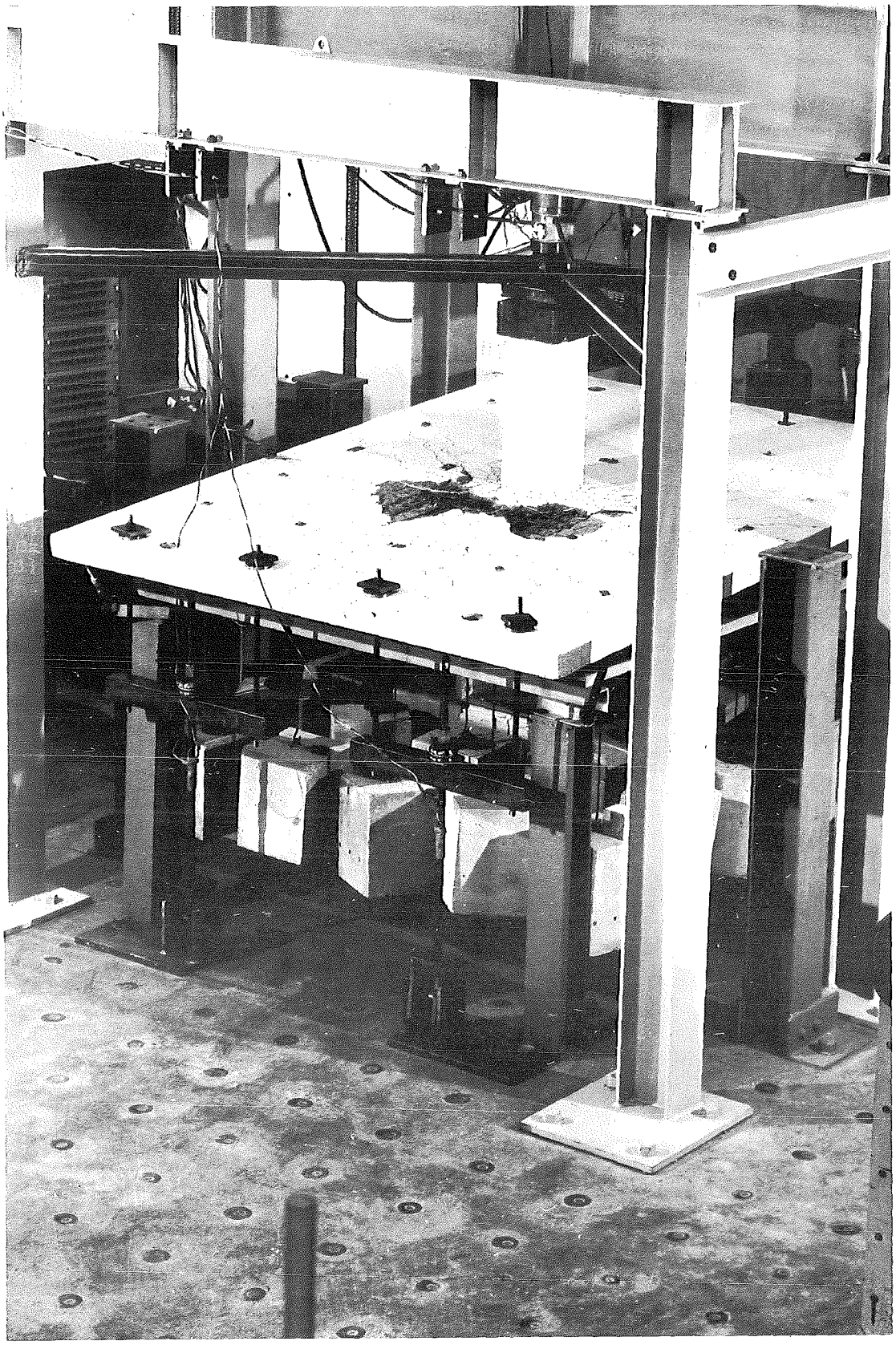

FIG. 3.16 SLAB-COLUMN SPECIMEN IN THE TEST RIG

the steel pins. The pins allowed free rotations but no lateral displacements at these points. Three types of loading were used during each test.

An axial load of 50 tons was applied to the column through a hydraulic jack and kept constant during testing. This load of approximately $\frac{1}{3}$ of the ultimate axial capacity of the column was chosen to represent the column loads in the lower storeys of a flat plate structure.

To simulate the prototype dead load plus some live load, 24 concrete blocks, each weighing 200 lbs., were suspended from the slab in a symmetrical manner. This suspended load applied 63.75 lb/ft^2 and was considered to be made up of the dead load of an extra $3\frac{1}{2}$ in. of slab (to bring the dead load up to that of the prototype) plus a live load of 20 lb/ft^2 (i.e. $\frac{1}{3}$ of the service live load of 60 lb/ft^2 was considered to be present during the earthquake). The location of these load points are shown in Fig. 3.9. The total shear force applied around the slab-column junction in each test was thus 8040 lb. which included the dead weight of the $3\frac{1}{2}$ in. thick test slab. This value was used in the design of shear reinforcement for the five specimens in Section 3.3.2 (iv).

The unbalanced moment loading was simulated by an upward edge load at one of the shorter sides of the slab and a downward edge load at the opposite side. In testing specimen 1 the edge load was applied through $3\frac{1}{2}$ in. x $3\frac{1}{2}$ in. steel tube seated in plaster along the slab edge by two 1 in. diameter high tensile bars spaced at 4'-6" apart as shown in Fig. B.9 of Appendix B. This method was not found to be satisfactory. Due to shrinkage effects the loading edges of the slab became slightly convex on the top surface and concave on the bottom surface. As a result the steel tube was not in contact with the slab surface throughout its whole length and this resulted in uneven distribution of load. In all subsequent tests the steel tube was discarded in favour of point loads.

Point loads at each end were applied by equal deflections at two pairs

of steel tie bars which passed through 3 in. diameter holes placed 6 in. inside the slab edge as shown in Fig. 3.9. Each pair of tie bars was loaded through a crosshead and a centrally placed high tensile bar by means of a mechanical screw device. These details are given in Figs. B.10 and B.12. The use of screw device permitted controlled deformations to be applied at each end. The edge loadings were increased and decreased in order to apply moment cycles simulating the effect of earthquake loading on the specimen.

Deflections were measured by dial gauges along the centre lines of the column and the slab at selected points in the longer direction. The location of dial gauges is shown in Fig. B.15. Steel strains were measured by electrical resistance strain gauges in the slab reinforcement as well as in shear reinforcement. Strain gauge locations are shown in corresponding diagrams of stress distribution in steel such as Figs. 3.19, 3.31, 3.40 etc.

The first step in the test procedure was to set up the slab-column specimen in the test rig carefully. The top and bottom ends of the column were enclosed within steel cappings set in 1:2 cement sand mortar in position in the test rig. After capping a load of about 2 tons was applied on the capping to squeeze out excess mortar and this load was sustained until the time of testing.

Before the commencement of actual testing this load on the column was removed. The initial readings were recorded for all dial gauges, strain gauges and load cells. A load of 50 tons was then applied to the column. The dial gauge and strain gauge readings were again noted. The next step was to hang the 200 lb. concrete blocks from the slab at 24 positions. This was done by taking the concrete blocks one by one and placing them symmetrically over the allocated 24 positions. Another set of dial and strain gauge readings were taken. After the column was loaded and the

concrete blocks were suspended from the slab equal and opposite edge deflections were imposed on the two edges of the slab in increments of 0.1 in. After each increment loads in the high tensile bars, by means of which edges were loaded, were recorded from the Budd bridge and a set of dial gauge and strain gauge readings were noted.

The upward and downward edge deflections were maintained equal but the edge loads were not equal. This was due to the fact that at the downward loading end the applied edge load and the weight of concrete blocks were acting in the same direction whereas they were acting in the opposite directions at the upward loading end.

For specimen Nos. 1 , 2 , 4S and 5S the upward and downward edge loadings were increased gradually in the same directions until failure occurred. For specimens 3C , 6CS , 7CS and 8CS the edge loads were reversed several times to simulate earthquake loading cycles described in the following section on the test results and performance of each specimen separately. The time to perform each of these tests was about 5 to 10 working days.

3.3.4 TEST RESULTS

The test results presented include the strength and ductility of slab-column junctions, load displacement graphs, failure modes and stresses in the slab reinforcing bars and shear reinforcement for all the specimens tested.

As a measure of ductility the ratio of maximum edge displacement to the edge displacement at which first yielding occurs in a slab reinforcing bar has been used in this thesis. This ratio is similar in concept to the ductility factor which is used in reinforced concrete frames and defined as the ratio of lateral deflection at ultimate to lateral deflection at first yield.

(i) Description of Loading Cycle

In testing specimens 1 , 2 , 4S and 5S monotonously increasing bending moment was applied. The specimens 3C , 6CS , 7CS and 8CS were subjected to several cycles of bending moment reversals. The loading cycle used for specimen 3C is shown in Fig. 3.29. This loading sequence was not intended to simulate any particular earthquake but it was rather regulated by the edge displacements to generate elastic and post-elastic loading history.

Fig. 3.49 shows the loading cycle used for specimens 6CS , 7CS and 8CS , all of which contained shear reinforcement. Edge displacements imposed on these specimens were considerably larger than those used for specimen 3C which was without any shear reinforcement. This cycle was adopted because it was felt that these specimens would exhibit large ductility and that the important requirement of the loading simulation was to generate a post-elastic loading history covering the likely range of deformations from moderate to severe earthquakes.

Static cyclic loading was used because of the convenience of applying this type of loading. The use of slow reversals of load to represent dynamic loading is thought to be conservative because the strength of concrete and steel increases with increasing rates of strain.

(ii) Strength and Ductility of Slab-Column Connections

The ultimate shear force transferred from the slab to the column due to the self weight of the slab and the suspended concrete blocks simulating $\frac{1}{3}$ of the live load was 8040 lb. in the case of each test specimen. The experimental moment and the ductility characteristics of all the test specimens are given in Table 3.2. This Table lists the moment at first yield, the maximum moment reached during testing and the moment at the maximum edge displacement. Also shown in the Table are the edge displacements at which first yielding occurs, the edge displacement at maximum moment and the maximum edge displacement. The ratio of maximum edge

TABLE 3.2

MOMENT AND DUCTILITY CHARACTERISTICS

SPECIMEN NO.	SHEAR REINFORCEMENT	MOMENT AT FIRST YIELD K.in.	MAXIMUM MOMENT K.in.	MOMENT AT MAXIMUM DISPLACEMENT K.in.	RATIO OF MOMENT AT MAXIMUM DISPLACEMENT TO MAXIMUM MOMENT	EDGE DISPLACEMENT AT WHICH FIRST YIELDING OCCURS in.	EDGE DISPLACEMENT AT MAXIMUM MOMENT in.	MAXIMUM EDGE DISPLACEMENT in.	RATIO OF MAXIMUM EDGE DISPLACEMENT TO EDGE DISPLACEMENT AT YIELD	FAILURE MODE
1	NIL	133	270	227	0.84	0.40	2.0	2.40	6.00	BRITTLE SHEAR
2	NIL	178	334	261	0.78	0.60	2.2	2.70	4.50	BRITTLE SHEAR
3C	NIL	191	317*	235**	0.74	0.60	2.0	2.80	4.67	BRITTLE SHEAR
4S	CRANKED BARS	207	367	295	0.81	0.70	2.6	2.90	4.14	BRITTLE SHEAR
5S	SHEARHEAD	200	350	208	0.59	0.70	2.5	6.55	9.36	DUCTILE
6CS	CLOSED STIRRUPS 4 LEGGED 3/16" Ø	179	340*	177**	0.52	0.50	2.4	9.60	19.20	DUCTILE
7CS	CLOSED STIRRUPS 2 LEGGED 1/4" Ø	192	369*	181**	0.48	0.60	2.2	11.2	18.70	DUCTILE
8CS	CLOSED STIRRUPS 2 LEGGED 3/16" Ø	162	309*	171**	0.51	0.60	3.0	10.7	17.80	DUCTILE

* Maximum moment reached in all cycles

** Moment at maximum displacement in last load cycle

displacement to edge displacement at first yield gives a measure of the ductility of slab-column connections. This Table also indicates the degradation of load carrying capacity which is given as the ratio of moment at the maximum edge displacement to the maximum moment attained during testing.

From these edge displacements of the test specimens the interstorey deflections of the prototype structure could be approximately obtained. Since the height of the column was half the longest span of the slab in the test specimens the lateral floor to floor deflections measured between the top and bottom ends of the column works out to be nearly equal to the edge displacement at one end of the slab. Therefore, the interstorey deflections of the prototype structure which is twice the size of the test specimens would be twice the edge displacements of the test specimens.

(iii) Behaviour of Specimen No. 1

Type of Loading

This specimen was subjected to an increasing bending moment applied in one direction only. The applied shear force was constant at 8040 lb.

Load-displacement Curve

The plots of applied upward and downward edge loads versus corresponding edge displacements of the slab are shown in Fig. 3.17 and 3.18. The displacements plotted were measured at the centre of the edge. The load-displacement curve becomes non-linear after the first increment of loads. In both the curves there are several kinks which coincide with the break during testing and are due to creep effects. The maximum moment was reached when both the upward and downward edge displacements were 2.0 in. At this edge displacement the upward edge load was 2780 lb. and the downward edge load was 2215 lb. The specimen failed when the edge displacement was being increased from 2.4 in. to 2.6 in. The failure was of a sudden punching shear type which took place in the slab. At the edge displacement of 2.4 in. the upward end load was 2540 lb. and the downward end load was 1660 lb.

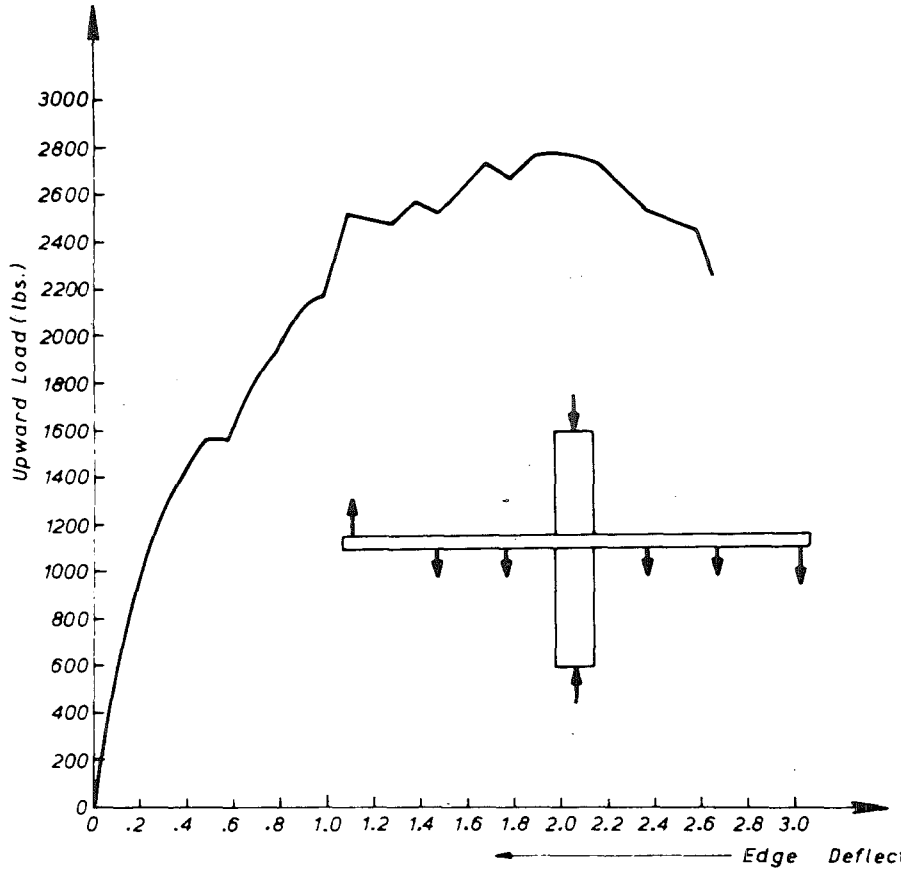

Fig. 3.17 – UPWARD LOAD

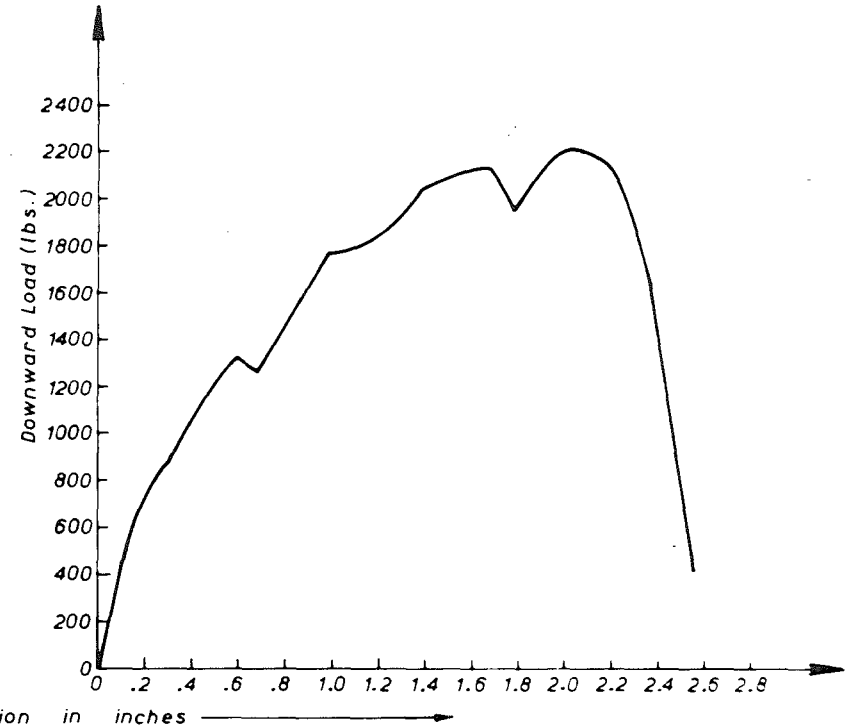

Fig. 3.18 – DOWNWARD LOAD

– LOAD–DISPLACEMENT CURVES FOR SPECIMEN 1 –

Stresses in Slab Bars

Fig. 3.19 shows the stresses in five slab reinforcement bars attained at the maximum applied moment and also at the moment at the maximum edge displacement. First yielding occurred in the top bar, T3 , passing through the centre of the column at an imposed edge displacement of 0.4 in., when the applied moment was 133 kip. in. At the maximum applied moment of 270 kip. in. strain gauges T2, T3 and T4 placed on the top bars and B2, B3 and B4 placed on the bottom bars indicated yielding of steel at those positions. The top bars T1 and T5 and the bottom bars B1 and B5 did not yield at the time of failure.

Crack Propagation

Small cracks formed near the junction of the column and the tension face of the slab after the first increment of upward and downward edge loadings. Cracks were marked and their widths measured during testing. The maximum crack widths recorded were 0.005 in. at 0.6 in. edge displacement, 0.007 in. at 0.9 in. edge displacement and 0.010 in. at 1.7 in. edge displacement. At 2.0 in. of edge displacement when the maximum applied moment was recorded the crack at the slab-column junction on the tension face of the slab at the downward loading end opened up to 1/16 in. The crack pattern at this edge displacement is shown in Fig. 3.20. Apart from the big crack just mentioned other cracks were numerous and very fine, none exceeding 0.010 in.

Mode of Failure

The specimen failed in punching shear which occurred in the slab suddenly near the column face subjected to downward edge loading. The inclined cracks extended from the intersection of the column face and the compression face of the slab toward the tension face of the slab at a distance of about 1'-3" from the column face, making an average angle of about 13° with the horizontal. The failure surface is shown in Fig. 3.21 and the deflected shape of the slab at failure is shown in Fig. 3.22.

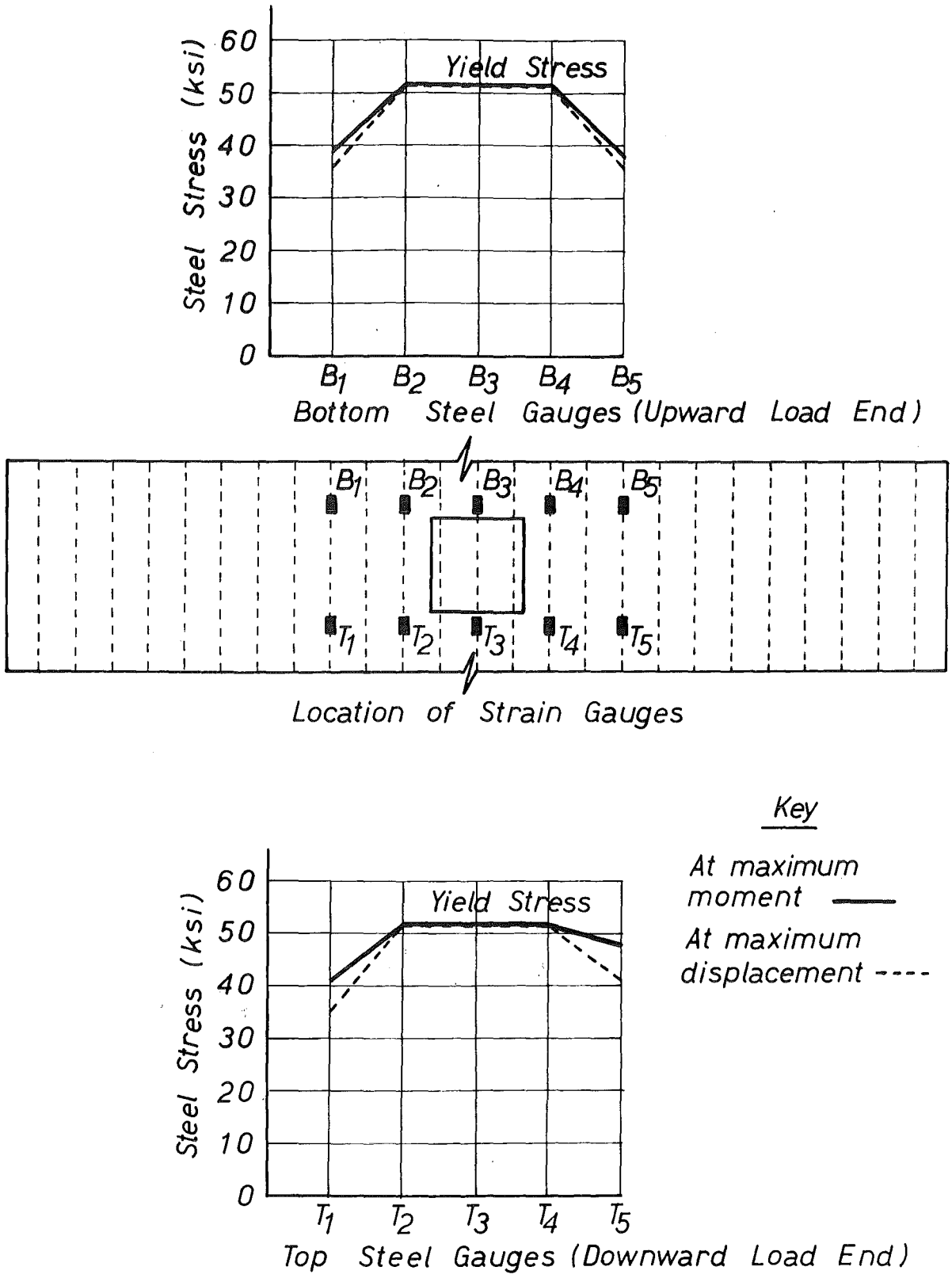

FIG. 3.19 STRESSES IN SLAB STEEL OF SPECIMEN 1

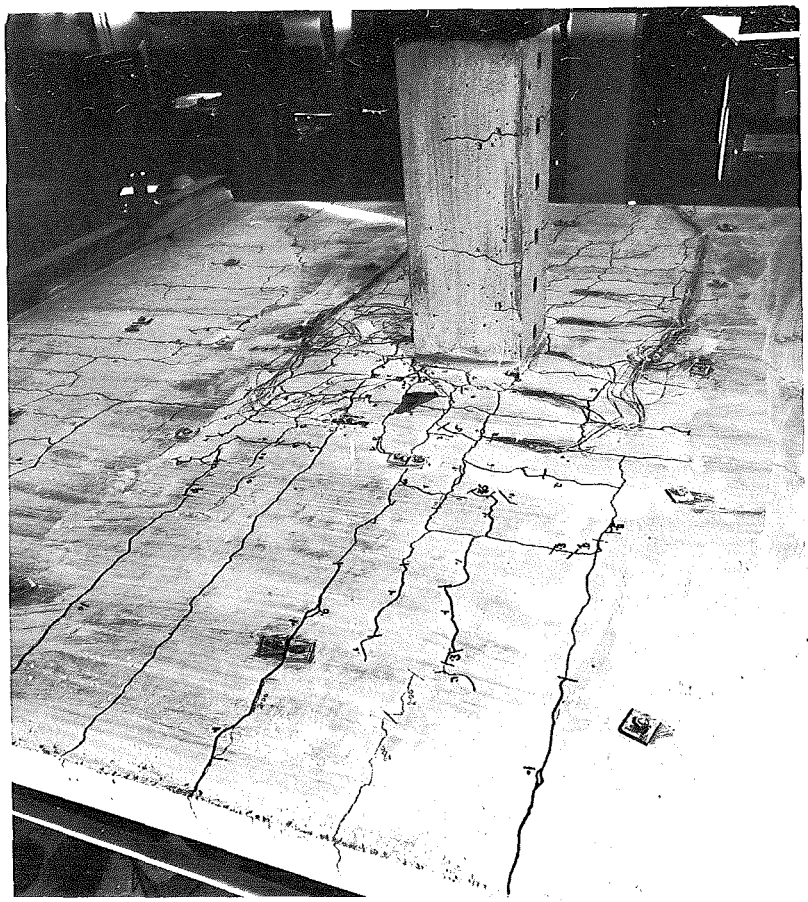

FIG.3.20 CRACK PATTERN OF SPECIMEN 1 AT 2 IN. DEFLECTION

FIG. 3.21 FAILURE SURFACE OF SPECIMEN 1

(iv) Behaviour of Specimen No. 2

Type of Loading

This specimen was loaded to failure in one way bending similar to the specimen No. 1 with a constant shear force of 8040 lb. acting at the slab-column junction.

Load-displacement Curve

Figs. 3.23 and 3.24 show the plots of upward and downward edge loads versus corresponding edge displacements of the slab. These are similar to those for specimen No. 1 but the upward load-displacement curve indicates higher load carrying capacity than the previous one. The maximum moment was reached when both the upward and downward edge displacements were 2.2 in. At this stage the upward edge load was 3970 lb. and the downward edge load was 2210 lb. The specimen failed when the edge displacement was being increased from 2.7 in. to 2.8 in. The failure was of punching shear type occurring in the slab quite suddenly.

Stresses in Slab Bars

The stresses in five slab reinforcement bars obtained at the maximum applied moment and just before failure are shown in Fig. 3.25. The top bar, T3 , yielded first at an imposed edge displacement of 0.6 in. when the applied moment was 179 kip.in. At the maximum applied moment of 334 kip. in. the top bars T2 , T3 and T4 and the bottom bars B1 , B2 , B3 and B4 yielded in tension. The top bars T1 and T5 and the bottom bar B5 did not reach yield point at failure.

Crack Propagation

The crack pattern just before failure on the tension face of the slab at the downward loading end is shown in Fig. 3.26. The imposed edge displacements are shown marked in the figure at the time of formation of these cracks. The largest crack again formed at the junction of the column and the tension face of the slab at the downward loading end. This crack

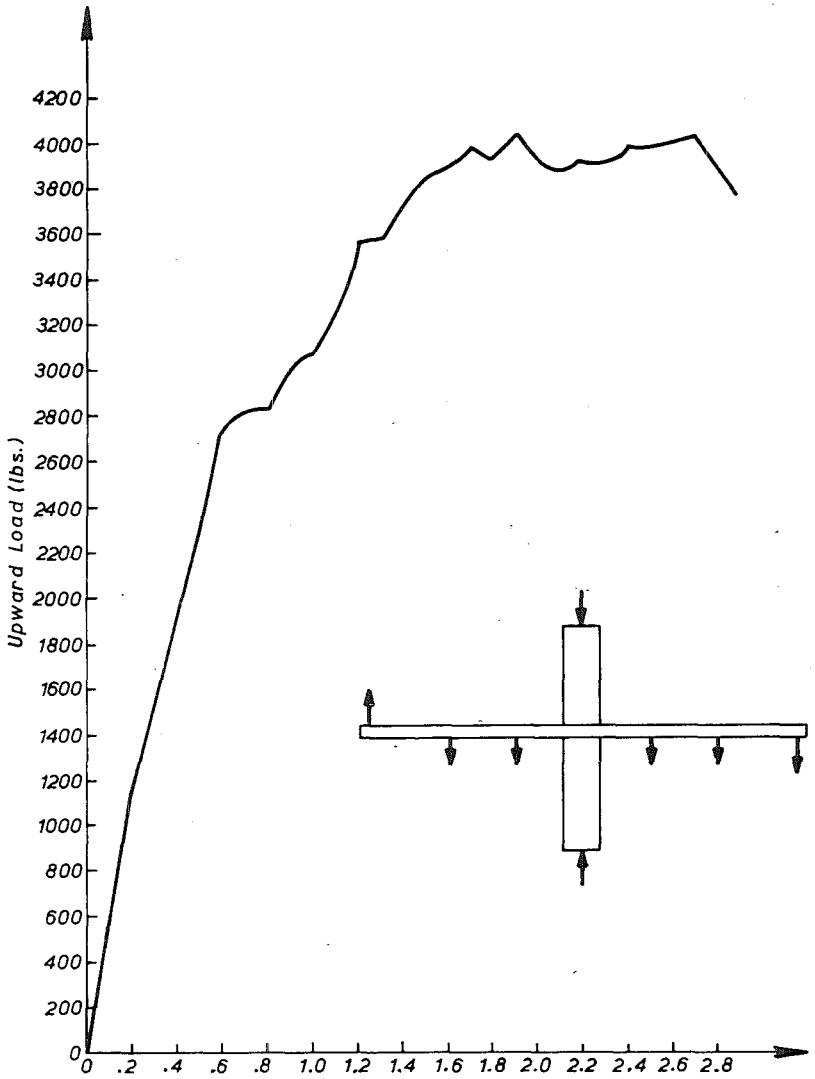

Fig. 3.23 — UPWARD LOAD

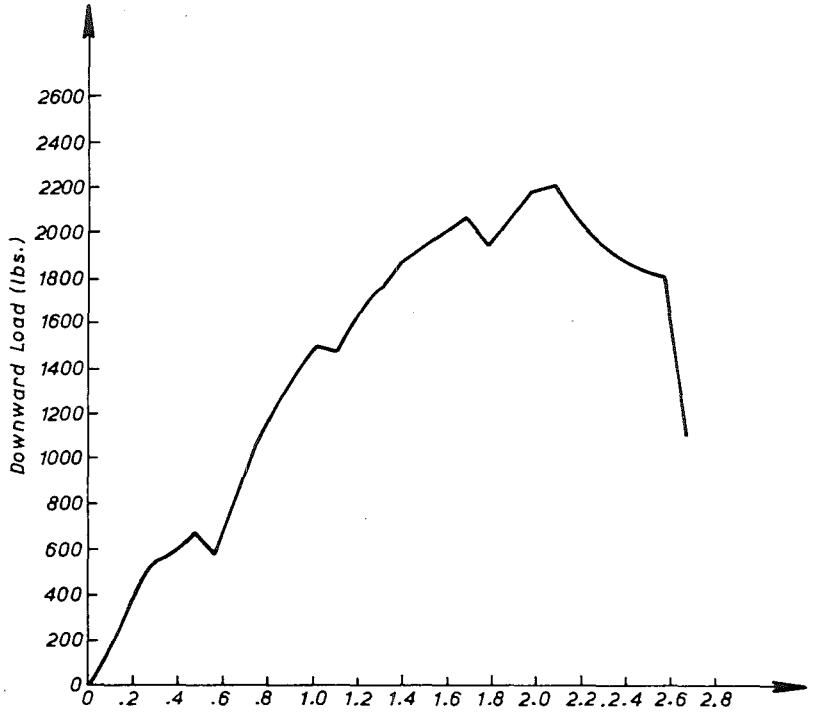

Fig. 3.24 — DOWNWARD LOAD

Edge Deflection in inches

— LOAD — DISPLACEMENT CURVES FOR SPECIMEN 2 —

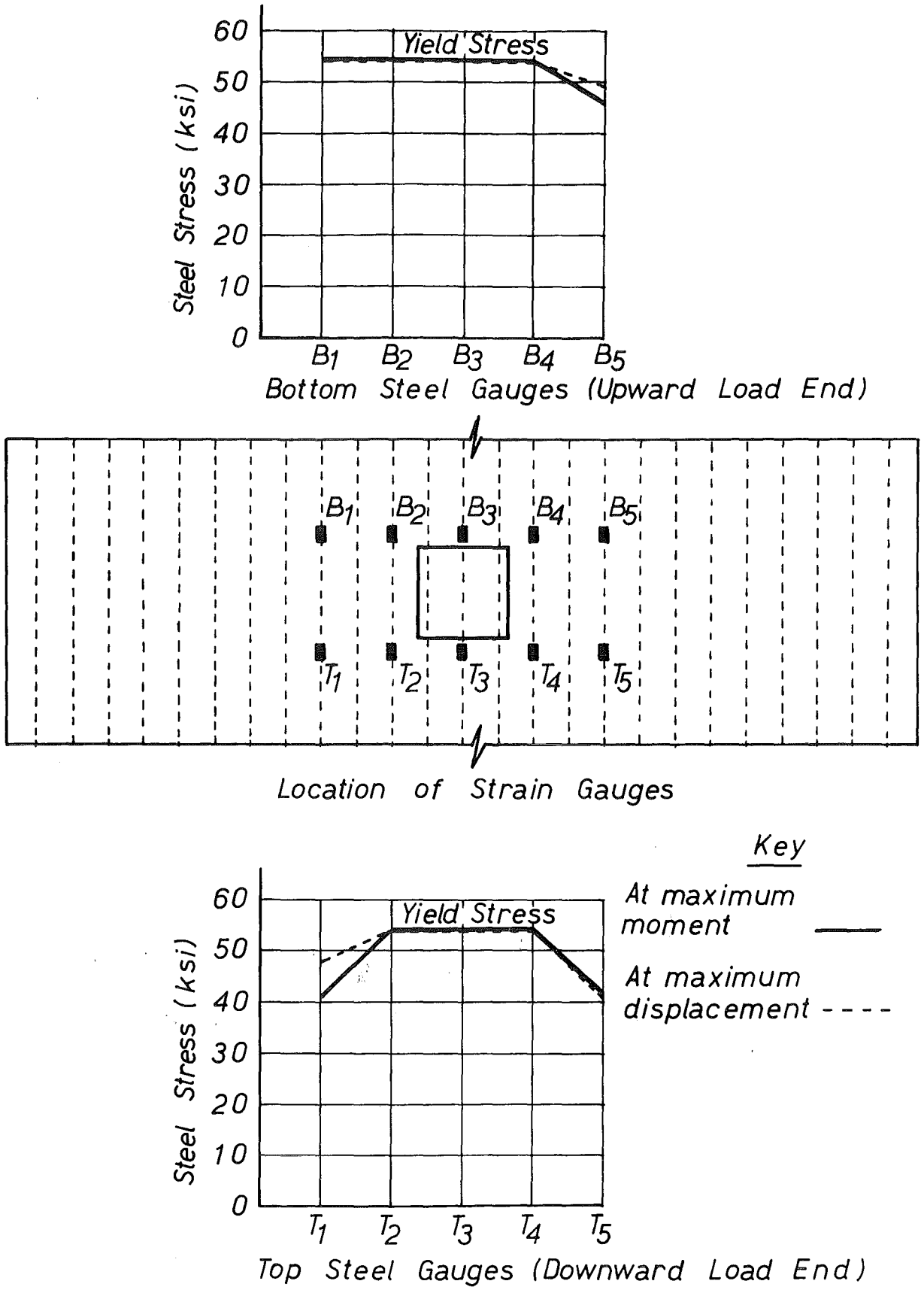

FIG. 3.25 STRESSES IN SLAB STEEL OF SPECIMEN 2

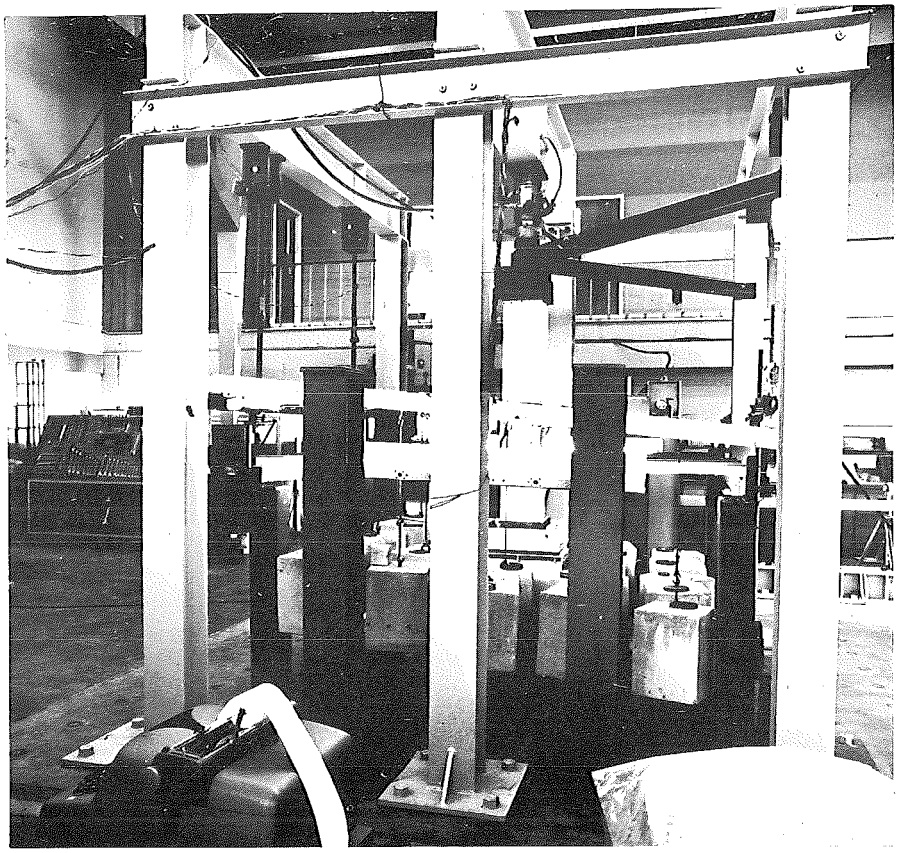

FIG. 3.22 DEFLECTED SHAPE OF SPECIMEN 1

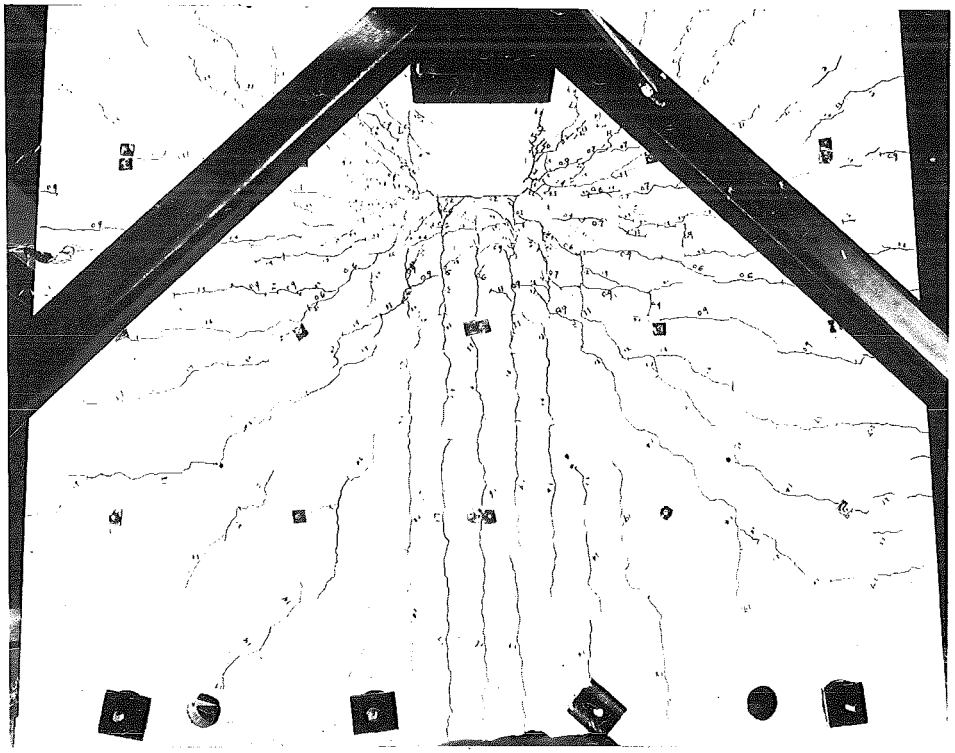

FIG. 3.26 CRACK PATTERN OF SPECIMEN 2 AT FAILURE

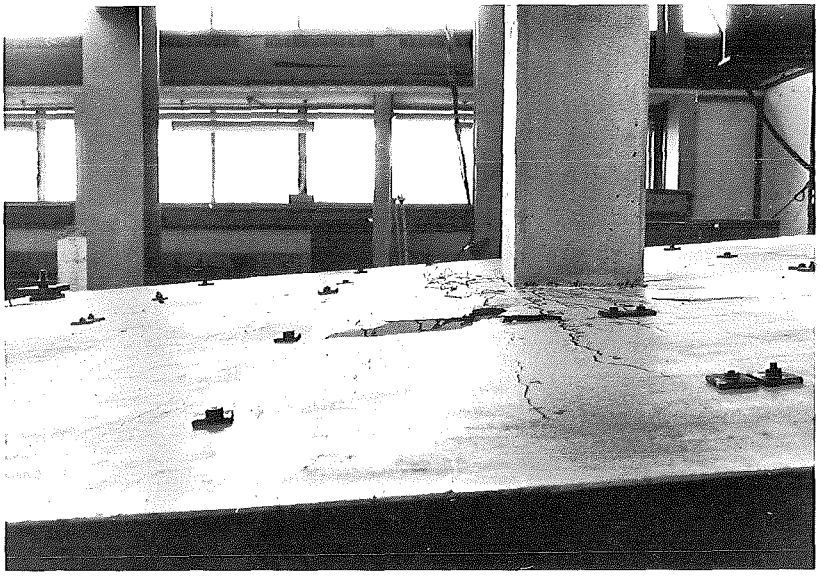

FIG. 3.27 FAILURE SURFACE OF SPECIMEN 2

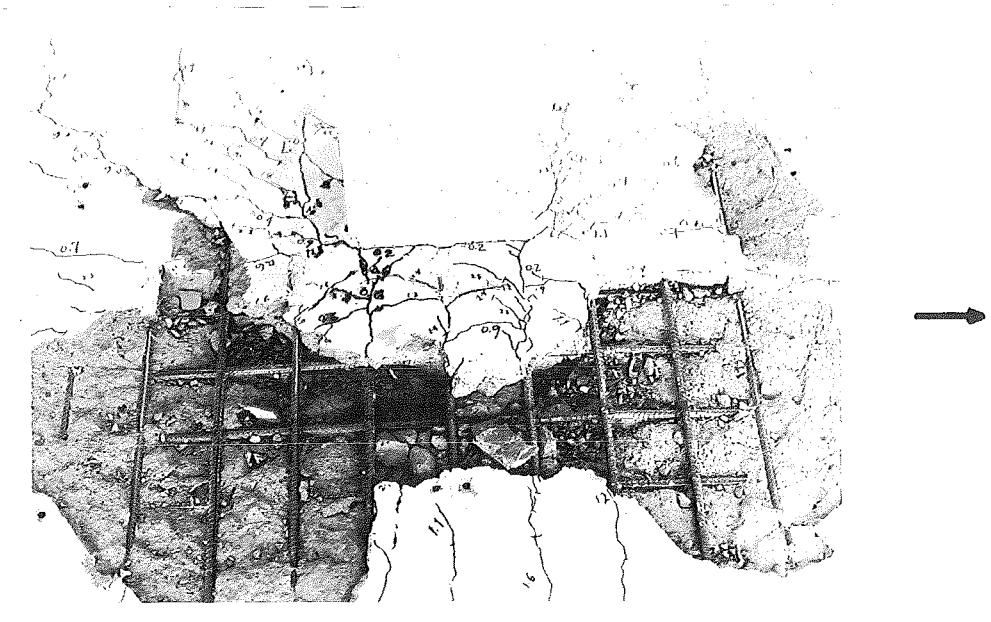

FIG. 3.28 VIEW OF SPECIMEN 2 AFTER REMOVAL OF BROKEN CONCRETE

width measured 0.003 in. at an edge displacement of 0.6 in. and 0.020 in. at 1.7 in. displacement. Other cracks were fine and none of them exceeded 0.010 in. just before failure.

Mode of Failure

The slab failed in shear near the column face at the downward loading end. A view of the failure surface is shown in Fig. 3.27. The failure was sudden and the inclined cracks extended from the intersection of the column and the compression face of the slab at the downward loading end. On the tension face of the slab the extent of cracking roughly formed a semicircular shape with a radius of about 1'-3" from the column face. A view of the failure after removal of broken concrete is shown in Fig. 3.28.

(v) Behaviour of Specimen No. 3C

Type of Loading

This specimen was subjected to reversals of bending moment several times. The sequence of loading cycles is shown in Fig. 3.29.

Load-displacement Curves

The load-displacement characteristics for the two edges of the slab obtained during the loading cycles are shown in Figs. 3.30 and 3.31. The numbers on all of the curves correspond to the cycle numbers given in Fig.3.30. The maximum moment was attained at the end of cycle 5 when the upward edge load was 3290 lb. and the downward edge load was 2580 lb. The specimen failed when the edge displacement was being increased from 2.8 in. to 3.0 in. Just before failure the upward edge load was 2010 lb. and the downward edge load was 2350 lb. The failure was again of sudden punching shear type.

Stresses in Slab Bars

The stresses in five top bars and five bottom bars are shown in Fig. 3.32. First yielding occurred in the top bar T3 at an edge deflection of 0.6 in. during cycle 1. At the end of cycle 5 all the five top bars had yielded and only three of the bottom bars, B2 , B3 and B4 , indicated yielding. By the end of cycle 13 the bottom bar B5 also yielded but the stress in B1

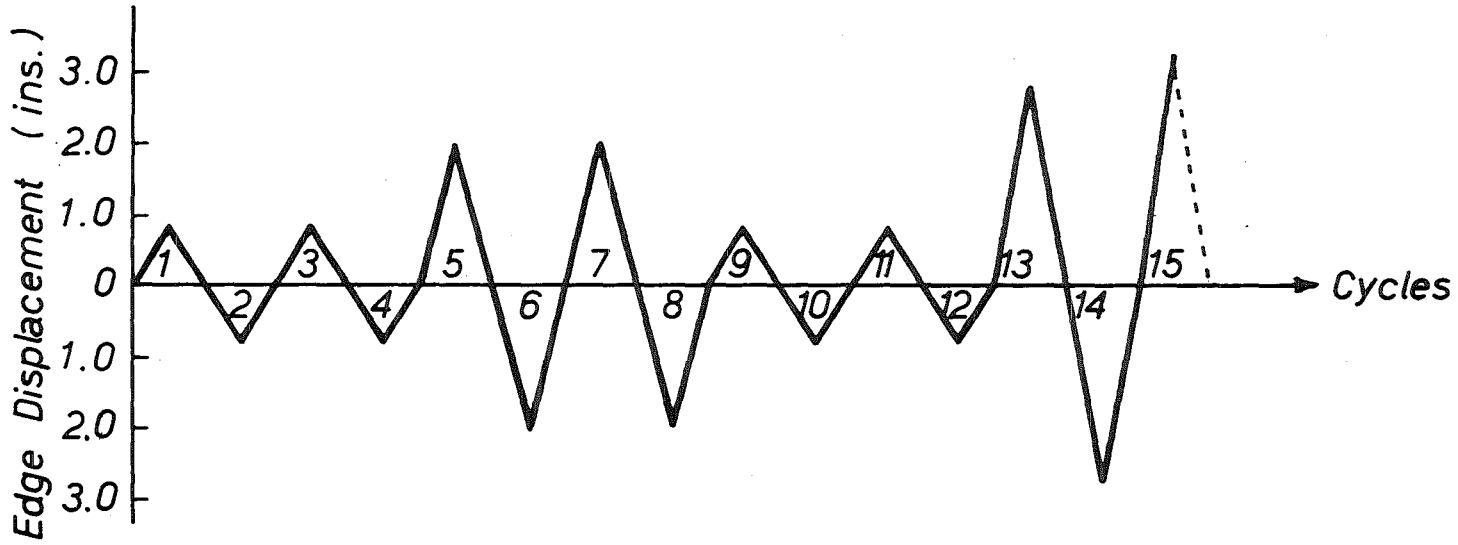

FIG. 3.29 LOADING CYCLES FOR SPECIMEN 3C

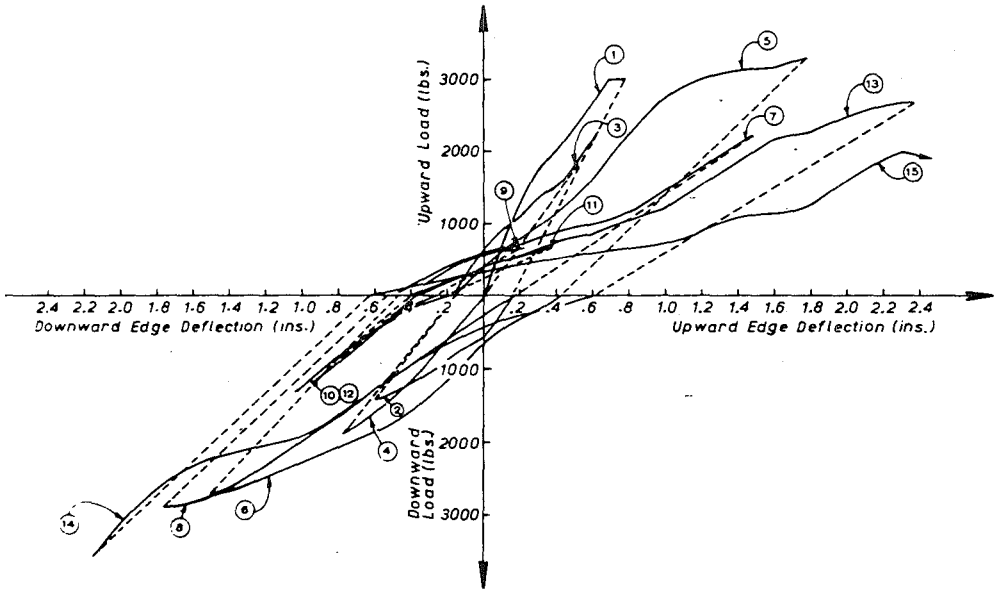

Fig. 3.30 – EDGE 'A'

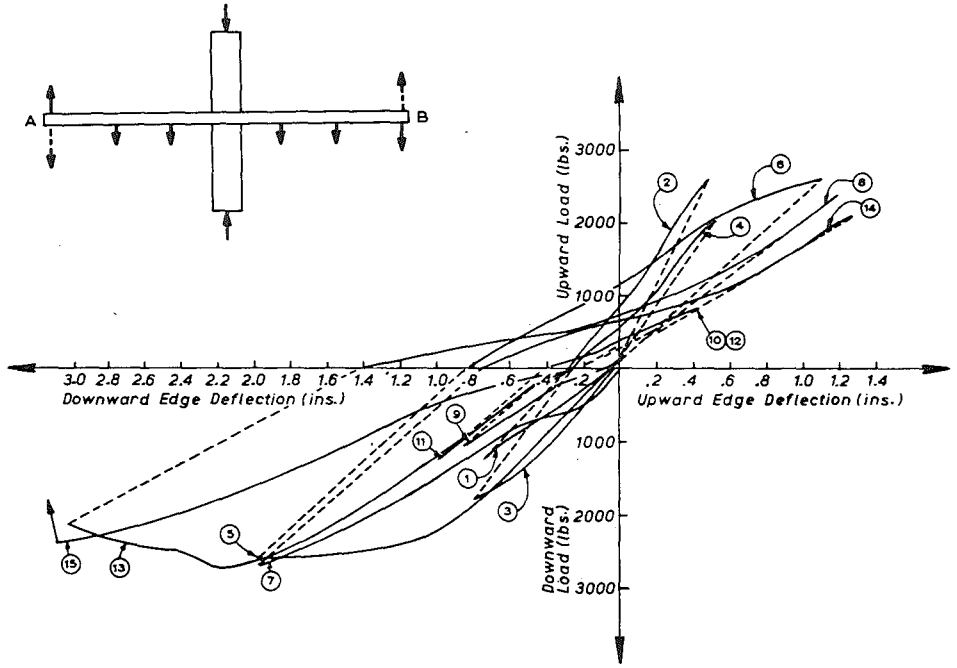

Fig. 3.31 – EDGE 'B'

– LOAD-DISPLACEMENT CURVES FOR EDGES 'A' & 'B' OF SPECIMEN 3C –

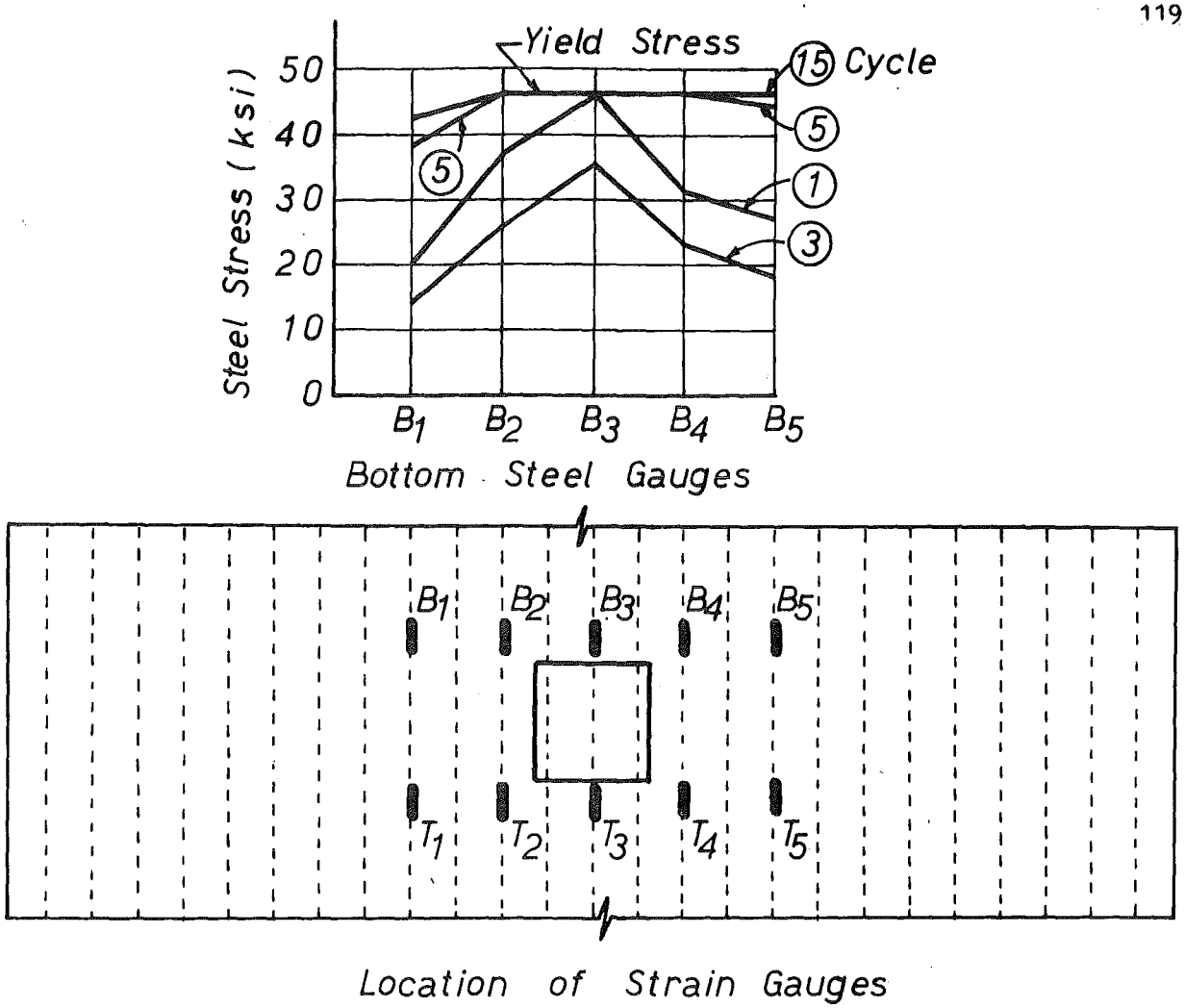

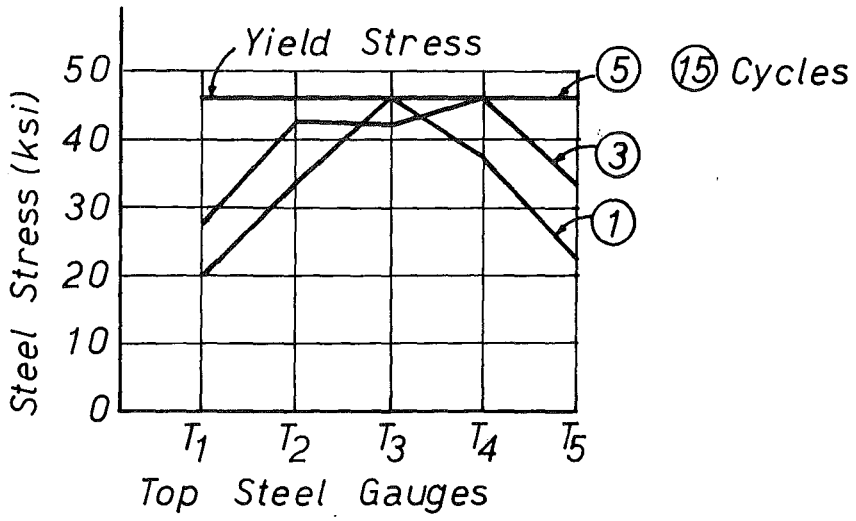

FIG. 3.32 STRESSES IN SLAB STEEL OF SPECIMEN 3C

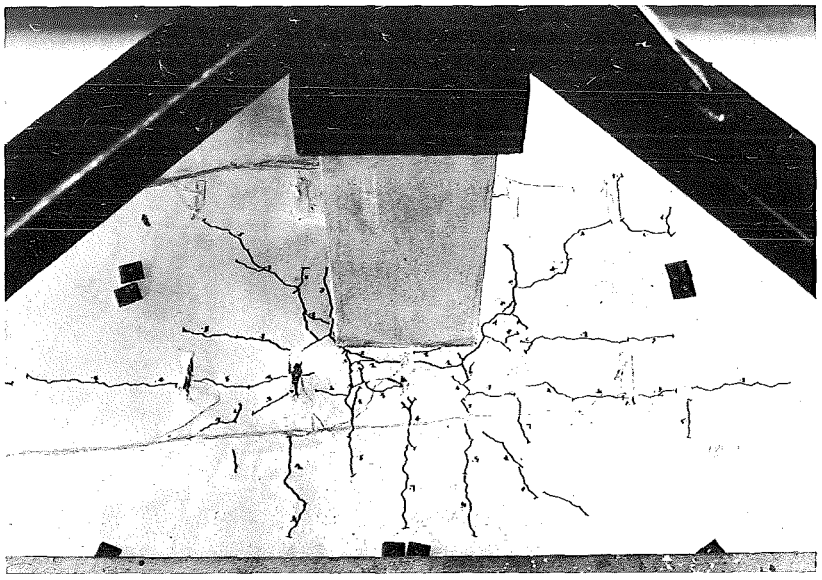

FIG. 3.33 CRACK PATTERN OF SPECIMEN 3C AFTER CYCLE 1

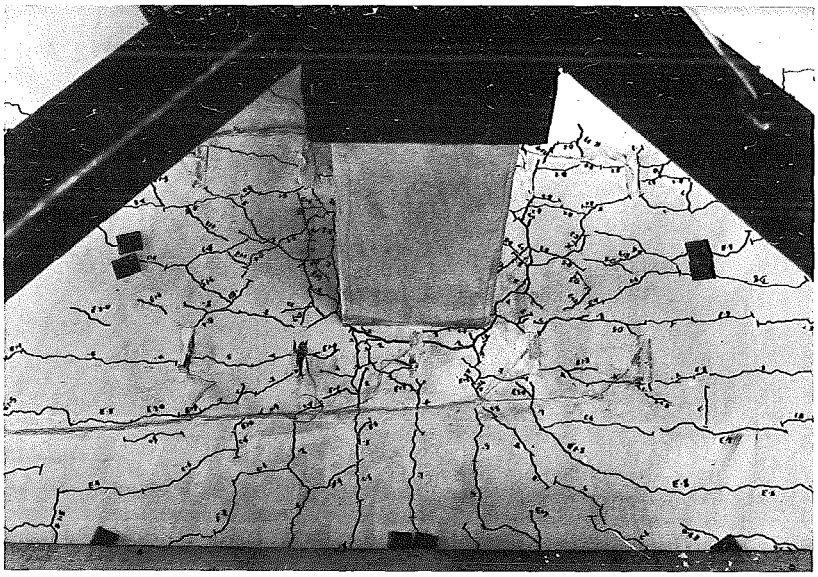

FIG. 3.34 CRACK PATTERN OF SPECIMEN 3C AFTER CYCLE 5

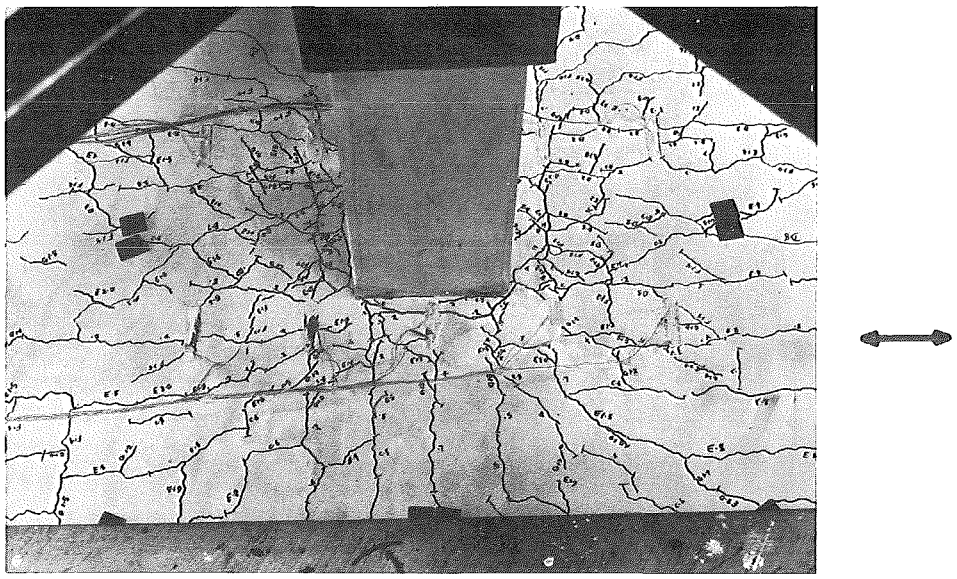

FIG. 3.35 CRACK PATTERN OF SPECIMEN 3C AFTER CYCLE 9

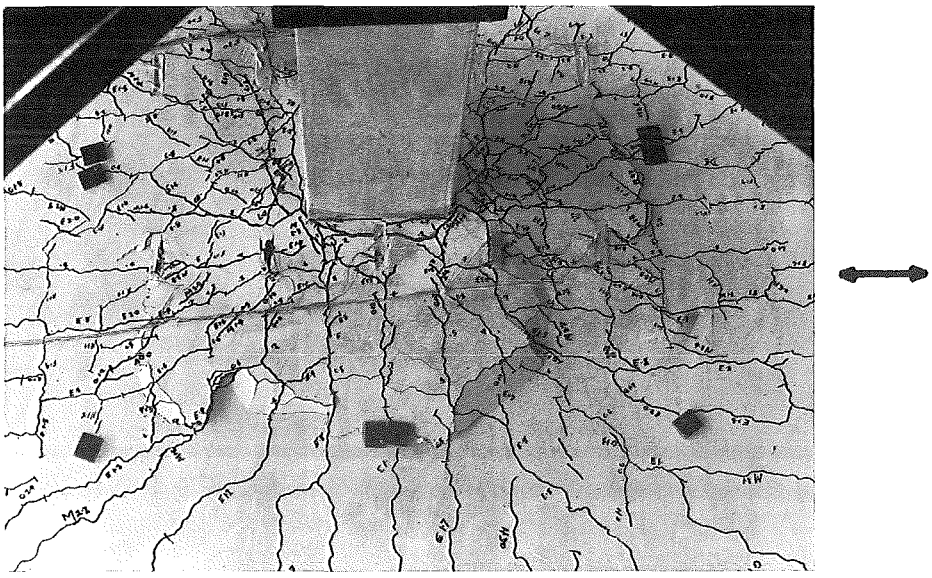

FIG. 3.36 FAILURE SURFACE OF SPECIMEN 3C

remained below the yield point at the time of failure.

Crack Propagation

Figs. 3.33 to 3.35 show the propagation of cracks on the top surface at cycles 1 , 5 , and 9. The cracking around the column was extensive and the largest crack once again developed at the junction of the column and the tension face of the slab.

Mode of Failure

The failure was by punching shear in the slab around the column face subjected to downward edge loading. The failure surface after cycle 15 is shown in Fig. 3.36.

(vi) Behaviour of Speciman 4S Containing Cranked Bars

Type of Loading

This specimen was subjected to one way bending with a constant shear force of 8040 lb. at the slab-column junction.

Load-displacement Curve

The load-displacement curves for the two loading edges of the slab are shown in Figs. 3.37 and 3.38. These curves indicate greater load carrying capacity than those for specimens without any shear reinforcement. The maximum moment was reached when both the upward and downward edge displacements were 2.5 in. At this edge displacement the upward edge load was 4050 lb. and the downward edge load was 2750 lb. The specimen failed when the edge displacement was being increased from 2.9 in. to 3.0 in. At the edge displacement of 2.9 in. the upward edge load was 3880 lb. and the downward edge load was 1580 lb.

Stresses in Slab Bars and Shear Reinforcement

Fig. 3.39 shows the stresses in nine top bars and nine bottom bars attained at the maximum applied moment and also at the moment at the maximum displacement. First yielding occurred in the top bar T5 at an imposed edge displacement of 0.7 in., when the applied moment was 207 kip. in. At the maximum applied moment of 367 kip. in. top bars T4 , T5 and T6 and bottom bars B3 , B4 , B5 , B6 and B7 yielded. The stresses in the

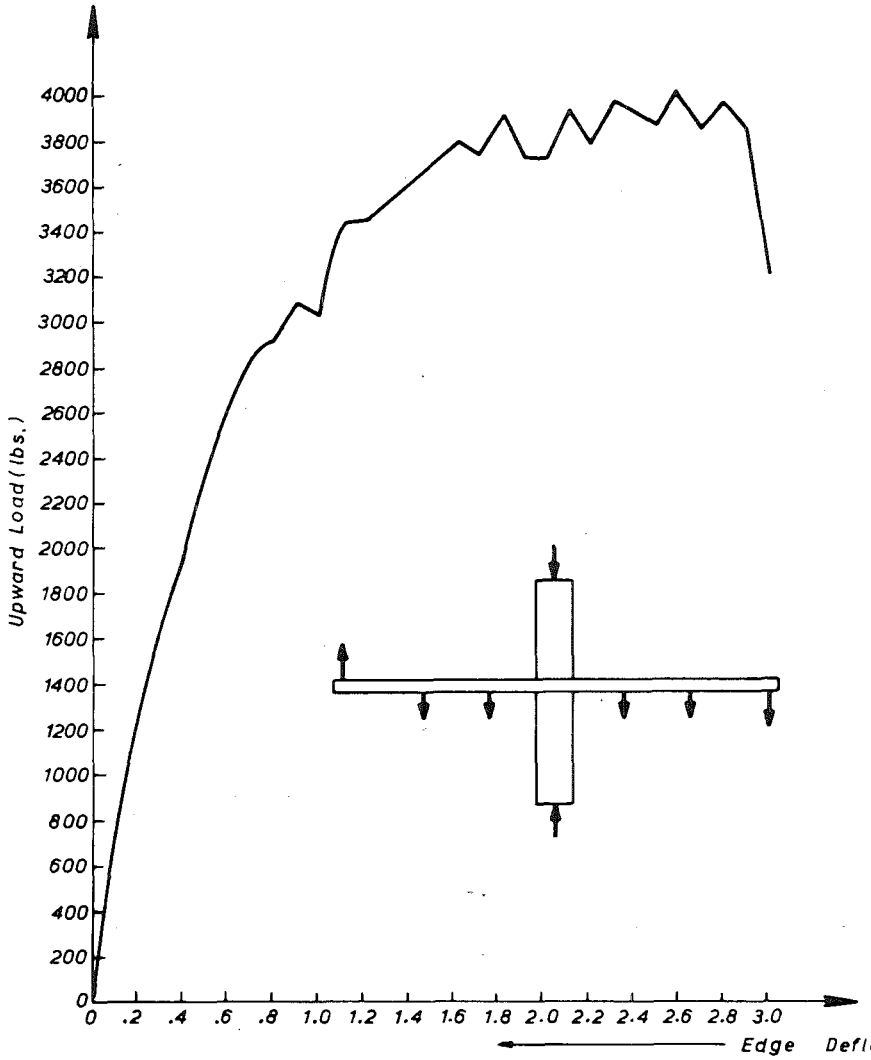

Fig. 3.37 — UPWARD LOAD

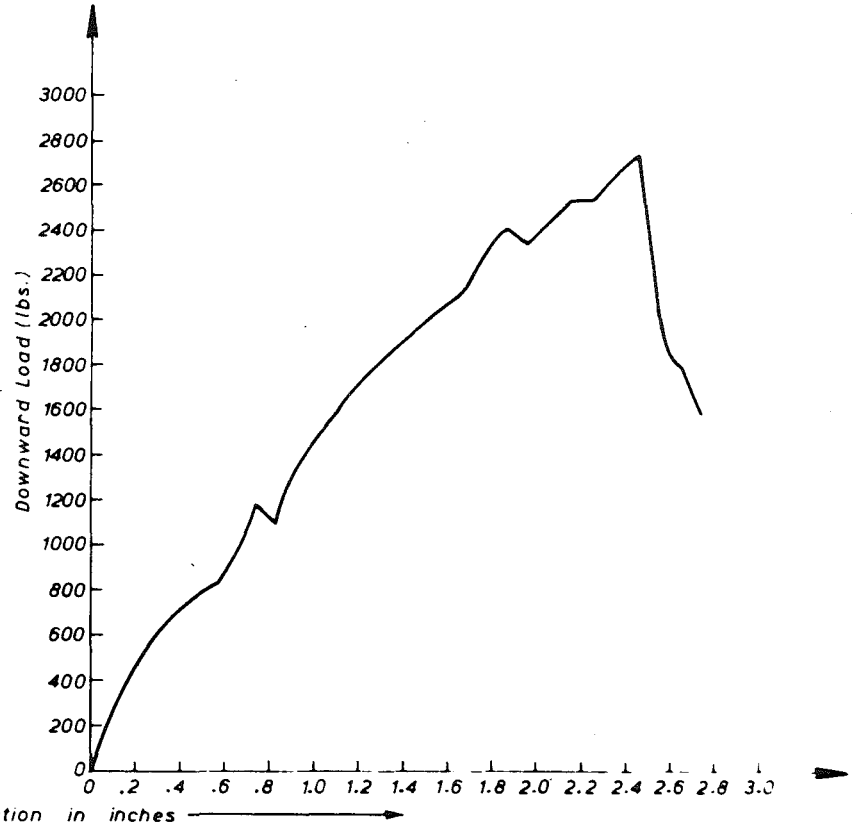

Fig. 3.38 — DOWNWARD LOAD

- LOAD—DISPLACEMENT CURVES FOR SPECIMEN 4S -

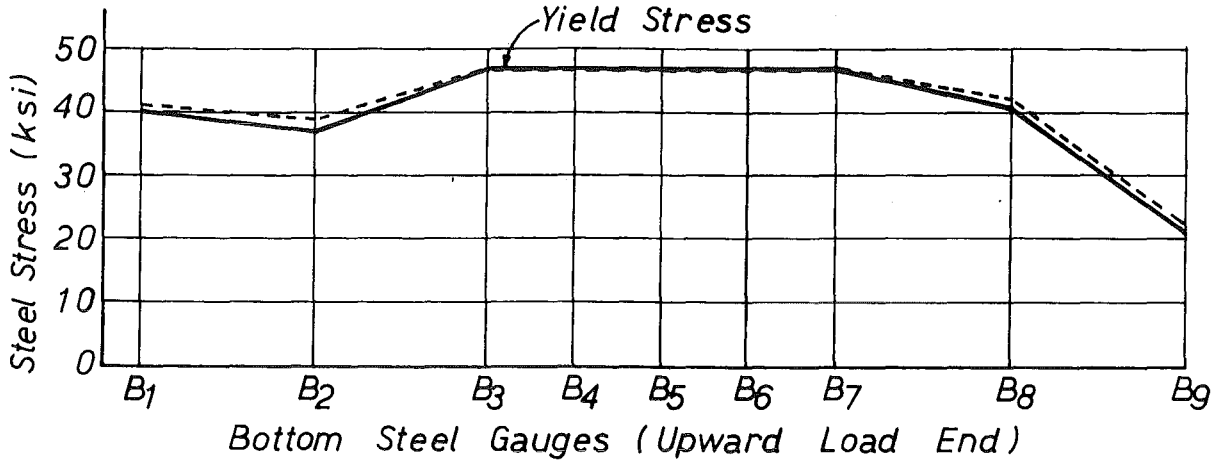

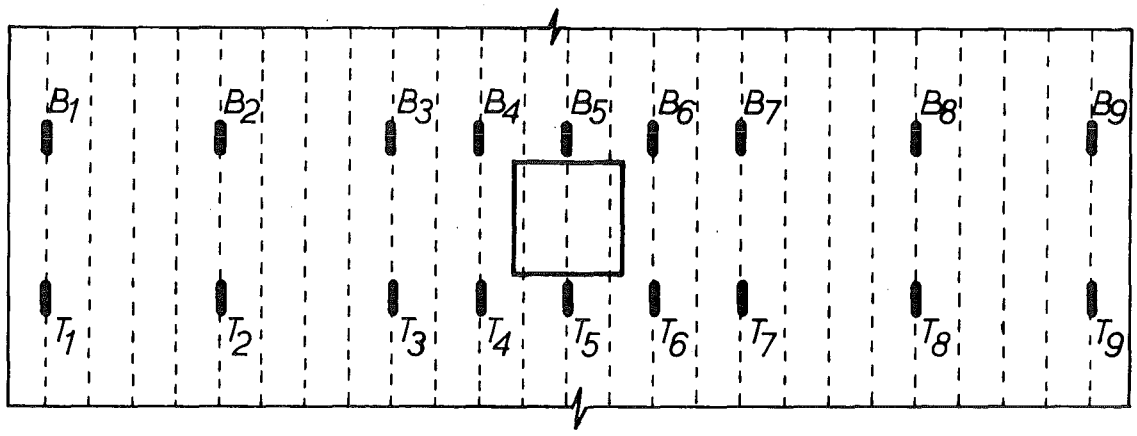

Location of Strain Gauges

At maximum moment ——

At maximum displacement - - - -

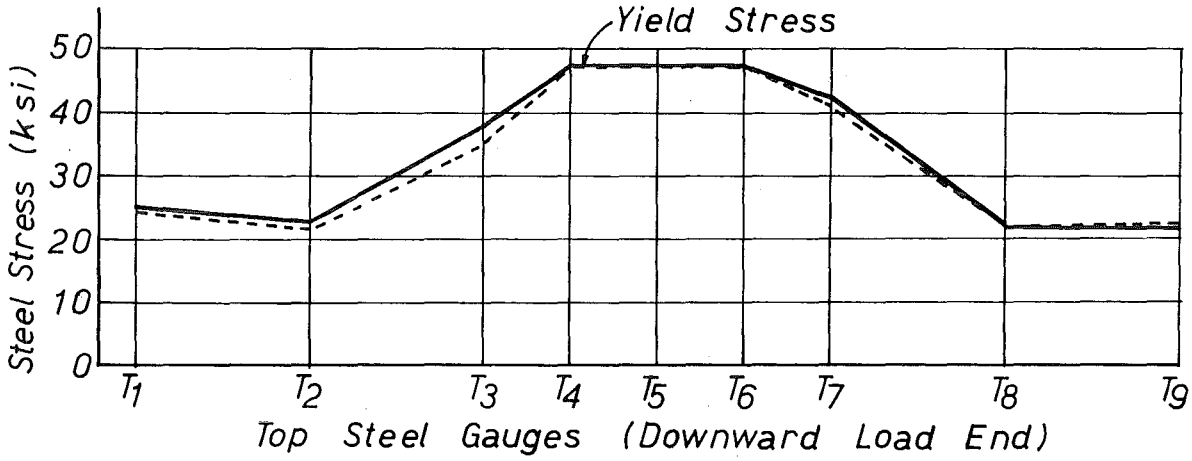

FIG. 3.39 STRESSES IN SLAB STEEL OF SPECIMEN 4S

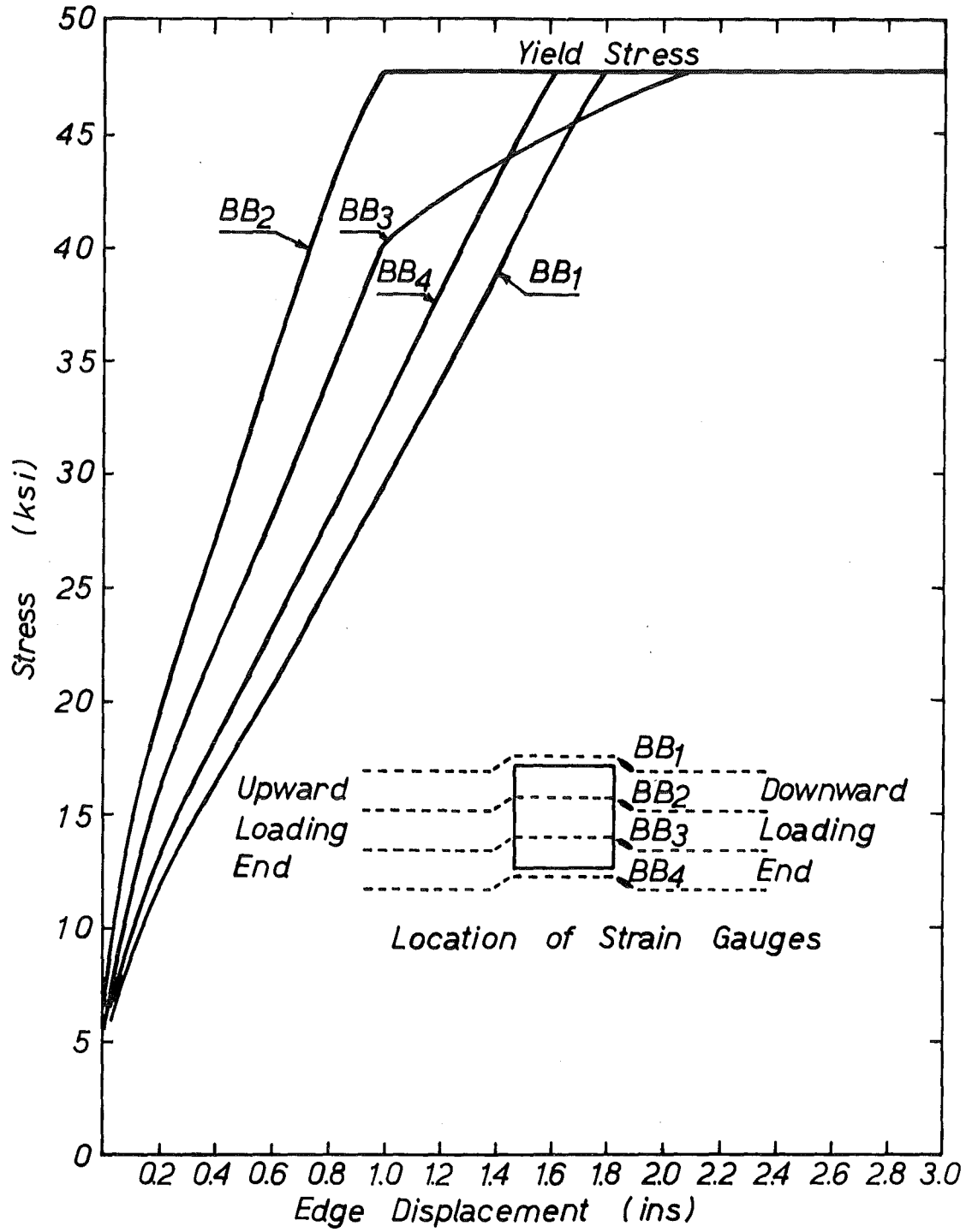

FIG. 3.40 STRESSES IN CRANKED BARS OF SPECIMEN 4S

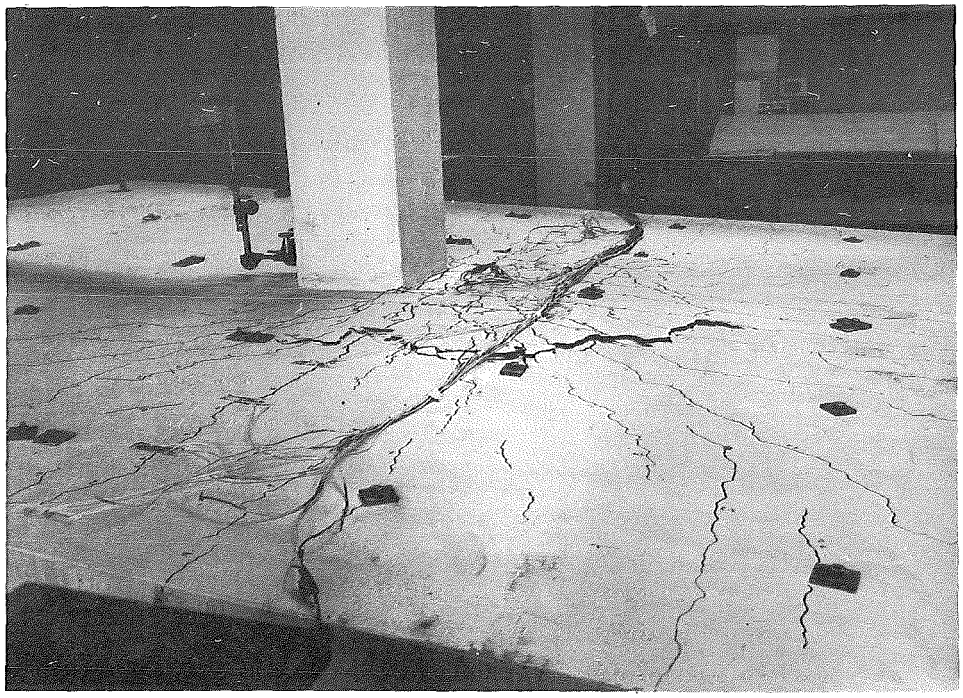

FIG. 3.41 CRACK PATTERN OF SPECIMEN 4S

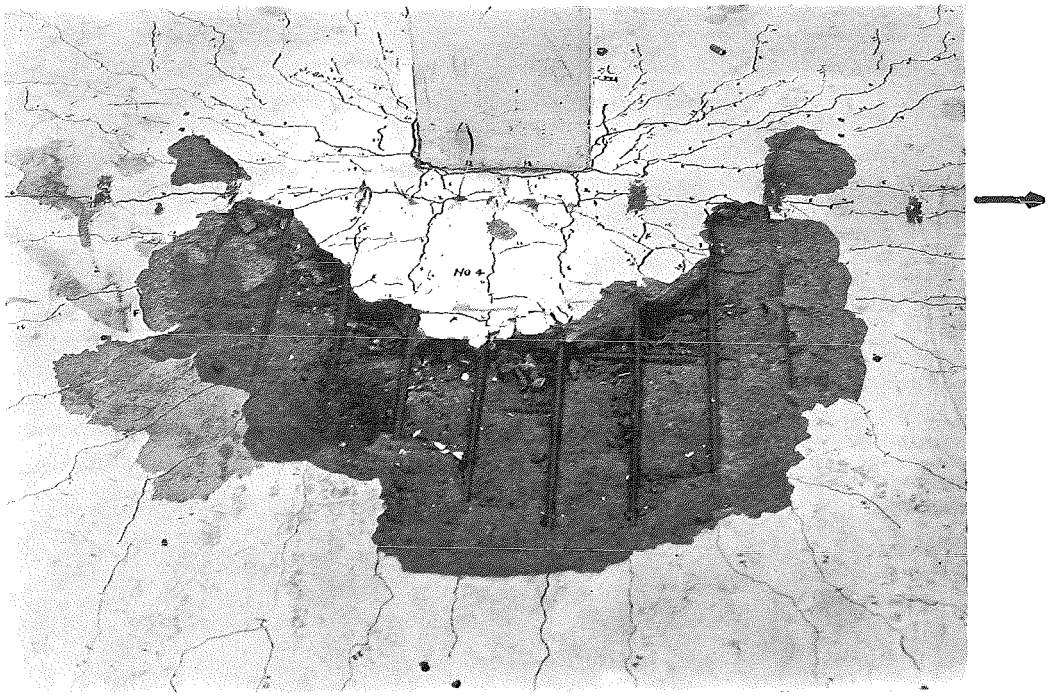

FIG. 3.42 FAILURE SURFACE OF SPECIMEN 4S

slab bars just before failure were similar to those obtained at the maximum moment. Yielding of bars was confined within a distance of 14 in. on either side of the column centre line.

The stresses measured on the inclined portion of the four cranked bars are shown in Fig. 3.40. All the bars yielded before the maximum moment was reached.

Crack Propagation

The development of cracks followed in a similar manner as for specimens without any shear reinforcement. A view of the crack pattern just before failure is shown in Fig. 3.41.

Mode of Failure

The slab failed in punching shear around the column face subjected to downward loading. The failure was sudden and it occurred outside the region which was reinforced with cranked bars. The inclined cracks originated from the intersection of the column face and the compression face of the slab and extended towards the tension face of the slab at an angle of about 13^{o} with the horizontal. The failure surface is shown in Fig. 3.42.

(vii) Behaviour of Specimen 5S Containing Shearhead

Type of Loading

This specimen was first subjected to a one way bending until the edge deflections reached 4.0 in. and then the loading was reversed and gradually increased.

Load-displacement Curves

The load-displacement curves for the two edges of the slab are shown in Figs. 3.43 and 3.44. During the first cycle the maximum moment of 350 kip.in. was reached at the imposed edge displacement of 2.5 in. when the upward edge load was 3850 lb. and the downward load was 2630 lb. At the edge displacement of 4.0 in. the upward load was 3900 lb. but the downward load decreased to 1650 lb. On unloading the downward loading end was left with a permanent set of 2.54 in. and the upward loading end recovered to

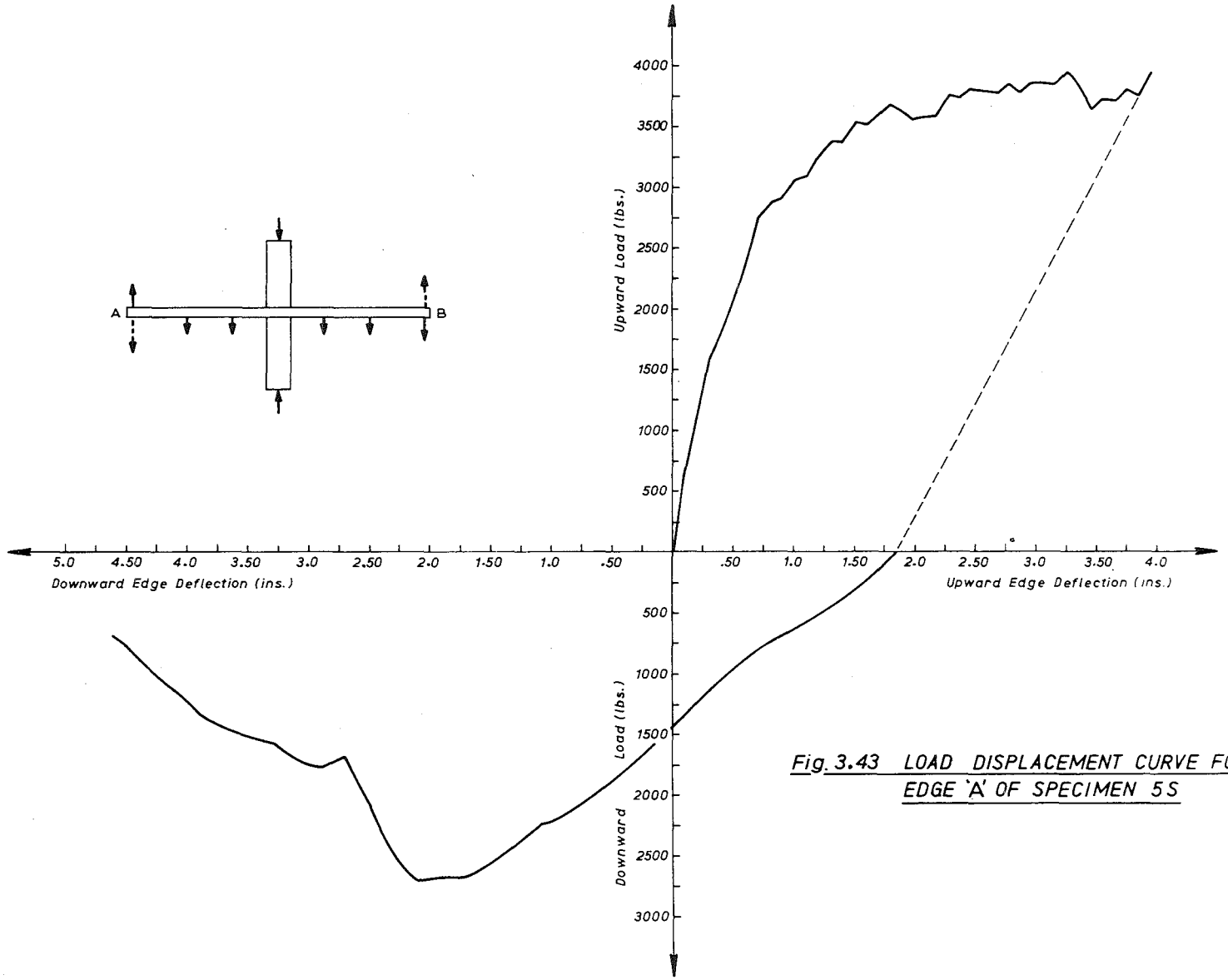

Fig. 3.43 LOAD DISPLACEMENT CURVE FOR EDGE 'A' OF SPECIMEN 5S

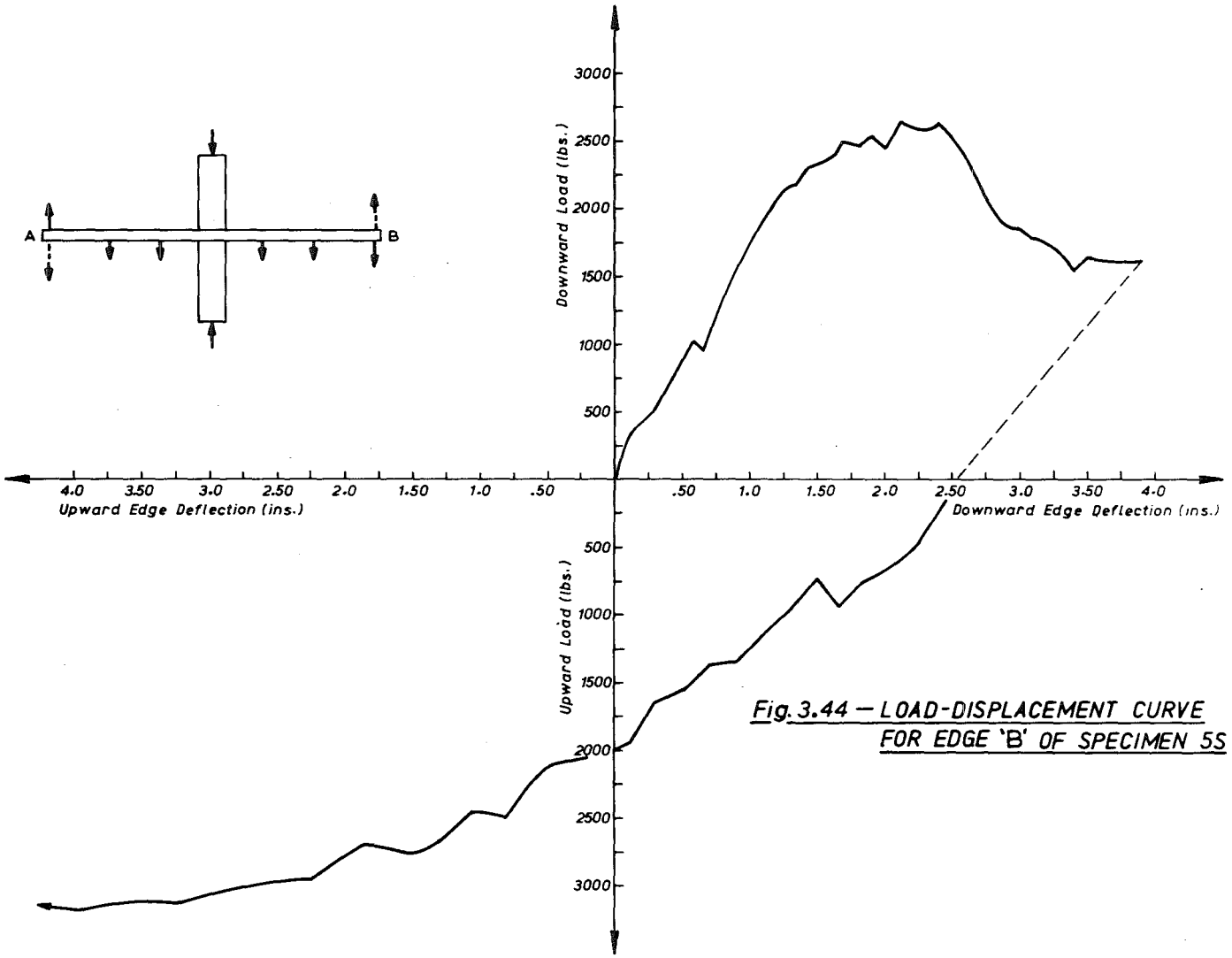

Fig. 3.44 — LOAD-DISPLACEMENT CURVE FOR EDGE 'B' OF SPECIMEN 5S

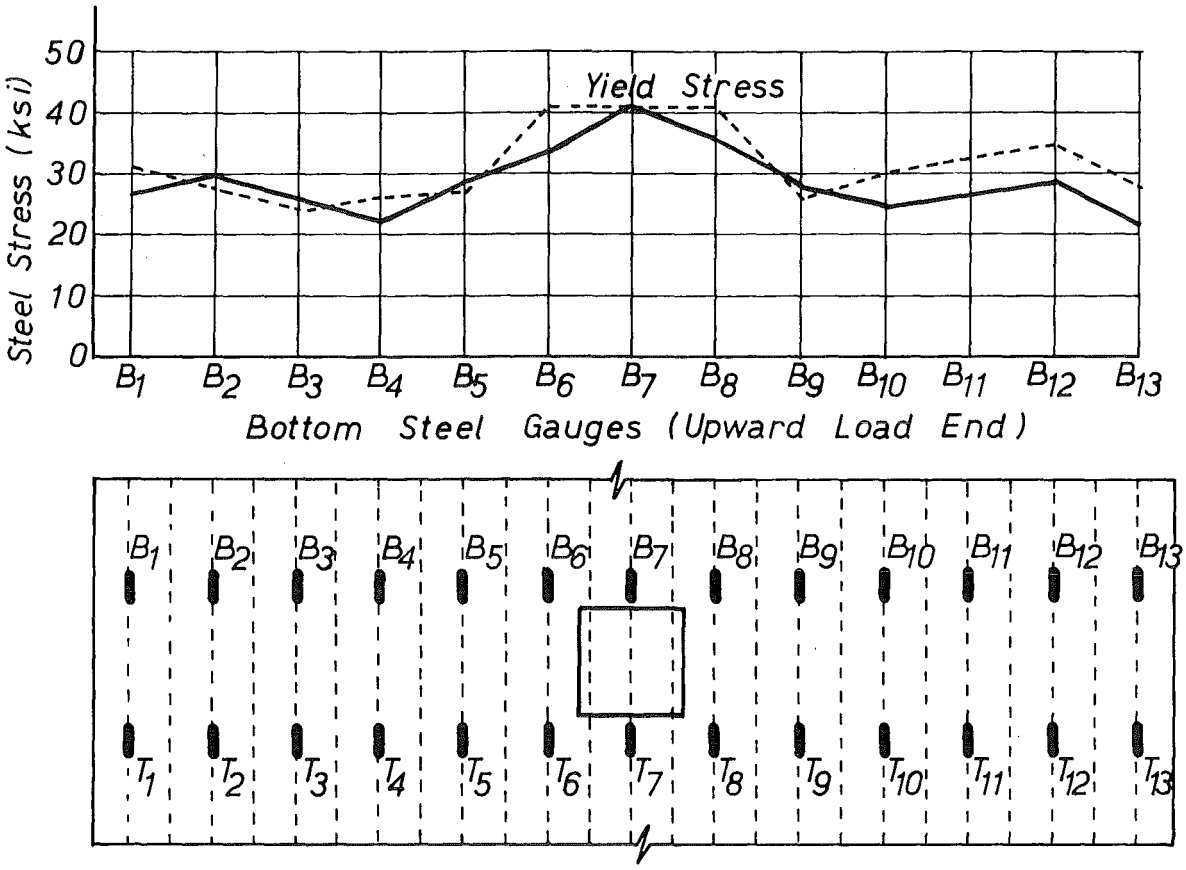

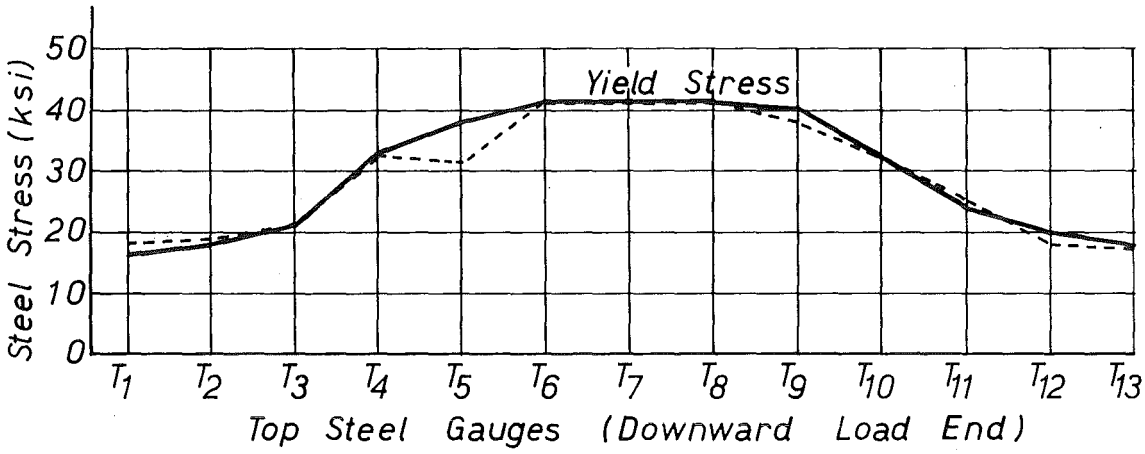

FIG. 3.45 STRESSES IN SLAB STEEL OF SPECIMEN 5S

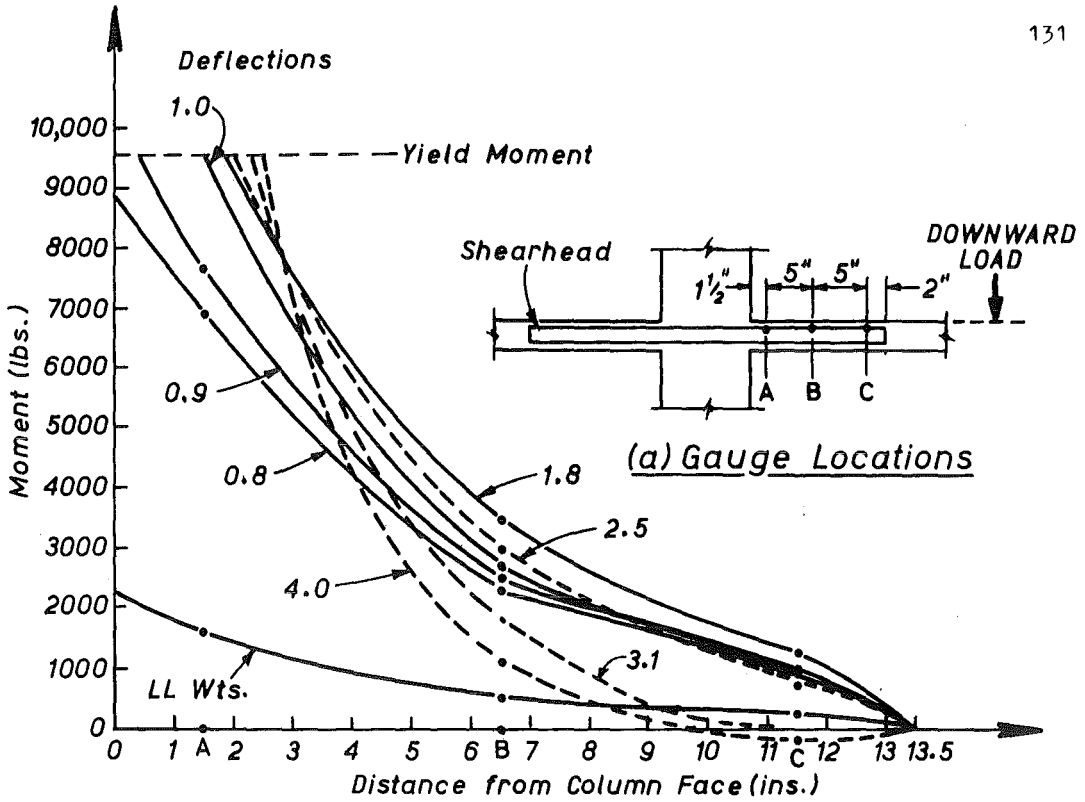

(b) Distribution of Moments on Channel Section

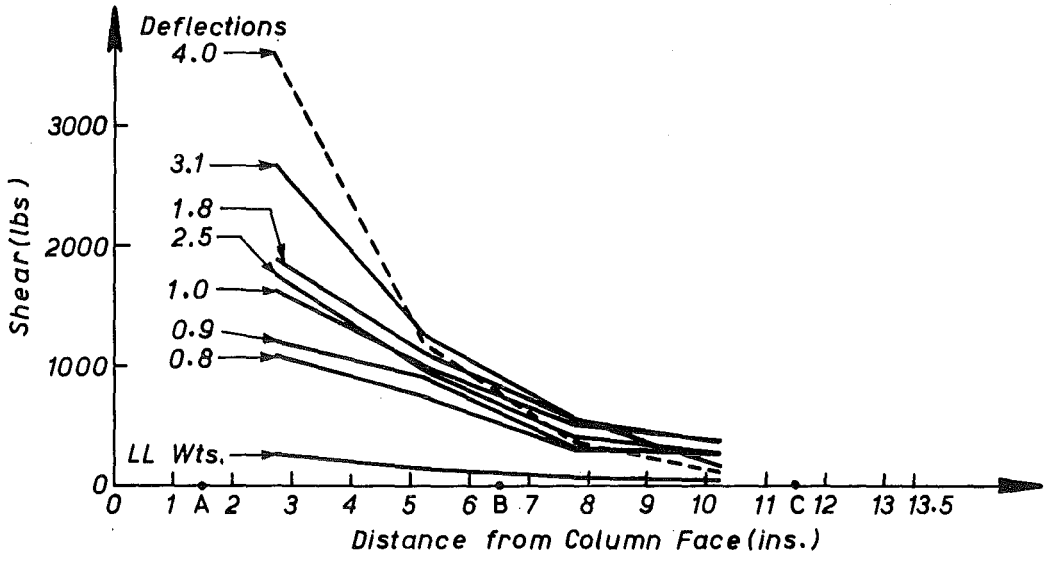

(c) Distribution of Shear Force on Channel Sections

Fig. 3.46 — STRESSES IN SHEARHEAD OF SPECIMEN 5S

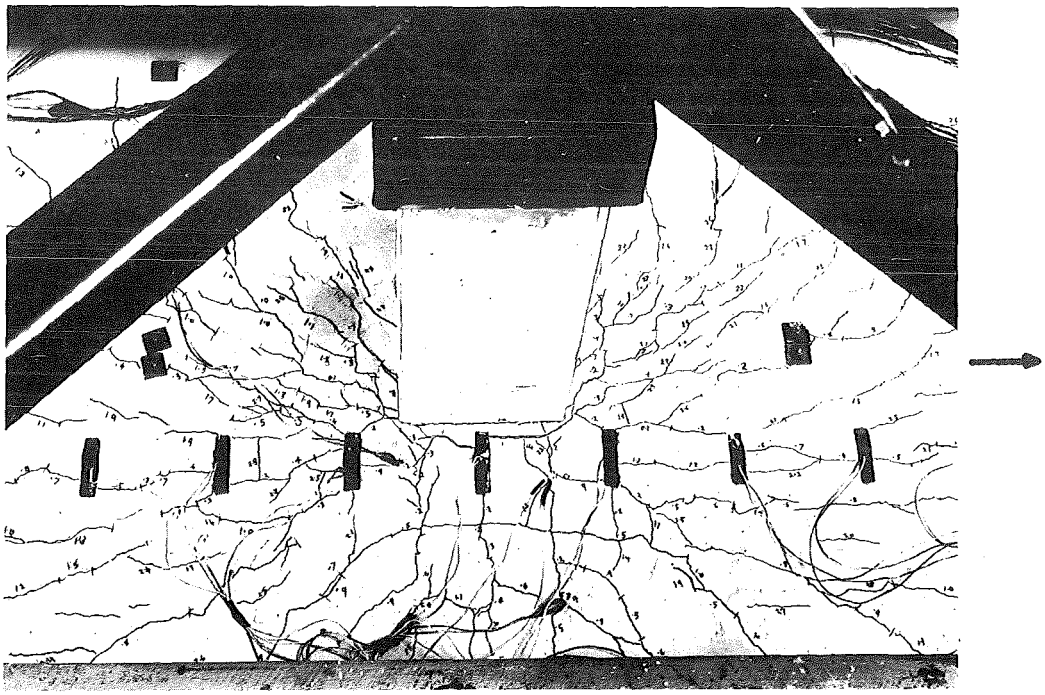

FIG. 3.47 CRACK PATTERN OF SPECIMEN 5S

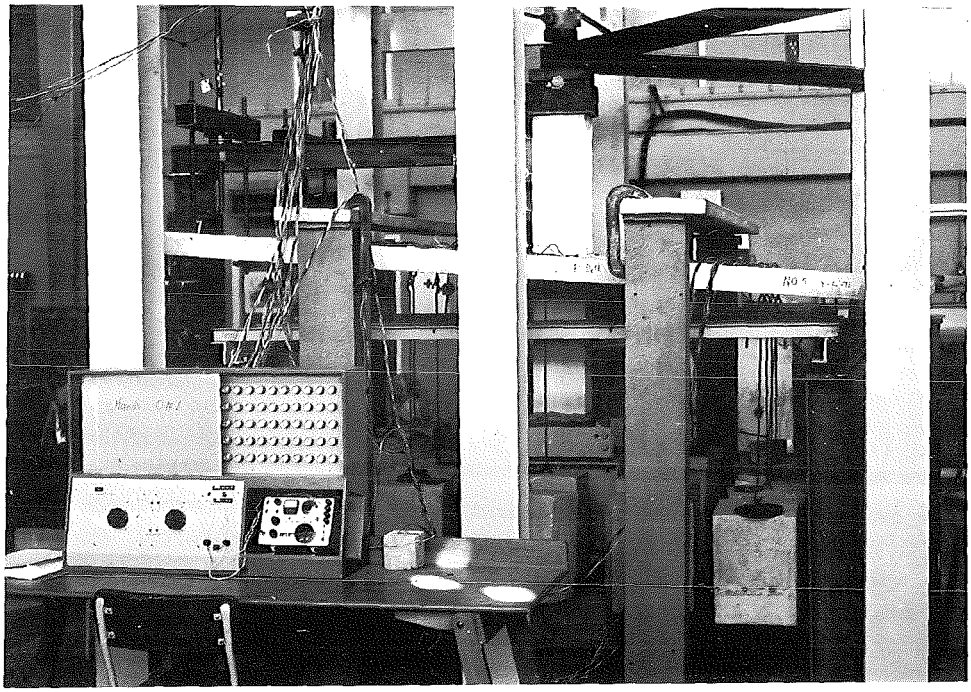

FIG. 3.48 SPECIMEN 5S AT 4 IN. EDGE DISPLACEMENT

1.85 in. of upward displacement. The loading was then reversed. During the reversed cycle of loading the maximum moment of 294 kip. in. was attained at the edge deflection of 4.05 in. which was measured from the unloaded position of the first cycle. At this edge deflection the upward edge load was 2750 lb. and the downward load was 2700 lb. The imposed edge deflections were increased to 6.55 in. when the upward load reached 3170 lb. and the downward load decreased to 680 lb.

Stresses in Slab Bars

The stresses in top and bottom bars measured across the whole width of the slab are shown in Fig. 3.45. The top bar T7 passing through the centre of the column yielded first at an edge deflection of 0.7 in. At the maximum applied moment top bars T6 , T7 and T8 yielded but only one bottom bar, B7 , indicated yielding. At the end of cycle 1 when the edge displacements were 4.0 in. the stress distribution in top bars was similar but this time bottom bars B6 , B7 and B8 had yielded.

Stresses in Shearhead

In order to determine the distribution of moment and shear force along the shearhead three strain gauges marked A, B, and C were placed on the shearhead arm at the downward loading end as shown in Fig. 3.46(a). From the measured strains bending moments were calculated at these locations. The distribution of moments along the shearhead arm for various edge displacements is shown in Fig. 3.46(b). The difference in moment at two locations along the shearhead divided by the distance between these locations provided a measure of the distribution of shear force. Fig. 3.46(c) shows the shear force distribution along the shearhead arm.

Crack Pattern and Failure Mode

The crack pattern and the deflected shape of the specimen at 4 in. of edge displacements are shown in Figs. 3.47 and 3.48 respectively. This specimen did not fail in shear while all the previous four specimens failed at edge displacements below 3.0 in. After the reversal of bending moment

edge displacements were increased up to 6.55 in. and at this edge displacement the specimens maintained 59% of the maximum moment attained during the first cycle. It behaved in a ductile manner without any danger of a shear failure.

(viii) Behaviour of Specimen 6CS Containing 4 Legged Stirrups of 3/16 in. Diameter

Type of Loading

This specimen was subjected to reversals of bending moment several times. The sequence of loading cycles is shown in Fig. 3.49.

Load-displacement Curves

The load-displacement curves for the two edges of the slab obtained during the loading cycles are shown in Figs. 3.50 and 3.51. During cycle 1 at an edge displacement of 2.4 in. the maximum moment of 340 kip. in. was reached when the upward end load was 3680 lb. and the downward end load was 2620 lb. This moment was never exceeded during subsequent cycles. On unloading the upwardly loaded end was left with a permanent set of 0.8 in. and the downward end has 1.26 in. of permanent set. The maximum moments attained during subsequent cycles of loading were 240 kip. in. at cycle 2, 202 kip. in. at cycle 3, 324 kip. in. at cycle 4, 252 kip. in. at cycle 5 and 177 kip. in. at cycle 6. During the last cycle the edge displacements were increased to 9.6 in. without failing the specimen.

Stresses in Slab Bars

Fig. 3.52 shows the stresses in top and bottom bars of the slab at the end of indicated loading cycles. First yielding occurred in the top bar T5 at an edge displacement of 0.5 in. At the end of cycle 1 top bars T3 , T4 , T5 , T6 and T7 yielded. Bottom bars B5 and B6 indicated yielding at this stage with B3 , B4 and B7 nearing the yield stress. During cycle 5 bottom bars B3 to B7 all yielded but top bars T1 , T2 ,T8 , T9 and bottom bars B1 , B2 , B8 , B9 remained below the yield point.

Stresses in Stirrups

Fig. 3.53 shows the stresses in stirrups at the end of each cycle of

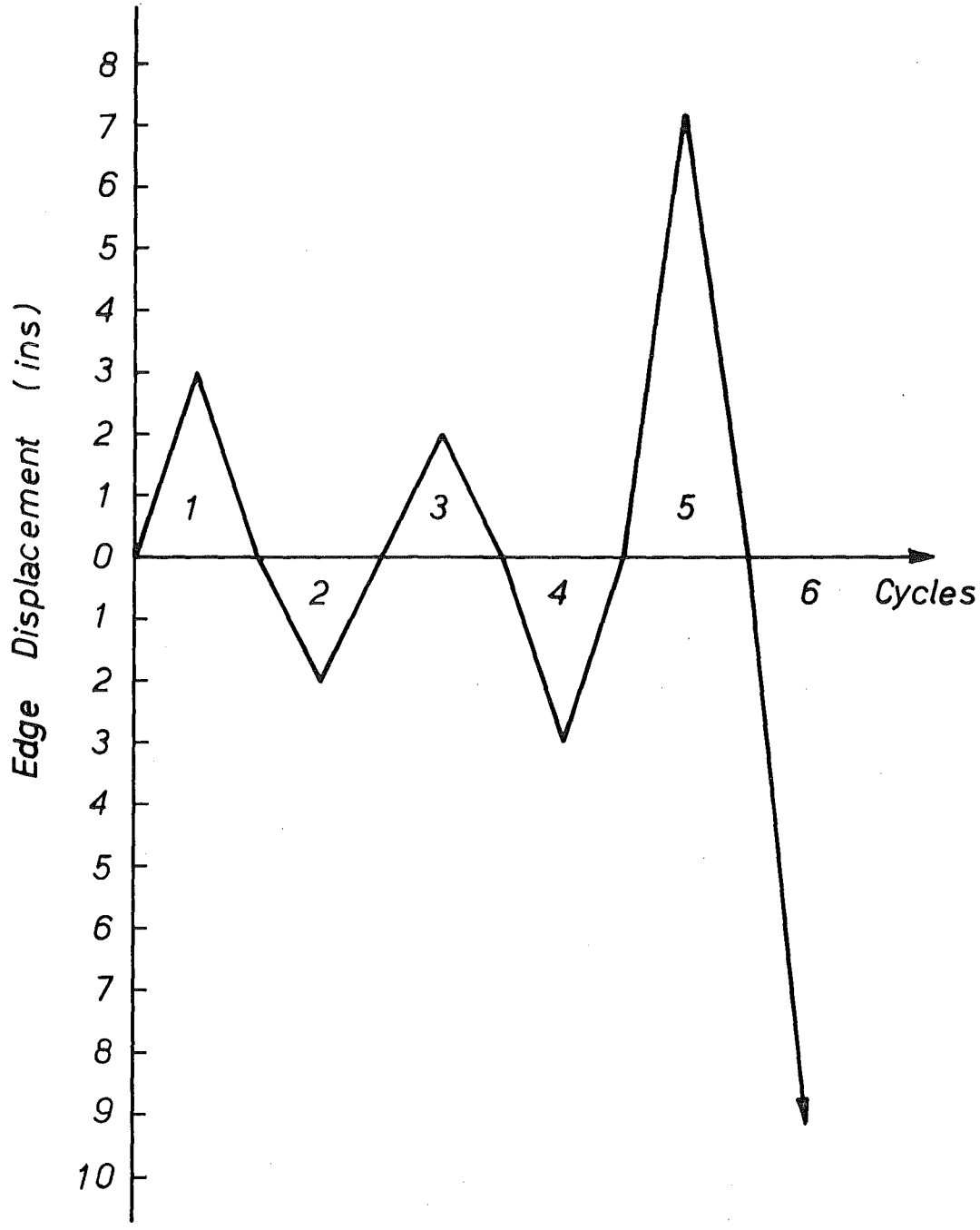

FIG. 3.49 LOADING CYCLES FOR SPECIMENS 6CS, 7CS AND 8CS

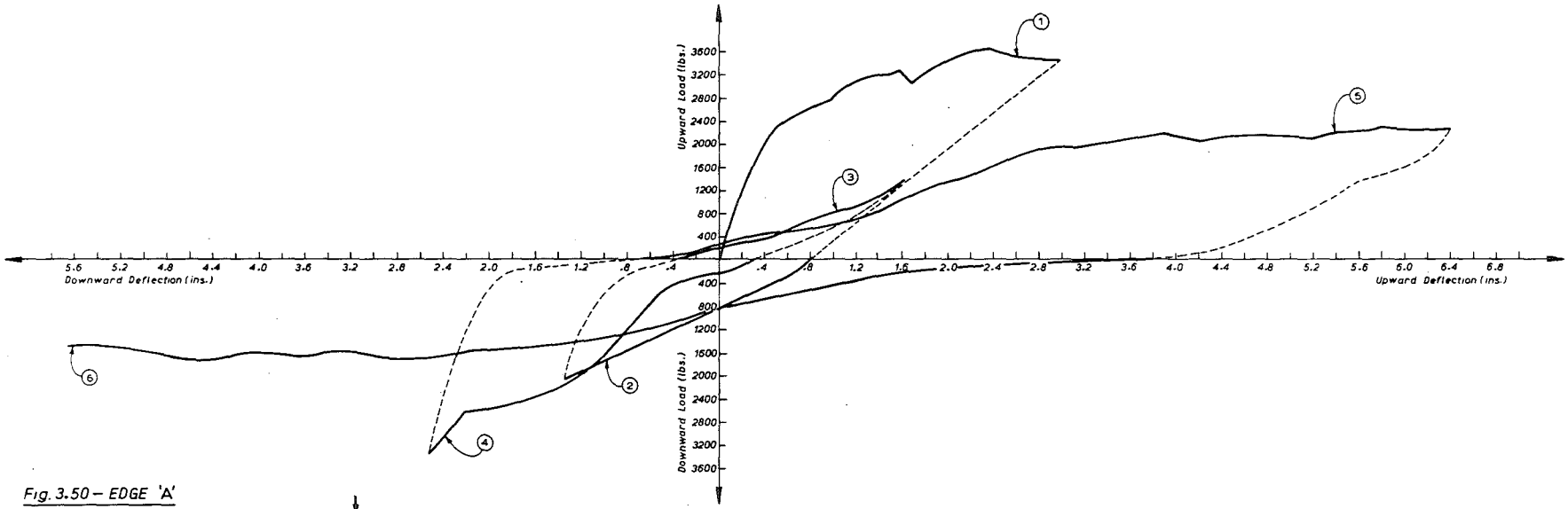

Fig. 3.50 – EDGE 'A'

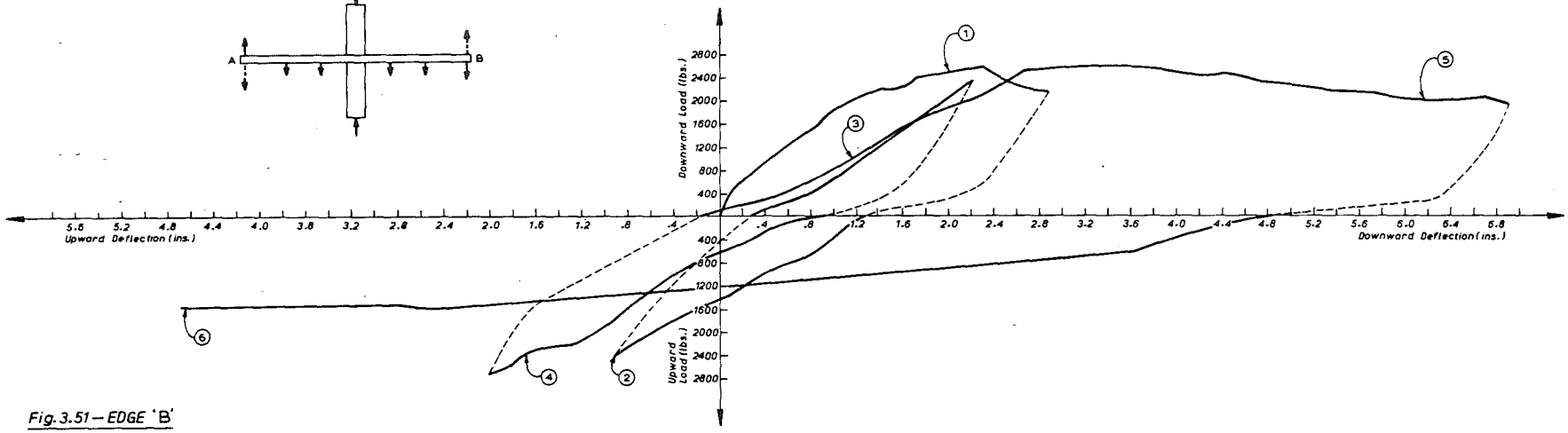

Fig. 3.51 – EDGE 'B'

– LOAD – DISPLACEMENT CURVES FOR EDGES 'A' & 'B' OF SPECIMEN 6CS –

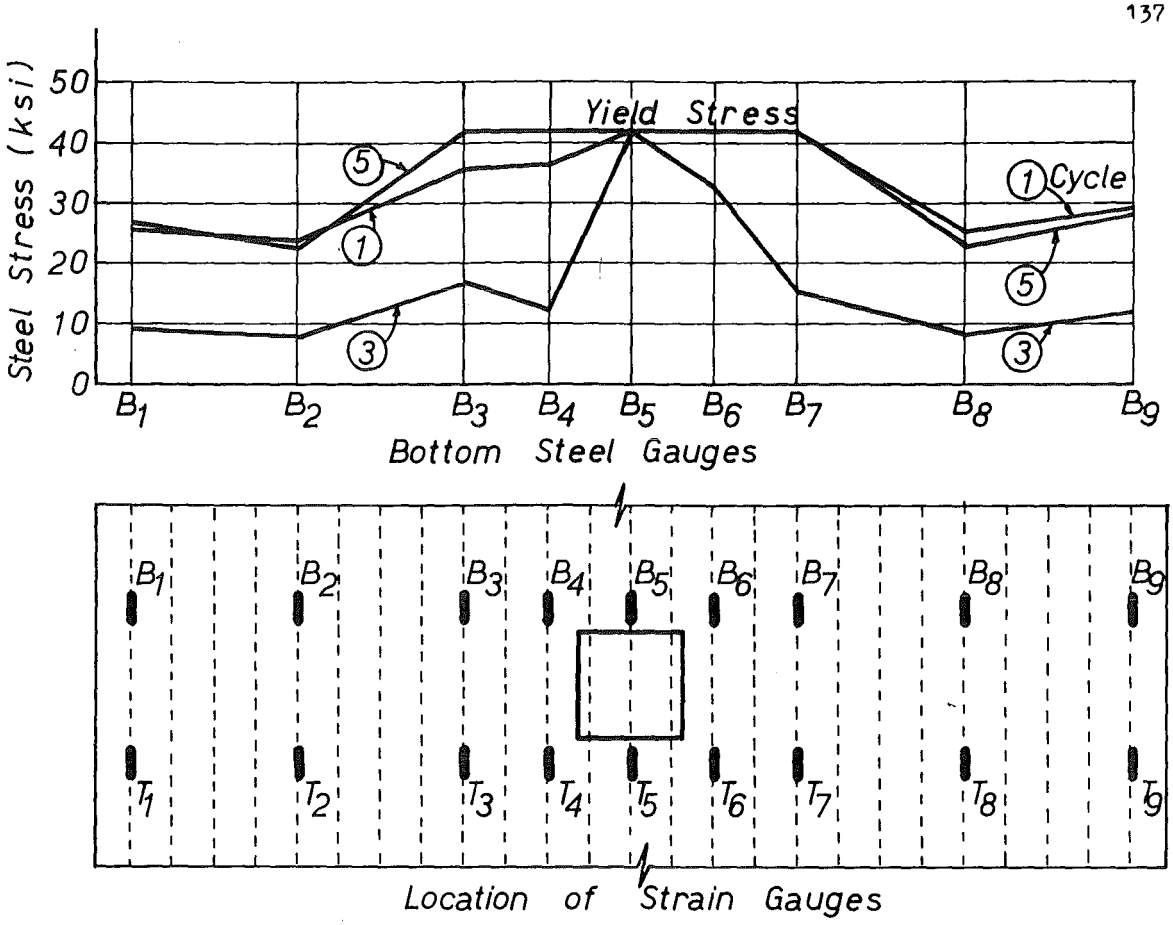

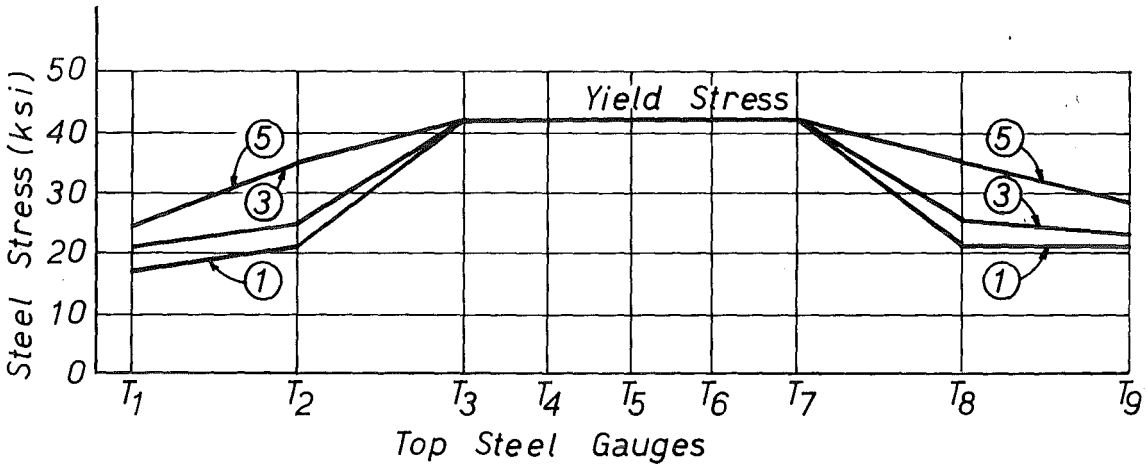

FIG. 3.52 STRESSES IN SLAB STEEL OF SPECIMEN 6CS

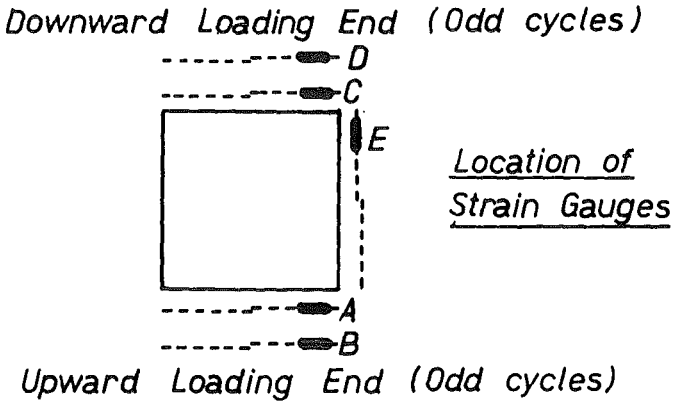

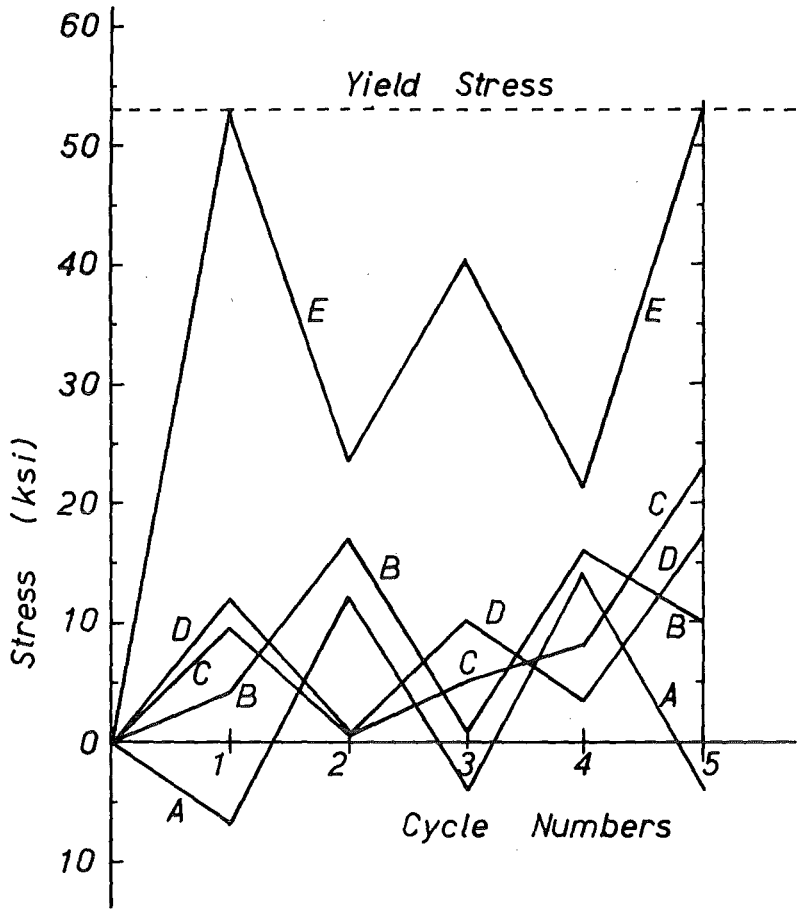

FIG. 3.53 STRESSES IN STIRRUPS OF SPECIMEN 6CS

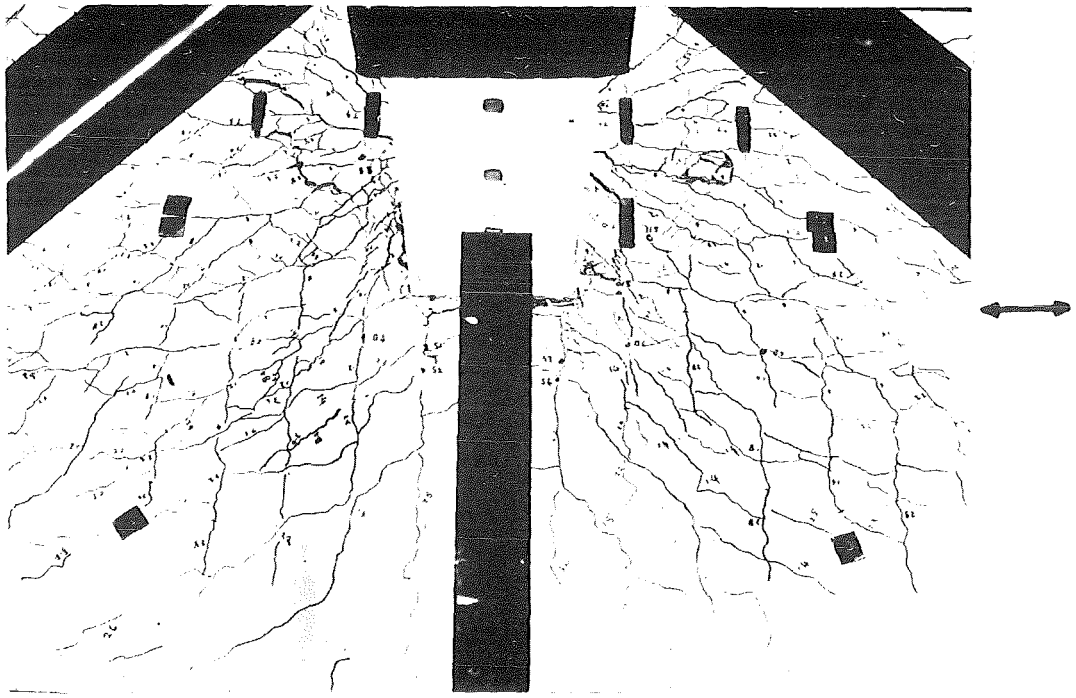

FIG. 3.54 CRACK PATTERN OF SPECIMEN 6CS

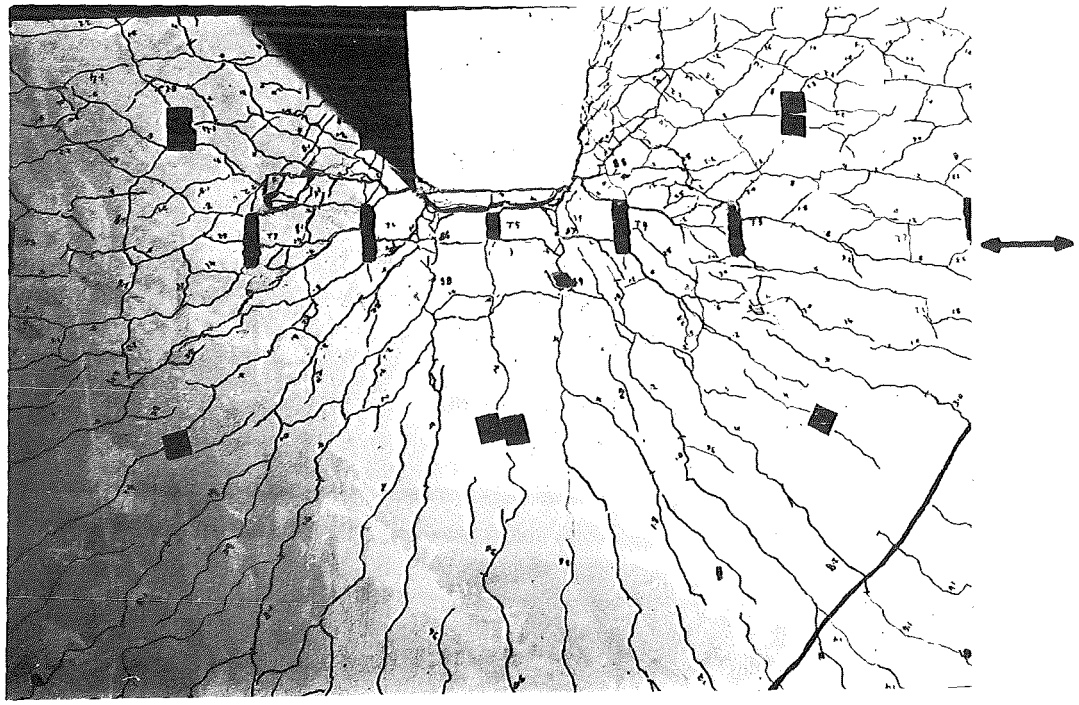

FIG. 3.55 CRACK PATTERN OF SPECIMEN 6CS

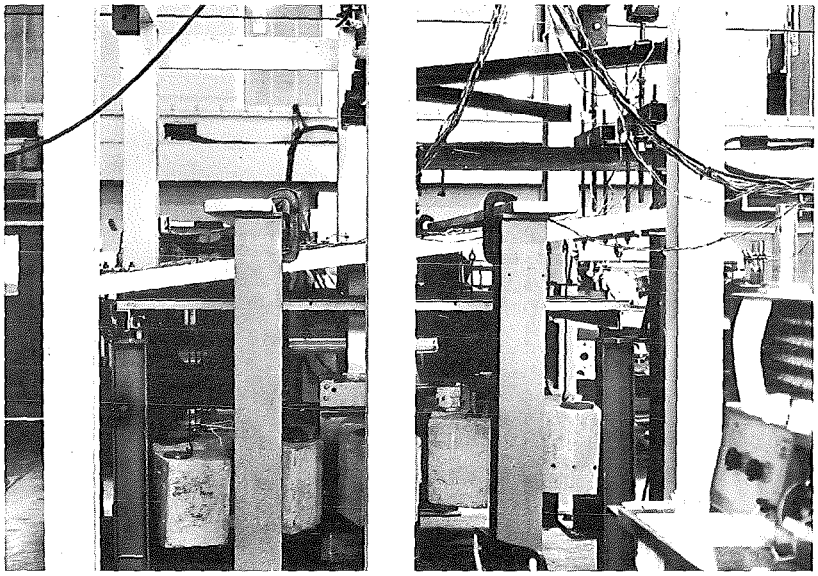

FIG. 3.56 SPECIMEN 6CS AT EDGE DISPLACEMENT OF 7.2 IN.

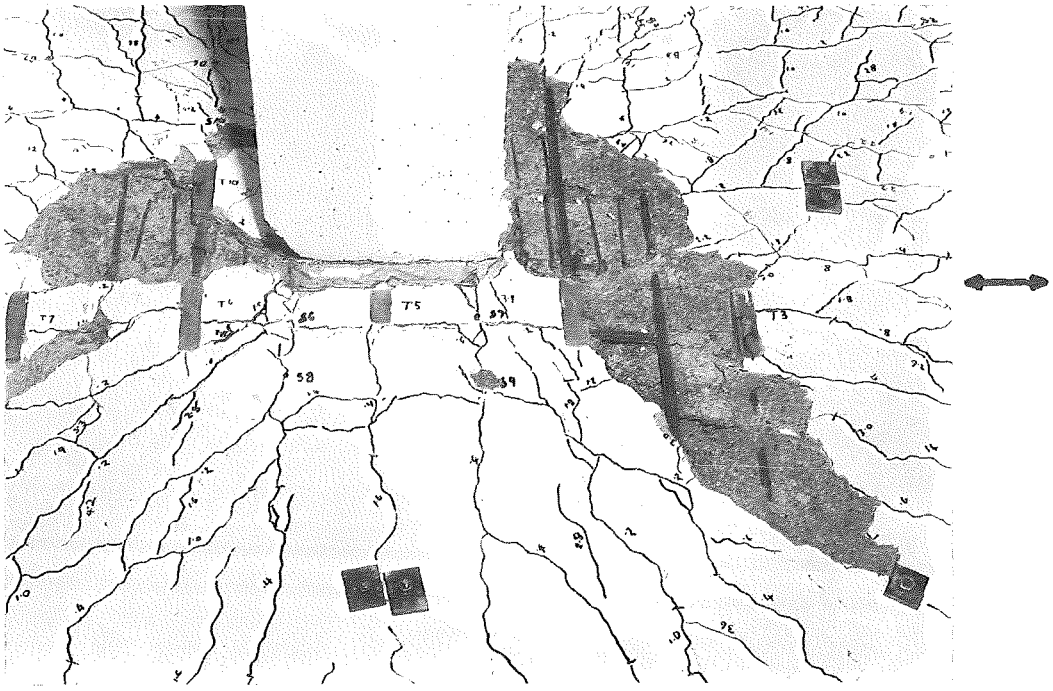

FIG. 3.57 SPECIMEN 6CS AT THE END OF TESTING

loading. Stirrups marked A, B, C and D did not yield at any stage of loading. This indicates that a smaller area of stirrup steel could be utilised. The stirrup E yielded at the end of cycle 1 indicating high torsional stresses set up on the column faces parallel to the direction of bending.

Cracking and Failure Mode

The crack patterns obtained on the top surface of the slab at the end of cycle 5 are shown in Figs. 3.54 and 3.55. The deflected shape at an edge displacement of 7.2 in. is shown in Fig. 3.56. This specimen did not fail in punching shear. The cracking on the slab surface was extensive but the specimen behaved in a ductile manner. A view of the slab-column junction at the end of the test is shown in Fig. 3.57. It shows that the stirrups of closed type prevented the punching shear failure in the slab near the column faces transverse to the direction of bending but the column faces parallel to the direction of bending are cracked in torsion.

(ix) Behaviour of Specimen 7CS Containing 2 Legged Stirrups of $\frac{1}{4}$ in. Diameter

Type of Loading

This specimen was subjected to several cycles of loading reversals as shown in Fig. 3.49.

Load-displacement Curves

The load-displacement characteristics for the two edges of the slab are shown in Figs. 3.58 and 3.59. The numbers on the curves correspond to the cycle numbers given in Fig. 3.49. The maximum moment of 369 kip. in. was reached at an edge displacement of 2.2 in. during cycle 1 when the upward edge load was 3900 lb. and the downward edge load was 2940 lb. The moments attained during subsequent cycles of loading were 213 kip. in. at cycle 2, 233 kip. in. at cycle 3, 304 kip. in. at cycle 4, 302 kip. in. at cycle 5 and 176 kip. in. at cycle 6. During the last cycle the edge displacements were increased up to 11.2 in. without failing the specimen.

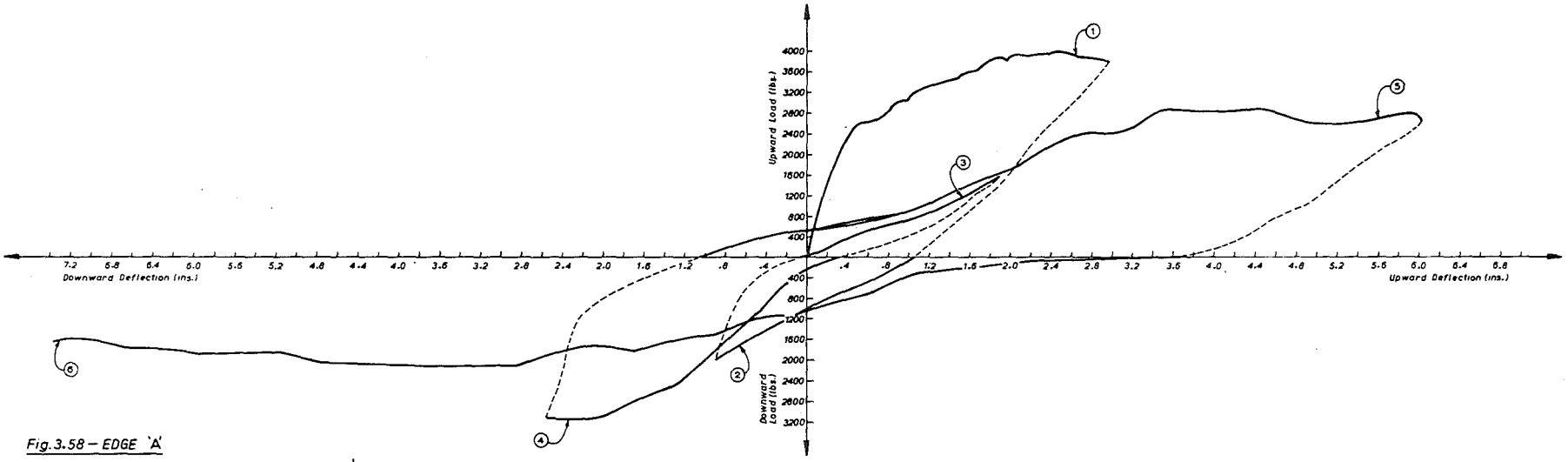

Fig. 3.58 – EDGE 'A'

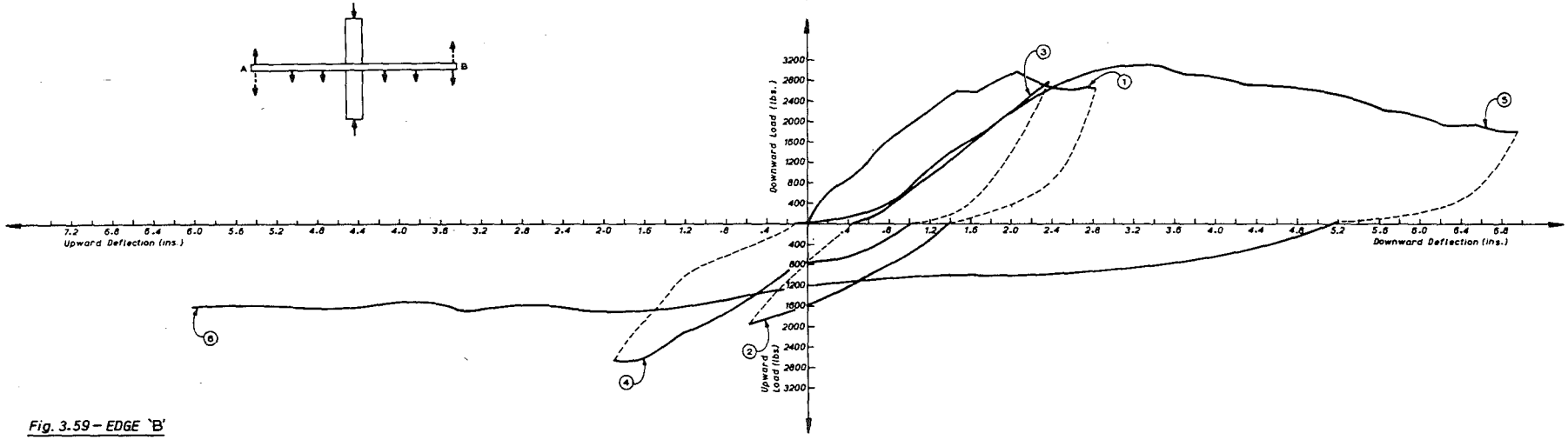

Fig. 3.59 – EDGE 'B'

– LOAD—DISPLACEMENT CURVES FOR EDGES 'A' & 'B' OF SPECIMEN 7CS –

The maximum moment attained during cycle 1 was never exceeded during subsequent cycles of loading.

Stresses in Slab Bars

Fig. 3.60 shows the stresses in top and bottom bars at selected locations across the width of the slab during loading cycles 1 , 3 and 5 . As before first yielding occurred in top central bar, T5 , at an imposed edge displacement of 0.6 in. During cycle 1 top bars T3 to T7 and bottom bars B3 to B7 all yielded. Top bars T1 , T2 , T8 , T9 and bottom bars B1 , B2 , B8 , B9 always remained below the yield stress level during all cycles of loading.

Stresses in Stirrups

The location of strain gauges on stirrups and the stresses attained at those locations during each loading cycle are shown in Fig. 3.61. During cycle 1 when the maximum applied moment was recorded stresses in stirrups A, B, C and D were far below the yield stress level but the stress at E was quite high. During cycle 5 yielding was observed to occur at A and E and during the last cycle of loading gauges at C and D also yielded. Unfortunately the strain gauge B ceased to function after cycle 3 and it was not possible to see whether this gauge also showed yielding during the last two cycles. The reason for yielding in 2 legged stirrups of this specimen may be due to the fact that the bulging action of the central top and bottom slab bars could have caused bending stresses in the extreme fibres of stirrup bars to exceed the yield point. In specimen 6CS the use of 4 legged stirrups prevented the bulging action of the central top and bottom slab bars and consequently the stresses were restricted below the yield point.

Cracking and Failure Mode

This specimen behaved in a ductile manner and did not fail in punching shear around the column. A view of the crack pattern at the end of testing is shown in Fig. 3.62. Major cracking took place at the side faces of the

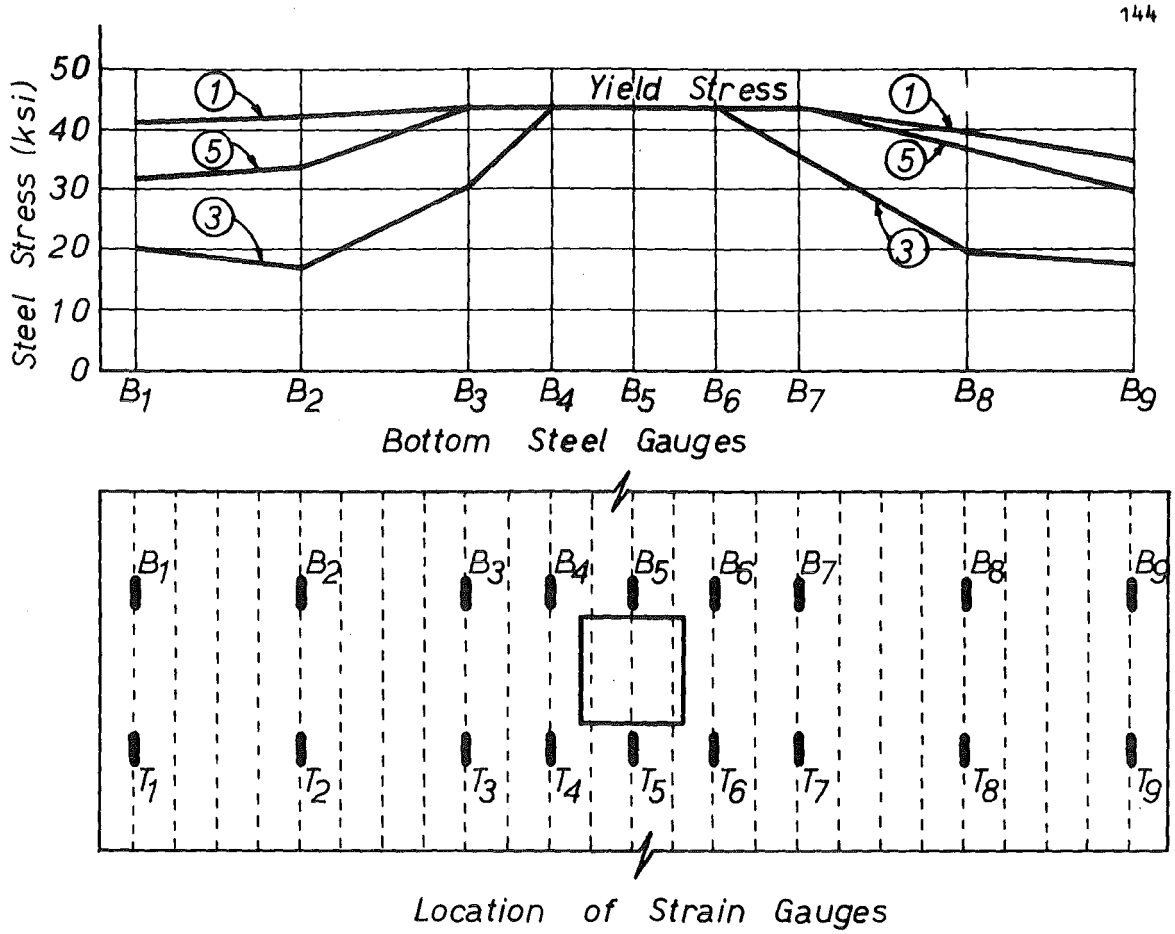

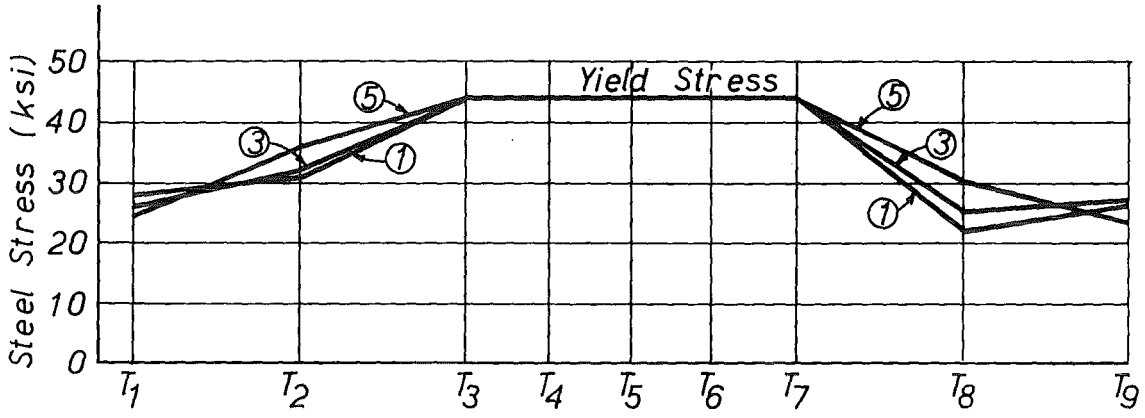

FIG. 3.60 STRESSES IN SLAB STEEL OF SPECIMEN 7CS

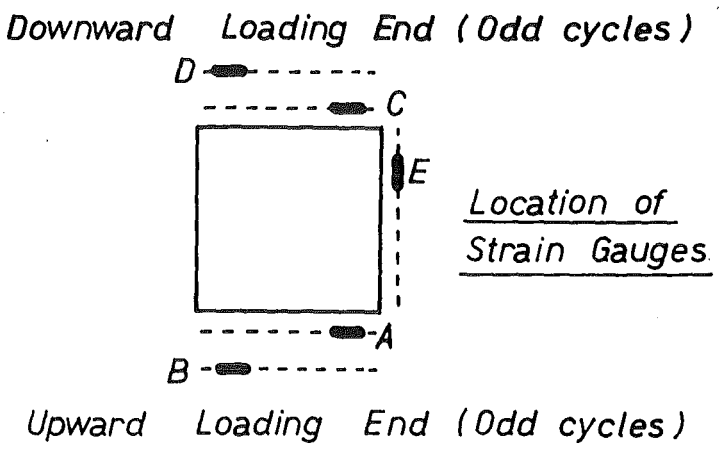

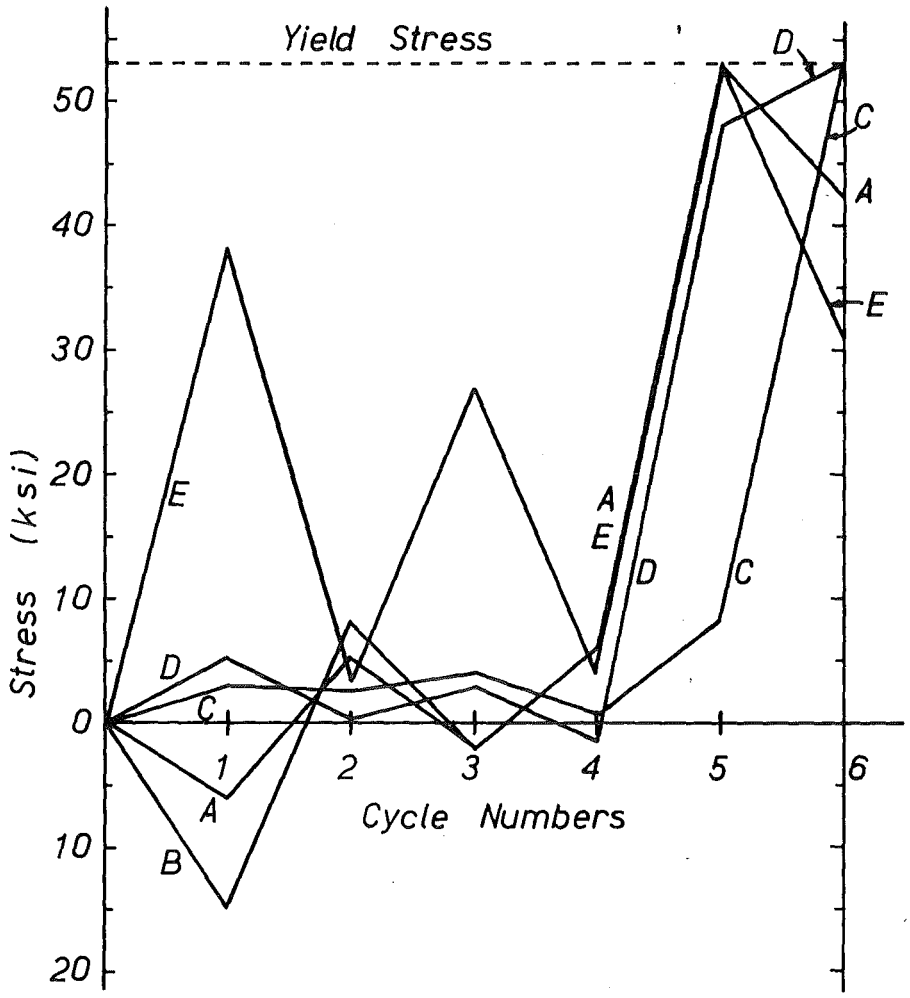

FIG. 3.61 STRESSES IN STIRRUPS OF SPECIMEN 7CS

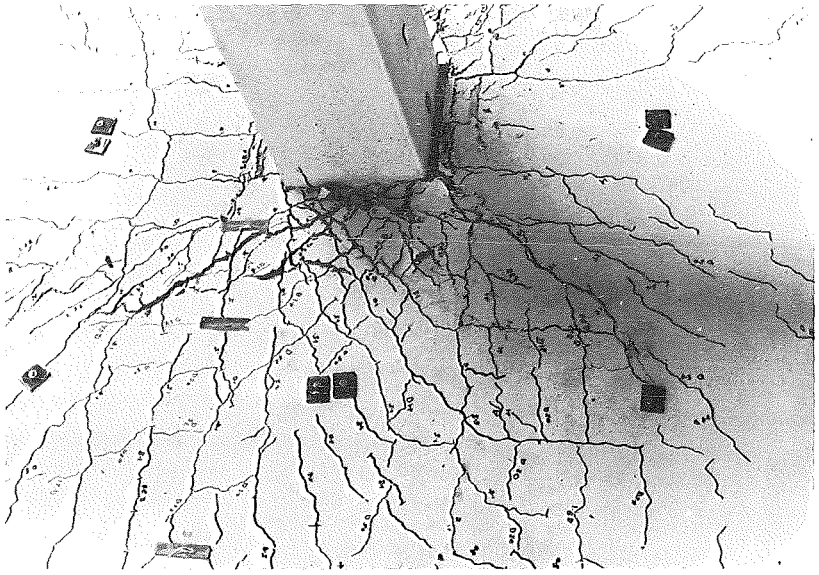

FIG. 3.62 VIEW OF SPECIMEN 7CS AFTER TEST

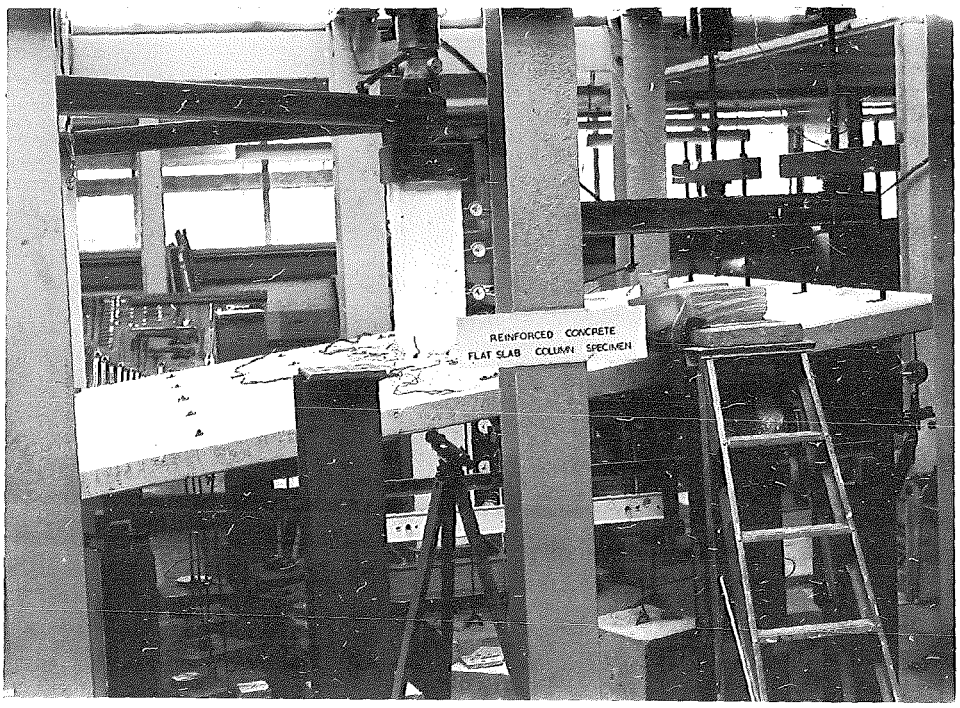

FIG. 3.63 DEFLECTED SHAPE OF SPECIMEN 7CS AFTER TEST

column-slab junction parallel to the direction of bending and also on the top surface of the slab at the downward loading end. In spite of these cracks the specimen maintained nearly 50% of the maximum moment attained during cycle 1 at the end of testing when the edge displacements were increased up to 11.2 in. A view of the deflected shape of the slab is shown in Fig. 3.63 at the end of testing.

(x) Behaviour of Specimen 8CS

Type of Loading

This specimen was also subjected to several cycles of loading reversals similar to those for specimens 6CS and 7CS.

Load-deflection Characteristics

The load-displacement curves for the two loading edges are shown in Fig. 3.64 and 3.65. The maximum moment of 309 kip. in. was attained at an edge displacement of 3.0 in. during cycle 1 when the upward edge load was 3280 lb. and the downward load was 2440 lb. The moments reached during subsequent cycles of loading were 169 kip. in. at cycle 2, 180 kip. in. at cycle 3, 267 kip. in. at cycle 4, 267 kip. in. at cycle 5 and 171 kip. in. at cycle 6. During the last cycle the edge displacements were increased up to 10.7 in. without causing failure in the specimen.

Stresses in Slab Bars

Fig. 3.66 shows the stresses in slab bars at selected positions during loading cycles 1, 3 and 5. As observed in other test specimens first yielding took place in the top central bar T5 , at an imposed edge displacement of 0.6 in. During cycle 1 top bars T3 to T7 and bottom bars B4 to B6 yielded. At the end of cycle 3 top bars T3 to T7 were past their yield stress levels but among the bottom bars only B5 indicated yielding. At the end of cycle 5 the stress distribution was similar to that obtained at cycle 1. Top bars T1 , T2 , T8 , T9 and bottom bars B1 , B2 , B3 , B7 , B8 , B9 always remained below their yield stress levels during all cycles of loading.

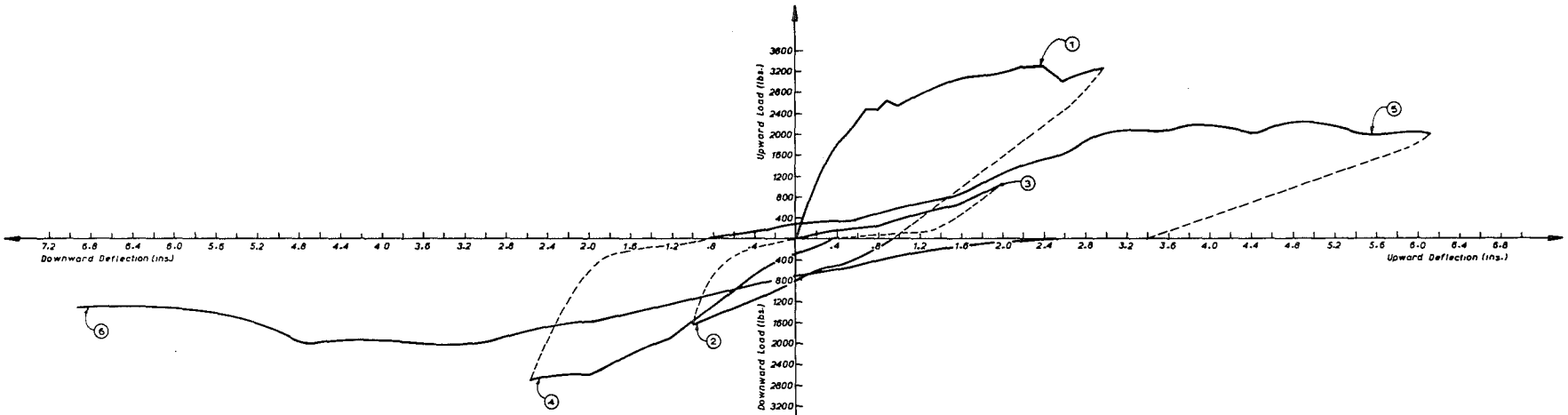

Fig.3.64 – EDGE 'A'

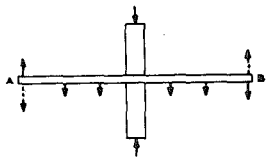

Fig.3 65 – EDGE B

– LOAD – DISPLACEMENT CURVES FOR EDGES A & B OF SPECIMEN 8 CS –

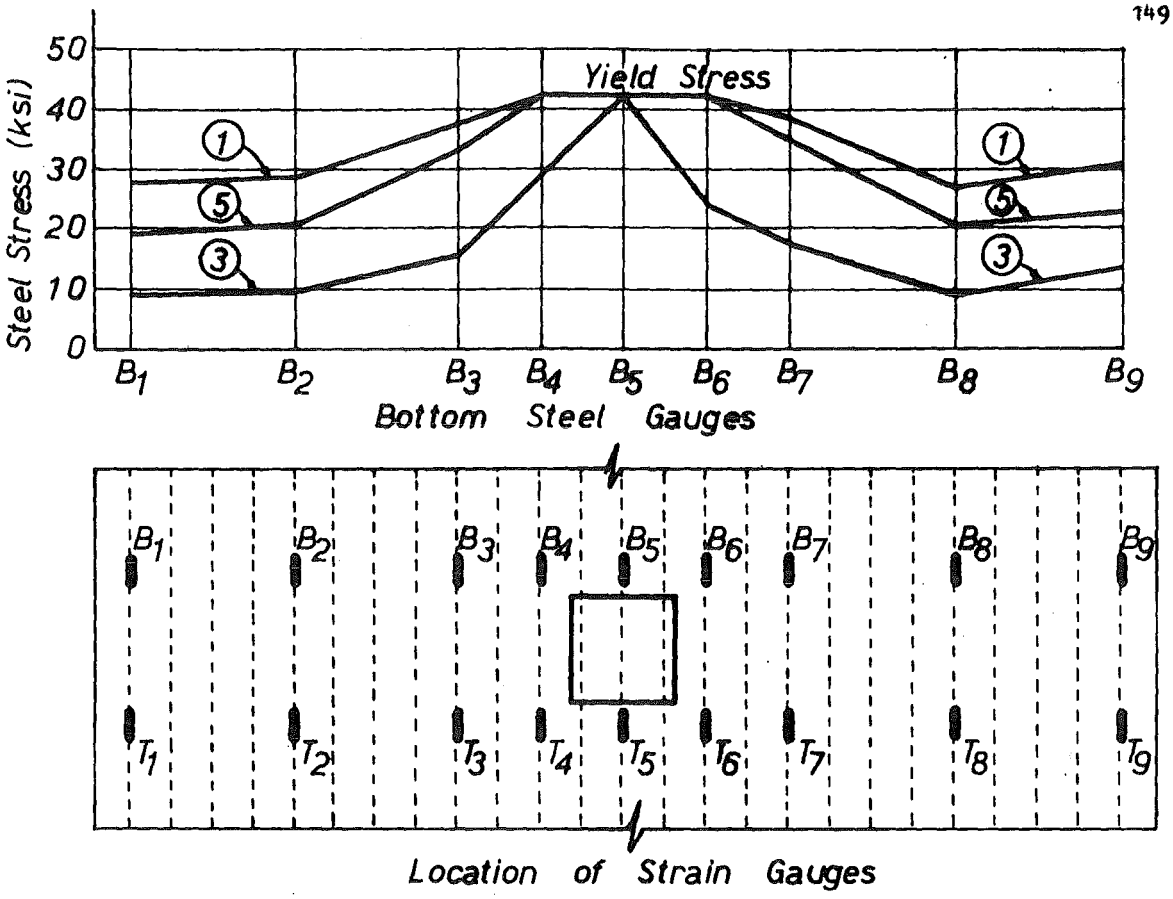

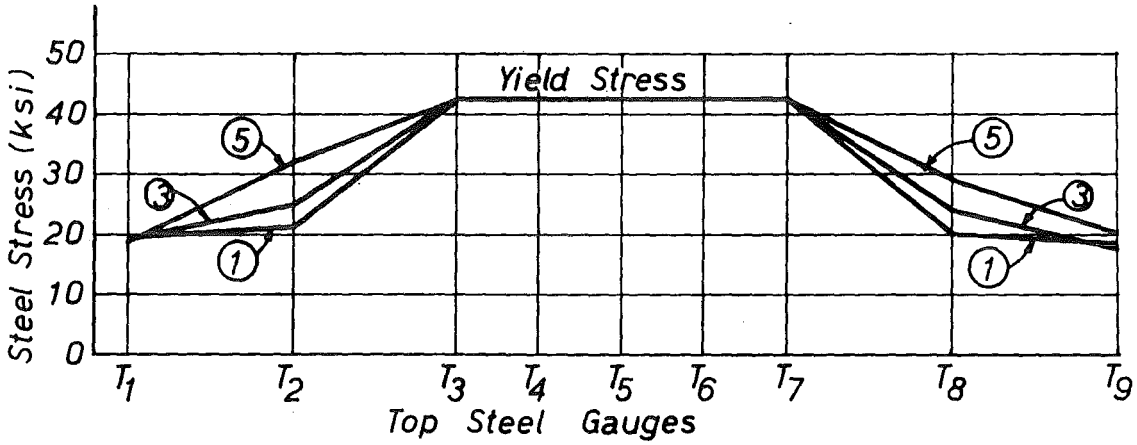

FIG. 3.66 STRESSES IN SLAB STEEL OF SPECIMEN 8CS

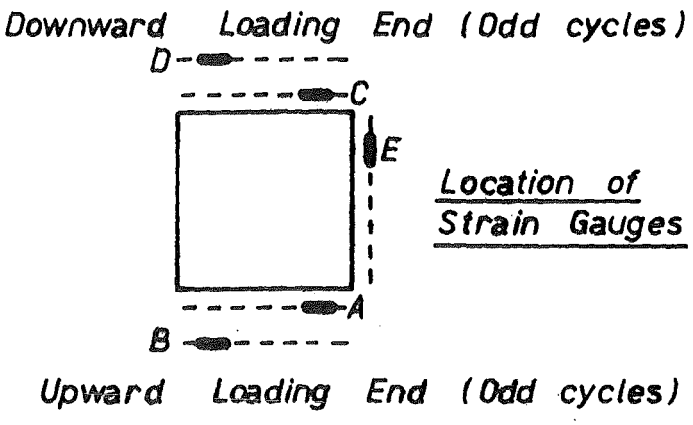

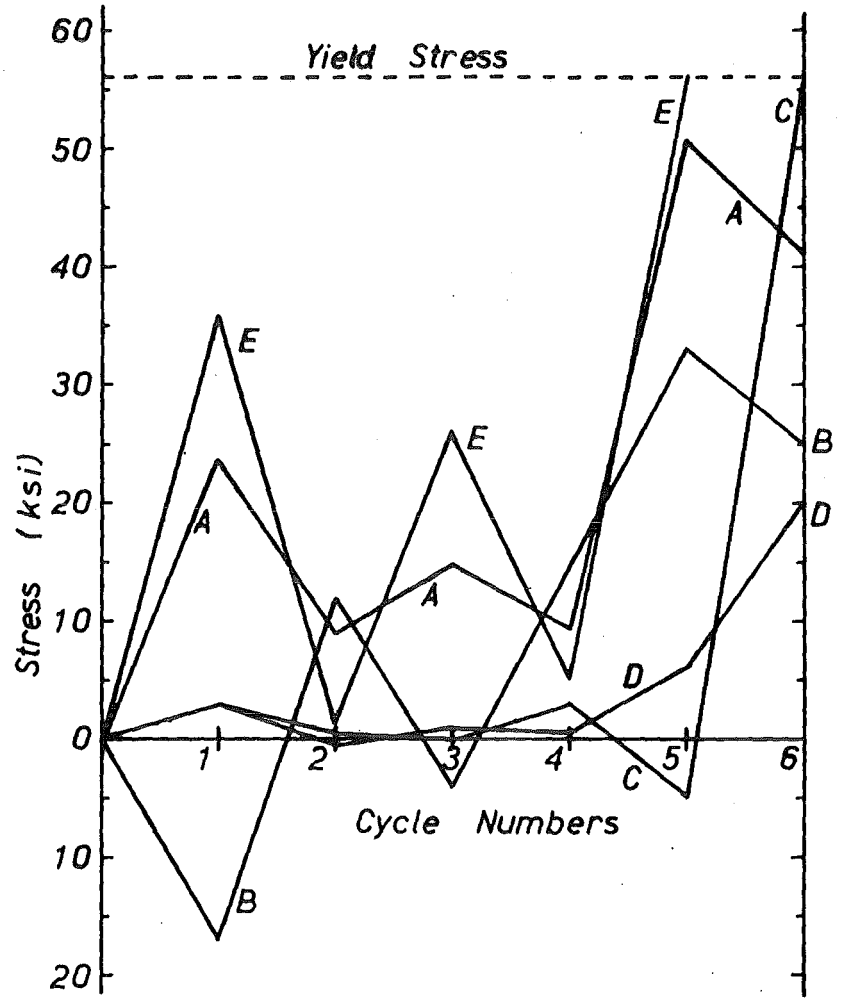

FIG. 3.67 STRESSES IN STIRRUPS OF SPECIMEN 8CS

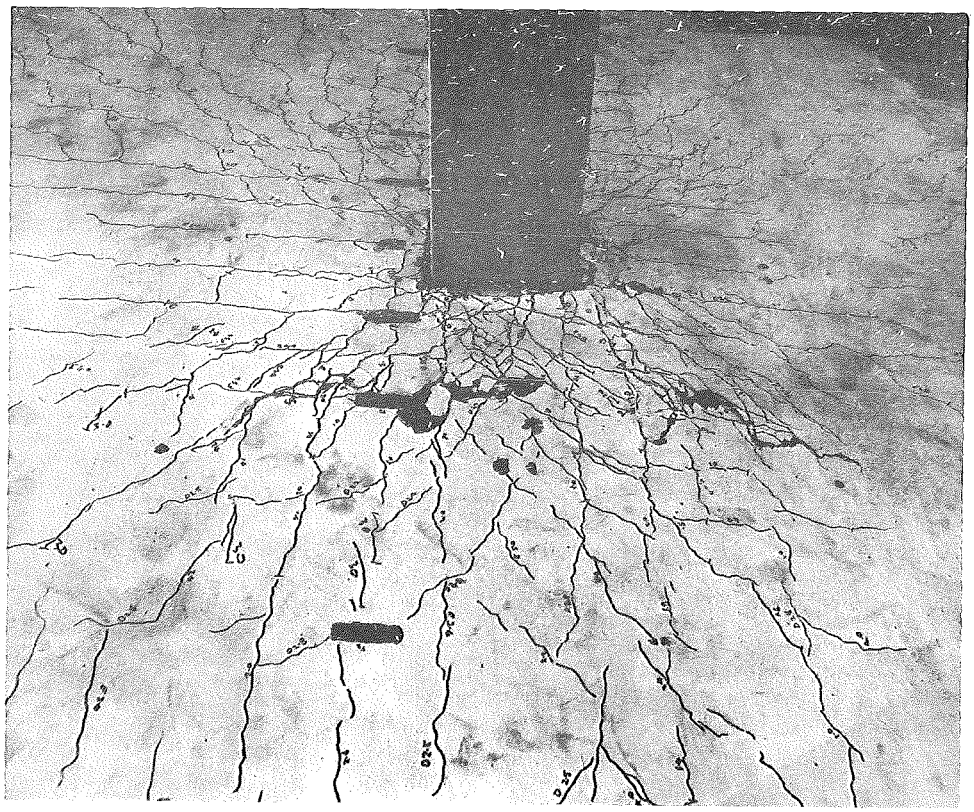

FIG. 3.68 CRACK PATTERN OF SPECIMEN 8CS AFTER TEST

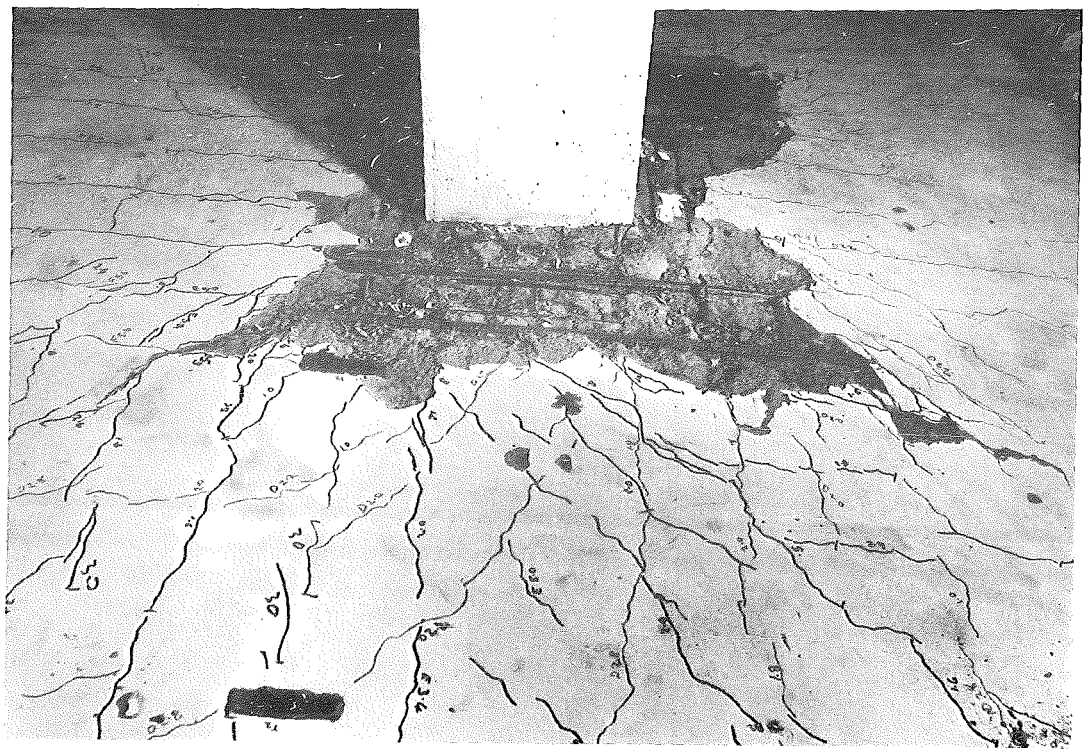

FIG. 3.69 VIEW OF SPECIMEN 8CS AFTER REMOVAL OF BROKEN CONCRETE

Stresses in Stirrups

The stresses attained in stirrups at selected locations during each loading cycle are shown in Fig. 3.61. The stresses in these stirrups remained below the yield point up to cycle 4. During cycle 5 stirrup E indicated yielding and stirrups A reached about 93% of the yield stress value. During cycle 6 stirrup C yielded but stirrups A, B and D remained below the yield stress level.

Cracking and Failure Mode

Like the specimens 6CS and 7CS with closed stirrups, this specimen also behaved in a ductile manner and did not exhibit any punching shear failure around the column. A view of the crack pattern at the end of testing is shown in Fig. 3.68. Primary cracking occurred at the side faces of the column parallel to the direction of bending and also on top surface of the slab at the downward loading end. Despite these cracks 50% of the maximum moment attained during cycle 1 was sustained by the specimen at the end of testing when the edge displacements were increased up to 10.7 in. Fig. 3.69 shows a view of the specimen after removal of broken concrete.

3.3.5 DISCUSSION OF TEST RESULTS

(i) Strength

Since all the eight test specimens were subjected to a constant shear force of 8040 lb. due to the self weight of the slab and the imposed live load, the strength of the slab-column connection in this discussion refers to the maximum unbalanced moment capacity that can be carried by the specimens. For the three specimens 1 , 2 and 3C without any shear reinforcement the maximum moment attained varied from 270 kip.in. to 334 kip. in. , while for the five specimens 4S , 5S , 6CS , 7CS and 8CS containing various shear reinforcement arrangements the maximum moment attained ranged from 309 kip. in. to 369 kip. in. Thus the mean strength of the slab-column connection has been increased to an extent of roughly 13% by the provision

of shear reinforcement at the connections. In case of the specimens without shear reinforcement the concrete compressive strength f'_c varied from 3960 psi to 4630 psi and the yield stress f_y of slab reinforcing bars ranged from 45,820 psi to 54,160 psi. In the specimens with shear reinforcement the range of f'_c was from 3210 psi to 4630 psi and that of f_y was from 41,230 psi to 47,740 psi. Due to the variation in the material strengths f'_c and f_y in each test specimen it is not exactly possible to determine the extent of increase in the strength experimentally. However, it can be seen that the unbalanced moment capacity of the specimens with shear reinforcement did not show marked increase over those specimens without shear reinforcement. The influence of the variation of concrete strength, f'_c, on the strength of slab-column connections may be regarded as small since theoretically it is the practice to assume direct proportionality between the nominal shear stress of concrete and the square root of its compressive strength. On the other hand the yield stress of slab reinforcing bars, f_y, has a marked influence on the strength of the connections as the flexural capacity of the slab depends largely on this value. Since the range of f_y in the specimens with shear reinforcement was lower than that for specimens without shear reinforcement it could be concluded that the extent of increase in the strength of the reinforced connections will be somewhat larger than what could be gauged from experimental results.

(ii) Ductility

The load-displacement curves indicate very little ductility for the specimens 1, 2 and 3C without shear reinforcement. The ratio of maximum edge displacement to the edge displacement at first yield in a slab reinforcing bar varied from 4.50 to 6.00. The maximum edge displacements that could be imposed on these specimens were of the order of 2.4 in. to 2.8 in. The maximum edge displacement to the edge displacement at

first yield ratio for the specimen 4S with cranked bars as shear reinforcement was found to be 4.14 . This ratio is even lower than those obtained for unreinforced slab-column connections. This is because straight portions of the cranked bars helped to increase the flexural resistance of the slab in the vicinity of the column thereby increasing the edge displacement at which first yielding could occur. The load-displacement curves for the specimen 5S with a shearhead and specimens 6CS , 7CS and 8CS with closed stirrups show large amounts of ductility which is available at the slab-column connections. The ratios of maximum edge displacement to the edge displacement at first yield range from 9.36 for a shearhead to 18 - 19 for closed stirrups. The lower ratio for the shearhead reinforcement is due to the fact that the onset of first yielding in a slab bar was delayed by the strengthening effect of the shearhead on the flexural resistance of the slab near the slab-column junction. In case of closed stirrups there was no addition to the flexural resistance of the slab and hence a greater displacement ratio could be achieved.

(iii) Stresses in Slab Bars and Shear Reinforcement

Strain measurements indicate yielding of all the slab bars passing through the column in all the test specimens. Table 3.3 gives a comparison of maximum steel stresses as a proportion of the yield stress reached in slab bars across the slab which extended from - 45 in. to + 45 in., i.e. a full width of 90 in. The mean steel stress over the full width of the slab is also indicated in the Table. A value of unity in the Table indicates yielding of slab steel.

In specimens 1 and 2 one more slab bar adjacent to either side of the column also yielded. In the specimen 3C which was subjected to cycles of bending moment reversals, yielding of slab bars extended to three more bars outside the column on either side of it before failure occurred. This is due to the loss in stiffness at the junction under

TABLE 3.3

COMPARISON OF MAXIMUM STEEL STRESSES AS A PROPORTION OF THE YIELD STRESS REACHED IN SLAB BARS ACROSS THE SLAB

SPECIMEN NOS.	TOP or BOTTOM	DISTANCE IN INCHES FROM THE SLAB-COLUMN CENTRE													MEAN STRESS OVER FULL WIDTH
		-42	-35	-28	-21	-14	-7	Column Centre	7	14	21	28	35	42	
1	Top					0.80	1.00	1.00	1.00	0.93					-
	Bottom					0.76	1.00	1.00	1.00	0.74					-
2	Top					0.76	1.00	1.00	1.00	0.77					-
	Bottom					1.00	1.00	1.00	1.00	0.85					-
3C	Top					1.00	1.00	1.00	1.00	1.00					-
	Bottom					0.91	1.00	1.00	1.00	1.00					-
4S	Top	0.53	0.51	0.48	0.63	0.80	1.00	1.00	1.00	0.89	0.68	0.46	0.46	0.46	0.68
	Bottom	0.84	0.82	0.78	0.88	1.00	1.00	1.00	1.00	1.00	0.93	0.86	0.65	0.44	0.86
5S	Top	0.41	0.43	0.51	0.80	0.92	1.00	1.00	1.00	0.96	0.80	0.58	0.48	0.43	0.72
	Bottom	0.65	0.72	0.63	0.53	0.70	1.00	1.00	1.00	0.67	0.60	0.65	0.70	0.53	0.72
6CS	Top	0.57	0.71	0.83	0.90	1.00	1.00	1.00	1.00	1.00	0.90	0.83	0.75	0.67	0.86
	Bottom	0.64	0.60	0.57	0.76	1.00	1.00	1.00	1.00	1.00	0.79	0.60	0.64	0.69	0.79
7CS	Top	0.64	0.68	0.82	0.91	1.00	1.00	1.00	1.00	1.00	0.84	0.68	0.60	0.61	0.83
	Bottom	0.93	0.95	0.96	0.98	1.00	1.00	1.00	1.00	1.00	0.95	0.89	0.84	0.80	0.94
8CS	Top	0.45	0.61	0.75	0.87	1.00	1.00	1.00	1.00	1.00	0.84	0.68	0.58	0.47	0.79
	Bottom	0.66	0.67	0.68	0.78	0.89	1.00	1.00	1.00	0.92	0.78	0.64	0.68	0.73	0.80

N.B. The slab extended from - 45" to 45" , i.e. a full width of 90".

155

repeated cyclic loading. In specimens with shear reinforcement the yielding of slab steel was observed to extend to three bars on either side of the column. This means that over the slab width of 90 in. yielding of steel was confined to a width of 28 in. centred on either side of the column and straight parallel yield lines never developed across the whole width of the slab. However, it is confirmed that the slab bars passing through the critical faces taken at a distance of d/2 from the column face do yield.

A study of Table 3.3 reveals a remarkable extent of slab participation in resisting moment outside the area of the column. The mean steel stress over the full width of the slab could be computed from strain measurements only in specimens with shear reinforcement because in specimens without shear reinforcement strain gauges were not used in slab bars across the entire width. The mean steel stress for slab bars in the top face varies from $0.68\ f_y$ to $0.86\ f_y$, whereas that for the bottom face ranges from $0.72\ f_y$ to $0.94\ f_y$.

The cranked bars used as shear reinforcement in the specimen 4S all yielded before failure and in spite of this fact they failed to achieve their purpose. The shear force distribution obtained from strain measurements in the shearhead of specimen 5S was found to be nearly parabolic and this fact was used in the derivation of the theory proposed for the design of shearhead in Section 3.3.2. The measurement of strains in closed type stirrups used in specimens 6CS, 7CS and 8CS showed that the stirrups placed adjacent to the column faces parallel to the direction of bending always yielded indicating their effectiveness in resisting torsional shear stresses set up on these faces. The stirrups placed on the column faces transverse to the direction of bending indicated yielding in specimens 7CS and 8CS but in the specimen 6CS none of these stirrups yielded. This may be due to the fact that in specimens 7CS and 8CS two legged stirrups of diameters $\frac{1}{4}$ in. and 3/16 in

respectively were used whereas in the specimen 6CS four legged stirrups of 3/16 in. diameter were used.

(iv) Effect of Bending Moment Reversals

The effect of cycles of bending moment reversals was studied in four specimens, namely 3C which was without shear reinforcement and 6CS , 7CS and 8CS which contained closed stirrups as shear reinforcement. The specimen 3C attained its maximum moment capacity at the end of cycle 5. In spite of repeated number of load reversals the degradation of moment capacity, measured as the ratio of the moment at the maximum displacement in the last load cycle to the maximum moment attained, was 0.74 as compared to 0.84 and 0.78 obtained for specimens 1 and 2 respectively under monotonic loading. Although successive loading cycles helped to spread yielding of slab reinforcing steel over a greater width of the slab there was no increase in the ductility factor which remained quite low,similar to those obtained under monotonic loading. Therefore it may be concluded that if a specimen without any shear reinforcement be subjected to a number of loading reversals within the same ductility factor as is obtained under monotonic loading, the deterioration in the load carrying capacity is not very pronounced.

On the other hand specimens 6CS , 7CS and 8CS exhibited a greater deterioration in the load carrying capacity under cycles of loading reversals. The degradation of moment capacity was nearly 0.50 but this was accompanied by a very large ductility factor of the order of 18 to 19 , which is desirable from the point of view of seismic-resistant design.

(v) Effectiveness of Various Shear Reinforcement Arrangements

The specimen 4S with cranked bars as shear reinforcement failed in punching shear and showed little ductility. There was some increase in the moment capacity as compared with the unreinforced junctions but otherwise there was very little difference in behaviour between this specimen and other specimens without any shear reinforcement. Therefore, cranked bar

are ineffective as shear reinforcement in thin slabs.

The shearhead used in the specimen 5S resulted in an increased ductility factor as compared to the previous specimens and behaved in a ductile manner without any danger of a shear failure. This specimen was also subjected to a reversal of bending moment after the first cycle and it maintained 59% of its maximum moment capacity at a ductility factor of 9.36. Therefore, a shearhead may be regarded as a satisfactory type of shear reinforcement in flat plates.

Closed stirrups used in specimens 6CS , 7CS and 8CS were found to form most suitable shear reinforcement in earthquake resistant flat plate-column junctions. In all these cases there was no shear failure in the slab and a large ductility was available at the slab-column junction when subjected to cyclic loading. The two specimens 7CS and 8CS containing two legged stirrups of diameters $\frac{1}{4}$ in. and 3/16 in. respectively behaved in a similar fashion as the specimen 6CS with four legged 3/16 in. diameter stirrups so far as the ductility and the degradation in the load carrying capacity are concerned. Because of reduced area of shear reinforcement the maximum moment capacity of the specimen 8CS was lower than that of the specimen 6CS but it achieved the same ductility factor after similar loading cycles and maintained the same load carrying capacity.

From the practical point of view tests with two legged stirrups were highly successful. The use of two legged stirrups makes fabrication and placing of stirrups simpler and quicker. These tests showed that even in $3\frac{1}{2}$ in. thick slabs stirrups of closed type can be fully effective in preventing punching shear failures and in addition they increase the ductility of the slab-column junctions by effectively confining the concrete within the slab.

(vi) Junction Failure Mechanisms

Punching shear failures in specimens 1 , 2 , 3C and 4S occurred in the slab near the column face which was subjected to the downward edge

loading. Failures took place along inclined cracks which extended from the intersection of the column face and the compression face of the slab toward the tension face of the slab at an angle of about 13^{o} with the horizontal. The reason for this very flat failure surface may be splitting of the concrete at the intersection of the inclined cracking and the tension reinforcement. Unlike symmetrically loaded slab-column junctions where punching shear failures occur along truncated pyramidal surfaces around the column failures in eccentrically loaded slab-column junctions take place in the slab region surrounding only one face of the column, which is subjected to the maximum shear force. It was observed that before failure the reinforcing steel passing through the column had yielded. This shows that yielding of the reinforcing steel at the column is a necessary requirement for punching shear failure.

The specimens 5S , 6CS , 7CS and 8CS did not fail in punching shear. Also there was no evidence of flexural failure by the formation of yield lines developing across the full width of the slab along sections adjacent to the column faces. On the top surface of the slab at the downward loading end there were a large number of cracks which originated radially from the two corners of the slab and some cracks formed at the intersection of the slab and the column along both directions, transverse and parallel to the direction of bending. Observed yield-line patterns followed substantially the theoretical pattern, A2 , adopted in Section 3.6 and shown in Fig. 3.83. There is, however, a disparity between the two patterns and this stems from torsional cracking of the column-slab interfaces parallel to the direction of bending. In the theoretical pattern, A2 , these column-slab interfaces were assumed to be uncracked whereas in the observed pattern torsional cracking does occur. This does not invalidate the theoretical pattern which can be realised if the torsional cracking could be suppressed by some means.

(vii) Effective Width and Stiffness of Slab-Column Specimens

The effective width of the slab is a useful concept for determining the stiffness of the structure. It is defined as the width of an imaginary slab strip having the same depth, span and flexural stiffness as the actual slab under consideration.

In order to determine approximately the effective width of the slab, load-displacement characteristics at the onset of first yielding of the slab reinforcing steel have been used. The computed edge displacement of the slab is assumed to consist of two components as shown in Fig. 3.70. The first deflection component is due to the column rotation which is calculated as $\ell.\theta$, where ℓ is half the span of the slab and θ is the column rotation computed as $\frac{M_c h_1}{3EI_c}$. M_c is the moment acting on the column, h, is the height of the column to midpoint measured from the slab-column joint and I_c is the moment of inertia of the column.

The second deflection component is due to the elastic deformation of slab due to the weight of the concrete blocks and the applied loads. Fig. 3.70 shows the slab-column specimen deformed elastically and also the method of computing the displacements. For comparison with the test results the average of upward and downward displacements has been considered. In computing the moment of inertia of the slab, I_s, the cracked transformed section has been used ; for the column the uncracked E I was used.

The effective width of the section was found by a trial and error approach. A width of 36 in. gives a good correlation between the measured and the computed edge displacements as shown in Table 3.4. This effective width is about 10 times the slab thickness and 0.4 of the width of the slab. Thus in computing the lateral deflection of this flat plate structure within the elastic stage, a width of 36 in. may be considered as effective.

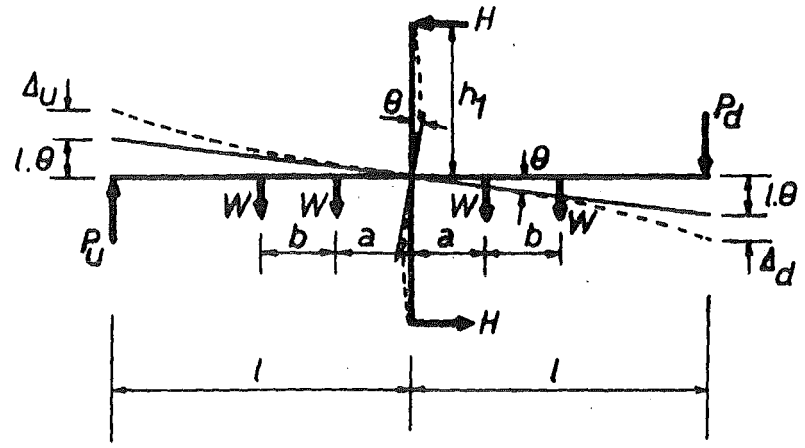

Edge displacement due to downward slab deformation

$$\Delta_d = \frac{P_d\, l^3}{3E I_s} + \frac{W a^3}{3E I_s} + \frac{W a^2 (l-a)}{2E I_s} + \frac{W(a+b)^3}{3E I_s} + \frac{W(a+b)^2(l-a-b)}{2E I_s}$$

Edge displacement due to upward slab deformation

$$\Delta_U = \frac{P_U\, l^3}{3E I_s} - \frac{W a^3}{3E I_s} - \frac{W a^2 (l-a)}{2E I_s} - \frac{W(a+b)^3}{3E I_s} - \frac{W(a+b)^2(l-a-b)}{2E I_s}$$

Edge displacement due to column rotation $= l.\theta$

$$\text{where } \theta = \frac{M_c\, h_1}{3E I_c}$$

$$\text{Computed edge displacement} = l.\theta + \frac{\Delta_U + \Delta_d}{2}$$

Notations: P_d = Downward load, P_U = Upward load
W = Weight of 5 concrete blocks = 1000 lb.
M_c = Column moment

FIG. 3.70 COMPUTATION OF EDGE DISPLACEMENT

TABLE 3.4

COMPARISON OF CALCULATED AND MEASURED EDGE DISPLACEMENTS

CIMEN O.	LOAD AT FIRST YIELD		CALCULATED EDGE DISPLACEMENT DUE TO				TOTAL CALCULATED EDGE DISPLACEMENT in.	MEASURED EDGE DISPLACEMENT in.	MEASURED / CALCULATED
	UPWARD lb. lb.	DOWNWARD lb. lb.	COLUMN ROTATION in.	UPWARD SLAB DEFORMATION in.	DOWNWARD SLAB DEFORMATION in.	AVERAGE OF UPWARD AND DOWNWARD DEFORMATIONS in.			
1	1404	1061	0.021	0.295	0.509	0.402	0.423	0.4	0.95
2	2476	819	0.026	0.631	0.420	0.526	0.552	0.6	1.09
3C	2635	911	0.029	0.689	0.453	0.571	0.600	0.6	1.00
4S	2864	967	0.030	0.756	0.467	0.612	0.642	0.7	1.09
5S	2762	939	0.030	0.728	0.461	0.595	0.625	0.7	1.12
6CS	2260	1060	0.028	0.571	0.503	0.537	0.565	0.5	0.88
7CS	2567	986	0.029	0.667	0.478	0.573	0.602	0.6	1.00
8CS	2083	911	0.028	0.533	0.473	0.503	0.531	0.6	1.13
								Mean	1.03

3.3.6 CONCLUSIONS

This series of tests showed that flat-plate column junctions reinforced with shearheads and closed stirrups as shear reinforcement behave in a satisfactory manner as earthquake resistant connections. Specific conclusions derived from this experimental study are as follows:

(a) The slab-column specimens without any shear reinforcement failed in shear and showed little ductility.

(b) Cranked bars as shear reinforcement are ineffective in thin slabs. Although they increased the moment capacity of the junction to some extent there was very little difference in behaviour between this junction and those junctions without any shear reinforcement.

(c) Shearheads and closed stirrups form suitable shear reinforcement in earthquake resistant flat plate-column connections. They ensure that the connection behaves in a ductile fashion when subjected to cyclic loading.

(d) The load carrying capacity with cyclic loading deteriorated by about 50% in junctions reinforced with closed stirrups but this was accompanied by very large cyclic deformations.

(e) Folding type failure mechanisms by the formation of parallel positive and negative yield lines running across the full width of the slab adjacent to the column faces were never realised. Observed yield-line patterns followed closely the theoretical pattern adopted in Section 3.6.

(f) Two legged closed stirrups were found to be as effective as four legged stirrups. From the practical constructional point of view two legged stirrups are recommended for seismic resistant flat plate-column connections.

(g) For predicting interstory displacements a slab strip may be considered effective in computing the flexural stiffness of the floor.

3.4 THEORY FOR SHEAR-FLEXURE FAILURE OF SLAB-COLUMN CONNECTIONS WITHOUT SHEAR REINFORCEMENT

SUMMARY

An ultimate strength procedure is derived for determining the shear and unbalanced moment capacity of interior column-flat plate junctions without any shear reinforcement. This theory is based on an extension of previous investigations. The strength of such junctions predicted by the theory is shown to give good agreement with test results.

3.4.1 INTRODUCTION

In most cases the strength of flat plate-column junctions without any shear reinforcement will be governed by a shear-flexure failure on some critical section surrounding the column before the formation of the complete yield-line pattern for the slab. On this critical section the applied shear and unbalanced moment are resisted by three actions within the slab, namely (i) flexure, (ii) shear, and (iii) torsion. The theory for the failure mode is based on the evaluation of these three quantities which are obtained from the results of previous investigations.

Fig. 3.71(a) shows the portion of a flat plate surrounding an interior column. Let V_u be the resultant shear and M_u the unbalanced moment about the X-X axis acting at the centroid of the slab-column junction at ultimate loading conditions. The forces and moments acting on some critical section ABCD within the slab and contributing to the transfer of the shear V_u and the moment M_u are indicated in the figure.

The unbalanced moment M_u is transferred by three actions, namely

(i) flexure on faces AB and CD,

(ii) vertical shear on faces AB and CD,

(iii) torsion on faces AD and BC.

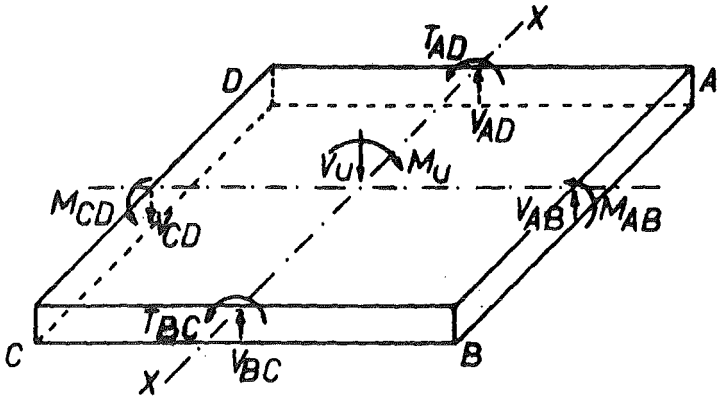

(a) Moments and Forces

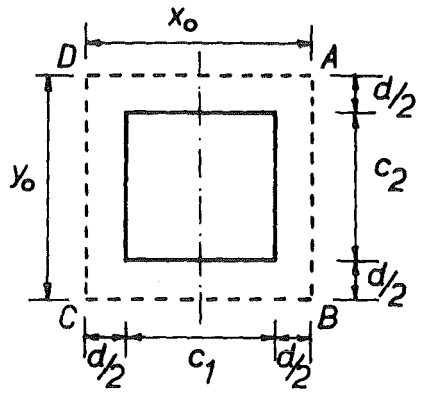

(b) Critical Section

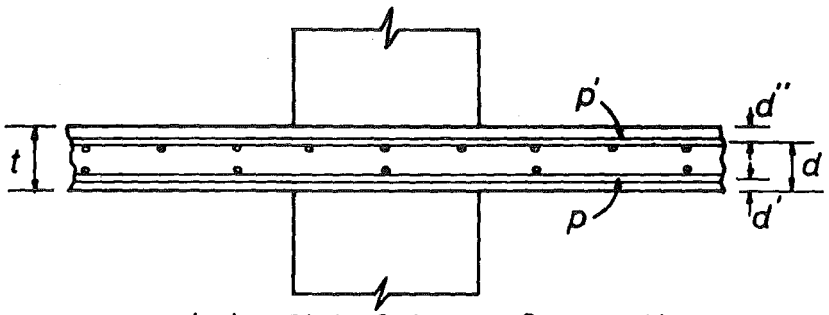

(c) Slab-Column Connection

FIG. 3.71 MOMENTS AND FORCES AT SLAB-COLUMN CONNECTION

The individual contributions of these actions will be determined and summed to obtain the total unbalanced moment that can be transferred with shear force at the interior column-flat plate junction.

The distribution of stresses in the slab around the column at the ultimate load is very complex. Mast[37] has obtained the distribution of stresses in flat plates near columns due to the moment transfer in accordance with the theory of elastic plates. This elastic stress distribution does not apply at the ultimate load because of the effect of inclined cracking in the slab around the column, which has been ignored in the theory and is likely to alter the stress distribution very appreciably. Besides, the elastic theory does not account for the influence of the slab reinforcement and the concrete does not act like an elastic homogeneous material at the ultimate load of the junction. Because of this complex behaviour it is necessary to make some simplifying assumptions in order to derive design equations.

3.4.2 ASSUMPTIONS

The assumptions made in the derivation of design equations are as follows:-

(i) The critical section shown in Fig. 3.71(b) will be assumed to be located at a distance $d/2$ from the periphery of the column. For a concentrically loaded slab-column junction the failure surface takes the shape of a truncated pyramid with sides sloping roughly at 45°. The average shear stress in the concrete which fails in this manner can be taken as that which acts on vertical planes laid through the slab at a perimeter a distance $d/2$ from the faces of the column. This has been found to give safe results for concentrically loaded slab-column junctions and was recommended by ACI-ASCE Committee 326[12]. It has been found by other researchers[16,20] to give good results for eccentrically loaded columns and has been incorporated in the ACI building code (ACI 318-71)[13].

(ii) At failure all the slab reinforcement bars crossing the transverse faces AB and CD of the critical section are assumed to yield in tension. The ultimate flexural capacity is reached in positive bending on the face AB and negative bending on the face CD. The effect of membrane action on the flexural capacities of the faces AB and CD will be neglected although compressive membrane forces present in the plane of the slabs may considerably enhance the flexural strength of the sections. Membrane action could be taken into account if the extent of membrane forces could be predetermined. The effect of membrane action will be discussed in more detail later.

(iii) The maximum vertical shear stress on the critical faces AB and CD will be limited to $4\sqrt{f'_c}$ psi. This is the same assumption as recommended by ACI-ASCE Committee 326[12] and incorporated in the ACI Building Code (ACI 318-71)[13] for computing the shear strength of concentrically and eccentrically loaded slab-column junctions. The shear stress of $4\sqrt{f'_c}$ at the critical section at ultimate load for concentrically loaded junction is twice that used for beams. This higher value for slabs is due to the strengthening effects of two-way action. At the slab-column junction the slab concrete is subjected to horizontal compressive stresses due to negative bending at the column in two perpendicular directions in addition to vertical compression due to the reaction of the column. The simultaneous presence of these compressive stresses increases the shear resistance of the section. Tests[12] have indicated that, when punching shear failure occurs, the shear stress computed on the perimeter of the critical section is larger than in beams or one-way slabs and is approximately equal to $4\sqrt{f'_c}$.

(iv) The part of the vertical shear stress due to V_u on the faces AB and CD of Fig. 3.71 is uniformly distributed over the effective depth of the slab.

(v) The part of the vertical shear stress induced by the moment M_u on the faces AB and CD of Fig. 3.71 is assumed to be uniformly distributed

over the effective depth of the slab. This vertical shear stress is assumed to be the difference between $4\sqrt{f'_c}$ and the shear stress induced by V_u.

(vi) The ultimate torsional capacity is assumed to be developed on the side faces AD and BC of the critical section. This is the torsional capacity taking into account the reduction due to the part of the vertical shear stress caused by V_u on the faces AD and BC of Fig. 3.71. The ultimate torsional shear stress for the case of torsion without flexural shear is assumed to be $4.8\sqrt{f'_c}$, which is twice that normally recommended for beams in ACI 318-71 Code[13]. This enhanced torsional shear stress is assumed to be available due to the effect of membrane compressive stresses in the plane of the slab.

3.4.3 MOMENT TRANSFER BY FLEXURE

The ultimate flexural capacities of faces AB and CD of Fig. 3.71 are calculated by using the ultimate strength design formula for a rectangular reinforced concrete section. The moment transferred by flexure is given by

$$M_{ABO} + M_{CDO} = (m_u + m'_u)\, y_o \qquad \ldots (3.25)$$

For positive bending

$$m_u = \rho f_y \, (t - d')^2 \left(1 - \frac{0.59\, \rho f_y}{f'_c}\right) \qquad \ldots (3.26)$$

For negative bending

$$m'_u = \rho' f_y \, (t - d'')^2 \left(1 - \frac{0.59\, \rho' f_y}{f'_c}\right) \qquad \ldots (3.27)$$

where

m_u = postive ultimate flexural capacity of face AB per unit length

m'_u = negative ultimate flexural capacity of face CD per unit length

y_o = dimension of faces AB and CD of the critical section transverse to the direction of bending

ρ = positive or bottom reinforcement ratio

ρ' = negative or top reinforcement ratio

t = total depth of slab

f_y = yield stress of reinforcement bars

f'_c = cylinder compressive strength of concrete

d' = distance between the bottom face and the centroid of bottom reinforcement

d'' = distance between the top face and the centroid of top reinforcement

In each case, the effect of the reinforcement which is in compression has been ignored as the presence of compression steel does not appreciably increase the ultimate moment capacity of reinforced concrete sections failing in tension.

The effect of membrane action on the flexural capacities of the faces AB and CD has been neglected. This aspect is further discussed in the following section.

3.4.4 EFFECT OF MEMBRANE ACTION

It has been shown by Park[38,39] that in slabs with edges restrained against lateral movement, compressive membrane forces develop in the plane of the slab and increase the ultimate moments of resistance at the yield lines. When yielding of the slab reinforcement at the critical sections occurs under the application of unbalanced moment the slab-column junction will rotate as shown in an idealised manner in Fig. 3.72. The surrounding slab will impose a lateral restraint on the portion of the slab within the failure sections thereby forcing the neutral axis to remain deep in the critical sections as shown in Fig. 3.72. In the typical lightly reinforced slab used in practice the neutral axis lies quite close to the

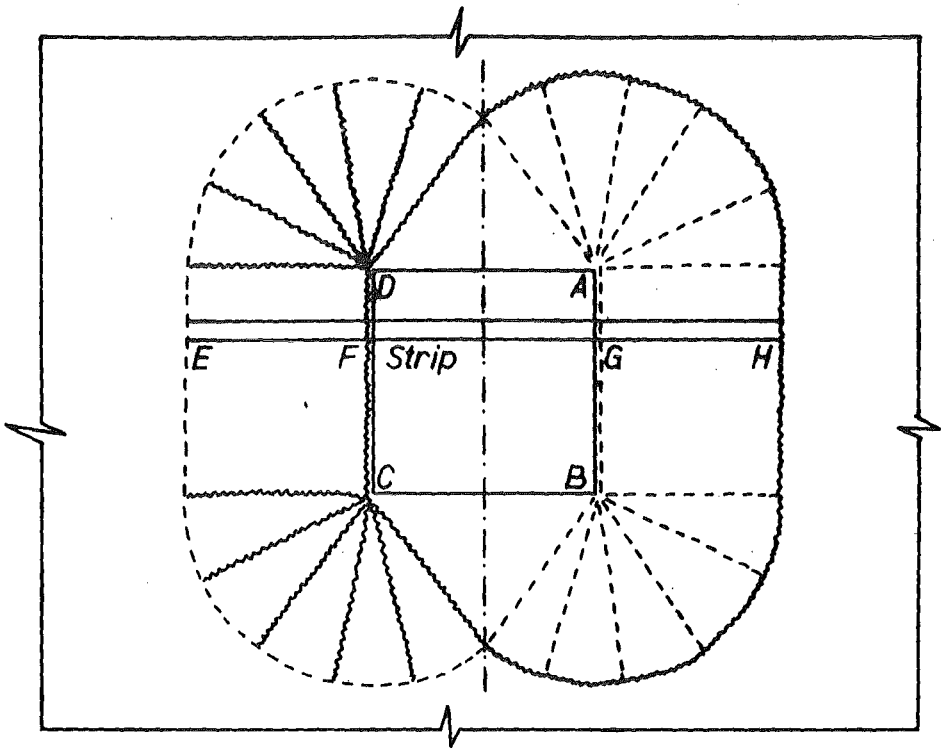

(a) Yield-line Pattern

Positive moment yield-line ~~~~~

Negative " " " ------

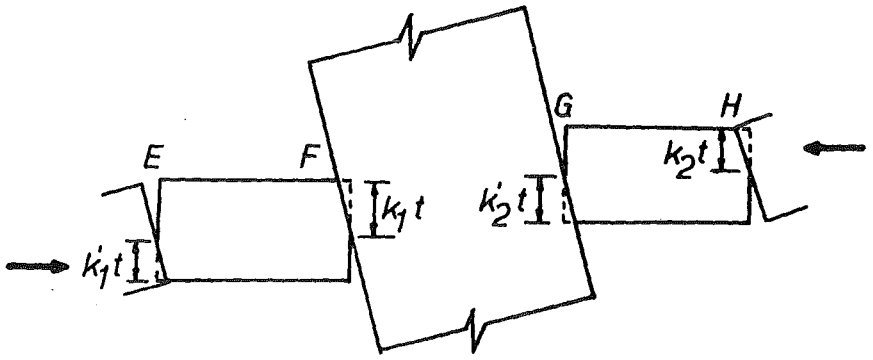

(b) Deformations of Portions EF and GH of the Strip

FIG. 3.72 MEMBRANE ACTION

compressed edge of the concrete if no compressive membrane forces are present. Hence if the lateral restraint imposed by the surrounding slab forces the neutral axis at the slab sections AB and CD to remain at a greater depth compressive membrane forces will be induced in the slab. Eccentrically loaded column theory shows that the ultimate moment of resistance of a section with moderate axial compression is greater than that of a section without axial compression. This means that the presence of compressive membrane forces will increase the flexural capacity of the slab.

Since membrane action has been neglected in computing the contribution of flexure towards the moment transfer between the slab and the column, the theory will be on the conservative side in predicting the ultimate strength of the slab-column junction.

3.4.5 MOMENT TRANSFER BY VERTICAL SHEAR STRESSES

If the vertical shear stress induced on the face AB by the shear force V_u is v_{AB}, the shear stress induced by the out of balance bending moment on the faces AB or CD will be $(4\sqrt{f'_c} - v_{AB})$. The face AB is the critical face for the combined shear stress due to V_u and M_u.

Thus the shear force induced by moment on the faces AB and CD will be given by $(4\sqrt{f'_c} - v_{AB})y_o\, d$ and the moment due to the shear couple is

$$M_v = (4\sqrt{f'_c} - v_{AB})\, y_o\, d\, x_o \qquad \ldots (3.28)$$

where

M_v = part of the moment transferred by shear stress on faces AB and CD

v_{AB} = shear stress induced by V_u on face AB

x_o = dimension of critical section parallel to the direction of bending

y_o = dimension of critical section transverse to the direction of bending

d = effective depth of slab measured from the extreme compression face to the mid depth of the top reinforcing mat

To determine v_{AB}, the shear force acting on the area tributary to the face AB may be divided by $y_o d$, the sectional concrete area of the face AB over the effective depth d. In practical cases it is quite difficult to determine the shear forces acting on the areas tributary to each of the faces AB, BC, CD and AD. For design purposes, where the floor loading is symmetrical, the shear stress induced by V_u on faces AB, BC, CD and AD of the critical section may be considered as uniformly distributed and calculated as

$$v_{AB} = v_{BC} = v_{CD} = v_{AD} = \frac{V_u}{2\,d\,(x_o + y_o)} \qquad \ldots (3.29)$$

All the terms are as defined previously.

3.4.6 MOMENT TRANSFER BY TORSION

The ultimate torsional capacity of the faces AD and BC may be calculated by using the approach recommended by the ACI Building Code (ACI 318-71)[13] for the ultimate torque of a reinforced concrete rectangular section with an enhanced ultimate torsional shear stress.

The ultimate torque for the face AD or BC is given by

$$T_{AD} = T_{BC} = \frac{4.8\sqrt{f'_c}}{\sqrt{1 + \left(\frac{1.2 v_{AD}}{\tau_{AD}}\right)^2}} \frac{x_o t^2}{3} \qquad \ldots (3.30)$$

where $\tau_{AD} = \dfrac{3T_{AD}}{x_o t^2}$ = the nominal ultimate torsional shear stress on the face AD or BC

$T_{AD} = T_{BC}$ = the ultimate resisting torsional moment acting on the face AD or BC

$v_{AD} = v_{BC}$ = vertical shear stress on the face AD or BC induced by V_u

All other terms are as defined previously.

It may be noted here that v_{AD} is strictly a variable along the faces AD and BC . In the above equation the uniform mean value has been assumed.

In the derivation of Eq. (3.30) the nominal torsional shear stress of $2.4\sqrt{f'_c}$ used in the ACI Building Code (ACI 318-71)[13] has been increased to $4.8\sqrt{f'_c}$. This is in keeping with the reasoning by which the nominal shear stress of $2\sqrt{f'_c}$ for a beam type shear failure is raised to $4\sqrt{f'_c}$ for slabs. In view of the triaxial stress conditions that exist in slabs near the columns, both these increases in the nominal shear stress and the torsional shear stress appear to be reasonable. Hence the factor 1.2 in the denominator of right hand side of Eq. (3.30) remains unchanged.

The limiting value of the torsional capacity of the face AD or BC will depend upon the vertical shear V_{AD} or V_{BC} and the moment M_{AD} or M_{BC} acting on the respective faces. Eq. (3.30) takes into account the interaction of shear and torsion. In most practical cases the moment M_{AD} or M_{BC} is small and hence the reduction in the torsional capacity due to shear only has been considered.

Substituting the value of τ_{AD} in Eq. (3.30) and rearranging the terms the following equation may be obtained:

$$T_{AD} = 4.8\sqrt{f'_c}\ \frac{x_o t^2}{3}\ \sqrt{1 - \left(\frac{v_{AD}}{4\sqrt{f'_c}}\right)^2} \qquad \ldots (3.31)$$

All other terms are as previously defined.

3.4.7 STRENGTH EQUATIONS

After evaluating the individual contributions of flexure, shear and torsion using Eqs. (3.25) to (3.31), the ultimate shear and moment transferred from the flat plate to the column can be calculated as

$$M_u = \left(m_u + m'_u\right) y_o + \left(4\sqrt{f'_c} - v_{AB}\right) x_o y_o d$$

$$+ \ 4.8\sqrt{f'_c} \ \frac{2}{3} \ x_o t^2 \sqrt{1 - \left(\frac{v_{AD}}{4\sqrt{f'_c}}\right)^2} \qquad \ldots (3.32)$$

$$V_u = 2 \, v_{AB} \, y_o d + 2 \, v_{AD} \, x_o d \qquad \ldots (3.33)$$

It is to be noted that the equation for M_u sums the maximum contributions from flexure, vertical shear and torsion. Thus it may represent an upper bound for M_u since it is possible that the maximum contribution from each effect may not occur simultaneously.

3.4.8 COMPARISON WITH TEST RESULTS

The theoretical strengths of 19 interior column-flat plate specimens without any shear reinforcement are shown compared with the experimental values in Table 3.5. Of these 19 tests, 7 were conducted by Hanson and Hanson[16], 9 by Moe[8] and 3 by the author, details of which are given in Section 3.3 of this thesis. The theoretical strengths of these test specimens were computed by using the equations presented in Section 3.4.7 and also by the methods given by the ACI Building Code (ACI 318-71)[13] and Hawkins and Corley[20].

(i) Comparison with Equations (3.32) and (3.33)

The theoretical method presented here gives the mean of $\frac{M_{test}}{M_u}$ as 1.35 with a coefficient of variation of 17.8% . For Hanson and Hanson's test specimens with a slab thickness of 3 in. and the author's specimens with a slab thickness of $3\frac{1}{2}$ in. this method gives a somewhat higher value of $\frac{M_{test}}{M_u}$ than the mean value of 1.35 . There is a good correlation between the predicted M_u and M_{test} for Moe's slabs having a thickness of 6 in. This may be due to the effect of membrane action which could enhance the flexural capacity of a thinner slab more prominently than that of a thicker slab.

Eqs. (3.32) and (3.33) can be used to plot interaction curves for shear and moment for these 19 test specimens. These curves are shown in

TABLE 3.5

STRENGTHS FOR SLAB-COLUMN SPECIMENS WITHOUT SHEAR REINFORCEMENT

TOR	SPECIMEN NO.	M_{test} Kip.in.	THEORY PRESENTED IN SECTION 3.40					ACI METHOD[13]		HAWKINS AND CORLEY'S METHOD[20]						FLEXURAL FAILURE MOMENTS		
			MOMENT TRANSFER BY			$Mu_{calc.}$ Eq.(3.32) Kip. in.	$\frac{M_{test}}{Mu_{calc.}}$	Mu_{calc} Eqs.(3.9,3.13) Kip. in.	$\frac{M_{test}}{Mu_{calc.}}$	M_m Kip.in.	$2T_o$ Eq.(3.15)x2 Kip. in.	M_t Eq.(3.14) Kip. in.	$\frac{M_m}{M_t}$	V_{AB} Kip.	V_{ABO} Eq.(3.18) Kip.	$\frac{V_{AB}}{V_{ABO}}$	$m_u + m'_u$ Kip.in/in.	M_{flex}	$\frac{M_{test}}{M_{flex}}$
			FLEXURE Kip. in. Eq.(3.25)	SHEAR Kip. in. Eq.(3.28)	TORSION Kip. in. Eq.(3.31)														
	A1	197.6	71.7	43.3	16.0	131.0	1.51	147.0	1.34	180.8	105.8	173.8	1.04	3.29	5.20	0.63	8.50	232.0	0.85
	A2	215.0	73.8	44.6	16.3	134.7	1.60	152.0	1.41	197.2	108.4	178.4	1.10	3.54	5.29	0.67	8.74	239.0	0.90
	A12	181.4	73.6	35.5	15.7	124.8	1.45	120.5	1.50	184.5	111.4	181.6	1.02	5.59	5.45	1.02*	8.72	238.0	0.76
	B7	316.0	70.2	79.3	28.8	178.3	1.77	270.0	1.18	263.4	179.8	246.8	1.07	4.94	5.42	0.91	8.32	380.0	0.83
	B16	242.0	67.4	58.4	25.8	151.6	1.60	198.5	1.21	218.4	173.2	237.2	0.92	7.28	5.22	1.39*	7.98	365.0	0.66
	C8	277.9	136.6	78.7	16.8	232.1	1.20	282.0	0.99	254.4	120.0	252.8	1.01	4.41	9.47	0.46	9.46	342.0	0.81
	C17	218.7	117.5	67.1	16.7	201.3	1.09	240.5	0.91	218.8	108.2	222.2	0.98	6.63	9.90	0.67	8.14	295.0	0.74
	M2A	349.0	275.5	61.9	38.2	375.6	0.93	210.5	1.66	349.0	-	-	-	16.0	14.9	1.07*	16.32	522.0	0.67
	M4A	553.0	287.0	145.2	75.2	507.4	1.09	494.0	1.12	553.0	-	-	-	14.4	15.9	0.91	17.00	544.0	1.02
	M2	506.0	310.0	62.6	38.2	410.8	1.23	213.0	2.38	506.0	-	-	-	22.1	19.3	1.15*	18.35	587.0	0.86
	M3	621.0	303.0	122.6	69.2	494.8	1.26	417.0	1.49	621.0	-	-	-	19.0	18.1	1.05*	17.95	574.0	1.08
	M6	356.0	174.0	62.0	44.4	280.4	1.27	212.5	1.68	356.0	-	-	-	17.8	16.9	1.05*	11.75	320.0	1.11
	M7	168.0	173.3	-	-	173.3	0.97	-	-	168.0	-	-	-	19.2	16.4	1.17*	11.70	318.0	0.53
	M8	578.0	257.4	127.5	77.0	461.9	1.25	436.0	1.32	578.0	-	575.0	1.01	15.1	16.3	0.93	17.38	473.0	1.22
	M9	300.0	172.1	22.6	16.8	211.5	1.42	77.3	3.88	300.0	-	-	-	18.5	15.8	1.17*	11.62	316.0	0.95
	M10	485.0	254.0	85.7	56.2	395.9	1.23	293.0	1.65	485.0	-	480.0	1.01	15.7	15.1	1.04*	17.13	466.0	1.04
	1	270.0	79.6	81.5	28.0	189.1	1.43	275.0	0.98	247.3	93.4	170.3	1.45	4.22	8.55	0.49	6.67	273.0	0.99
	2	334.0	84.2	90.1	30.2	204.5	1.63	304.0	1.10	306.2	99.0	180.2	1.70	4.21	9.25	0.46	7.05	289.0	1.16
	3C	317.0	71.6	86.1	29.4	187.1	1.69	291.0	1.09	290.6	86.8	156.9	1.85	4.58	8.95	0.51	6.00	246.0	1.29
					Mean		1.35		1.49				1.18						
					Standard Deviation		0.24		0.67				0.296						
					Coefficient of Variation		17.8%		45%				25%						

* Indicates shear-torsion failure

Figs. 3.73 to 3.79. Calculations are based on the average concrete strengths and yield stresses of steel for the number of test results shown in each figure. For comparison the straight line interaction graphs between shear and moment as given by Eq. (3.9) of the ACI method[13] are also plotted. Generally, for lower values of shear transferred, about 25% or less of the ultimate pure shear capacity of the slabs, the interaction curve given by Eq. (3.32) seems to underestimate the strength of the test specimens as can be seen in Figs. 3.73, 3.74 and 3.75. For higher values of shear transferred, about 50% or more of the ultimate pure shear capacity of the slabs, the interaction curve appears to be in good agreement with the test results as shown in Figs. 3.77 and 3.78.

In the case of a concentrically loaded slab-column junction the moment transferred between the slab and the column will be zero and the shear transferred will be the ultimate pure shear capacity of the slab. Under application of unbalanced moment a slab-column junction already subjected to its ultimate pure shear capacity will continue to resist the applied moment until the transverse faces AB and CD of the critical section shown in Fig. 3.71 reach their ultimate flexural capacities. In other words, the theory assumes that a slab-column junction loaded to its ultimate pure shear capacity is capable of resisting an unbalanced moment equal to the sum of the ultimate flexural capacities of the faces AB and CD of the critical section. This is expected to occur due to the redistribution of actions in the slab which is a statically indeterminate system.

Moe's specimen No.M7 shown in Fig. 3.77 and Table 3.5 justifies this behaviour. The specimen subjected to a shear stress of 246 psi, which was slightly greater than the allowable ultimate shear stress of $4\sqrt{f'_c}$ = 241 psi failed at an applied moment of 168 kip. in. This is nearly equal to the ultimate flexural capacity of 173.3 kip. in. of the faces AB and CD of the critical section.

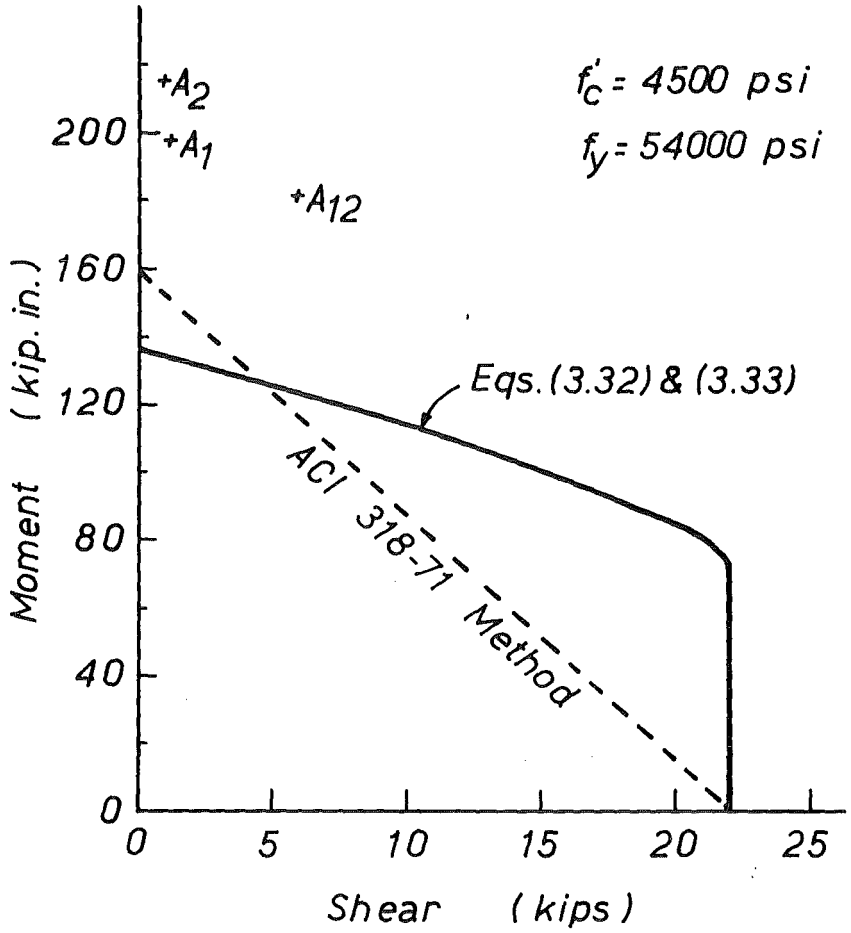

FIG. 3.73 INTERACTION DIAGRAMS FOR HANSON AND HANSON'S SPECIMENS A_1, A_2 & A_{12}

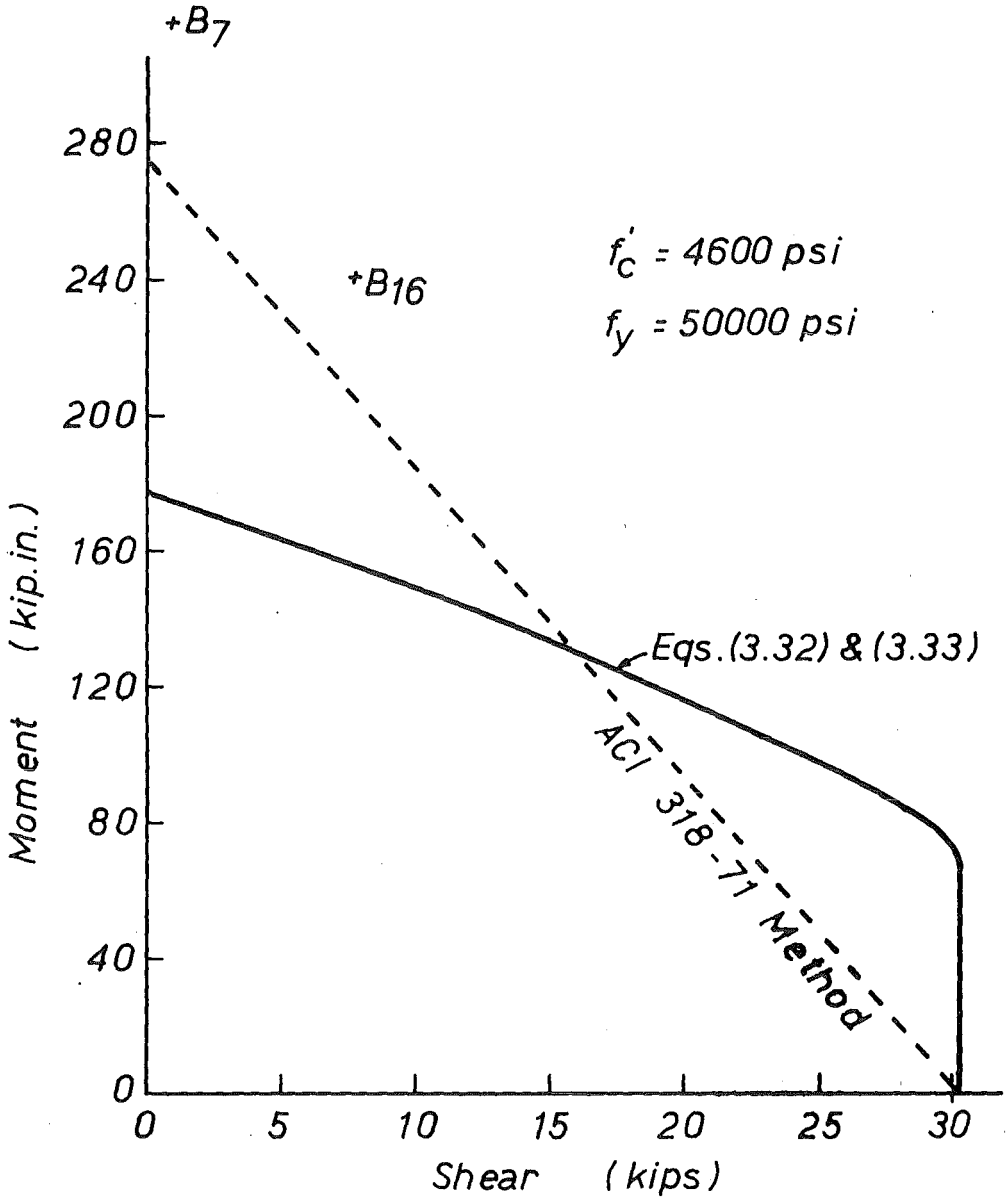

FIG. 3.74 INTERACTION DIAGRAMS FOR HANSON AND HANSON'S SPECIMENS B_7 AND B_{16}

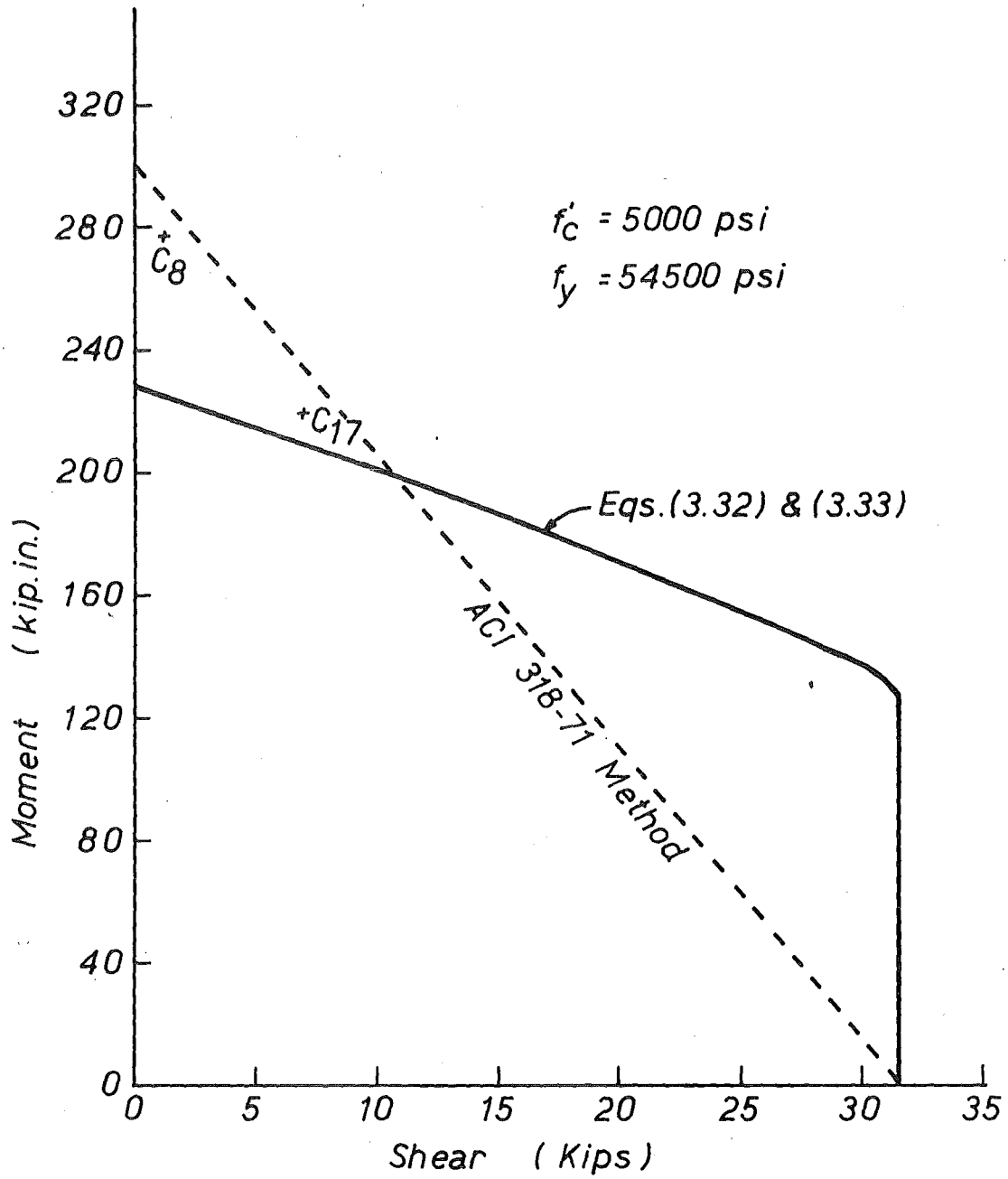

FIG. 3.75 INTERACTION DIAGRAMS FOR HANSON AND HANSON'S SPECIMENS C_8 AND C_{17}

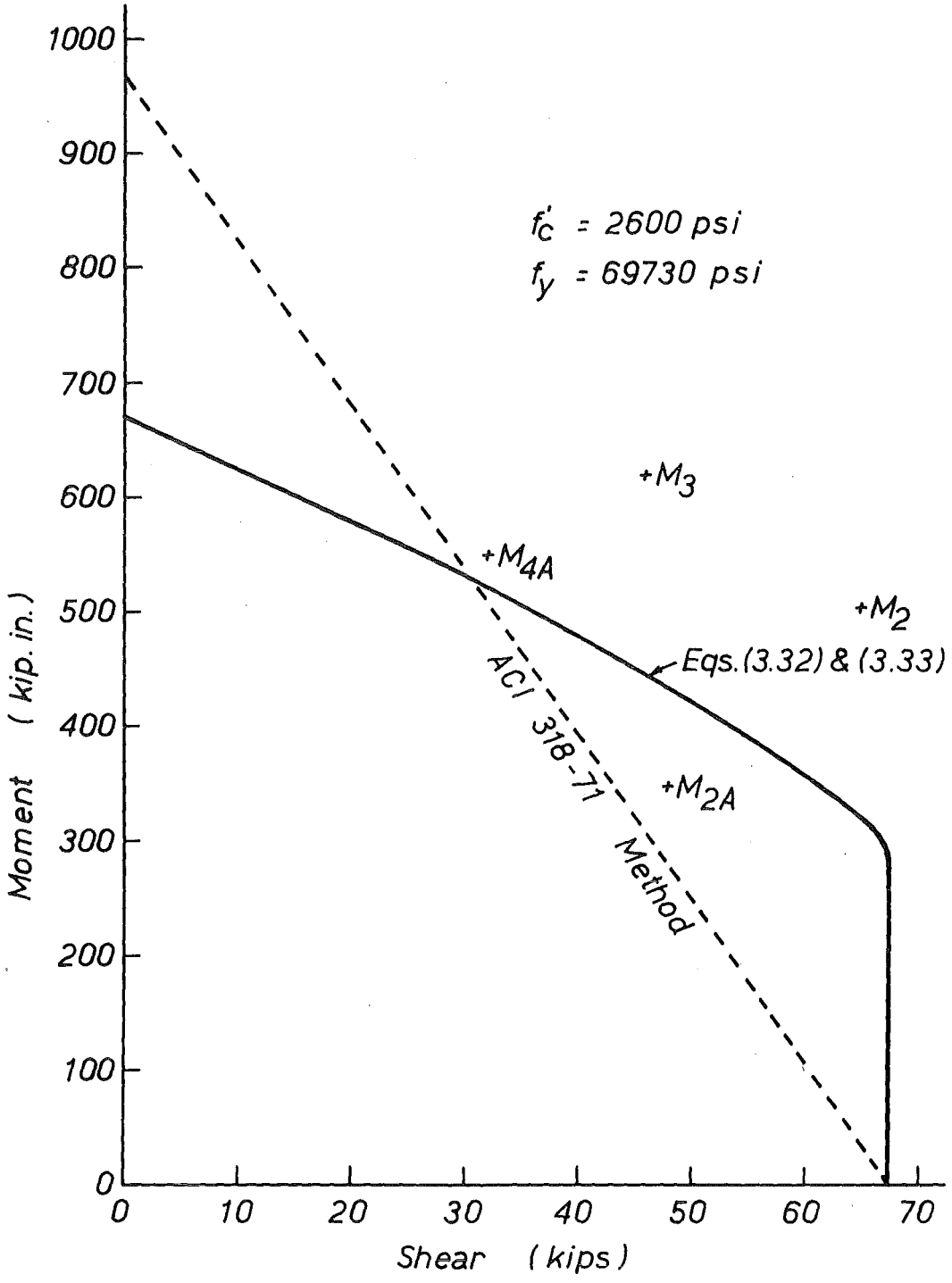

FIG. 3.76 INTERACTION DIAGRAMS FOR MOE'S SPECIMENS M_2, M_{2A}, M_3 & M_4

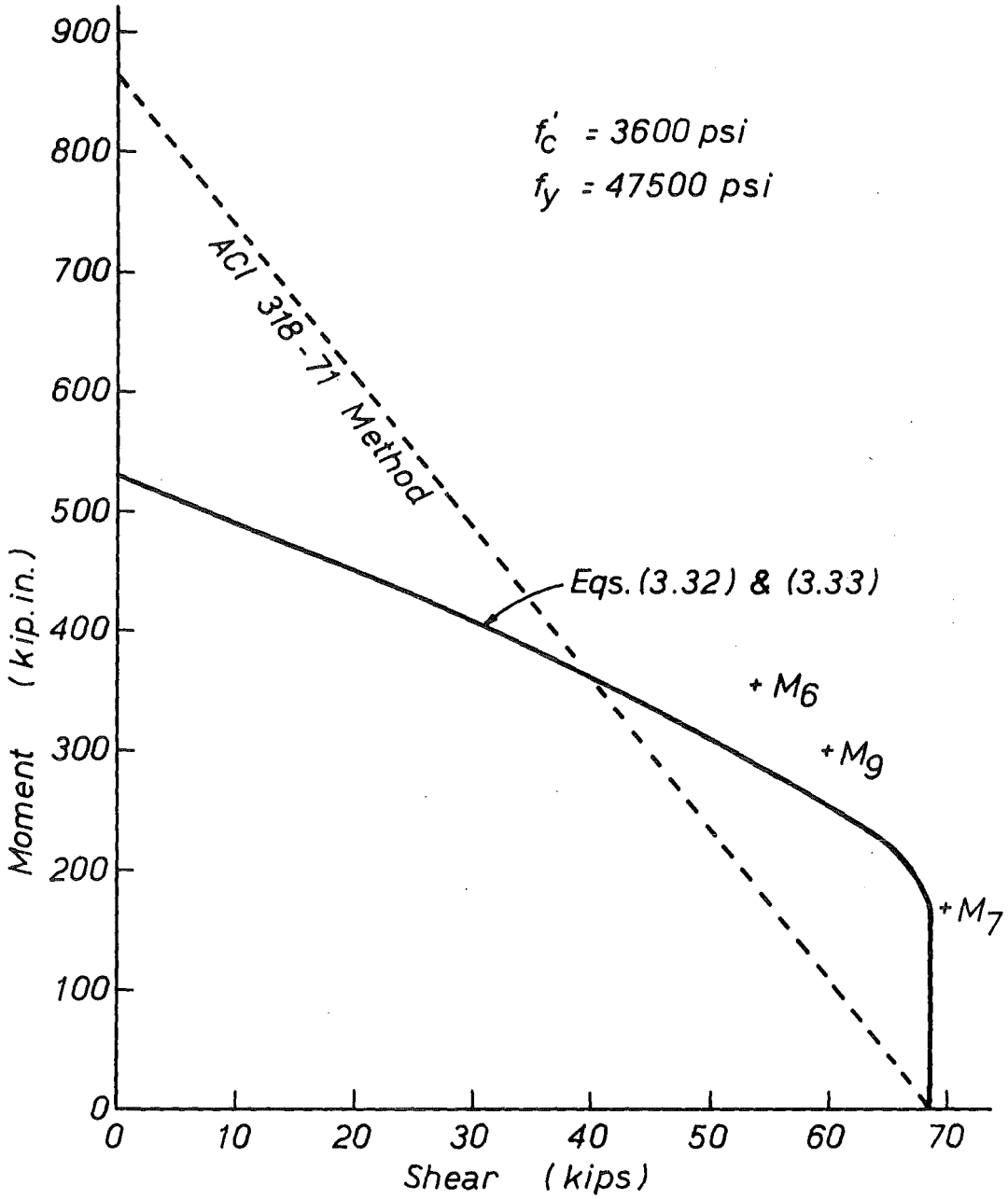

FIG. 3.77 INTERACTION DIAGRAMS FOR MOE'S SPECIMENS M_6, M_7 & M_9

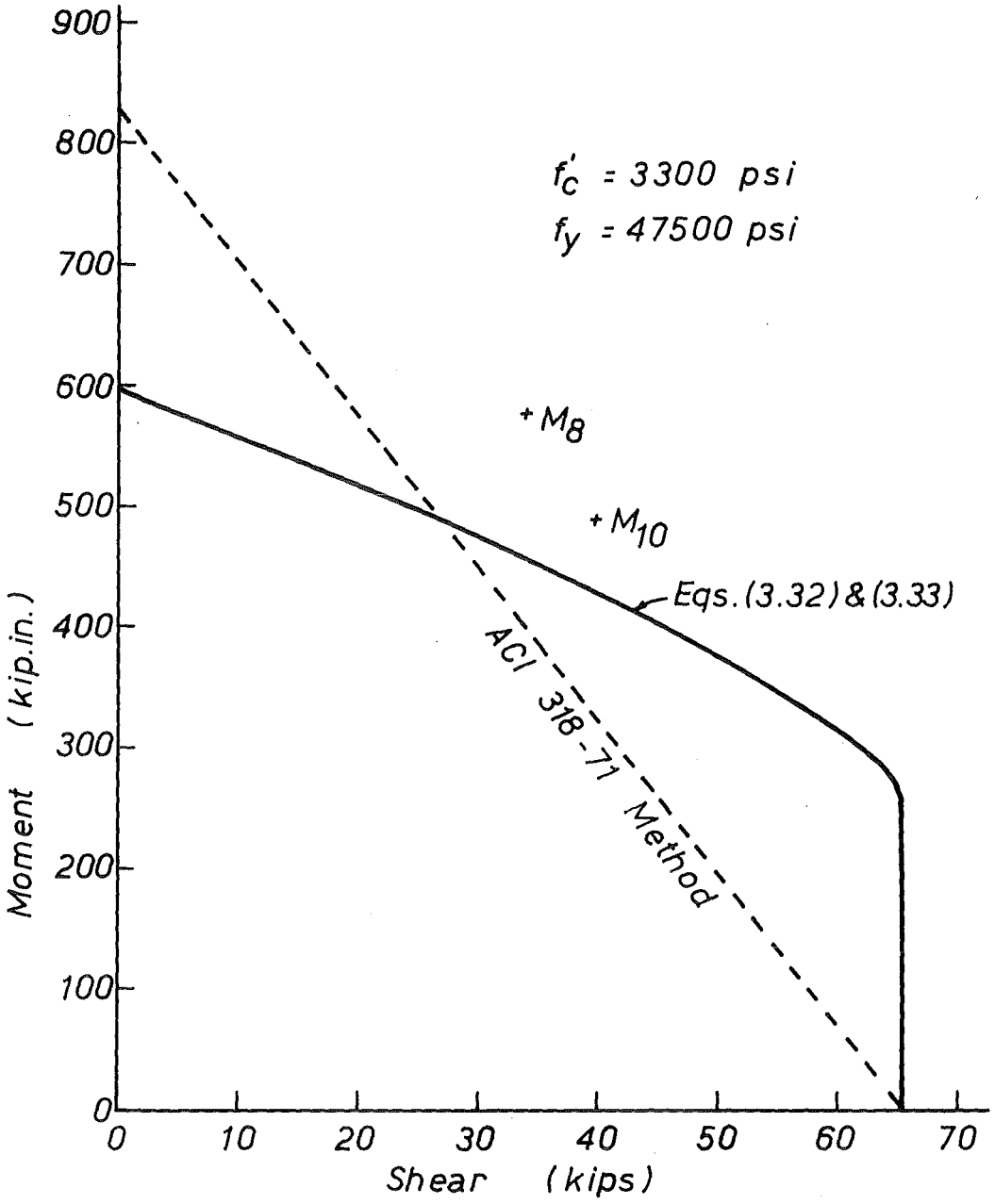

FIG. 3.78 INTERACTION DIAGRAMS FOR MOE'S SPECIMENS M_8 & M_{10}

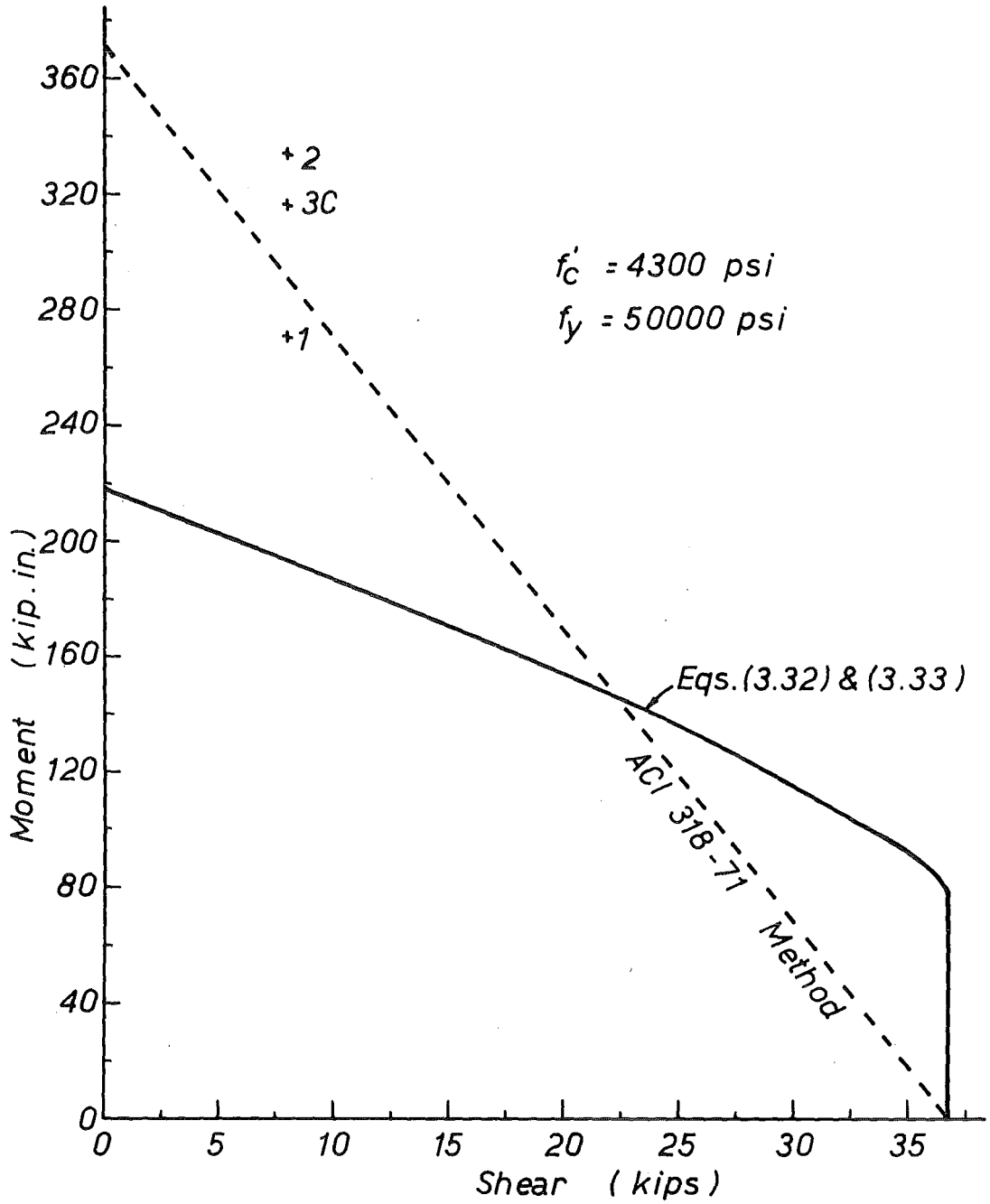

FIG. 3.79 INTERACTION DIAGRAMS FOR AUTHOR'S SPECIMENS 1, 2 & 3C

(ii) Comparison with ACI 318-71 Method[13]

The analysis of 19 test specimens shown in Table 3.5 by the ACI 318-71[13] method gives the mean of $\frac{M_{test}}{M_u}$ as 1.49 with a coefficient of variation of 45% . In case of the author's 3 specimens without shear reinforcement this method predicts very good results. The scatter in the test results arises mainly from Moe's slabs which, with the exception of the specimens M8 and M10, had reinforcement on one face only. The likely cause of this scatter is due to the neglect of the influence of slab reinforcement bars passing through the column on the proportion of moment assumed to be transferred by shear stresses. However, as in most practical cases there will be both top and bottom reinforcement in the slabs over the column regions, the coefficient of variation will be somewhat lesser than the indicated figure of 1.49.

(iii) Comparison with Method of Hawkins and Corley[20]

The method of Hawkins and Corley[20] gives accurate results for all Hanson and Hanson's specimens[16] and Moe's[8] specimens M8 and M10 which contained top reinforcement. For the author's 3 tests their method is very much on the conservative side. In Table 3.5 the comparison between the experimental moment and the predicted moment by their theory is expressed as the ratio of $\frac{M_m}{M_t}$ where M_m is the applied moment on the critical section and M_t is the computed moment capacity at the critical section for a moment torsion failure, The mean of $\frac{M_m}{M_t}$ for 12 test results is found to be 1.18 with a coefficient of variation of 25% . Since they are considering both the applied moment and the computed moment to be acting on the critical section the moment transferred by shear stresses acting on the transverse faces AB and CD of the critical section do not enter their Eq. (3.14) for the total moment capacity for a moment-torsion failure. Thus with their method it is not possible to determine the additional shear stresses caused by the application of unbalanced moment.

The torsional moment capacity of the faces AD and BC of the critical section given by Eq. (3.15) appears to have been overestimated by them. It is seen in Table 3.5 that the torsional moment $2T_o$ accounts for nearly 50% to 75% of the total moment M_t for a moment-torsion failure. As pointed out in Section 3.2.3 this may be partly due to the consideration of slab reinforcement as fully effective as closed hoops in resisting torsion and partly due to the neglect of the maximum limit for torsional capacity of reinforced concrete sections given in the ACI Building Code (ACI 318-71)[13]. For a moment-torsion failure no reduction in the torsional moment capacity due to the shear effects has been considered.

For Moe's slabs torsional strengths were calculated for specimens M8 and M10 only and for the remainder which did not contain reinforcement in both faces of the slab torsional strengths were not shown in their paper[20]. As the accuracy of their method is dependent on the torsional moment provided by the slab reinforcement the computed moment capacity for these specimens without top reinforcement will be quite low when compared with the test results.

According to their method, at loads less than the flexural capacity, there will be a moment-torsion failure if $\frac{V_{AB}}{V_{ABO}} < 1$ and a shear torsion failure if $\frac{V_{AB}}{V_{ABO}} > 1$, where V_{AB} is the shear force acting on the face AB and V_{ABO} is the ultimate resisting shear force for the face AB. In the case of a shear-torsion failure interaction between shear and torsion is considered in computing the torsional moment capacity as given by Eq. (3.16).

On the whole Hawkins and Corleys' method gives more accurate prediction of the theoretical strength than both the method presented here and the ACI (318-71)[13] method for slab-column specimens containing reinforcement in both faces of the slab. Their method is difficult to use for design purposes whereas the method presented here, although not so accurate as

their method, is more simplified and can be readily used by designers.

3.4.9 DISCUSSION OF THE THEORY PRESENTED

The theory presented for interior column-flat plate junctions without any shear reinforcement assumes that the individual maximum contributions of the three actions, namely, flexure, shear and torsion, can be summed to obtain the ultimate strength of the slab-column junction. It is implied that if their governing values are not reached simultaneously sufficient ductility exists for their maximum values to be sustained. The comparison of the test results with the theory indicates that this assumption is reasonable.

The slab is subjected to high moments in the column region and consequently the tension steel crossing the transverse faces AB and CD of the critical section will yield before the shear failure commences. For the typical lightly reinforced slab used in practice the moment-curvature relationship can be expected to show appreciable ductility at these faces of the critical section at failure. The vertical shears on the faces AB and CD can build up even if the moments are constant at the yield moment because the statically indeterminate system in flat plates will allow redistribution of actions before collapse.

The torsional moments are computed by using the ACI Building Code (ACI 318-71)[13] equations which are based on the circular interaction curve for torsion and shear. Torsion and flexure interaction effects have not been considered because external moments on faces AD and BC are usually small. The nominal torsional and flexural shear stresses used were twice those for beams, following existing findings for the flexural shear strength of concentrically loaded slabs, due to the existence of triaxial stress conditions at the slab-column junction. This stress condition may also result in sufficient ductility in the torsion-twist relationship for the faces AD and BC .

The assumptions seem to have been justified by the agreement of theory with the experimental results, deviations being on the safe side.

3.4.10 CONCLUSIONS

The theory presented gives more consistent and better results than those predicted by the current ACI Building Code (ACI 318-71)[13] and is more simplified than Hawkins and Corley's method[20]. The agreement with the test results is reasonably good and verifies the theoretical approach. With this method it is possible to compute the individual contributions of flexure, shear and torsion in transferring an unbalanced moment between a column and a slab.

3.5 THEORY FOR SHEAR-FLEXURE FAILURE OF SLAB-COLUMN CONNECTIONS WITH SHEAR REINFORCEMENT

SUMMARY

An ultimate strength method is presented to determine the shear and unbalanced moment capacity of interior column-flat plate junctions containing shear reinforcement in the form of either inclined cranked bars, vertical closed stirrups or structural steel shearheads. Strengths based on this theory are compared with test results and a conservative agreement obtained.

3.5.1 INTRODUCTION

Some type of shear reinforcement may often be necessary in flat plate floors around the junction of the column and the slab to strengthen the junction without increasing the slab thickness. Also it is desirable that a slab-column junction should not fail in a brittle manner but should show adequate ductility, particularly under earthquake conditions.

As mentioned in Section 3.2 there is no established procedure available for designing shear reinforcement in slab-column junctions which transfer both shear and moment. In the design procedures given here three types of shear reinforcement are considered, namely, (i) inclined cranked bars, (ii) vertical closed stirrups and (iii) shearheads fabricated from structural steel shapes. The strength of the junction is found by adding the contribution of the shear reinforcement in resisting shear and torsion to the strength of an unreinforced junction.

3.5.2 INCLINED CRANKED BARS

Fig. 3.80 shows an interior slab-column junction containing inclined bars as shear reinforcement and the assumed critical section ABCD located at a distance d/2 outside the column periphery. Let V_{max} be the maximum shear force which can be developed on the face AB of the critical

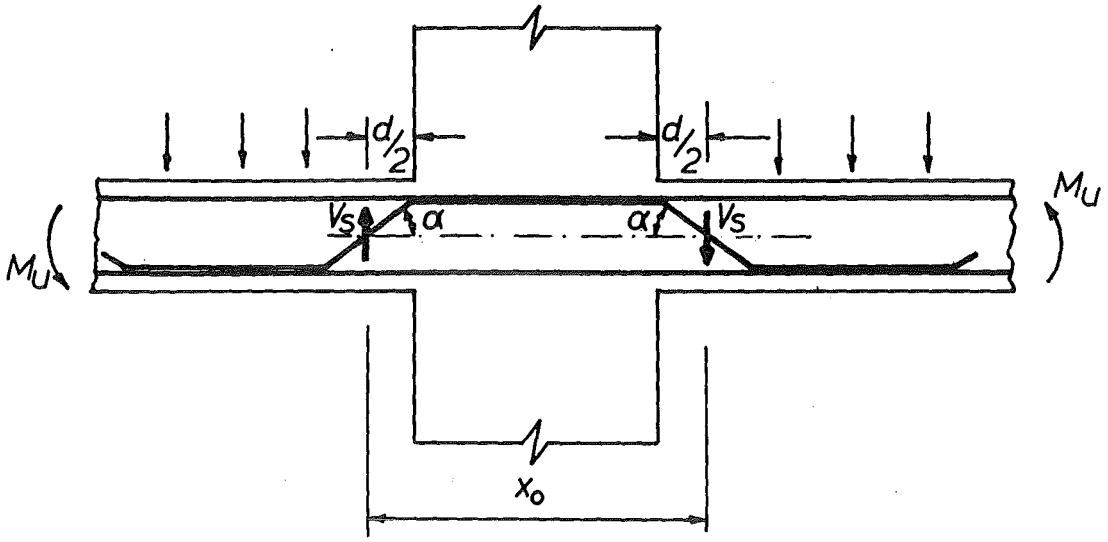

(a) Shear Force Carried by Cranked Bars

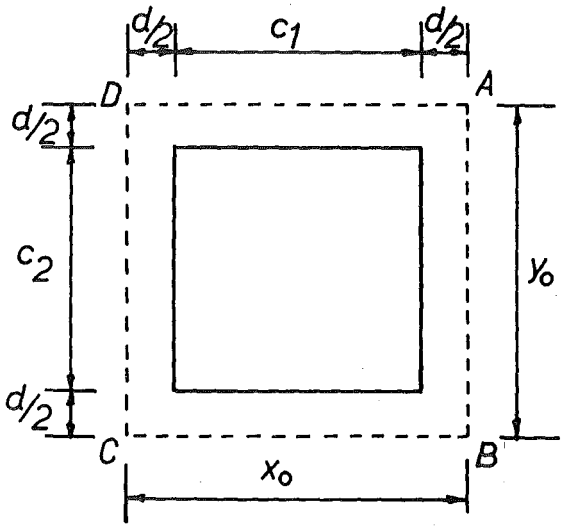

(b) Critical Section

FIG. 3.80 INCLINED CRANKED BARS

section by the combined action of the concrete and the inclined bars. The maximum nominal shear stress carried by the concrete is taken as $4\sqrt{f'_c}$. As discussed in Section 3.4.2 this shear stress of $4\sqrt{f'_c}$ at the critical section at ultimate loading conditions, representing twice the value used for beams, is considered effective due to the two-way action in slabs. The shear force carried by the concrete on the face AB is taken as $4\sqrt{f'_c}\, y_o d$ and the shear force carried by the cranked bars is considered as V_s, where V_s is the vertical component of the force carried by the cranked bars across the face AB and $y_o d$ is the sectional area of the face AB. Thus V_{max} may be written as

$$V_{max} = 4\sqrt{f'_c}\, y_o d + V_s$$

$$= 4\sqrt{f'_c}\, y_o d + \eta A_v f_y \sin\alpha \qquad \ldots (3.34)$$

where

η = efficiency of inclined bars as shear reinforcement

A_v = area of inclined bars crossing the critical section on faces AB or CD

f_y = yield stress of inclined bars

α = angle of inclination of the bars with the horizontal

y_o = dimension of critical section transverse to the direction of bending

d = effective depth of the slab

From Eq. (3.34) the maximum shear stress v_{max} on the face AB can be obtained by dividing V_{max} by the sectional area $y_o d$. The design of shear reinforcement is based on the critical face AB of Fig. 3.80.

Herzog[30] has shown that the efficiency of the shearing reinforcement as inclined bars or vertical stirrups can be taken as $\eta = 39\%$ in concentrically loaded slabs which do not transfer any moment to the columns. This value of 39% was derived from the analysis of 57 punching shear

tests on slabs containing shear reinforcement either as inclined bars or stirrups. The results were widely scattered, the coefficient of variation amounting to 49.5% . This wide variation and the low value of η = 39% may be attributed to the results of punching shear tests of many slabs[6,8,31] with inadequately anchored shear reinforcement.

If properly designed anchorage lengths are used for shear reinforcement as inclined bars the value of η could be assumed somewhat higher than 39% in determining the contribution of the inclined bars towards the shearing resistance of slabs carrying both shear and unbalanced moment. Further, the inclined bars on the faces AD and BC do not take part in resisting torsional shear stresses on these faces. Thus the total unbalanced moment that can be transferred with shear force at an interior column-slab junction containing inclined bars as shear reinforcement may be written as

$$M_u = \left(m_u + m'_u\right) y_o + \left(v_{max} - v_{AB}\right) x_o\, y_o\, d + 4.8\sqrt{f'_c}\ \frac{2}{3}\, x_o t^2 \sqrt{1 - \left(\frac{v_{AD}}{4\sqrt{f'_c}}\right)^2} \qquad \ldots (3.35)$$

$$V_u = 2\, v_{AB}\, y_o d + 2\, v_{AD}\, x_o d \qquad \ldots (3.36)$$

where

v_{AB}, v_{AD} = shear stress induced by V_u on faces AB, CD

v_{max} = maximum shear stress on the face AB due to the combined action of concrete and inclined bars

All other terms are as defined previously.

In Eq. (3.35) the first term on the right hand side gives the contribution of flexure on the faces AB and CD ; the second term is the contribution of the vertical shear stress on the faces AB and CD induced by M_u and the last term is that of torsion on the faces AD and BC . Eq. (3.35) is similar to the equation derived for the slab-column junction without any shear reinforcement excepting that $4\sqrt{f'_c}$ has been replaced by v_{max} which takes into account the effect of the shear

reinforcement.

3.5.3 VERTICAL CLOSED STIRRUPS

The procedure for designing vertical stirrups of closed type is similar to that of inclined bars. The maximum shear force V_{max} on the critical face AB is given by

$$V_{max} = 4\sqrt{f'_c}\, y_o d + V_s$$

$$= 4\sqrt{f'_c}\, y_o d + \eta A_v f_y \qquad \ldots (3.37)$$

All the terms are as defined previously.

An efficiency factor η is again included in the expression for V_{max} to consider the effectiveness of closed stirrups as shear reinforcement in slabs. The maximum shear stress v_{max} acting on the face AB may be obtained by dividing V_{max} as given by Eq. (3.37) by the sectional area $y_o d$. Unlike inclined bars, closed type stirrups placed on the faces AD and BC of the critical section will be effective in resisting torsional shear stresses on these faces. Additional torsional moment resisted by the closed stirrups on the face AD or BC may be calculated by using the procedure given by the ACI Building Code (ACI 318-71)[13]. This is given as

$$T_s = \frac{\Omega x_o (t - d' - d'') A_s f_y}{s} \qquad \ldots (3.38)$$

where

T_s = torsional moment resisted by stirrups on face AD or BC

Ω = coefficient = $0.66 + \frac{0.33 x_o}{t-d'-d''}$ but not greater than 1.5

x_o = dimension of critical section parallel to the direction of bending

t = total depth of slab

d' = distance between the bottom face and the centroid of bottom reinforcement

d'' = distance between the top face and the centroid of

top reinforcement

A_s = area of one leg of stirrup

s = spacing of stirrups

f_y = yield stress of stirrups.

The unbalanced moment and shear capacity of the slab-column junction provided with closed stirrups may now be calculated by using the following equations:

$$M_u = \left(m_u + m'_u\right) y_o + \left(v_{max} - v_{AB}\right) x_o y_o d + \left(4.8\sqrt{f'_c}\,\frac{2}{3}\,x_o t^2\right)\sqrt{1 - \left(\frac{v_{AD}}{4\sqrt{f'_c}}\right)^2} + \frac{2\Omega x_o (t-d'-d'')A_s f_y}{s} \quad \ldots (3.39)$$

$$V_u = 2\,v_{AB}\,y_o d + 2\,v_{AD}\,x_o d \quad \ldots (3.40)$$

v_{max} is given by Eq. (3.37). All other terms are as defined previously.

3.5.4 STRUCTURAL STEEL SHEARHEADS

The shearing resistance of the flat plate-column junction can be increased by providing a shearhead made of standard structural steel sections within the concrete slab. The shearhead will contribute towards the moment transfer between the slab and the column in three ways, namely, (i) flexure, (ii) shear, and (iii) torsion.

The flexural contribution of the shearhead is given by $2\Sigma m_p$, where m_p is the plastic moment capacity of an arm of the shearhead. Σm_p gives the total plastic moment of the arms of the shearhead on one face of the critical section which is again assumed to be at a distance $d/2$ from the column periphery. This is multiplied by 2 to take into account the contributions of both faces AB and CD of the critical section.

The shearing contribution of the shearhead will be worked out in a slightly different manner than the previous proposals for inclined bars

and vertical closed stirrups. To determine the shear force carried by the shearhead it would be necessary to know the shear force distribution along the arm of the shearhead. The assumed idealised shear force distribution shown in Fig. 3.81 is obtained from the experimental study of a flat plate-column specimen containing a shearhead, which is described in Section 3.3.4 (vii).

Let V_s be the shear force carried by the shearhead at the critical section. From the idealised shear force diagram the moment at the critical section may be obtained as

$$\Sigma m_p = \frac{V_s}{3}\left(L_c - \frac{d}{2}\right)$$

$$\therefore \quad V_s = \frac{3\Sigma m_p}{L_c - \frac{d}{2}} \qquad \ldots (3.41)$$

where

m_p = plastic moment capacity of a shearhead arm

L_c = length of shearhead arm measured from the column face

d = effective depth of slab.

The maximum shear force on the critical face AB is once again obtained as the sum of the shear force carried by the concrete and the shear force carried by the shearhead.

Thus $V_{max} = 4\sqrt{f'_c}\, y_o d + V_s$

$$= 4\sqrt{f'_c}\, y_o d + \frac{3\Sigma m_p}{L_c - \frac{d}{2}} \qquad \ldots (3.42)$$

where $y_o d$ represents the concrete area of the face AB of the critical section. The maximum shear stress v_{max} is obtained by dividing V_{max} by $y_o d$.

The shearhead arms placed transversely to the direction of bending will be subjected to torsion. Their resistance to torsion may be calculated as $2\Sigma m_t$, where Σm_t is the total plastic torque of the shearhead arms on the face AD or BC of the critical section.

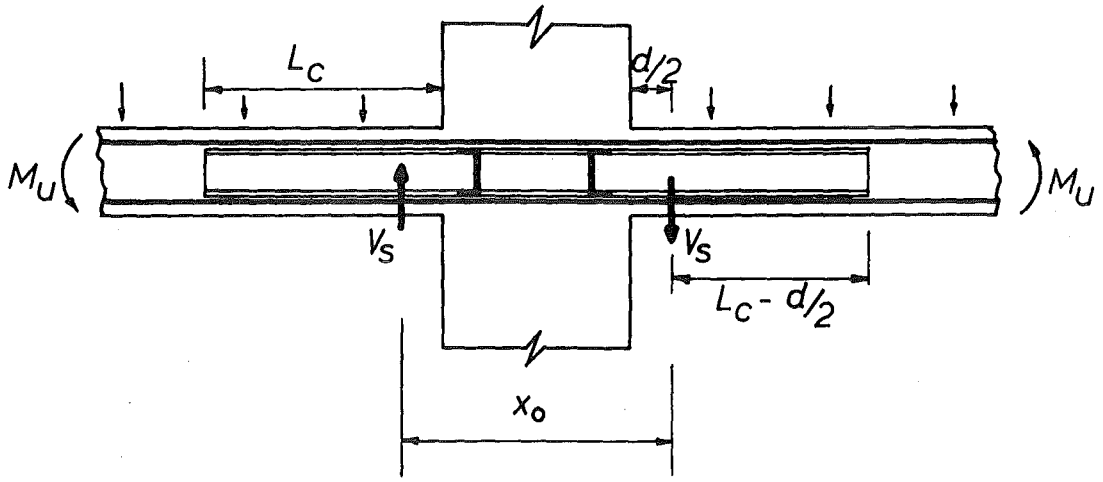

(a) Shear Force Carried by Shearhead

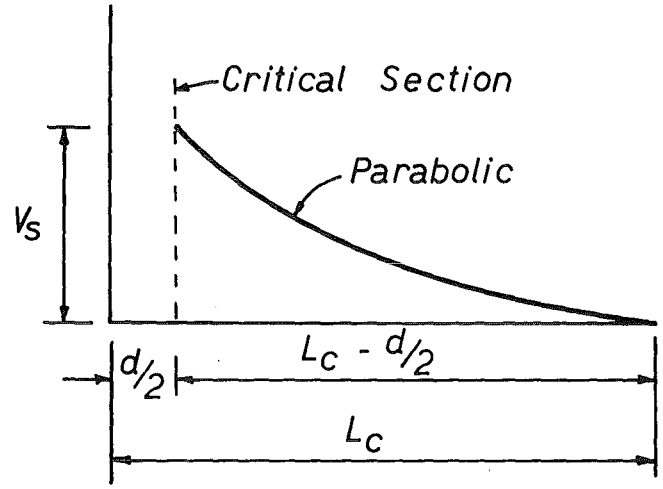

(b) Assumed Shear Force Distribution along the Shearhead Arm

FIG. 3.81 SHEARHEAD REINFORCEMENT

The unbalanced moment and shear capacity of the slab-column junction with a shearhead may be computed by using the following equations:

$$M_u = \left(m_u + m'_u\right) y_o + 2\Sigma m_p + \left(v_{max} - v_{AB}\right) x_o y_o d + 4.8\sqrt{f'_c}\ \frac{2}{3} x_o t^2 \sqrt{1 - \left(\frac{v_{AD}}{4\sqrt{f'_c}}\right)^2} + 2\Sigma m_t \quad \ldots (3.43)$$

$$V_u = 2 v_{AB} y_o d + 2 v_{AD} x_o d \quad \ldots (3.44)$$

v_{max} is obtained from Eq. (3.42) and all other terms are as defined previously.

In most practical cases Σm_t will be small and may be ignored for design purposes.

3.5.5 COMPARISON WITH TEST RESULTS

The test results reported on the transfer of unbalanced moment and shear between flat plates and columns containing shear reinforcement are very meagre. Of the few known tests one was carried out by Hollings[18] and four or five tests were known to have been conducted at the Portland Cement Association Laboratory, U.S.A., whose details were not available for comparison with the theory.

Five tests conducted on flat plate-column specimens containing various arrangement of shear reinforcement in the form of inclined cranked bars, vertical closed stirrups and a structural steel shearhead as part of this investigation are described in Section 3.3. The theoretical strengths of these five tests and the test conducted by Hollings[18] are shown compared with the experimental values in Table 3.6. The moment transferred by the junction without any shear reinforcement and the moment transferred by the shear reinforcement alone are shown separately.

When the efficiency of the shear reinforcement is taken as $\eta = 100\%$. The mean of $\frac{M_{test}}{M_{u\ calc}}$ for the six test results shown in Table 3.6 is found to be 1.17 with a coefficient of variation of 13%. With the efficiency

TABLE 3.6

STRENGTHS FOR SLAB-COLUMN SPECIMENS WITH SHEAR REINFORCEMENT

ATOR	SPECIMEN NO.	TYPE OF SHEAR REINFORCEMENT	M_{test} Kip.in.	MOMENT TRANSFERRED WITHOUT SHEAR REINFORCEMENT				MOMENT TRANSFERRED BY SHEAR REINFORCEMENT				TOTAL MOMENT TRANSFERRED η = 1 assumed Mu_{calc} Kip. in.	$\frac{M_{test}}{Mu_{calc}}$	FLEXURAL FAILURE MOMENTS		
				FLEXURE Kip.in.	SHEAR Kip.in.	TORSION Kip. in.	TOTAL Kip. in.	FLEXURE Kip. in.	SHEAR Kip. in.	TORSION Kip. in.	TOTAL Kip. in.			$M_u + m'_u$ Kip.in/in.	M_{flex} Kip.in.	$\frac{M_{test}}{M_{flex}}$
	4S	4 Nos. $\frac{3}{8}$" Ø cranked bars	367	74.9	90.0	31.1	196.0	-	139.1xη	-	139.1xη	335.1	1.10	6.27	257.0	1.43
	5S	Shearhead 2 Nos. $1\frac{1}{2}$" x 1" x .128" thick channels	350	61.9	87.5	30.4	179.8	38.2	56.9	-	95.1	274.9	1.27	5.19	251.2	1.39
R	6CS	Closed stirrups 4 legs 3/16" Ø at $1\frac{1}{2}$" c/c	340	62.9	83.2	29.2	175.3	-	71.9xη	72.4	71.9xη+72.4	319.6	1.06	5.27	216.0	1.57
	7CS	Closed stirrups 2 legs $\frac{1}{4}$" Ø at $1\frac{1}{2}$" c/c	369	65.9	85.9	30.0	181.8	-	62.0xη	124.0	62.0xη+124.0	367.8	1.00	5.52	226.0	1.63
	8CS	Closed stirrups 2 legs 3/16" Ø at $1\frac{1}{2}$" c/c	309	62.4	70.9	25.6	158.9	-	37.2xη	74.4	37.2xη+74.4	270.5	1.14	5.23	214.0	1.44
S^{18}		Shearhead 2 Nos. 3" x 2" x 4.5 lb. I-Beams	2365	410.0	411.0	149.4	970.4	220.0	432.4	-	652.4	1622.8	1.46	21.60	1595.0	1.48
												Mean	1.17			
												Standard Deviation	0.153			
												Coefficient of Variation	13%			

$\eta = 39\%$ as recommended by Herzog[30] the mean of $\frac{M_{test}}{M_{u\ calc}}$ is found to be 1.30 with a coefficient of variation of 9.7% . Since the shear reinforcement for the five test specimens listed in the table fulfilled the requirements for anchorage as given in the ACI Building Code (318-71)[13] a higher value of η can be used with some justification. A value of $\eta = 70\%$ for the inclined bars and vertical closed stirrups gives the mean of $\frac{M_{test}}{M_{u\ calc}}$ as 1.23 with a coefficient of variation of 10% . This brings the mean value down to 1.23 from 1.30 when $\eta = 39\%$ and at the same time reduces the coefficient of variation to 10% from 13% when $\eta = 100\%$. As there is some uncertainty about the full effectiveness of shear reinforcement in thin slabs and as the theoretical strength of slab-column junctions is somewhat underestimated by the theory presented in Section 3.4, it appears reasonable to accept the efficiency of shear reinforcement as $\eta = 70\%$. With this value the predicted strengths of slab-column junctions are on the conservative side with a good degree of consistency.

In case of the author's five tests where the basic slab reinforcement pattern was unchanged the computed moments carried by the unreinforced junction do not differ much. This slight variation is mainly due to differing values of f'_c and f_y . The moment carried by the various arrangement of shear reinforcement is seen to vary appreciably. With the efficiency taken as $\eta = 70\%$ for inclined cranked bars and vertical closed stirrups the shear reinforcement carries 33% of the total computed moment for specimen No. 4S with cranked bars, 35% for specimen No. 5S with a shearhead, 41% for specimen No. 6CS with 4 legs of 3/16 in. diameter closed stirrups, 48% for specimen No. 7CS with 2 legs of $\frac{1}{4}$ in. diameter closed stirrups and 39% for specimen No. 8CS with 2 legs of 3/16 in. diameter closed stirrups. In the case of Holling's specimen, the shearhead carries 40% of the total computed moment. Of the three types of shear reinforcement investigated it appears that both closed stirrups and the shearhead are more efficient in carrying additional moment than the cranked bars.

3.5.6 DISCUSSION OF THE THEORY PRESENTED

The shear strength problem is complex and even for reinforced concrete beams a precise and rational analysis of shear behaviour has yet to be developed. The concepts which underlie present design practice are based partly on rational analysis, partly on test evidence and partly on successful experience with structures in which certain procedures for designing shear reinforcement have resulted in a satisfactory performance.

The design procedure presented here for slabs follows the same pattern and logic as those for beams. In order to design shear reinforcement for a flat plate-column junction carrying an ultimate shear V_u and an ultimate moment M_u, first of all v_{AB} and v_{AD}, which are assumed to be equal, are computed by using any one of the Eqs. (3.36), (3.40) and (3.44). The maximum shear stress v_{max} is then obtained from Eqs. (3.35), (3.39) and (3.43) for the type of shear reinforcement selected. The design of shear reinforcement may then be carried out by using Eqs. (3.34), (3.37) and (3.42) as appropriate for the selected type.

In these design equations an efficiency factor of 0.7 has been taken into account to consider the effectiveness of shear reinforcement in slabs owing to anchorage problems. Since it is difficult to achieve good anchorage of shear reinforcement in slabs by bond and bearing the best way to develop anchorage is to transfer the force in the shear bar to other reinforcement, such as by rigidly attaching stirrups to longitudinal reinforcement or by tightly wrapping stirrups around the longitudinal reinforcement.

In the case of shearhead reinforcement no reduction has been made on its effectiveness as the problem of anchorage does not arise here. Corley and Hawkins[28] have shown that shearhead reinforcement is fully effective in thin slabs. A parabolic distribution of shear force has been assumed along the length of the shearhead arm up to the critical face AB. This

has been experimentally verified in Section 3.3. Based on this distribution the shear force carried by the shearhead at the critical section has been estimated as given by Eq. (3.41).

Once the shear forces carried by the various shear reinforcement are known the shear and unbalanced moment capacity of a slab-column junction can be computed in a similar manner as given for slab-column junctions without shear reinforcement.

3.5.7 CONCLUSIONS

The predicted strengths computed by using the theoretical approach outlined here for interior flat plate-column junctions containing shear reinforcement are found to be on the conservative side with a good degree of consistency. As verified by the experimental results it would appear to be quite safe to use these equations for designing shear reinforcement for slab-column junctions.

Of the three types of shear reinforcement considered closed stirrups and shearheads are more efficient in carrying additional moment than the inclined cranked bars.

3.6 THEORY FOR FLEXURAL FAILURE OF SLAB-COLUMN CONNECTIONS

SUMMARY

The ultimate flexural strength of interior flat plate-column specimens under combined shear and unbalanced moment loadings tested by various investigators is obtained by using the yield-line theory for reinforced concrete slabs. When compared with the experimental flexural capacity this is found to be greater in most specimens without shear reinforcement and lower in all specimens with shear reinforcement.

3.6.1 INTRODUCTION

One important object of the design of flat plate floors is the need to prevent shear failures of slab-column junctions. In order to achieve this requirement it is essential to know the ultimate flexural strength of flat plate floors. Once this is known it would be possible to design for shear reinforcement which may be required to prevent premature shear failure of slab-column junctions.

The ultimate flexural strength of several different models of interior flat plate-column specimens subjected to combined shear and unbalanced moment loadings and tested by Hanson and Hanson[16], Moe[8], Hollings[18] and the author is determined here by using the yield-line theory for reinforced concrete slabs. As mentioned in Section 2.2 the yield line theory is an upper bound method and it is always necessary to examine all the possible collapse mechanisms to ensure that the load carrying capacity of the slab is not overestimated. Several different yield-line patterns which model various flat plate-column test specimens will now be analysed. The yield-line flexural capacity of these test specimens is then compared with the experimental moment capacity obtained from tests for slab-column junctions with or without shear reinforcement.

3.6.2 DEVELOPMENT OF EQUATIONS

Fig. 3.82(a) shows a flat plate floor supported by columns with a grid $L_1 \times L_2$. The slab is loaded uniformly with both dead load and live load and is also subjected to an unbalanced moment in the direction of the span L_1. The slab reinforcement is considered to be isotropic with positive and negative yield moments per unit length m and m' respectively. For the purpose of analysis a portion of the floor containing an interior column and the surrounding slab as shown by dotted lines in Fig. 3.82(a) is considered. The column is taken as rectangular and passes through the centre of the slab as shown in Fig. 3.82(b).

Two possible yield-line patterns are considered. The first pattern A1 shown in Fig. 3.82(c) involves two parallel yield lines running along the sides of the column transverse to the direction of bending. The second pattern A2 shown in Fig. 3.83 involves a mixed pattern of straight and curves yield lines placed symmetrically about the column centroid.

(i) Pattern A1

Let the positive yield-line AB be given a unit downward displacement and the negative yield-line A'B' be given a unit upward displacement. This collapse mechanism, shown in Fig. 3.82(d), gives

$$\theta_1 = \frac{2}{L_1 - c_1}, \quad \theta_2 = \frac{2}{c_1}$$

$$\text{and} \quad \theta = 2\left(\frac{1}{L_1 - c_1} + \frac{1}{c_1}\right)$$

Total internal work done by the yield lines

$$= (m + m')\, L_2\, \theta$$

$$= 2\,(m + m')\, L_2 \left(\frac{1}{L_1 - c_1} + \frac{1}{c_1}\right)$$

Total work done by the applied moment M and the uniformly distributed load w

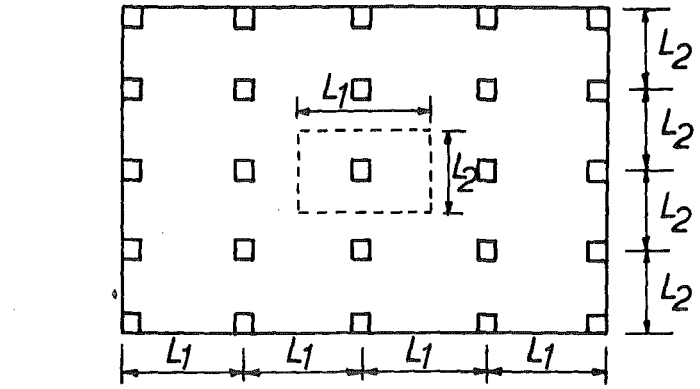

(a) Flat Plate Floor

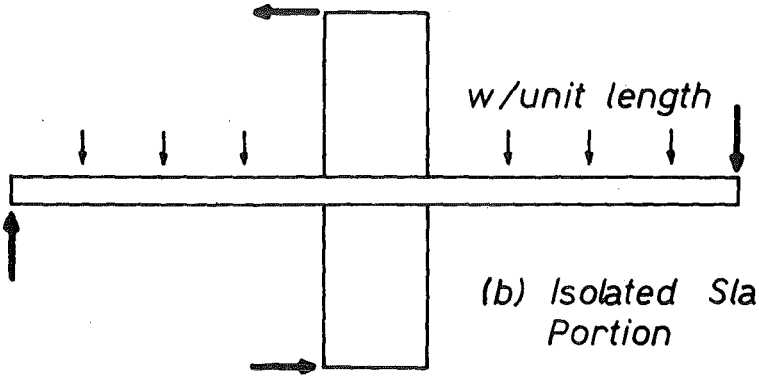

(b) Isolated Slab-Column Portion

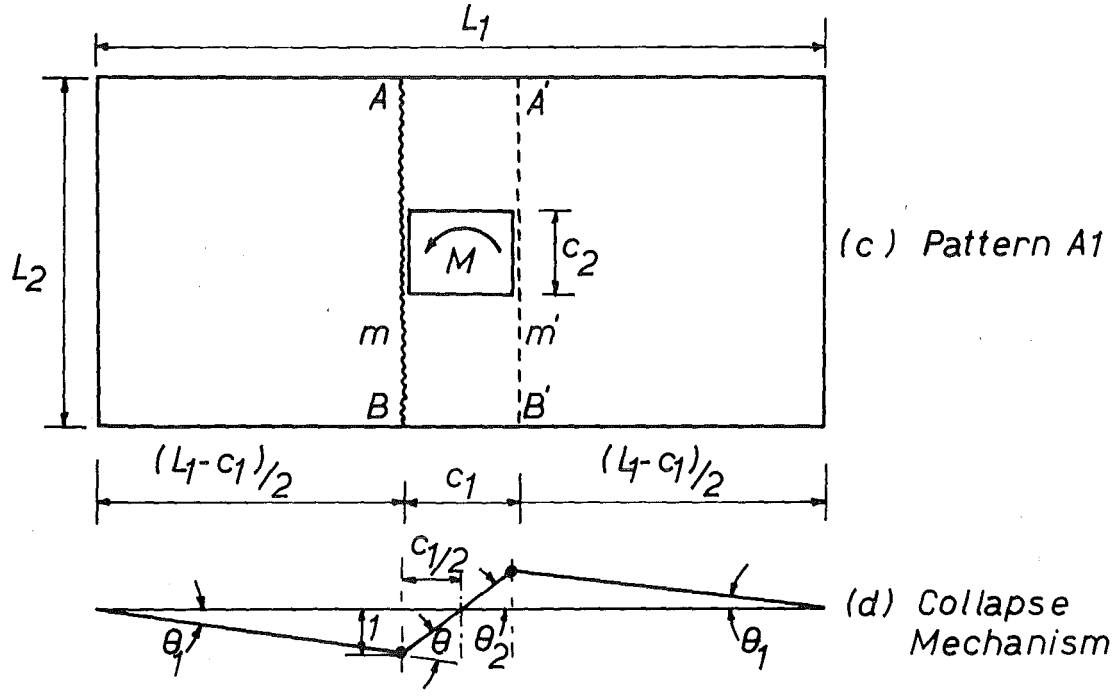

(c) Pattern A1

(d) Collapse Mechanism

FIG. 3.82 YIELD-LINE PATTERN A1

$$= M\theta + wL_2\frac{(L_1 - c_1)}{4} - wL_2\frac{(L_1 - c_1)}{4}$$

$$= 2M\left(\frac{1}{L_1 - c_1} + \frac{1}{c_1}\right)$$

Equating total internal work to total external work, one obtains

$$M = (m + m')\, L_2 \qquad \ldots (3.45)$$

This equation is applicable to specimens with either square or rectangular columns as it is independent of the column dimension.

(ii) Pattern A2

The collapse mechanism is shown in Fig. 3.83(a). The unknown angle ϕ defines the pattern fully. The radius R of the "fans" can be expressed in terms of ϕ and the known column dimension c_1. The positive yield-line CD is given a downward displacement of unity and the negative yield-line AB is given a unit upward displacement. From the collapse mechanism of Fig. 3.83(b) it is seen that

$$\theta_1 = \frac{1}{R} \quad \text{and} \quad \theta_2 = \frac{2}{c_1}$$

$$\theta = \frac{1}{R} + \frac{2}{c_1}$$

From Fig. 3.19(c)

$$c_1 = 2R\cos\phi$$

$$\theta = \frac{2\cos\phi}{c_1} + \frac{2}{c_1} = \frac{2}{c_1}(\cos\phi + 1)$$

The total internal energy dissipation by the yield lines may be calculated by dividing the pattern into 4 "fans" (e.g. F D E), 2 "rectangles" (e.g. C D F G) and 2 "triangles" (e.g. A D E). The internal energy dissipation for

4 "fans" (F D E) $= 4(m + m')(\pi - \phi)$

2 "rectangles" (C D F G) $= 2(m + m')(2\cos\phi + 1)\frac{c_2}{c_1}$

2 "triangles" (A D E) $= 2(m + m')\tan\phi$

Total internal work done by yield moments is given by

$$2(m + m')\left[2(\pi - \phi + 2\frac{c_2}{c_1}\cos\phi + \frac{c_2}{c_1} + \tan\phi\right]$$

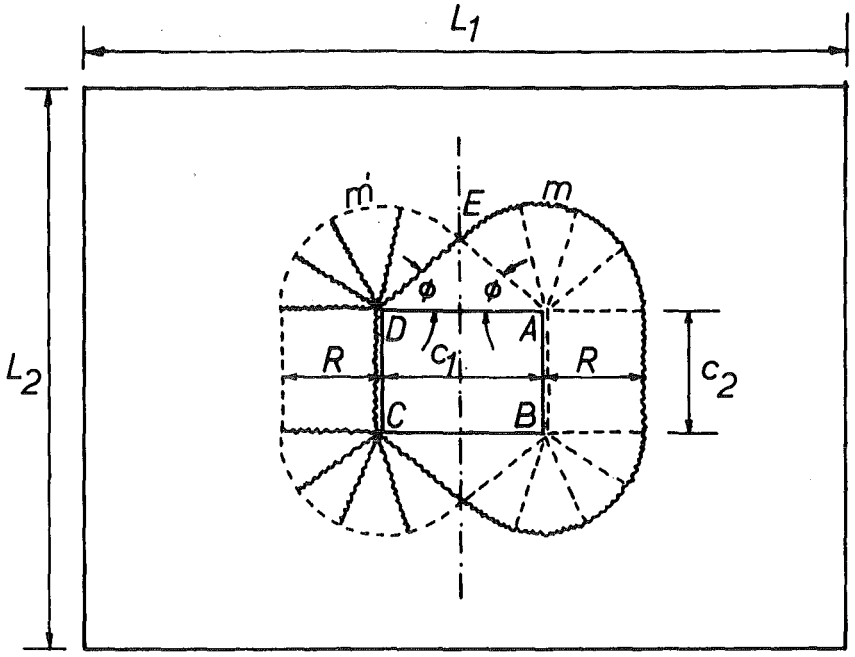

(a) Pattern A2

Positive yield line ~~~~
Negative " " ----

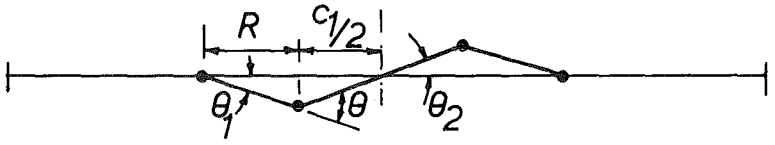

(b) Collapse Mechanism

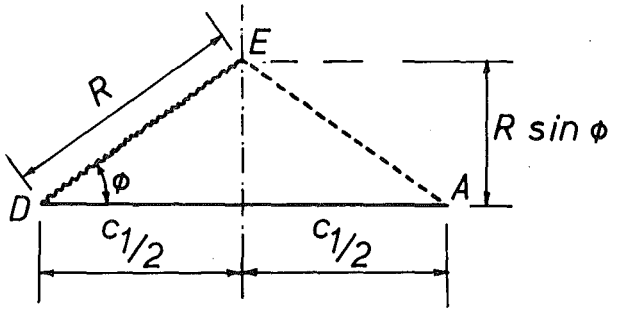

(c) Enlarged View of the Portion ADE

FIG.3.83 YIELD-LINE PATTERN A2

Total external work done by the applied moment $M = M\theta = \frac{2M}{c1}(1 + \cos \phi)$. Equating internal work done by yield moments to external work done by loading one finds that

$$M = (m + m') c_1 \frac{\left[2(\pi - \phi) + 2\frac{c2}{c1} \cos \phi + \frac{c2}{c1} + \tan \phi\right]}{1 + \cos \phi} \quad \ldots (3.46)$$

where c_1 is the column dimension parallel to the direction of bending and c_2 is the column dimension transverse to the direction of bending.

To determine the minimum value of M, Eq. (3.46) needs to be minimised.

For square columns with $c_1 = c_2 = c$, Eq. (3.46) is reduced to

$$M = (m + m') c \frac{[2(\pi - \phi) + 2 \cos \phi + 1 + \tan \phi]}{1 + \cos \phi} \quad \ldots (3.47)$$

A value of $\phi = 20^\circ$ gives the minimum value of $M = 4.551 (m + m')c$

$$\ldots (3.48)$$

For rectangular columns with the ratio of sides $\frac{c_2}{c_1} = \frac{1}{2}$, Eq. (3.46) is reduced to

$$M = (m + m') c_1 \frac{[2(\pi - \phi) + \cos \phi + 0.5 + \tan \phi]}{1 + \cos \phi} \quad \ldots (3.49)$$

The minimum value of M is obtained as

$$M = 3.809 (m + m') c_1 \quad \ldots (3.50)$$

for a value of $\phi = 17^\circ 30'$.

For rectangular colums with $\frac{c_2}{c_1} = 2$, the moment is given by

$$M = (m + m') c_1 \frac{[2(\pi - \phi) + 4 \cos \phi + 2 + \tan \phi]}{1 + \cos \phi} \quad \ldots (3.51)$$

The minimum value of M is

$$M = 6.033 (m + m') c_1 \quad \ldots (3.52)$$

when the value of $\phi = 23^\circ$.

3.6.3 COMPARISON WITH TEST RESULTS

The ultimate flexural strength of test specimens obtained by the yield-line analysis is shown compared with the experimental values in Tables 3.5 and 3.6.

(i) Author's Specimens

For the author's test specimens with square columns the dimensions L_2 = 90 in. and c = 9 in.

Pattern A1 gives $M = 90 (m + m')$

Pattern A2 gives $M = 41 (m + m')$

Thus the pattern A2 is always critical for the author's test specimens. The ultimate flexural capacity of the author's specimens without shear reinforcement is shown in Table 3.5 and that with shear reinforcement is given in Table 3.6. The values of $\frac{M_{test}}{M_{flex}}$ for specimen nos. 1, 2 and 3C are 0.99 , 1.16 and 1.29 respectively. These specimens failed in shear rather than in flexure. It appears that the ultimate flexural strength has been underestimated. Strain hardening of slab reinforcing bars and membrane forces generally result in the flexural strength being greater than that predicted by a yield-line analysis.

It may be pointed out here that specimens 1 and 2 were subjected to a one way bending but specimen no. 3C was subjected to several cycles of reversal of bending. M_{test} represents the maximum moment reached during testing. If the actual experimental moment which was recorded just at the time of failure is compared with the computed flexural strength the values of $\frac{M_{failure}}{M_{flex}}$ for specimens 1 , 2 and 3C will become 0.83 , 0.90 and 0.96 respectively, which are all less than unity indicating a shear failure. As expected the values of $\frac{M_{test}}{M_{flex}}$ for all the specimens with shear reinforcement are greater than unity, the values ranging from 1.39 to 1.63 .

(ii) Hanson and Hanson's Specimens[16]

Their specimens are similar to the author's specimens. The columns are 6 in. square or 6 x 12 in. rectangular columns. For specimens

A1 , A2 and A12 with 6 in. square columns and $L_2 = 48$ in. pattern A1 gives $M = 48\ (m + m')$ and pattern A2 gives $M = 27.3\ (m + m')$. Thus pattern A2 is always critical.

For specimens B7 and B16 with $\frac{c_2}{c_1} = \frac{6}{12} = \frac{1}{2}$ pattern A1 gives $M = 48\ (m + m')$ and pattern A2 gives $M = 45.7\ (m + m')$, which is the governing pattern.

For specimens CB and C17 with $\frac{c_2}{c_1} = \frac{12}{6} = 2$ pattern A1 gives $M = 48\ (m + m')$ and pattern A2 gives $M = 36.2\ (m + m')$, which is again the critical pattern.

The ultimate flexural capacity of all Hanson and Hanson's specimens is given in Table 3.5. The experimental failure moment of all their specimens is less than the computed ultimate flexural strength. This indicates a shear failure in all the cases. The ratio of $\frac{M_{test}}{M_{flex}}$ ranges from 0.66 to 0.90 .

(iii) Moe's Specimens[8]

Moe's 6 ft. square slabs were supported along all four edges and moment was applied through a centrally located square column stub.

A possible collapse mechanism is given by the pattern A2, shown in Fig. 3.83. This pattern gives an equation which is independent of the side dimension of the slab and the moment is expressed as

$$M = 4.551\ (m + m')\ c \qquad \ldots (3.48)$$

Another possible collapse mechanism is given by the simple yield-line pattern B1 , shown in Fig. 3.84, in which corner levers have been ignored. The total internal work done by the yield lines is computed as $2(m + m')\ \frac{(3L - 2c)}{(L - c)}$ and the total external work is given by $\frac{2\ M\ L}{c(L-c)}$. Equating internal work to external work, one obtains

$$M = (m + m')\ \frac{c}{L}\ (3L - 2c) \qquad \ldots (3.53)$$

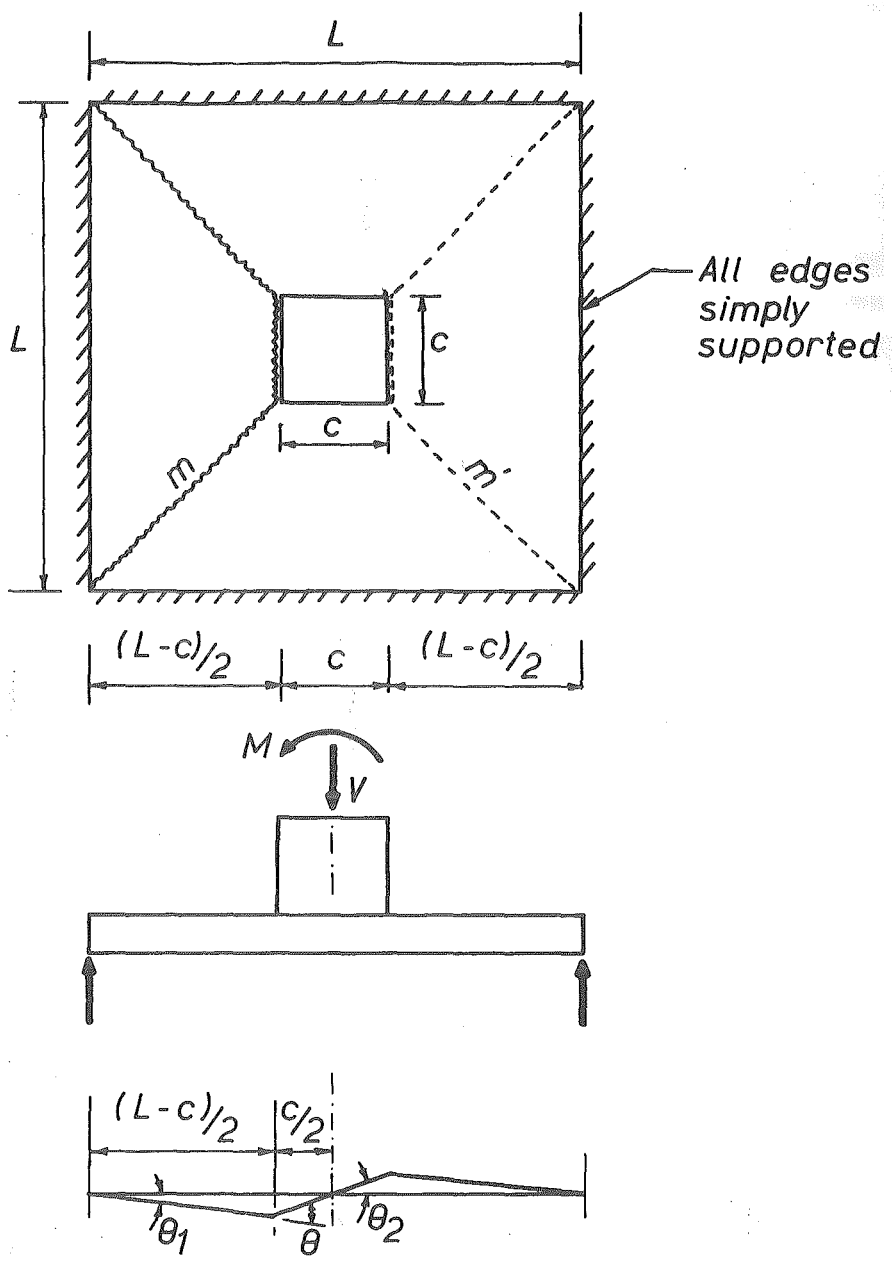

FIG. 3.84 YIELD LINE PATTERN B1 FOR MOE'S SPECIMENS

For Moe's specimens with 12 in. square columns and L_2 = 72 in., the governing pattern is that given by the pattern B1 and the moment M = 32 (m + m').

For specimens with 10 in. square columns and L_2 = 72 in., pattern B1 is again the critical pattern, which gives M = 27.2 (m + m').

The yield-line flexural capacity of all Moe's specimens are shown in Table 3.5. The ratio of $\frac{M_{test}}{M_{flex}}$ is less than unity for specimens M2A, M2, M7 and M9 whereas specimens M4A, M3, M6, M8 and M10 give values of $\frac{M_{test}}{M_{flex}}$ greater than one indicating a flexural failure. Actually these specimens failed in shear. This discrepancy may be due to the effect of strain hardening and membrane forces in the slab.

(iv) Holling's Specimen[18]

Eq. (3.48) for square columns is also applicable to Holling's specimen with a shearhead. The ultimate flexural capacity of the specimen is shown in Table 3.6. In this case the plastic moment capacity of the shearhead arms crossing the yield lines has been taken into account. The ratio of $\frac{M_{test}}{M_{flex}}$ is found to be 1.48 which indicates a flexural failure.

3.6.4 CONCLUSIONS

The ultimate flexural capacity of the slab obtained from the yield-line theory gives a useful criteria in determining whether the slab-column junction will fail in shear or in flexure. If this is greater than the ultimate strength of the slab-column junction under combined moment and shear loadings appropriate shear reinforcement can be provided at the junction to prevent a shear failure and thereby achieve the desirable flexural failure of the junction. Equations derived here give a conservative indication of the ultimate flexural capacity when shear failure is prevented.

3.7 CONCLUSIONS AND SUGGESTED FUTURE RESEARCH

3.7.1 GENERAL

The experimental investigation shows that flat plate construction can be used as an earthquake resistant structure if the slab-column connections are reinforced with shear reinforcement in the form of shearheads or closed vertical stirrups. The theory presented here for the prediction of shear and unbalanced moment capacity of flat plate-column connections gives consistent and safe results.

3.7.2 SUMMARY OF CONCLUSIONS

The discussion and conclusions presented at the end of each section may be summarised as follows:

(a) The recommended ACI 318-71 method for designing flat plate-column connections transferring shear and unbalanced moment does not accurately assess the relative contributions to strength from shear, torsion and flexure at the connection.

(b) Hawkins and Corley's method gives an accurate prediction of the strength of slab-column connections but their method is too involved to be used as a practical design method.

(c) The theory presented here is more simplified than Hawkins and Corley's method and gives better results than the ACI 318-71 method.

(d) The method presented here for determining the strength of slab-column connections containing shear reinforcement is found to be quite safe and consistent when compared with test results.

(e) The test results indicate that slab-column connections without any shear reinforcement have little ductility and failure takes place suddenly by diagonal tension cracking and splitting away of the concrete cover.

(f) Cranked bars as shear reinforcement result in an increase in the moment capacity of the connection but do not cause any increase in the ductility of the connection.

(g) Shearheads and closed stirrups are suitable as shear reinforcement in earthquake-resistant flat plate-column connections. They ensure that the connection behaves in a ductile fashion when subjected to cyclic loading.

(h) For use in practical seismic-resistant flat plate construction two-legged closed stirrups are recommended as they are relatively easy to fabricate and equally effective as four-legged closed stirrups.

(i) The interstorey deflections of flat plate structures within the elastic range can be approximately determined using the concept of effective width.

(j) The deterioration in the load carrying capacity of slab-column connections reinforced by closed stirrups can be reduced to about 50% of the maximum value when subjected to repeated cyclic loading well into the post-elastic range.

(k) Both the experimental and theoretical investigations show that the folding type failure mechanisms with parallel yield lines across the full width of the slab adjacent to the column faces may not occur in flat plate floors. A yield-line pattern involving fan mechanisms in the slab around the column is the one which will generally govern the ultimate flexural capacity of the slab-column connection.

3.7.3 SUGGESTED FUTURE RESEARCH

It has been evident from this study that several areas regarding the behaviour of slab-column connections require further research.

(a) Most of the test data available on the flat plate-column connection behaviour are on the specimens with square columns only. Experimental investigations are necessary on specimens with rectangular columns

whose longer side dimension may be parallel or transverse to the direction of applied bending moment.

(b) In the study presented the unbalanced moment capacity of slab-column connections was determined with a constant level of vertical shear force at the junction. In future experimental work various levels of vertical shear force could be used in order to find the moment capacities of the junctions and to check the interaction equations.

(c) Both the theoretical and experimental work need to be extended to the case of exterior slab-column connections.

APPENDIX A

BIBLIOGRAPHY

1. JOHANSEN, K.W., "Yield-line Theory", Cement and Concrete Association, London, 1962, p.181.

2. Draft "British Standard Code of Practice for the Structural Use of Concrete", 1969.

3. LASH, S.D. and BANERJEE, A., "Strength of Simply Supported Square Plates with Central Square Openings", Transaction of the Engineering Institute of Canada, Vol. 10, No. A-5, June, 1967, p.3-11.

4. ZASLAVSKY, A., "Yield-line Analysis of Rectangular Slabs with Central Openings", ACI Journal, Proceedings V.64, December, 1967, p.838-844.

5. JOHANSEN, K.W., "Pladeformler", Kobenhaun, Akademisk Forlag, 1963.

6. ELSTNER, R.C. and HOGNESTAD, E., "Shearing Strength of Reinforced Concrete Slabs", ACI Journal, Proceedings V.53, July, 1956, p.29-58.

7. KINNUNEN, S. and NYLANDER, H., "Punching of Concrete Slabs Without Shear Reinforcement", Transactions of the Royal Institute of Technology, Stockholm, No. 158, 1960.

8. MOE, J., "Shearing Strength of Reinforced Concrete Slabs and Footings Under Concentrated Loads", Development Department Bulletin D47, Portland Cement Association, Skokie, Illinois, April, 1961, 130 pages.

9. TASKER, H.E. and WYATT, K.J., "Shear in Flat Plate Construction Under Uniform Loading", Special Report No. 23, Department of Works, Commonwealth Experimental Building Station, Sydney, 1963.

10. YITZHAKI, D., "Punching Strength of Reinforced Concrete Slabs", Comite Europeen du Beton Bulletin d'Information No. 58, October, 1966, p.83-115.

11. WHITNEY, C.S., "Ultimate Shear Strength of Reinforced Concrete Flat Slabs, Footings, Beams and Frame Members Without Shear Reinforcement", ACI Journal, Proceedings V.54, October, 1957, p.265-298.

12. ACI-ASCE COMMITTEE 326, "Shear and Diagonal Tension", ACI Journal, Proceedings V.59, March, 1962, p.353-395.

13. ACI COMMITTEE 318, "Building Code Requirements for Reinforced Concrete (ACI 318-71)", American Concrete Institute, Detroit, 1971.

14. DI STASIO, J. and VAN BUREN, M.P., "Transfer of Bending Moment Between Flat Plate Floor and Column", ACI Journal, Proceedings V.57, September, 1960, p.299-314.

15. ACI COMMITTEE 318, "Commentary on Building Code Requirements for Reinforced Concrete (ACI 318-63)", Publication SP-10, American Concrete Institute, Detroit, 1965.

16. HANSON, N.W. and HANSON, J.M., "Shear and Moment Transfer Between Concrete Slabs and Columns", Journal of the PCA Research and Development Laboratories, Vol. 10, No. 1, January, 1968, p.2-16. Also PCA Development Department Bulletin D129.

17. KREPS, R.R. and REESE, R.C., Discussion of "Transfer of Bending Moment Between Flat Plate Floor and Column", by Di Stasio and Van Buren, M.P., ACI Journal, Proceedings V.57, March, 1961, p.1261-1263.

18. HOLLINGS, J.P., "The Rotational Capacity of a Reinforced Concrete Flat Slab to Column Connection", Journal of New Zealand Engineering, Vol. 22, No. 8, August, 1967, p.317-320.

19. CARPENTER, J.E., KAAR, P.H. and HANSON, N.W., Discussion of "Proposed Revision of ACI 318-63: Building Code Requirements for Reinforced Concrete", by ACI Committee 318, ACI Journal, Proceedings V.67, September, 1970, p.696-697.

20. HAWKINS, N.M. and CORLEY, W.G., "Transfer of Unbalanced Moment and Shear From Flat Plates to Columns", Tentative Report, PCA R/D Ser. 1482, Portland Cement Association, Skokie, Illinois, October, 1970.

21. ACI COMMITTEE 318., "Building Code Requirements for Reinforced Concrete (ACI 318-56)", ACI Journal, Proceedings V.52, May, 1956, p.913-986.

22. ACI COMMITTEE 318., "Building Code Requirements for Reinforced Concrete (ACI 318-63)", American Concrete Institute, Detroit, June, 1963.

23. ACI COMMITTEE 318., "Commentary on Building Code Requirements for Reinforced Concrete (ACI 318-71)", American Concrete Institute, Detroit, 1971.

24. HSU, T.T.C., "Ultimate Torque of Reinforced Rectangular Beams", Journal of Structural Division, Proceedings, ASCE, Vol.94, ST2, February, 1968, p.485-510. Also PCA Development Department Bulletin D127.

25. HSU, T.T.C., "Torsion of Structural Concrete-Plain Concrete Rectangular Sections", Publication SP-18, American Concrete Institute, Detroit, 1968, p.203-238. Also PCA Development Department Bulletin D134.

26. HSU, T.T.C., "Torsion of Structural Concrete - Behaviour of Reinforced Concrete Rectangular Members", Publication SP-18, American Concrete Institute, Detroit, 1968, p.261-306. Also PCA Development Department Bulletin D135.

27. HSU, T.T.C., "Torsion of Structural Concrete - Interaction Surface for Combined Torsion, Shear and Bending in Beams Without Stirrups", ACI Journal, Proceedings V.65, January, 1968, p.51-60. Also PCA Development Department Bulletin D138.

28. CORLEY, W.G. and HAWKINS, N.M., "Shearhead Reinforcement for Slabs", ACI Journal, Proceedings V.65, October, 1968, p.811-824. Also PCA Development Department Bulletin D144.

29. PRIVATE COMMUNICATION from Carpenter, J.E., Portland Cement Association, Skokie, Illinois, May 5, 1969.

30. HERZOG, M., "A New Evaluation of Earlier Punching Shear Tests", Concrete, Journal of the Concrete Society, London, Vol.4, No. 12, December, 1970, p.448-450.

31. GRAF, O., "Strength Tests of Thick Reinforced Concrete Slabs Supported on All Sides Under Concentrated Loads", Deutscher Ausschuss fur Eisenbeton, Bulletin No. 88, Berlin, 1938.

32. ROSENTHAL, I., "Experimental Investigation of Flat Plate Floors", ACI Journal, Proceedings V.56, August, 1959, p.153-166.

33. ANDERSSON, J.L., "Punching of Concrete Slabs With Shear Reinforcement", Transactions of the Royal Institute of Technology, Stockholm, No. 212, 1963.

34. FRANZ, G., "The Column Region of Reinforced Concrete Flat Plates", Comite Europeen du Beton Bulletin d'Information No. 58, October, 1966, p.38-50 (In German).

35. RUSSELL, H.G., "Flat-Slab and Column Construction - A Preliminary Investigation of the Design of Column-Slab Joints With Reference to Punching-Shear and Bending-Moment Transmission", Building Research Station, Garston, England, 1969.

36. TSUBOI, Y. and KAWAGUCHI, M., "On Earthquake Resistant Design of Flat Slabs and Concrete Shell Structures", Proceedings of the Second World Conference on Earthquake Engineering, Japan, Vol. III, July, 1960, p.1693-1708.

37. MAST, P.E., "Stresses in Flat Plates Near Columns", ACI Journal, Proceedings V.67, October, 1970, p.761-768.

38. PARK, R., "Ultimate Strength of Rectangular Concrete Slabs Under Short-Term Uniform Loading with Edges Restrained Against Lateral Movement", Proceedings of the Institution of Civil Engineers, Vol. 28, June, 1964, p.125-150.

39. PARK, R., "The Ultimate Strength and Long-Term Behaviour of Uniformly Loaded Two-Way Concrete Slabs with Partial Lateral Restraint at All Edges", Magazine of Concrete Research, Vol. 16, No. 48, September, 1964, p.139-152.

40. PARK, R., "Ultimate Strength Design of Reinforced Concrete Structures", Vol. 2 - "Limit Design of Reinforced Concrete Slabs", University of Canterbury, Christchurch, 1969.

41. AALAMI, B., "Moment-Rotation Relation Between Column and Slab", ACI Journal, Proceedings V.69, May, 1972, p.263-269.

APPENDIX B

MATERIALS, EQUIPMENT AND TESTING PROCEDURE FOR SLAB-COLUMN SPECIMENS

B.1 MATERIALS

B.1.1 Concrete

(a) Mix Properties

The concrete used in all specimens was a specially mixed mortar, AD-$\frac{1}{4}$, supplied by Certified Concrete Limited, Christchurch, and was made with ordinary portland cement and a graded aggregate with a maximum size of $\frac{1}{4}$ in. The design strength of the mix was 4000 psi at 28 days. The mix proportions by weight were:

aggregate : cement : water = 4.20 : 1 : 0.69

The slumps measured for the mix ranged from $3\frac{1}{4}$ in. to $5\frac{1}{2}$ in.

(b) Control Specimens

For the slab and the lower column in each specimen, four 6 in. diameter x 12 in. cylinders and three 12 in. x 3 in. x 3 in. modulus of rupture prisms were cast in machined steel forms. Three additional 6 in. diameter x 12 in. cylinders were cast for the concrete in the upper column which was poured one day after the slab and the lower column were placed. The control specimens were tested immediately after each slab-column experiment. The cylinders were capped with plaster at both ends and were loaded at 2000 psi per minute to failure. The modulus of rupture prisms were tested slowly. The 12 in. x 3 in. x 3 in. prisms were simply supported over 9 in. point loads being applied 3 in. from the supports.

The results of the concrete control specimen tests are given in Table B.1.

TABLE B.1

CONCRETE PROPERTIES AT TIME OF TESTING

SPECIMEN NO.	AGE days	SLAB AND LOWER COLUMN		UPPER COLUMN
		CYLINDER STRENGTH f'_c psi	MODULUS OF RUPTURE f_r psi	CYLINDER STRENGTH f'_c psi
1	110	3960	620	3880
2	39	4630	680	5250
3C	41	4310	687	5080
4S	31	4630	690	4650
5S	39	4430	562	4520
6CS	42	4090	568	4620
7CS	58	4310	726	5120
8CS	91	3210	506	4160

B.1.2 Steel

(a) Slab Reinforcement

Deformed mild steel reinforcing bars of $\frac{3}{8}$ in. diameter were used as top and bottom reinforcement in the slab. The reinforcing bars were obtained from one manufacturer but in different lots. For tension tests six 18 in. long samples were taken from the batch of reinforcing bars used in each slab-column specimen. Care was taken to ensure that some of the test samples came from bars which passed through the column in the longer direction. Tension tests were conducted on these samples and values of yield stress f_y and ultimate stress f'_s shown in Table B.2 were averages of these tests. In addition, stress-strain curves were found for selected steel specimens using a Baty mechanical extensometer on a 2 in. gauge length, and an Avery 25,000 lb. Universal Testing Machine. Fig. B.1 shows the shape of a representative stress-strain curve for a typical $\frac{3}{8}$ in. diameter bar used in the slab.

(b) Column Reinforcement

The column was reinforced with 8 Nos. of $\frac{3}{4}$ in. diameter deformed mild steel bars and ties were made of $\frac{1}{4}$ in. diameter plain mild steel bars. The reinforcing bars for columns were obtained in two batches and their strengths are given in Table B.2.

(c) Shear Reinforcement

$\frac{3}{8}$ in. diameter deformed bars used as shear reinforcement in the form of inclined cranked bars in specimen 4S came from the same batch of reinforcement as used in the slab. Measured yield and ultimate stresses are given in Table B.2.

TABLE B.2

STEEL PROPERTIES

CIMEN O.	SLAB REINFORCEMENT		COLUMN REINFORCEMENT		SHEAR REINFORCEMENT			
	$\frac{3}{8}$" Dia. Bar		$\frac{3}{4}$" Dia. Bar		3/16" Dia. Bar		$\frac{1}{4}$" Dia. Bar	
	Yield Stress f_y psi	Ultimate Stress f'_s psi	Yield Stress f_y psi	Ultimate Stress f'_s psi	Yield Stress f_y psi	Ultimate Stress f'_s psi	Yield Stress f_y psi	Ultimate Stress f'_s psi
	51,610	73,630	42,800	65,000	-	-	-	-
	54,160	74,070	42,800	65,000	-	-	-	-
	45,820	66,220	42,800	65,000	-	-	-	-
	47,740	66,360	42,800	65,000	-	-	-	-
	41,230	60,000	43,710	64,920	-	-	-	-
S	42,120	61,200	43,710	64,920	54,830	64,130	-	-
S	44,090	62,970	43,710	64,920	-	-	52,970	71,580
S	42,480	61,360	43,710	64,920	56,250	64,740	-	-

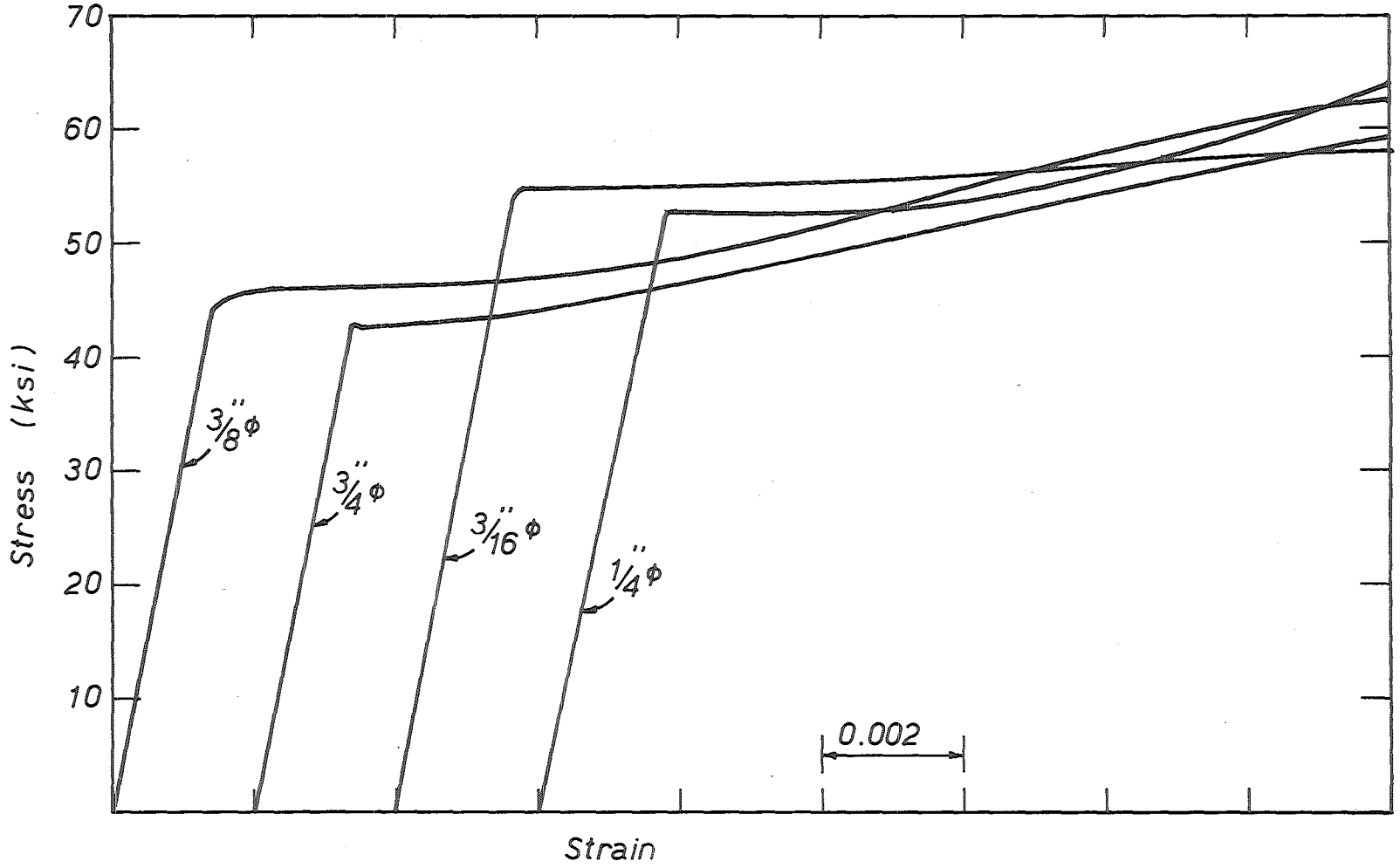

FIG. B.1 STRESS-STRAIN CURVES FOR STEEL

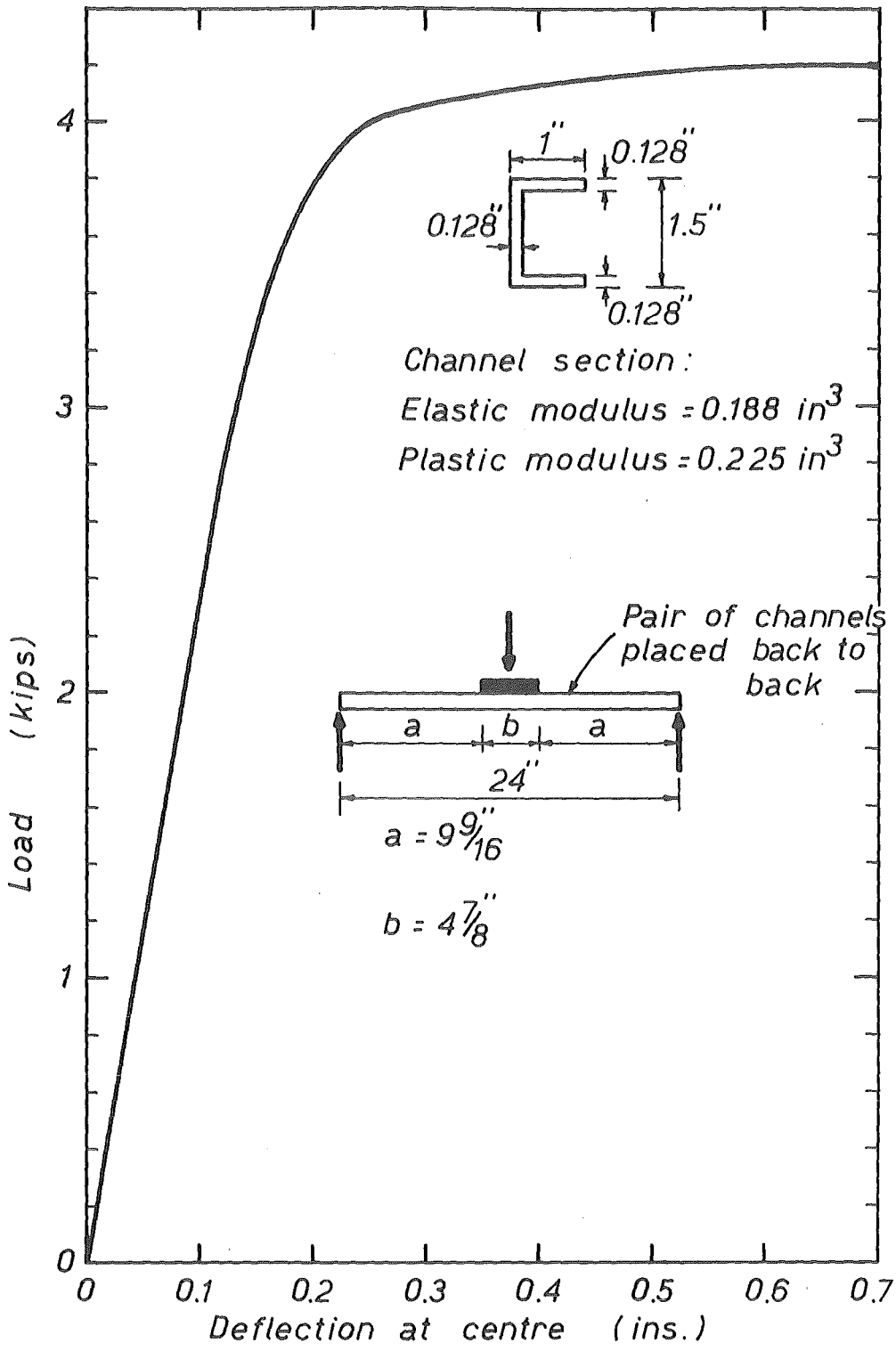

FIG. B.2 LOAD-DEFLECTION CURVE FOR SHEARHEAD

For the shearhead used in specimen 5S a load-deflection curve was obtained from a bending test. Fig. B.2 shows the arrangement for the bending test as well as the load-deflection curve. The yield stress computed from the test data and the properties of the section was found to be 42,500 psi. From this test it was found that the plastic moment capacity of each arm of the shearhead was 9,600 lb. in.

Yield and ultimate stresses for 3/16 in. diameter plain bars used as stirrups in specimens 6CS and 8CS, and those for $\frac{1}{4}$ in. diameter plain bars used in specimen 7CS are given in Table B.2. The representative stress-strain curves for 3/16 in. and $\frac{1}{4}$ in. diameter bars are also shown in Fig. B.1.

B.2 FABRICATION

B.2.1 Formwork

The form for the test specimens was made of $\frac{3}{4}$ in. thick coreboard suitably stiffened with 4" x 2" channel sections. Unequal angles of size $3\frac{1}{2}$" x $2\frac{1}{2}$" x $\frac{1}{4}$" were used to form the boundary of the slab. The moulds for the lower and upper column were made of $\frac{1}{4}$ in. thick steel plates. The form was constructed in such a way that the entire slab and the lower column could be cast at one time. The mould for the upper column could be placed in position on the following day for subsequent casting. Prior to each casting all the steel moulds were coated with a light mould oil and the coreboard surface was varnished with a coat of Duropon.

It was necessary to make provisions for 24 holes in the slab for suspending the concrete blocks. This was done by using $\frac{1}{4}$ in. diameter plain bars which were held on the board vertically by means of screws. These bars were covered with thin plastic tubing for the ease of removal later on. Provisions for four 3 in. diameter holes along each of the two

shorter edges of the slab were also made by fixing 3 in. diameter hollow cylindrical blocks on the board by screws.

Fig. B.3 shows a view of the form and reinforcement arrangements prior to casting of specimen 1.

B.2.2 Placing Reinforcement

The column reinforcement was assembled and placed in position in the form prior to placing of slab reinforcement. Both top and bottom layers of slab reinforcing bars were tied together with iron wires. The bottom layers of bars were supported on $\frac{3}{8}$ in. thick precast cement mortar blocks which provided the same margin of clear cover as their thicknesses. The top layers were supported on the bottom layers by $\frac{3}{8}$ in. diameter studs which were tack welded to the reinforcing bars at selected positions.

A photograph of specimen 1 before casting is shown in Fig. B.3. This basic reinforcement pattern was used in all the specimens tested. Fig. B.4 shows the inclined cranked bars used as shear reinforcement in specimen 4S. The shearhead reinforcement used in specimen 5S can be seen in Fig. B.5. Closed stirrups with 4 legs which were used in specimen 6CS are shown in Fig. B.6. A view of 2 legged closed stirrups used in specimens 7CS and 8CS is shown in Fig. B.7.

B.2.3 Placing Concrete

Before concrete was placed all the joints in the form were taped to prevent leakage of mortar. The form and the reinforcement were thoroughly cleaned. About one cubic yard of ready mixed concrete delivered by Certified Concrete Ltd. was required to cast each slab-column specimen and its 6 x 12 in. test cylinders. The lower column and the entire slab were placed at one time. An internal vibrator was used to consolidate the concrete. The slab was screeded and the surface finished with a steel float. The top column was cast on the following day. For this purpose concrete was mixed in the laboratory using the same proportions of dry mix as supplied by Certified Concrete Ltd for casting the slab. Slump tests

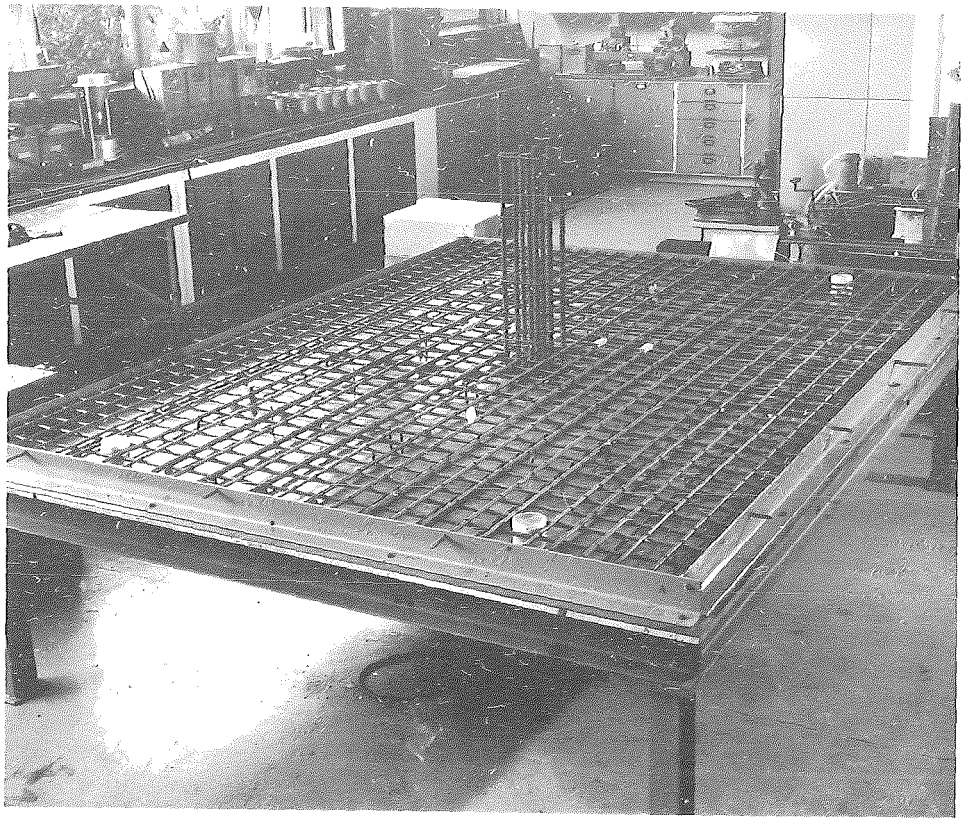

FIG. B.3 FORMWORK AND REINFORCEMENT

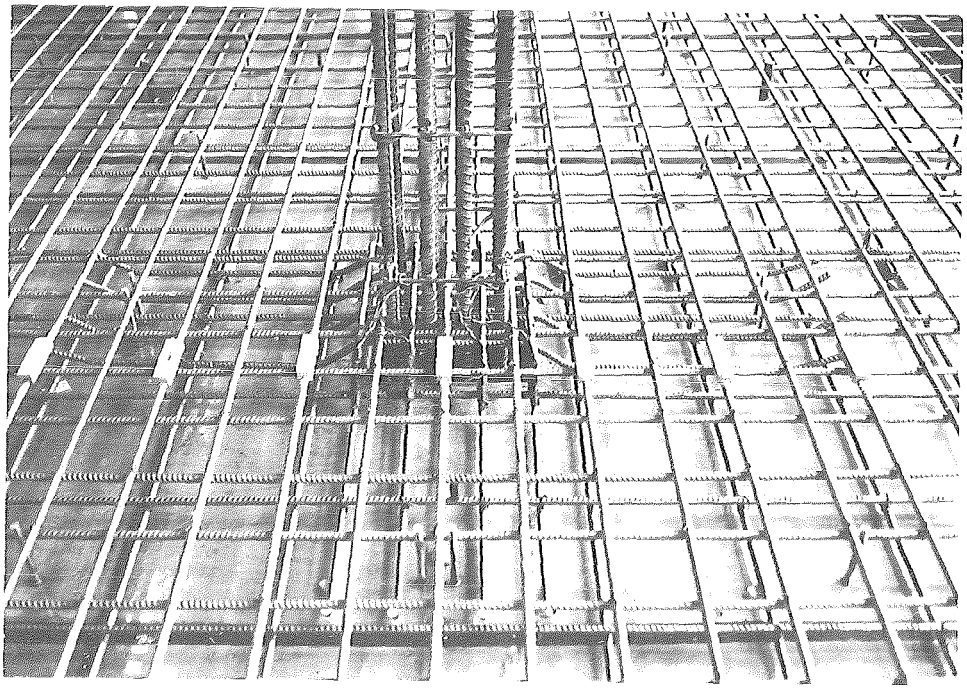

FIG. B.4 INCLINED CRANKED BARS IN SPECIMEN 4S

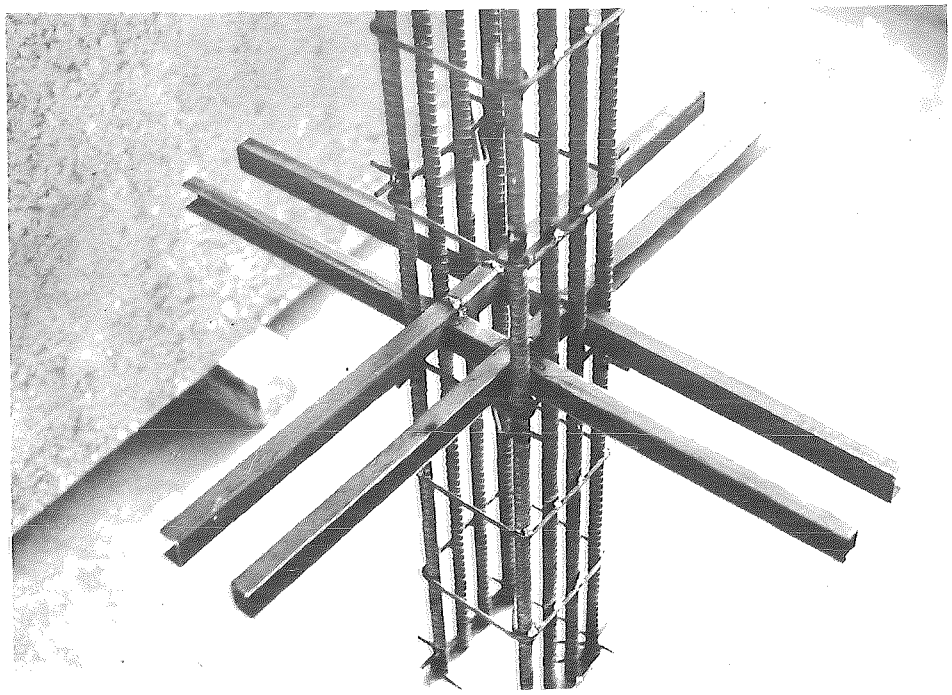

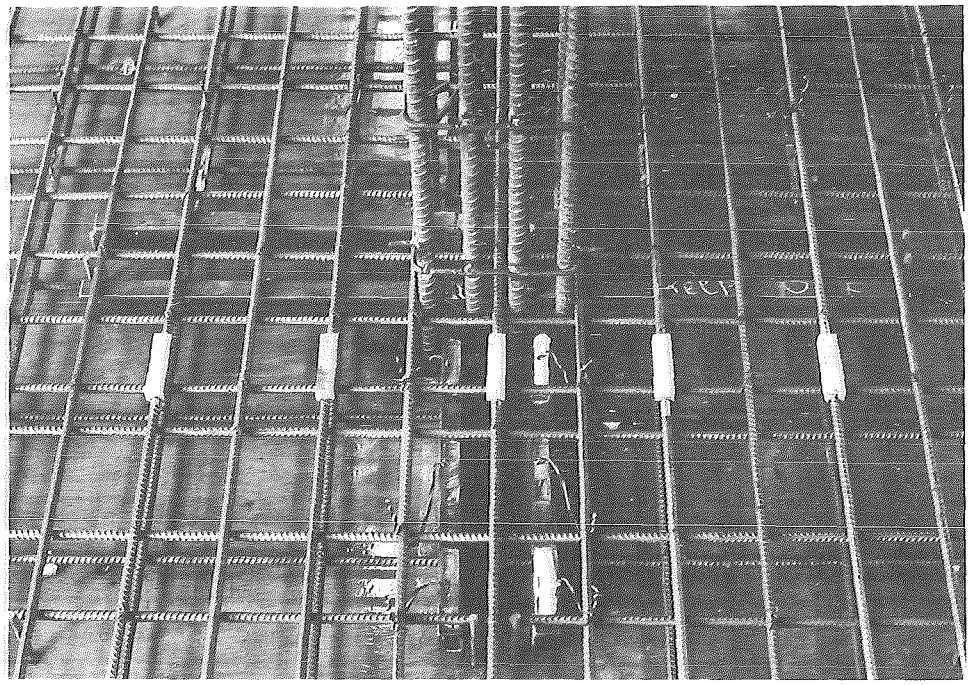

FIG. B.5 SHEARHEAD IN SPECIMEN 5S

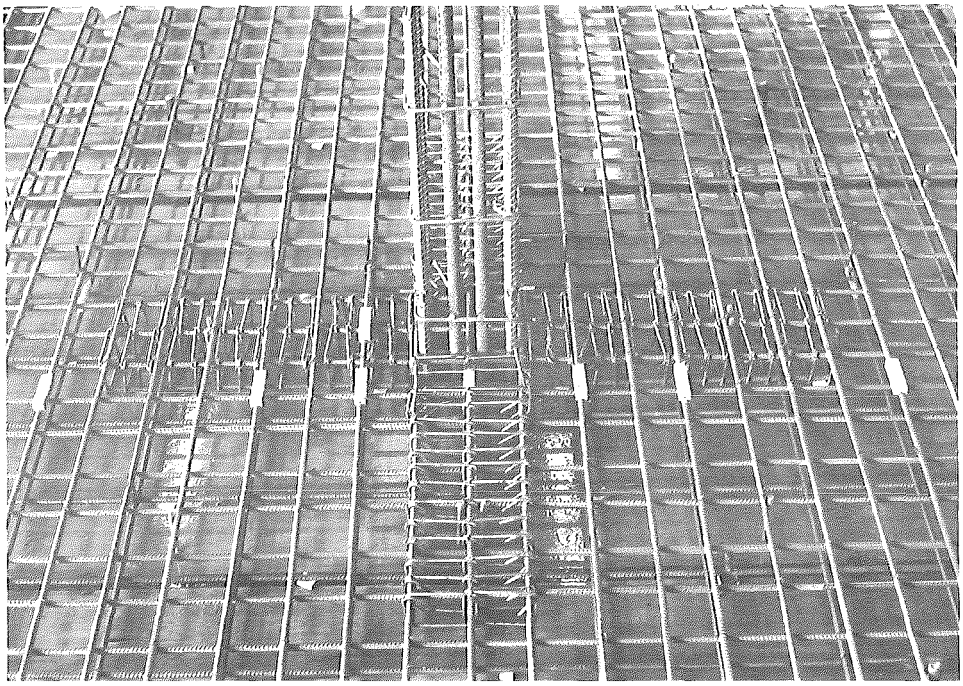

FIG. B.6 CLOSED STIRRUPS IN SPECIMEN 6CS

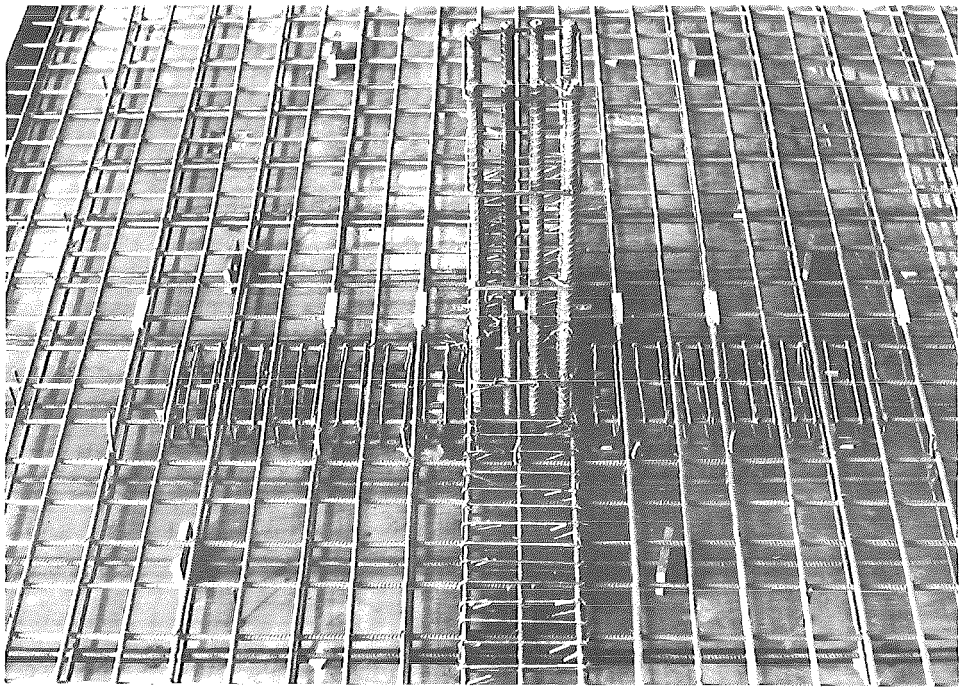

FIG. B.7 CLOSED STIRRUPS IN SPECIMENS 7CS & 8CS

were made to check the given water cement ratio. About 24 hours after the concrete was placed the slab surface was covered with wet sacks and plastic sheets. This moist curing continued for eight to ten days. The test cylinders and prisms for modulus of rupture test were cast in steel moulds. They were vibrated internally and were cured in the same way as the slab-column specimens.

B.3 TEST EQUIPMENT AND PROCEDURE

B.3.1 Test Frame

The test frame is shown in Figs. 3.16 and B.8. It consisted of three portal frames rigidly braced at the top. The central portal frame for application of axial load on the column was designed for a maximum vertical load of 60 tons. The two end portals were designed for an upward vertical slab edge loading of 5 tons. The downward slab edge loading was transmitted to the floor base plates, details of which are shown in Figs. B.9 and B.10. For horizontal loads from the top of the column a V-type reaction frame was designed for a load of 10 tons. The ends of the V-frame were pin connected to the flanges of the columns to transmit the horizontal forces. The section sizes of the frames were increased considerably over those required in order to reduce frame deflections. Column reactions were transferred through a steel column cap (made to a close fit, but with mortar placed between the cap and the column end to give uniform bearing) to a 2" diameter steel pin, greased to allow rotations, and thence to the reaction frame at the top and a floor base plate at the bottom.

B.3.2. Load Application and Measurement

The axial load on the column was applied through a 60-ton hydraulic jack, Simplex "Re-Mo-Trol" Ram Model No. R613 as shown in Fig. B.11. The oil pressure was applied and regulated throughout the test by a hand pump with a maximum capacity of 10,000 psi. The column load was measured

by a 50-ton Phillips load cell, type PR9226/50. The load cell was calibrated on an Avery 250,000 lb. Universal Testing Machine with a Budd Strain Bridge.

The slab edge loading was applied by tightening nuts against threaded 1" diameter high tensile bars. This was considered more suitable than hydraulic jacks as it allows the application of controlled displacements rather than constant loads, the former being preferable for determining deformations in the post-elastic range. Further, for a constant deflection system the creep that occurs at an increment is mainly in the magnitude of load, rather than in all the strain and deflection readings as would occur for a constant load hydraulic system.

Two systems of slab edge loading were used. In testing specimen No. 1 live loads were applied through a $3\frac{1}{2}$" x $3\frac{1}{2}$" hollow steel section seated in plaster on the slab surface as shown in Fig. B.9. Loading was applied through two 1" diameter high tensile bars by tightening nuts against the hollow steel section. As pointed out earlier in Section 3.3.3, due to uneven distribution of load resulting from lack of contact of the steel tube with the slab surface near the outer ends, this method was abandoned in favour of point loads in the remaining tests. In this system the slab edge loading was applied by two pairs of $\frac{3}{4}$" diameter steel rods. Each pair was loaded through a $3\frac{1}{2}$" x $3\frac{1}{2}$" steel tube crosshead by a centrally located 1" diameter high tensile bar as shown in Fig. B.10. The methods of applying upward and downward edge loads are shown in Figs. B.12 and B.13.

The load in the 1" diameter high tensile bars was measured by strain gauges. Four Kyowa KF-10-C1-11 (temperature compensated for steel) 10 mm foil strain gauges were glued to each bar. Two gauges diametrically opposed and aligned axially formed the active strain gauges, and the other two gauges diametrically opposed and aligned circumferentially formed the compensating strain gauges. The gauges were connected together to form one four-arm bridge circuit. The gauges were waterproofed with micro-wax and

the bars loaded in direct tension and calibrated with a Budd Strain Bridge Model P-350. The load-strain plot for each high tensile bar was very consistent and linear as shown in Fig. B.14.

To apply a uniformly distributed load of 63.75 lb/ft^2 on the slab 24 concrete blocks, each weighing 200 lbs were suspended from the slab. The location of these point loads are shown in Fig. 3.9. The size of each concrete block was 12" x 12" x 16" (height) and their actual weights were found to vary slightly, all remaining under weight. Extra weights of varying amounts had to be placed on these blocks to make the weight of each block exactly 200 lbs. The concrete blocks were suspended from the slab by $\frac{1}{4}$ in. diameter plain bars.

B.3.3 Deflections

The deflections along the centre lines of the column and the slab in the longer direction were measured by a number of 2"-travel and 1"-travel, 0.001" dial gauges. The dial gauge locations are shown in Fig. B.15. For loading the slab edges by controlled deformations dial gauges were also placed at each corner of the slab.

B.3.4 Steel Strains

Steel strains were measured by electrical resistance strain gauges glued to the surface of both slab reinforcing bars and shear reinforcement. The strain gauge locations are shown in corresponding stress diagrams for slab bars and shear reinforcement such as Figs. 3.19, 3.40, 3.45, etc. The slab reinforcement gauges were placed in position after removing a cork block fixed between the bar and the mould surface on casting. However, for the various shear reinforcement arrangements used it was more practicable to place and waterproof the gauges prior to casting.

The strain gauges used for $\frac{3}{8}$" diameter bars and the shearhead were BLH SR-4 Type A-12 gauges, a wire gauge length of 1". For 3/16 in. diameter and $\frac{1}{4}$ in. diameter stirrups it was necessary to use Kyowa KF-15-C8-11 gauges

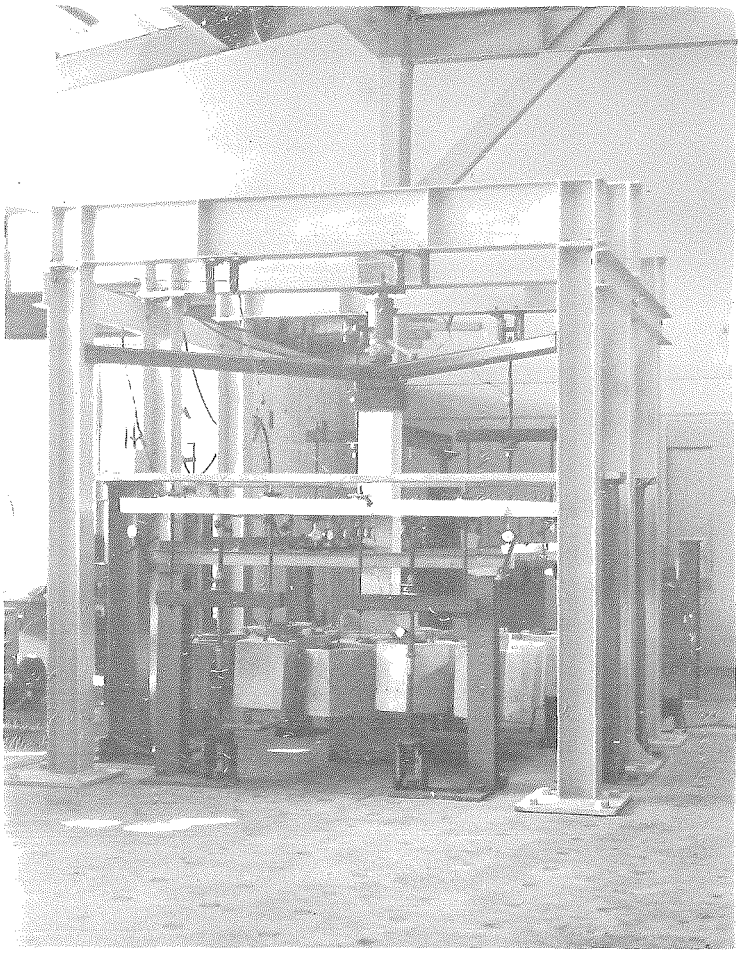

FIG. B.8 — TEST FRAME

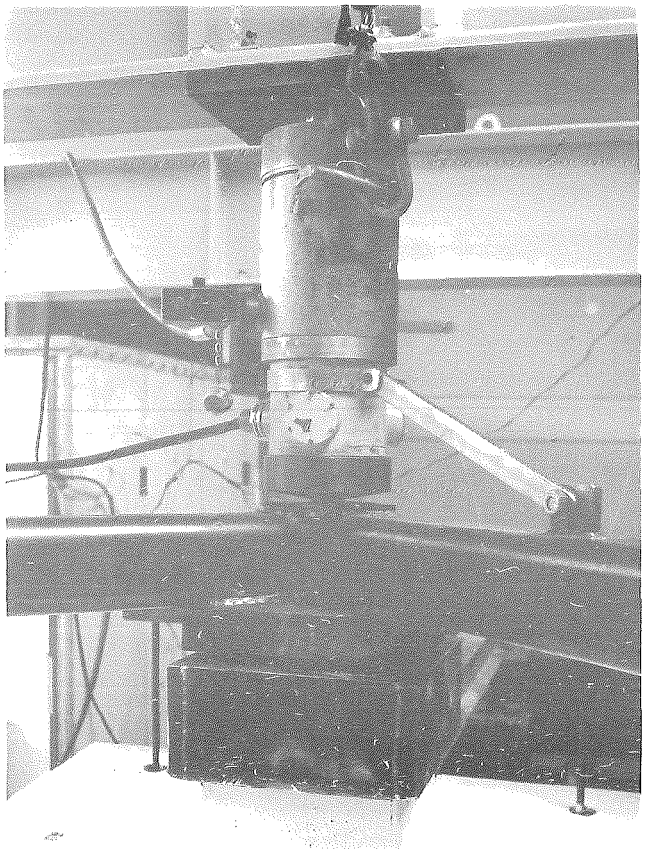

FIG. B.11 — APPLICATION OF COLUMN LOAD

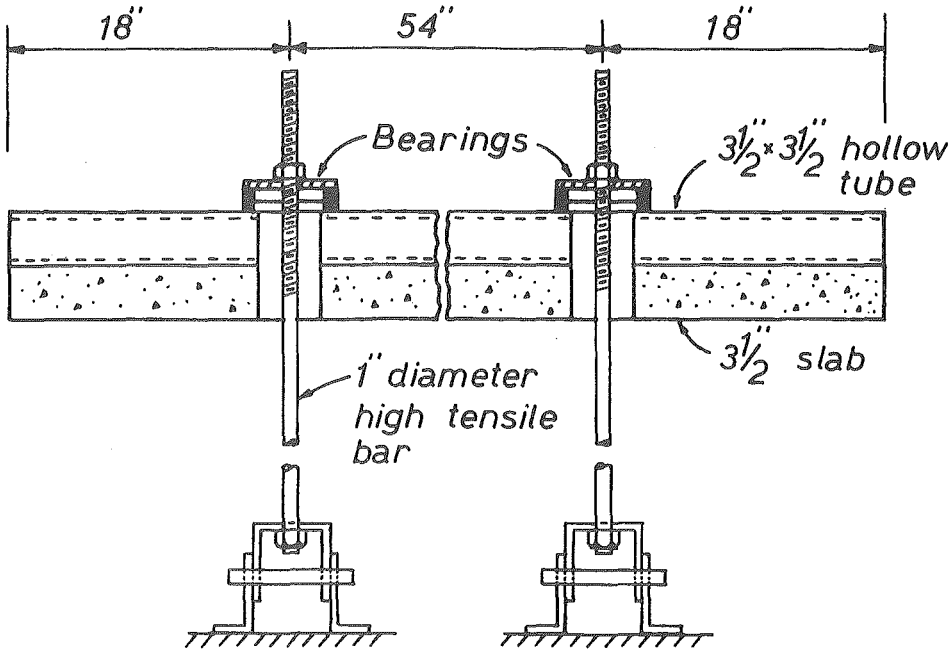

FIG. B.9 METHOD OF APPLYING LINE LOAD AT EDGE

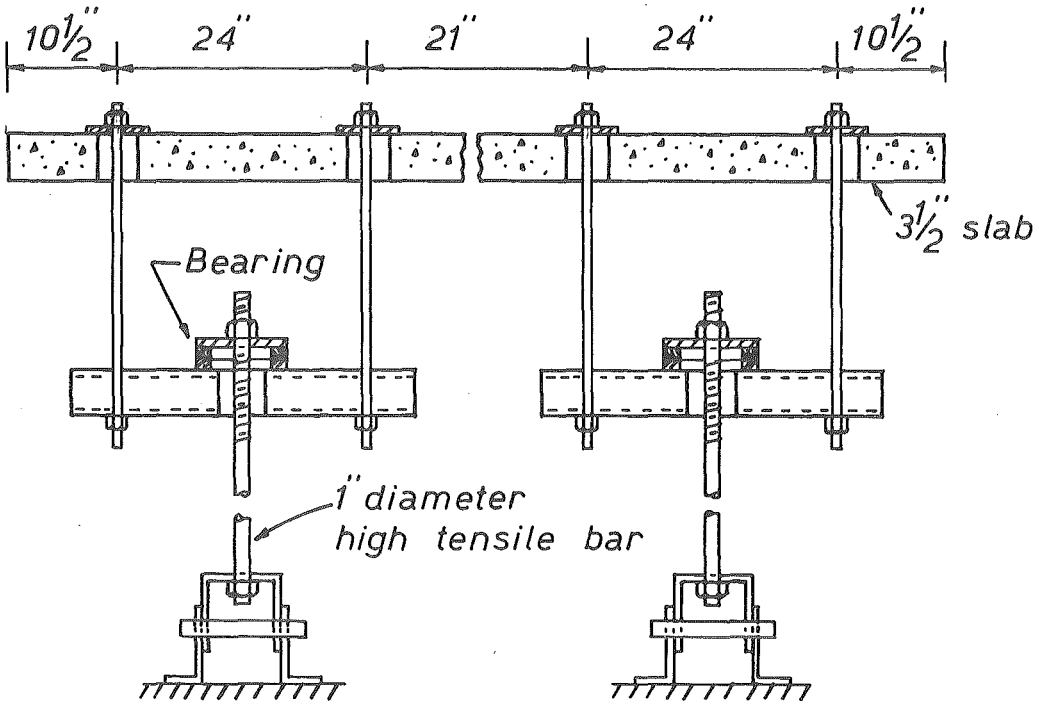

FIG. B.10 METHOD OF APPLYING EDGE LOAD THROUGH 4 POINTS

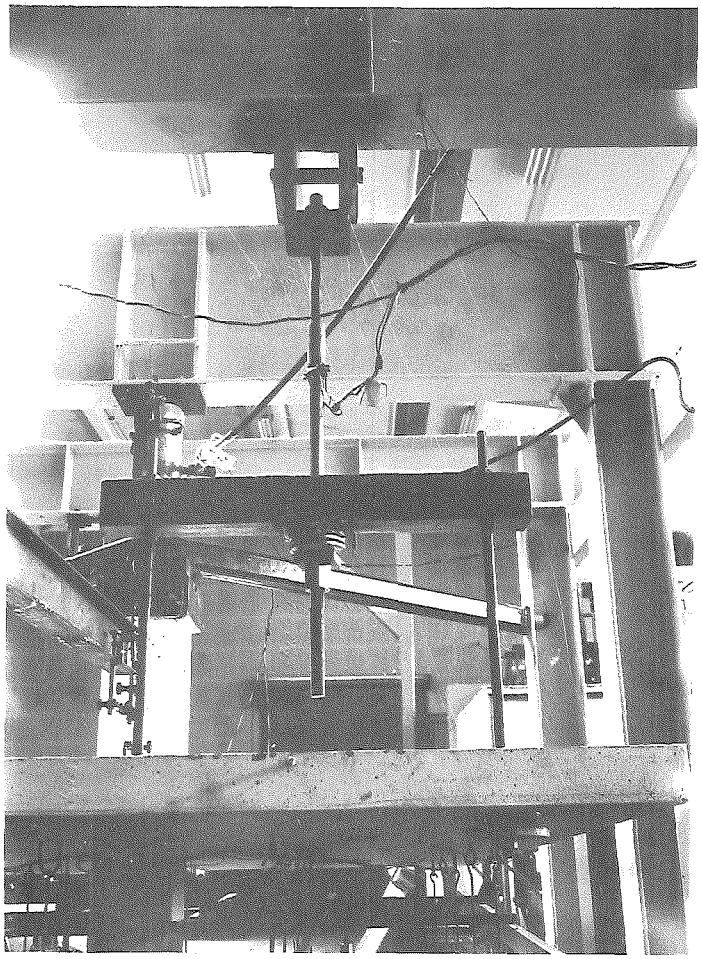

FIG. B.12 APPLICATION OF UPWARD EDGE LOAD

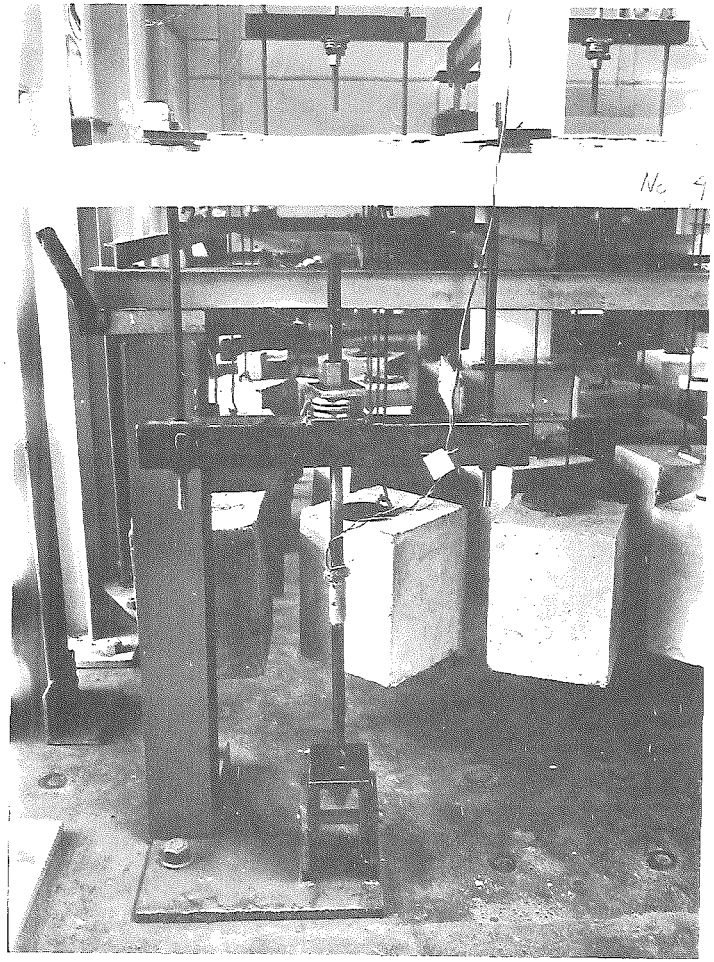

FIG. B.13 APPLICATION OF DOWNWARD EDGE LOAD

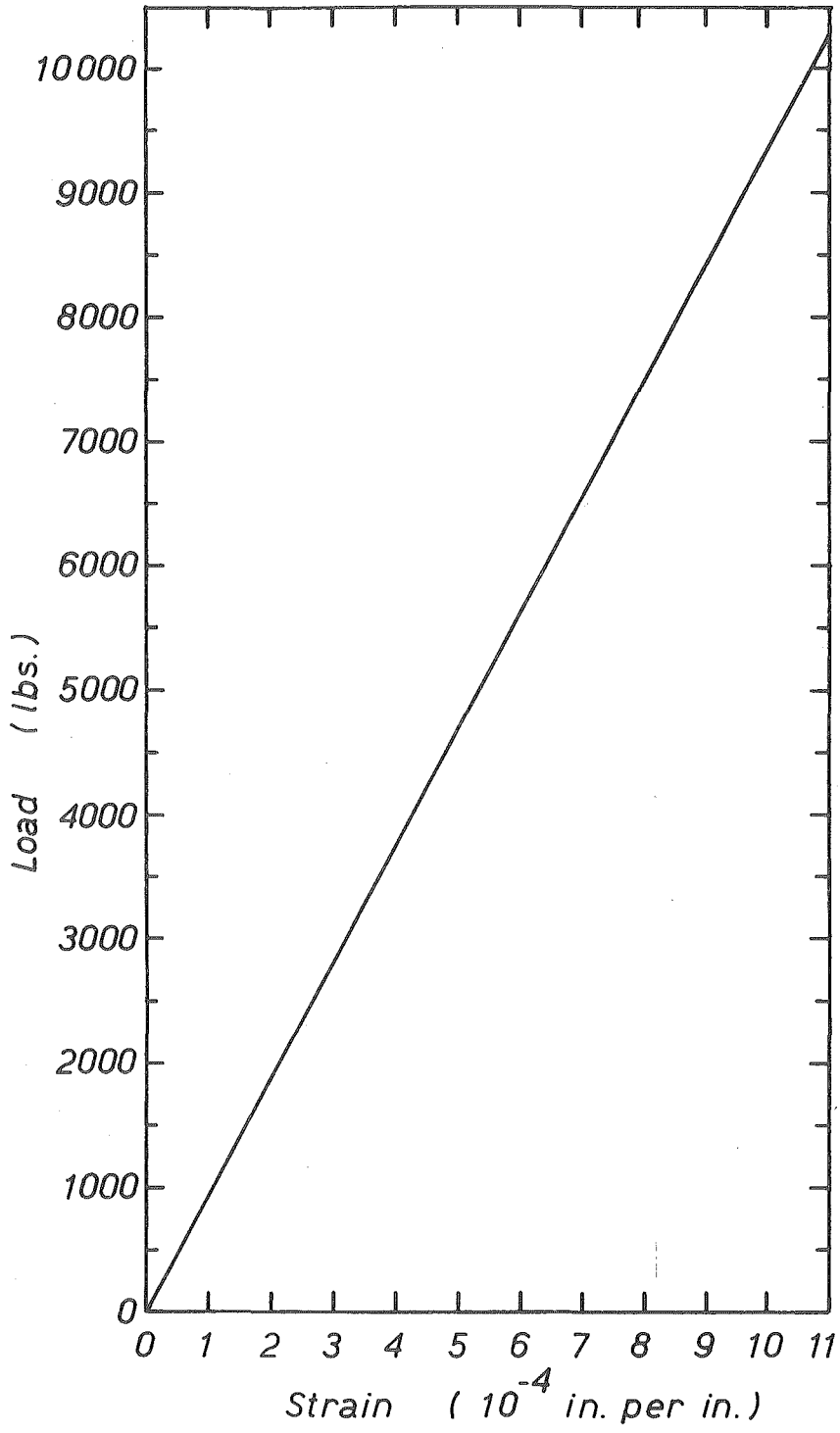

FIG. B.14 LOAD-STRAIN PLOT FOR HIGH TENSILE BAR

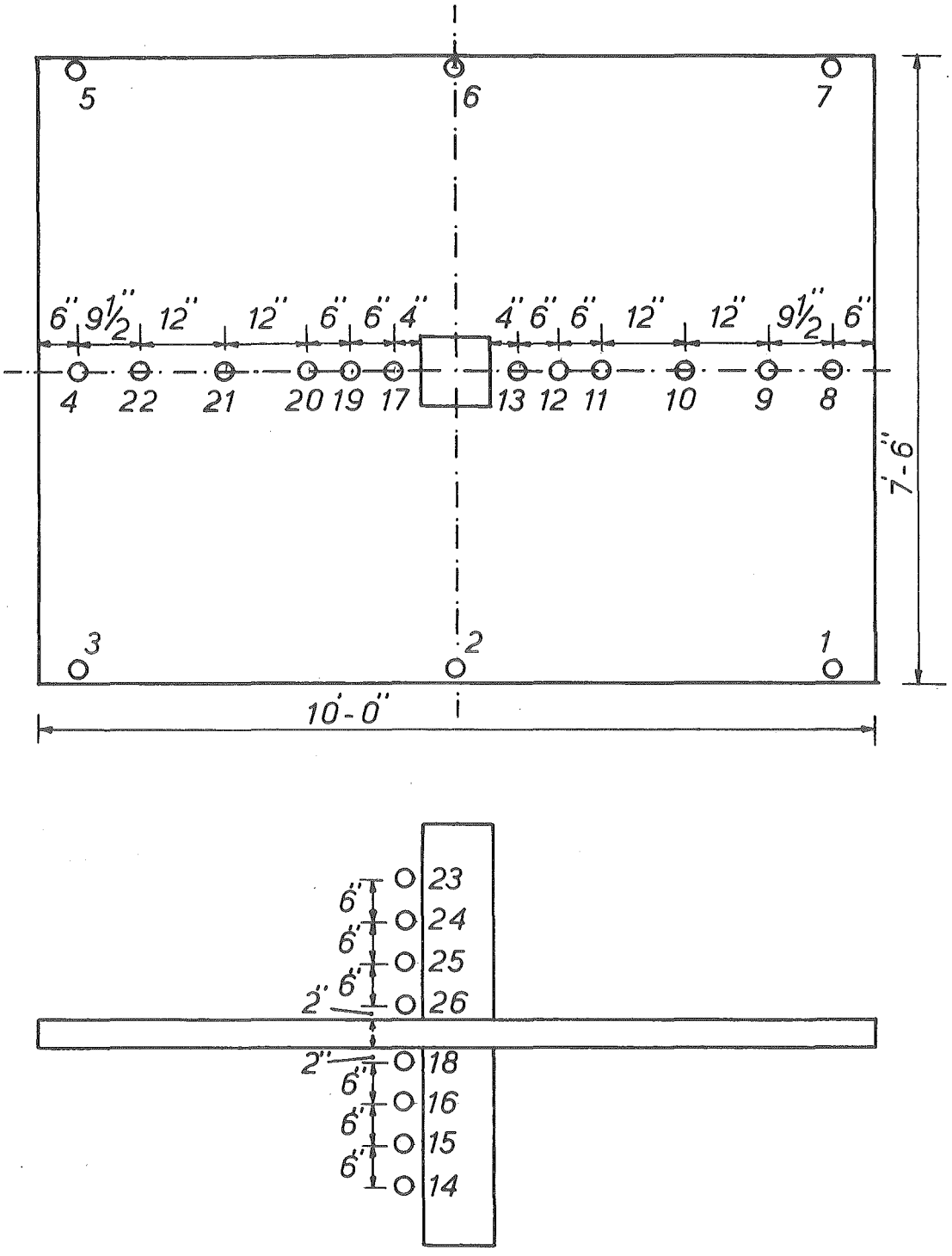

FIG. B.15 DIAL GAUGE LOCATIONS

which could be glued to bars of smaller diameters. Gauges of these types were tested initially and found to be satisfactory up to a strain of 8,000 microstrains. A rapid setting adhesive, Eastman 910 , was used and found to be most satisfactory. For waterproofing all strain gauges petroleum based microcrystalline wax was used.

A 140-channel strain data logger was used to read strains for the first six slab-column specimens tested. A digital voltmeter incorporated in the logger provided output, in microstrains, on a typewriter. For the remaining two tests the data logger was not available. The strain gauges were wired to a switch box and strains were read by a Budd strain bridge. The strain gauges behaved satisfactorily throughout all tests.

B.3.5 Crack Detection

Each specimen was painted white prior to testing to aid detection of cracks. At each load increment cracks were observed with magnifying glasses and marked with felt-tipped pens to give better definition in the photographs of the specimen. Crack widths were also measured at selected points with high magnification microscopes, capable of reading to 0.001".

B.3.6 Sequence of Operations

At the start of each test an initial set of dial gauge and strain gauge readings was taken before application of any load on the specimen. The first loading that was applied was the constant axial load of 50 tons on the column. Another set of dial gauge and strain gauge readings was taken. The next operation was to suspend the 200 lb. weight concrete blocks from the slab at 24 points. This loading was applied in a symmetrical manner so as to avoid any unbalanced moment occurring at the slab-column connection. Again a set of dial gauge and strain gauge readings was taken. After this operation equal and opposite displacements were applied to the edges of the slab. The increment for each edge displacement was 0.1 in. The procedure at each increment was as follows:

(i) Calculate the dial gauge readings at each corner of the slab by adding 0.1 in. to the previous readings for the downward loading end and deducting 0.1 in. from the previous readings for the upward loading end.

(ii) Check column load.

(iii) Apply edge loads by tightening nuts on the high tensile bars to bring the dial gauge readings at each corner to the required marks.

(iv) Read dial gauges.

(v) Record all electrical resistance strain gauge readings.

(vi) Read load in the high tensile bars.

(vii) Mark cracks.